

**SYNTHESIS OF NEW SCHIFF BASES AND  
COMPLEXATION WITH METALS**


**YENİ SCHİFF BAZLARININ SENTEZİ VE BAZI  
METALLERLE KOMPLEKSLEŞME REAKSİYONLARININ  
İNCELENMESİ**


**MAHİR TİMUR**

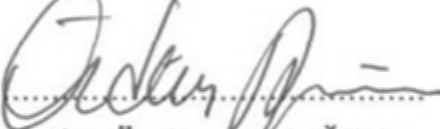
Submitted to Institute of Sciences of  
Hacettepe University as a partial fulfillment  
to the requirements for the award of the degree of  
DOCTOR OF PHILOSOPHY  
in  
CHEMISTRY

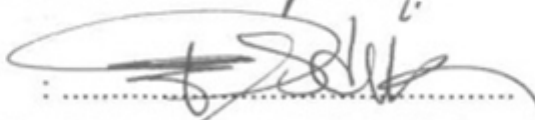
2008


This is to certify that we have read this thesis and that in our opinion it is fully adequate, in scope and quality, as a thesis for degree of **Doctor of Philosophy in Chemistry**.

Head :   
Prof. Dr. Zeynel KILIÇ

Member (Advisor) :   
Prof. Dr. Nazan TUNOĞLU

Member :   
Prof. Dr. Özdemir DOĞAN

Member :   
Prof. Dr. Fatma SEVİN DÜZ

Member (Co-advisor) :   
Doç. Dr. Hülya ŞENÖZ

## APPROVAL

This thesis has been certified as a thesis for the Degree of Doctor of Philosophy by the above Examining Committee Members on 25/06/2008.

...../...../2008

Prof. Dr. Erdem YAZGAN  
Director of the Graduate School of  
Natural and Applied Sciences

# YENİ SCHIFF BAZLARININ SENTEZİ VE BAZI METALLERLE KOMPLEKSLEŞME REAKSİYONLARININ İNCELENMESİ

**Mahir Timur**

## **Özet**

Doktora tezi olarak sunulan bu çalışmada amacımız ilk olarak yeni Schiff bazlarını sentezlemek ve ardından bu Schiff bazlarının Cu(II), Co(II), ve Ni(II) ile kompleksleştirme reaksiyonlarını gerçekleştirmektir.

Çalışmamızda diketon olarak 5,5-dimetil-1,3-sikloheksandion, 1,3-sikloheksandion ve amin olarak p-amino difenilamin, trietilentetramin, 1,3-sikloheksanbis(metilamin) ve m-ksililen diamin kullanılarak beş yeni Schiff bazı sentezlenmiştir. Sentezlenen bu Schiff bazlarının, yapılan spektroskopik çalışmalar sonucunda  $\beta$ -enaminon formunda olduğu belirlenmiştir.

Sentezlenen bileşikler kromatografik yöntemlerle veya kristallendirme ile saflaştırılmış, yapıları element analizi LC-MS,  $^1\text{H}$  NMR, APT, COSY NMR, FT-IR ve UV-VİS spektroskopik teknikleriyle aydınlatılmıştır.

Kompleksleştirme reaksiyonlarında kompleks oluşumu için iki farklı yöntem uygulanmıştır.

İlk yöntem olarak sentezlenen Schiff bazları Cu(II), Co(II), ve Ni(II) ile reaksiyona girerek değişik renklerde metal kompleksleri elde edilmiştir. İkinci yöntemde Schiff bazı oluşumu ile kompleksleşme aynı basamakta gerçekleştirilmiştir.

Sentezlenen metal kompleksleri ICP-AES, magnetik susseptibilite, FT-IR, TGA ve UV-VİS spektroskopik teknikleri kullanılarak karakterize edilmiştir.

**Anahtar Kelimeler:** Schiff bazı, Enaminon, Diamin, Diketon, Metal Kompleksleri, Tautomerizm.

Danışman: Prof. Dr. Nazan Tunođlu, Hacettepe Üniversitesi, Fen Fakóltesi, Kimya Bölümü, Organik Kimya Anabilim Dalı.

İkinci danışman: Doç. Dr. Hülya Şenöz, Hacettepe Üniversitesi, Fen Fakóltesi, Kimya Bölümü, Organik Kimya Anabilim Dalı.

# SYNTHESIS OF NEW SCHIFF BASES AND COMPLEXATION WITH METALS

**Mahir Timur**

## ABSTRACT

First aim of this study presented as a PhD thesis, is the synthesis of new Schiff bases and second aim is the complexation of them with Cu(II), Co(II) and Ni(II) metal ions.

In our study five new Schiff bases were synthesized by using 5,5-dimethyl-1,3-cyclohexanedione, 1,3-cyclohexanedione as diketones and p-amino diphenylamine, triethylenetetramine, 1,3-cyclohexanebis(methylamine) and m-xylylene diamine as amines. According to spectroscopic study, all Schiff bases were synthesized as  $\beta$ -enaminone tautomers.

Synthesized compounds were purified by chromatographic methods and their structures were identified by elemental analysis, LC-MS,  $^1\text{H}$  NMR, APT, COSY NMR, FT-IR and UV-VIS-NIR spectroscopic techniques.

Syntheses of complexes carried out by two different methods.

In first method, all synthesized Schiff bases were directly reacted with Cu(II), Co(II), and Ni(II) and various coloured powder metal complexes were obtained. As the second method, the ketone, amine and metal salt were all mixed together and allowed to react in-situ to yield the corresponding complex.

The structures of the metal complexes were identified by elemental analysis, ICP-AES, magnetic susceptibility, FT-IR, TGA and UV-VIS-NIR spectroscopic techniques.

**Keywords:** Schiff base, Enaminone, Diamine, Diketone, Metal complexes, Tautomerisation.

Advisor: Prof. Dr. Nazan Tunođlu, Hacettepe University, Faculty of Science,  
Department of Chemistry, Organic Chemistry Division.

Co-advisor: Doç. Dr. Hülya Şenöz, Hacettepe University, Faculty of Science,  
Department of Chemistry, Organic Chemistry Division.

## **ACKNOWLEDGMENT**

I would like to express my thanks to advisors Prof. Dr. Nazan Tunođlu and Doç. Dr. Hülya Őenöz for their invaluable help, support, professional advice and encouragement through my studies.

I would like to thank to Prof. Dr. Zeynel Kılıç and Prof. Dr. Birgül Karan their help and interest in my work.

I would like to thank to Hacettepe University Scientific Research Unit for funding part of this work.

I am also thankful to all the members of Organic and Inorganic Chemistry Divisions for the friendly working atmosphere.

I wish to express my sincere thanks to my colleagues Ahmet Nedim Ay and Halil Erdoğan for their helps during my studies.

I wish to express my deep gratitude to my family for their love, encouragement and patience.

Finally, I want to thank to my wife Suat Gür Timur and my son Fevzi Başar Timur for their love and support was my strenght during this study.

*This work is dedicated to my Dad !*

## CONTENTS

	<b>Page</b>
<b>ÖZET</b> .....	i
<b>ABSTRACT</b> .....	iii
<b>ACKNOWLEDGMENTS</b> .....	v
<b>CONTENTS</b> .....	vi
<b>FIGURES</b> .....	ix
<b>TABLES</b> .....	xiv
<b>SCHEMES</b> .....	xv
<b>ABBREVIATIONS</b> .....	xvi
<b>1. INTRODUCTION</b> .....	<b>1</b>
<b>2. GENERAL INFORMATION</b> .....	<b>3</b>
<b>2.1. Synthesis of Schiff Bases, <math>\beta</math>-Enaminone Formation</b> .....	<b>3</b>
<b>2.2. Synthetic Importance of Schiff Bases</b> .....	<b>4</b>
<b>2.3. Chemistry and Biological Importance</b> .....	<b>6</b>
<b>2.4. Tautomerism in Schiff Bases, <math>\beta</math>-enaminone Formation</b> .....	<b>8</b>
<b>2.5. Electronic Spectra</b> .....	<b>12</b>
<b>2.5.1. Metal-metal bonds</b> .....	<b>14</b>
<b>2.5.2. Electronic Spectra of Ligands and Complexes</b> .....	<b>14</b>
<b>2.5.3. Electronic Spectral Data and Magnetic Properties of Copper(II)</b> ...	<b>15</b>
<b>2.5.4. Electronic Spectral Data and Magnetic Properties of High-Spin Octahedral and Tetrahedral Complexes of Cobalt(II)</b> .....	<b>16</b>
<b>2.5.5. Electronic Spectral data and Magnetic Properties of Complexes of Nickel(II)</b> .....	<b>19</b>
<b>2.6. Metal Complexes</b> .....	<b>21</b>
<b>2.6.1. Metal Ion Control in Macrocycle Synthesis</b> .....	<b>22</b>
<b>2.6.2. Analytical Applications</b> .....	<b>23</b>
<b>2.7. Characterization of Schiff Bases and Metal Complexes</b> .....	<b>24</b>
<b>2.7.1. Complexes of Polyamines</b> .....	<b>24</b>
<b>2.7.2. Lattice Water and Aqua Complexes</b> .....	<b>25</b>
<b>2.8. Stabilities of Coordination Compounds</b> .....	<b>26</b>



2.8.1	Effect of Metal Ion .....	26
2.8.2.	Classification of Metal Acceptor Properties .....	27
2.8.3.	Basicity and Structure of Ligand .....	28
2.9.	IR Spectroscopy .....	29
2.10.	NMR Spectroscopy.....	31
<b>3.</b>	<b>THE AIM OF THE WORK .....</b>	<b>32</b>
<b>4.</b>	<b>EXPERIMENTAL .....</b>	<b>33</b>
4.1.	General Procedures .....	33
4.2.	Experiments .....	35
4.2.1.	Synthesis of $\beta$ -enaminones .....	35
4.2.1.1	Synthesis of 3,3'-(2,2'-(ethane-1,2-diylbis(azanediyl))bis(ethane-2,1-diyl))bis(azanediyl)bis(5,5-dimethylcyclohex-2-enone) (L1).....	35
4.2.1.2.	Synthesis of 3,3'-(cyclohexane-1,3-diylbis(methylene))bis(azane diyl)bis(5,5dimethyl cyclohex-2-enone) (L2).....	36
4.2.1.3.	Synthesis of 3,3'-(1,3-phenylenebis(methylene))bis(azanediyl)bis(5,5-dimethyl cyclo hex-2-enone) (L3).....	37
4.2.1.4	Synthesis of 5,5-dimethyl-3-(4-(phenylamino)phenylamino)cyclo Hex-2-enone (L4).....	38
4.2.1.5.	Synthesis of 3-(4-(phenylamino)phenylamino)cyclohex-2-enone (L5).....	39
4.2.2.	Synthesis of Metal Complexes .....	40
4.2.2.1	Procedure 1: (in-situ method) .....	41
4.2.2.2.	Procedure 2: .....	41
<b>5.</b>	<b>EXPERIMENTAL RESULTS AND DISCUSSION .....</b>	<b>48</b>
5.1.	Compound 3,3'-(2,2'-(ethane-1,2-diylbis(azanediyl))bis(ethane-2,1-diyl))bis(azanediyl)bis(5,5-dimethylcyclohex-2-enone) (L1).....	48
5.2.	Compound 3,3'-(cyclohexane-1,3-diylbis(methylene))bis(azanediyl)bis(5,5dimethylcyclohex-2-enone) (L2).....	54

5.3.	Compound 3,3'-(1,3-phenylenebis(methylene))bis(azanediyl)bis (5,5- dimethyl cyclohex-2-enone) (L3).....	60
5.4.	Compound 5,5-dimethyl-3-(4-(phenylamino)phenylamino)cyclohex- 2-enone (L4).....	66
5.5	Compound 3-(4-(phenylamino)phenylamino)cyclohex-2-enone (L5)...	71
5.6	$\beta$ -enaminone- Metal Complexes .....	80
5.6.1	L1-Nickel Complexes.....	80
5.6.2.	L2-Cobalt Complexes .....	85
5.6.3.	L3-Copper Complexes.....	90
5.6.4.	L1-Copper Complexes.....	94
5.6.5.	L1-Cobalt Complexes.....	98
5.6.6.	L3-Cobalt Complexes .....	102
5.6.7.	L3-Nickel Complexes.....	105
5.6.8.	L2-Copper Complexes .....	108
5.6.9.	L2-Nickel Complexes.....	110
6.	<b>CONCLUSIONS</b> .....	113
	<b>REFERENCES</b> .....	116
	<b>CURRICULUM VITAE</b> .....	124

## FIGURES

	<b>Page</b>
<b>Figure 1.</b>	Tautomeric forms of a Schiff base..... 9
<b>Figure 2.</b>	The E and Z forms of $\beta$ -enaminone..... 11
<b>Figure 3.</b>	The three rotational modes of H <sub>2</sub> O in the solide state..... 26
<b>Figure 4.</b>	Infrared spectra of metal hexamine complexes..... 30
<b>Figure 5.</b>	Colors of Ligand L1 and its complexes..... 42
<b>Figure 6.</b>	Colors of Ligand L2 and its complexes..... 42
<b>Figure 7.</b>	Colors of Ligand L3 and its complexes..... 42
<b>Figure 8.</b>	The IR spectrum of 3,3'-(2,2'-(ethane-1,2-diylbis(azanediy))bis(ethane-2,1-diyl))bis(azanediy))bis(5,5-dimethylcyclohex-2-enone) (L1)..... 48
<b>Figure 9.</b>	The <sup>1</sup> H-NMR spectrum of 3,3'-(2,2'-(ethane-1,2-diylbis(azanediy))bis(ethane-2,1-diyl))bis(azanediy))bis(5,5-dimethylcyclohex-2-enone) (L1)..... 49
<b>Figure 10.</b>	The APT spectrum 3,3'-(2,2'-(ethane-1,2-diylbis(azanediy))bis(ethane-2,1-diyl))bis(azanediy))bis(5,5-dimethylcyclohex-2-enone)(L1)..... 50
<b>Figure 11.</b>	The UV spectrum of 3,3'-(2,2'-(ethane-1,2-diylbis(azanediy))bis(ethane-2,1-diyl))bis(azanediy))bis(5,5-dimethylcyclohex-2-enone)(L1)..... 51
<b>Figure 12.</b>	The LC-MS spectrum of 3,3'-(2,2'-(ethane-1,2-diylbis(azanediy))bis(ethane-2,1-diyl))bis(azanediy))bis(5,5-dimethylcyclohex-2-enone)(L1)..... 52
<b>Figure 13.</b>	The COSY spectrum of 3,3'-(2,2'-(ethane-1,2-diylbis(azanediy))bis(ethane-2,1-diyl))bis(azanediy))bis(5,5-dimethylcyclohex-2-enone)(L1)..... 53
<b>Figure 14.</b>	The IR spectrum of 3,3'-(cyclohexane-1,3-diylbis(methylene))bis(azanediy)) bis(5,5dimethylcyclohex-2-enone) (L2)..... 54
<b>Figure 15.</b>	The <sup>1</sup> H-NMR spectrum of 3,3'-(cyclohexane-1,3-diyl bis(methylene)) bis(azanediy)) bis(5,5dimethylcyclohex-2-enone) L2..... 55

<b>Figure 16.</b>	The APT spectrum of 3,3'-(cyclohexane-1,3-diyl bis(methylene))bis (azanediy) bis(5,5dimethylcyclohex-2-enone) (L2).....	56
<b>Figure 17.</b>	The UV spectrum of 3,3'-(cyclohexane-1,3-diyl bis(methylene))bis(azanediy) bis(5,5dimethylcyclohex-2-enone)(L2).....	57
<b>Figure 18.</b>	The LC-MS spectrum of 3,3'-(cyclohexane-1,3-diyl bis(methylene))bis(azanediy) bis(5,5dimethylcyclohex-2-enone)(L2).....	58
<b>Figure 19.</b>	The COSY spectrum of 3,3'-(cyclohexane-1,3-diyl bis(methylene))bis (azanediy)bis(5,5dimethylcyclohex-2-enone) (L2).....	59
<b>Figure 20.</b>	The IR spectrum of 3,3'-(1,3-phenylenebis(methylene))bis (azanediy) bis(5,5-dimethylcyclohex-2-enone) (L3).....	60
<b>Figure 21.</b>	The <sup>1</sup> H-NMR spectrum of 3,3'-(1,3-phenylenebis(methylene)) bis(azanediy)bis(5,5-dimethylcyclohex-2-enone) L3.....	61
<b>Figure 22.</b>	The APT spectrum of 3,3'-(1,3-phenylenebis(methylene)) bis(azanediy)bis(5,5-dimethylcyclohex-2-enone) (L3).....	62
<b>Figure 23.</b>	The UV spectrum of 3,3'-(1,3-phenylenebis(methylene)) bis(azanediy)bis(5,5-dimethylcyclohex-2-enone) (L3).....	63
<b>Figure 24.</b>	The LC-MS spectrum of 3,3'-(1,3-phenylenebis(methylene)) bis(azanediy)bis(5,5-dimethylcyclohex-2-enone) (L3).....	64
<b>Figure 25.</b>	The COSY spectrum of 3,3'-(1,3-phenylenebis(methylene)) bis (azanediy) bis(5,5-dimethylcyclohex-2-enone) (L3) .....	65
<b>Figure 26.</b>	The IR spectrum of 5,5-dimethyl-3-(4-(phenylamino) phenylamino) cyclohex-2-enone (L4).....	66
<b>Figure 27.</b>	The <sup>1</sup> H-NMR spectrum of 5,5-dimethyl-3-4-(phenylamino) phenylamino) cyclohex-2-enone (L4).....	67
<b>Figure 28.</b>	The APT spectrum of 5,5-dimethyl-3-(4-(phenylamino) phenylamino) cyclohex-2-enone (L4).....	68
<b>Figure 29.</b>	The UV spectrum of 5,5-dimethyl-3-(4-(phenylamino) phenylamino) cyclohex-2-enone (L4).....	69
<b>Figure 30.</b>	The COSY spectrum of 5,5-dimethyl-3-(4-(phenylamino) phenylamino) cyclohex-2-enone (L4).....	70

<b>Figure 31.</b>	The IR spectrum of 3-(4-(phenylamino)phenylamino) cyclohex-2-enone (L5).....	71
<b>Figure 32.</b>	The <sup>1</sup> H-NMR spectrum of 3-(4-(phenylamino)phenylamino) cyclohex-2-enone (L5).....	72
<b>Figure 33.</b>	The APT spectrum of 3-(4-(phenylamino)phenylamino) cyclohex-2-enone (L5).....	73
<b>Figure 34.</b>	The UV spectrum of 3-(4-(phenylamino)phenylamino) cyclohex-2-enone (L5).....	74
<b>Figure 35.</b>	The COSY spectrum of 3-(4-(phenylamino)phenylamino) cyclohex-2-enone (L5).....	75
<b>Figure 36.</b>	Molecular structure of 3-(4-(phenylamino)phenylamino) cyclohex-2-enone, showing 50% probability displacement ellipsoids.....	75
<b>Figure 37.</b>	Packing diagram showing molecular orientation and hydrogen bonded chains of Ligand L5.....	79
<b>Figure 38.</b>	Possible structure of L1-Nickel complex.....	82
<b>Figure 39.</b>	UV-VIS Spectrum of Complex 3.....	82
<b>Figure 40.</b>	IR Spectrum of Complex 3.....	83
<b>Figure 41.</b>	DTA-TGA Thermogram of Complex 3 .....	83
<b>Figure 42.</b>	UV-VIS Spectrum of Complex 6.....	84
<b>Figure 43.</b>	IR Spectrum of Complex 6.....	84
<b>Figure 44.</b>	DTA-TGA Thermogram of Complex 6 .....	85
<b>Figure 45.</b>	Possible structure of L2-Cobalt complex.....	86
<b>Figure 46.</b>	UV-VIS Spectrum of Complex 8.....	87
<b>Figure 47.</b>	IR Spectrum of Complex 8.....	87
<b>Figure 48.</b>	DTA-TGA Thermogram of Complex 8.....	88
<b>Figure 49.</b>	UV-VIS Spectrum of Complex 11.....	88
<b>Figure 50.</b>	IR Spectrum of Complex 11.....	89
<b>Figure 51.</b>	DTA-TGA Thermogram of Complex 11.....	89
<b>Figure 52.</b>	Possible structure of L3-Copper complex.....	90
<b>Figure 53.</b>	UV-VIS Spectrum of Complex 13 .....	91
<b>Figure 54.</b>	IR Spectrum of Complex 13.....	91
<b>Figure 55.</b>	DTA-TGA Thermogram of Complex 13.....	92
<b>Figure 56.</b>	UV-VIS Spectrum of Complex 16.....	92

<b>Figure 57.</b>	IR Spectrum of Complex 16.....	93
<b>Figure 58.</b>	DTA-TGA Thermogram of Complex 16.....	93
<b>Figure 59.</b>	Possible structure of Complex 1.....	94
<b>Figure 60.</b>	Possible structure of Complex 4.....	94
<b>Figure 61.</b>	UV-VIS Spectrum of Complex 1.....	95
<b>Figure 62.</b>	IR Spectrum of Complex 1.....	95
<b>Figure 63.</b>	DTA-TGA Thermogram of Complex 1.....	96
<b>Figure 64.</b>	UV-VIS Spectrum of Complex 4.....	96
<b>Figure 65.</b>	IR Spectrum of Complex 4.....	97
<b>Figure 66.</b>	DTA-TGA Thermogram of Complex 4.....	97
<b>Figure 67.</b>	Possible structure of Complex 2.....	98
<b>Figure 68.</b>	Possible structure of Complex 5.....	98
<b>Figure 69.</b>	UV-VIS Spectrum of Complex 2.....	99
<b>Figure 70.</b>	IR Spectrum of Complex 2.....	99
<b>Figure 71.</b>	DTA-TGA Thermogram of Complex 2.....	100
<b>Figure 72.</b>	UV-VIS Spectrum of Complex 5.....	100
<b>Figure 73.</b>	IR Spectrum of Complex 5.....	101
<b>Figure 74.</b>	DTA-TGA Thermogram of Complex 5.....	101
<b>Figure 75.</b>	Possible structure of L3-Cobalt complex .....	102
<b>Figure 76.</b>	UV-VIS Spectrum of Complex 14.....	102
<b>Figure 77.</b>	IR Spectrum of Complex 14.....	103
<b>Figure 78.</b>	DTA-TGA Thermogram of Complex 14.....	103
<b>Figure 79.</b>	UV-VIS Spectrum of Complex 17.....	104
<b>Figure 80.</b>	IR Spectrum of Complex 17.....	104
<b>Figure 81.</b>	Possible structure of L3-Nickel complex.....	105
<b>Figure 82.</b>	UV-VIS Spectrum of Complex 15.....	105
<b>Figure 83.</b>	IR Spectrum of Complex 15 .....	106
<b>Figure 84.</b>	UV-VIS Spectrum of Complex 18.....	106
<b>Figure 85.</b>	IR Spectrum of Complex 18.....	107
<b>Figure 86.</b>	DTA-TGA Thermogram of Complex 18.....	107
<b>Figure 87.</b>	UV-VIS Spectrum of Complex 7.....	108
<b>Figure 88.</b>	IR Spectrum of Complex 7.....	108
<b>Figure 89.</b>	UV-VIS Spectrum of Complex 10.....	109
<b>Figure 90.</b>	IR Spectrum of Complex 10 .....	109

<b>Figure 91.</b>	UV-VIS Spectrum of Complex 9.....	110
<b>Figure 92.</b>	IR Spectrum of Complex 9 .....	111
<b>Figure 93.</b>	UV-VIS Spectrum of Complex 12.....	111
<b>Figure 94.</b>	IR Spectrum of Complex 12.....	112

## TABLES

	<b>Page</b>
<b>Table 1.</b>	Electronic Spectral Data of Complexes of Cobalt(II) ..... 18
<b>Table 2.</b>	Electronic Spectral Data of Some Complexes of Ni(II). ..... 20
<b>Table 3.</b>	Classification of metals according to acceptor properties..... 28
<b>Table 4.</b>	Structures of the starting compounds..... 32
<b>Table 5.</b>	The experimental results of 3,3'-(2,2'-(ethane-1,2-diyl bis(azanediyl))bis(ethane-2,1-diyl))bis(azanediyl)bis(5,5-di methyl cyclohex-2-enone) (L1) and its metal complexes ..... 43
<b>Table 6.</b>	The experimental results of 3,3'-(cyclohexane-1,3-diyl bis (methylene))bis (azanediyl)bis(5,5dimethylcyclohex-2- enone) (L2) and its metal complexes ..... 44
<b>Table 7.</b>	The experimental results of 3,3'-(1,3-phenylenebis(methylene))bis (azanediyl) bis (5,5-dimethylcyclohex-2-enone) (L3) and its metal complexes..... 45
<b>Table 8.</b>	Characteristic IR bands of the Ligands and the Complexes (cm <sup>-1</sup> )..... 46
<b>Table 9.</b>	Solubilities of All New Compounds..... 47
<b>Table 10.</b>	L1 COSY Hydrogen-interaction data..... 52
<b>Table 11.</b>	L3 COSY Hydrogen-interaction data..... 58
<b>Table 12.</b>	L3 COSY Hydrogen-interaction data..... 64
<b>Table 13.</b>	L4 COSY Hydrogen-interaction data .....70
<b>Table 14.</b>	L5 COSY Hydrogen-interaction data..... 74
<b>Table 15.</b>	Crystal structural data and details of the structure determination of 3-(4- (phenylamino) phenylamino)cyclohex-2-enone..... 76
<b>Table 16.</b>	Some geometrical parameters of 3-(4-(phenylamino) phenylamino) cyclohex-2-enone..... 77
<b>Table 17.</b>	Hydrogen bonding geometry (Å, °) for 3-(4-(phenylamino) phenylamino) cyclohex-2-enone..... 79



## SCHEMES

	<b>Page</b>
<b>Scheme 1.</b> Formation of a Schiff base .....	4
<b>Scheme 2.</b> Intramolecular H-bonding of a Schiff base.....	10
<b>Scheme 3.</b> Intermolecular H-bonding of a Schiff base .....	10
<b>Scheme 4.</b> Keto-Enol Forms of Acetylacetone .....	23
<b>Scheme 5.</b> Synthesis of 3,3'-2,2'-(ethane-1,2-diylbis(azanediy))bis (ethane-2,1-diyl))bis(azanediy))bis (5,5-dimethylcyclo hex-2-enone) (L1).....	35
<b>Scheme 6.</b> Synthesis of 3,3'-(cyclohexane-1,3-diylbis(methylene)) bis(azane diyl))bis(5,5dimethyl cyclohex-2-enone) (L2).....	36
<b>Scheme 7.</b> Synthesis of 3,3'-(1,3-phenylenebis(methylene))bis (azanediy) bis(5,5-dimethyl cyclo hex-2-enone) (L3) .....	37
<b>Scheme 8.</b> Synthesis of 5,5-dimethyl-3-(4-(phenylamino)phenylamino) cyclohex- 2-enone (L4) .....	38
<b>Scheme 9.</b> Synthesis of 3-(4-(phenylamino)phenylamino) cyclohex-2-enone (L5) .....	39

## ABBREVIATIONS

br	: Broad
d	: Doublet
FT-IR	: Fourier Transform Infrared
m	: Multiplet
NMR	: Nuclear magnetic resonance
TGA	: Thermal gravimetric analysis
q	: Quartet
s	: Singlet
t	: Triplet
DMSO	: Dimethyl sulfoxide
TLC	: Thin layer chromatography
UV	: Ultraviolet

## 1. INTRODUCTION

Schiff bases belong to a widely used group of organic intermediates important for the production of chemical specialties, e.g. pharmaceuticals, or rubber additives and as amino protective groups in organic synthesis. The biological importance of Schiff bases formed between amino acids and pyridoxal stimulated intensive studies in this area. Schiff base complexes are also noted for their significant antimicrobial activities. A large number of Schiff base compounds are often used as ligands in coordination chemistry for their metal binding ability. Schiff bases also have uses as liquid crystals, and in analytical, medicinal and polymer chemistry. A basic reaction synthesis involves an amine and an aldehyde or a ketone.

It is well known in the literature that reactions of  $\beta$ -diketones with 1,2-diamines generally yield symmetrical 2:1 tetradentate Schiff bases whatever their proportion. However, relatively few studies on tridentate 1:1 condensation products have been reported. These compounds, synthesized by a single condensation reaction of a carbonyl function of a  $\beta$ -diketone with only one amine group of an aliphatic or aromatic diamine, are referred to as "half units" or "hemi-Schiff bases" and in solution they can exist as a tautomeric mixture of the keto-amine (enaminone) and keto-imine (iminone) forms.

Alkaline, alkaline earth and transition-metal ion recognition with particular metal ion binding applications are of fundamental importance to broad areas of inorganic, coordination and biochemistry. An important number of the ligands that have been reported to date are Schiff bases or  $\beta$ -enaminones.

$\beta$ -enaminone complexes have been amongst the most widely studied coordination compounds in the past few years, in the development of catalysis and enzymatic reactions, molecular architectures and materials chemistry and they are becoming increasingly important as biochemical, analytical and antimicrobial reagents.

These complexes, exhibiting versatile magnetic behaviors such as light switchable magnets and single molecule magnets have attracted special attention. The

molecule based magnetic materials consisting of d-transition metal ions have been well developed, and the magnetochemistry of d-f transition metal complexes will be one of the future targets in this field. In fact, the recent investigations of the magnetic properties of heteropolymetallic compounds have made important contributions to the development of molecular ferromagnetism. Magnetic studies of d-transition metal polynuclear complexes have shown great progress from experimental and theoretical contributions.

Since the chemistry of metal complexes of Schiff bases has a wide variety of applications in most fields, their synthesis has a great importance. In this thesis five new  $\beta$ -enaminones were synthesized and they were complexed with metals.

## 2. GENERAL INFORMATION

### 2.1 Synthesis of Schiff Bases, $\beta$ -Enaminone Formation

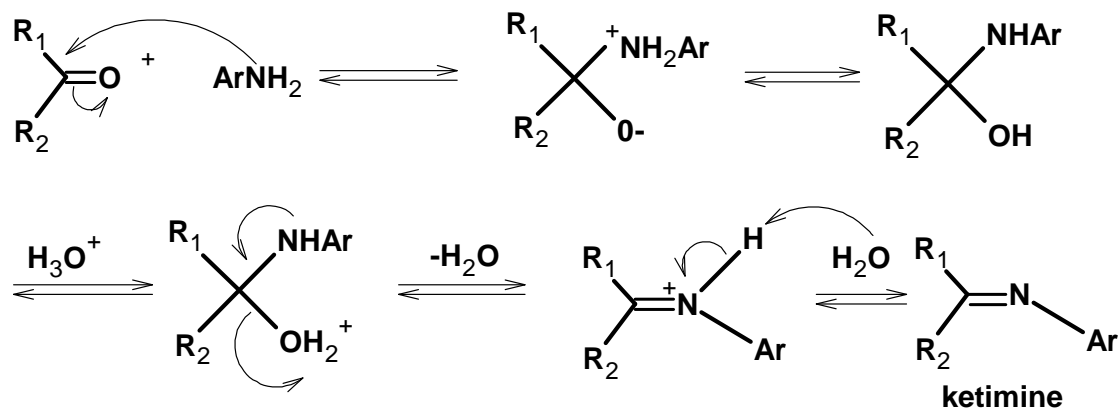
Schiff bases, imines and azomethines are amongst the various names commonly used for carbon-nitrogen double bond. It is well known in the literature that reactions of  $\beta$ -diketones with 1,2-diamines generally yield symmetrical 2:1 tetradentate Schiff bases whatever their proportion. However, relatively few studies on tridentate 1:1 condensation products have been reported. These compounds, synthesized by a single condensation reaction of a carbonyl function of a  $\beta$ -diketones with only one amine group of an aliphatic or aromatic diamine, are referred to as "half units" or "hemi-Schiff bases" and in solution they can exist as a tautomeric mixture of the keto-amine (enaminone) and keto-imine (iminone) forms (Gallardo et al., 2007)

As the polarity of carbon-nitrogen double bond is comparatively much less than carbonyl function, therefore the reactivity of these compounds have also been investigated in comparison to carbon-carbon double bonds (Sandhu and Sain, 1987).

The condensations of carbonyl compounds with amines have been broadly used reactions since they were discovered by Schiff in 1864 and have been implement in numerous processes, such as the synthesis of Salen type ligands for metal ion coordination and the synthesis of macrocycles of diverse structures often via reductive amination for which imine formation serves as an intermediate step. Mostly these reactions have been carried out in different organic solvents in order to shift reversible imine formation towards the condensation product. The creation of libraries of constitutionally dynamic combinatorial chemistry, in addition to organic solvents, aqueous organic mixtures and aqueous solutions have been employed as reaction media (Alcantar, et al., 2005).

Primary amines have an unshared electron pair on the nitrogen atom and act as nitrogen nucleophiles toward the carbonyl carbon atom. The first product formed is a dipolar ion. The positive nitrogen loses a proton and the negative oxygen gains a

proton, thus forming a tetrahedral addition product. The elimination of water then gives the observed Schiff base product (Dorris, 1999).



Scheme 1. Formation of a Schiff base

The reaction is reversible ending in a equilibrium composition dependent on reaction conditions. Similarly, reactions of amines with ketones provide Schiff bases of a ketimine type (Macho, et al., 2004). Conventionally Schiff bases have been prepared by refluxing mixtures of the amine and the carbonyl compound in an organic solvent, for example, ethanol or methanol, but variations are known, much as treatment of the same mixture at room temperature, refluxing the mixture in heptane in the presence of acetic acid or azeotropic mixture with benzene in a Dean-Stark apparatus in the presence of acid (Vazzana, et al., 2004). In general, ketones react more slowly than aldehydes and higher temperatures and longer reaction times are often required as a result. In addition, the equilibrium must often be shifted, usually by removal of the water, either azeotropically by distillation or with suitable drying agents.

## 2.2. Synthetic Importance of Schiff Bases

Schiff bases have a large number of synthetic uses in organic chemistry, some of which are given as below:

Acylation of Schiff bases (Layer, 1963; Harada, 1970; Ivanov, et al., 2007) by acid anhydrides, acid chlorides and acyl cyanides is initiated by attack at the nitrogen atom and leads to net addition of the acylating agent to the carbon - nitrogen double bond. Reactions of this type have been put to good use in natural product syntheses.

Also the base-catalyzed condensation of acetyl chlorides (bearing an electron withdrawing group and at least one hydrogen atom at the  $\alpha$ -position) with *N*-aryldimines occurs by initial acylation at the nitrogen atom and leads to  $\beta$ -lactams of interest in penicillin chemistry.

The reaction of 4-substituted benzenediazonium tetrafluoroborates with 3-amino-1-phenylbut-2-en-1-one, 4-amino-4-phenylbut-3-en-2-one and their *N*-aryl derivatives has been used to prepare the azo coupling products from enaminone (Simunek, et al., 2005).

Iminium salt (Blaha and Cervinka, 1966). ( $R_2C = N^+R_2$ ) at the other extremes are very rapidly hydrolyzed by water and have to be prepared under rigorously anhydrous conditions. The facility of iminium salt hydrolysis has been put to use in a synthesis of secondary amines from primary amines which involves conversion into the aldimine ( $R'CH = NR_2$ ) and then by alkylation into the iminium salt [ $R'CH = N^+R''(R''')X^-$ ] followed by hydrolysis to give the secondary amines ( $R'NHR''$ ). Because of the involvement of Schiff base hydrolysis in a number of enzyme-mediated processes, the detailed mechanism of the hydrolytic cleavage of carbon-nitrogen double bonds has been the subject of close scrutiny both under *in vivo* and under *in vitro* conditions (Cockenill and Harrison, 1977; Kayser and Pollack, 1977). Imine hydrolysis is also a key step in the Sommelet, Stephen, Sonn-Muller and Gattermann aldehyde syntheses (Angyal, 1954; Olah and Kuhn, 1964).

Enaminones were readily converted into an unexpected spiran by formaldehyde and dilute hydrochloric acid at room temperature. The suggested mechanism involved an internal Mannich reaction (Chaaban, et al., 1978).

Enaminones have attracted much interest recently not only because they can be used as good chelating ligands for transition metals but also because the anions generated from them offer potential isoelectronic alternatives to cyclopentadienyl-

based anions and therefore their transition metal complexes can act as possible alternatives for olefin polymerization catalysts (Shi, et al.,2004).

Schiff bases also have uses as liquid crystals, and in analytical, medicinal and polymer chemistry. A basic reaction synthesis involves an aromatic amine and an aldehyde or a ketone (Macho, et al., 2004; Jarrahpour, and Khalili, 2006).

### **2.3. Chemistry and Biological Importance**

A comprehensive review (Holm, et al., 1966) covers much of the Schiff base chemistry known up to 1966 and it has been followed by others (Calligaris, et al., 1972; Casellato and Vigato, 1979; Iqbal, et al., 1993). Structure and mechanism of the formation of the Schiff base complexes and stereochemistry of four-coordinate chelate compounds from Schiff bases and their analogues have been discussed in a review (Panova, et al., 1980). The configuration of the chelate group in the four-coordinate complexes may be square-planer, tetrahedral, distorted tetrahedral or distorted pyramidal with the metal atom at the apex. The configuration depends primarily on the nature of the metal atom and also on the magnitude and symmetry of the ligand field.

Alkyl 3-(dimethylamino)propenoates and related enaminones have been recently used as building blocks for the preparation of dehydro-alanine derivatives and many heterocyclic systems such as fused pyridines, pyrimidines, pyranones, and other compounds, including some natural products (e.g., indole alkaloids) and their synthetic analogues (Wagger, et al., 2006).

Schiff base complexes can be classified as mononuclear, binuclear and polynuclear, based on the number of metal atoms present, and as monodentate, bidentate and polydentate. The use of transition metal i.e. Cu (II), Ni (II) and Zn (II) complexes of tridentate Schiff bases derived from salicylaldehydes and N-(pyridyl)-2-hydroxyl-3-methoxy-5-aminobenzylamine as chelating agents to form binuclear centers has been well documented . These complexes have been found to be active against *Bacillus subtilis* IMG 22 (bacteria), *Micrococcus luteus* LA 2971 (bacteria), *Saccharomyces cerevisiae* WET 136 (yeast) and *Candida albicans*



CCM 314 (yeast). Some of them are capable of reversibly binding molecular oxygen, being consequently employed as models in the study of oxygen's reversible fixation such its natural carries (hemoglobins, hemocianines, etc.). Other complexes - due to their capacity of acting as catalyst- may be employed as models in the study of oxygenases, peroxidases and mono- and di-oxygenases (Niederhoffer, et al., 1984;Shikama, 1998).

Sargeson and Searle first studied cobalt complexes containing the tetradentate ligand triethylenetetramine nearly three decades ago. Triethylenetetramine can be considered the prototype linear tetradentate ligand, and in the years that followed this initial work many complexes were isolated that contained tetradentate derivatives of triethylenetetramine (McClure and Holcombe, 2004).

A large of reports are available on the chemistry and the biocidal activities of transition metal complexes containing O,N and S,N donor atoms. The transition metal complexes having oxygen and nitrogen donor Schiff bases possess unusual configuration, structural lability and a resensitive to molecular environment. The environment around the metal centre "as coordination geometry, number of coordinated ligands and their donor groups" is the key factor for metalloproteins to carry out specific physiological functions (Golcu, et al., 2005).

$\beta'$ -Hydroxy- $\beta$ -enaminones containing a 4-hydroxy-2-pyrone ring are of interest as synthetic intermediates for the preparation of large number of heterocyclic compounds. Recent development in the design of potent HIV protease inhibitors, that led to the discovery of a novel class of inhibitors containing 2-pyrone structure, stimulated investigation in the field of 2-pyrone derivatives and their metal complexes. Also, such complexes have been studied as models for beter understanding of interaction between metal ions and flavonoides and in the attempts to explain the role of metal centres in some catalytic processes (Cindric, et al., 2004).

Complexes of Ni (II), Co (II) and Cu (II) with Schiff base ligands derived from  $\beta$ -diketones (acetylacetone) and p-anisidine have been reported (Raman, et al., 2003). Spectral and magnetic studies on these complexes indicate that they are

four-coordinates with square-planar geometry. It has been found that all the complexes are antimicrobially active and show higher activity than the free ligands.

Ni (II), Cu (II), Pd (II) and Pt (II) complexes of thiophene-2-carboxaldehyde Schiff bases of S-methyl- and S-benzyl dithiocarbazate have also been reported. Magnetic and spectroscopic evidences support a square-planar structure for these complexes.

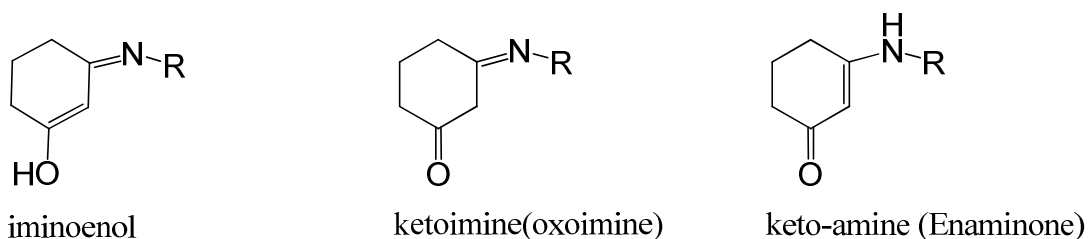
Binuclear copper systems are implicated in a wide variety of biochemical processes, especially in transport and multi-electron redox reactions of molecular oxygen. A number of mononuclear planar Cu (II) complexes have been found to exist as dimers in crystals and in solutions. A study of ferro- and antiferromagnetic coupling in Cu(II) complexes with tridentate Schiff bases may lead to a better understanding of the phenomenon in magnetically condensed complexes (Hatfield and Inman, 1969). Two tetrameric Cu (II) complexes with Schiff bases derived from acetylacetone and isomeric  $\alpha$ -aminoalcohol have been reported. Metal complexes have also been reported with other ligands mixed with Schiff bases (Turner, et al., 1999).

The chemistry of Schiff base complexes has developed rapidly in the last 40 years solving problems related to stereochemistry and fertilizing related fields in coordination chemistry. Stereochemistry and electronic factors largely govern the reactivity and stability of chelate compounds. The stereochemistry and the electronic structure of chelates determine many properties, such as their redox properties and reactivity and ability to form adducts. These properties are important for understanding many catalytic processes and phenomena occurring in living organisms. Schiff base complexes of Cu (II) are believed to be key intermediates of pyridoxal dependant enzymes. Consequently, a number of studies of the Schiff bases derived from amino acids have been reported using pyridoxal as the cocondensent (Bukhari, 2002).

#### **2.4. Tautomerism in Schiff Bases, $\beta$ -enaminone Formation**

Schiff bases can exist as three tautomeric forms; A ketoamine, an iminoenol and ketoimine form, however the enaminone form is favored in general because of

increased resonance between  $sp^3$ -nitrogen and the carbonyl group (Gilli, et al., 2000; Katritzky, et al., 1997; Rodriguez, and Hamilton, 2006; Zhuo, 1998; Zhuo, 1997; Sinha, et al., 2007; Scott, et al., 1995). (Figure 1).



R: Alkyl or aromatic group

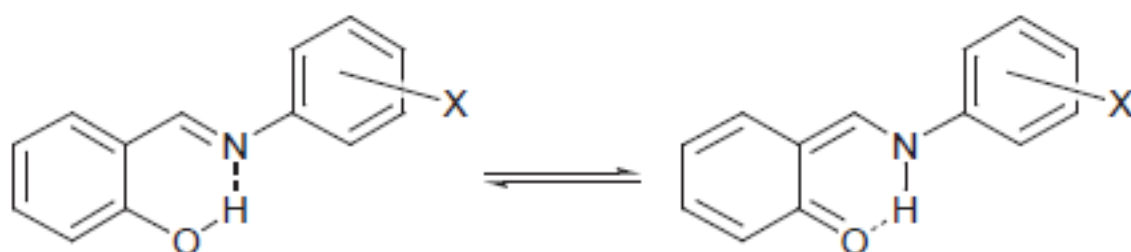
Figure 1. Tautomeric forms of a Schiff base.

N-Substituted aminoethylene derivatives having carbonyl function(s) in the  $\beta$ -position- known as enaminones –have been extensively investigated because of their interesting structural characteristics, such as distinct geometric forms and tautomerism (Eberlin et al., 1990) They can also be viewed as push-pull ethylenes, a class of reactive and versatile compounds presenting an unusually low rotational barrier around the C=C double bond with an absorption in the near ultraviolet and visible regions due to the delocalization of  $\pi$ -electrons (Wennerbeck, 1973). Therefore, such compounds have found widespread applications in pharmaceutical and medicinal chemistry, e.g. as prodrugs of primary amines or intermediates in the preparation of antiulcer and antibacterial drugs (Naringrekar and Stella, 1990) as well as in the chemical industry (organic dyes and agrochemicals).

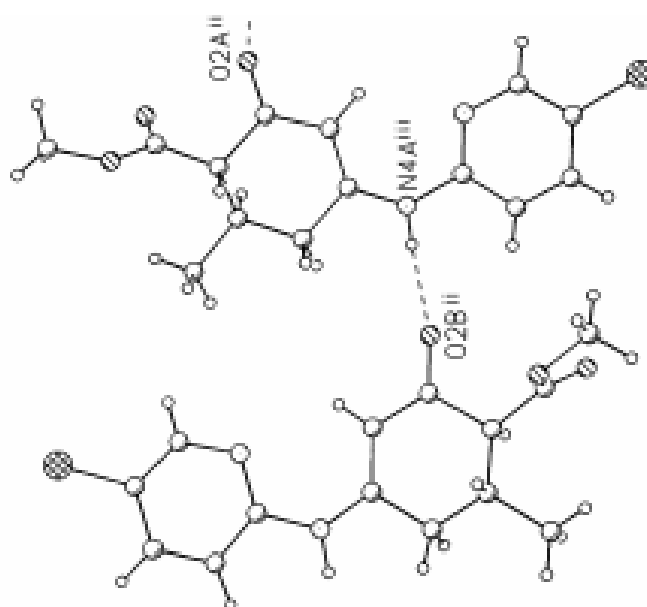
When, a 1,3-diketone is used in Schiff base synthesis a more stable  $\beta$ -enaminone derivative, is formed by means of isomerization. A keto-enol tautomerism ( $A \rightleftharpoons B$ ) is resulted when only one carbonyl group of 1,3-diketone forms the corresponding Schiff base because of added conjugation which covers the three carbons of hexane ring. The keto-enol form is stabilized both by the formation of intermolecular hydrogen bonding and resonance (Junior et al., 2007; Schiøtt et. al., 1998).

Schiff base ligands are of interest mainly due to the existence of (O–H...N) and (O...H–N) type hydrogen bonds and tautomerism between enol–imine and keto–amine forms (Schilf, et. al., 2004) Two types of intramolecular hydrogen bonds, either N–H...O (keto-amine form) or N...O–H (enol-imine form) can exist in enamminones (Elmalı, et al., 1999; Yıldız, et al., 1998; Nazır, et al., 2000; Ünver, 2001; Yıldız, 2004).  $\beta$ -Enaminones, derived from cyclic 1,3-dicarbonyl compounds are significantly more stable than acyclic analogs (Scott, et al., 1995). (Scheme 2,3).

Scheme 2: Intramolecular H-bonding of a Schiff base (Ligtenberg, et al., 1999)



Scheme 3: Intermolecular H-bonding of a Schiff base (Kubickia, et al., 2000)



E and Z isomers are observed for  $\beta$ -enaminones. The E and Z forms can easily be identified by means of  $^1\text{H-NMR}$  spectra. The N-H signal of the Z isomer appears at 9-13 ppm while the same signal of E isomer appears at 4-8 ppm due to strong intermolecular hydrogen bonding (Zhuo, 1997; Zhuo, 1998; Rodriguez, and Hamilton, 2006).

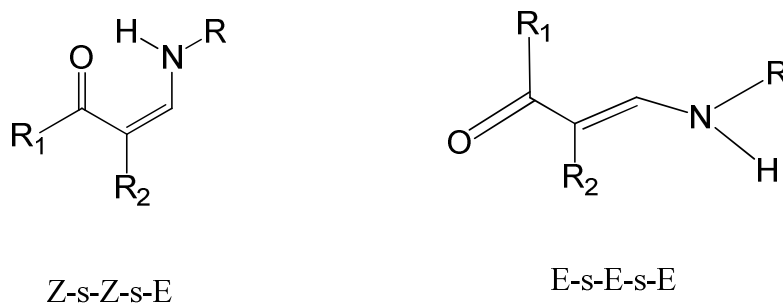


Figure 2 : The E and Z forms of  $\beta$ -enaminone

$\beta$ -enaminones are a class of enamines which are stabilized relative to enamines of monocarbonyl compounds due to intramolecular hydrogen bonding. Because of the significant reactivity of the conjugated  $\text{N-C=C-C=O}$  system,  $\beta$ -enaminones are used as important intermediates in synthetic organic chemistry (Schilf, et al., 2004; Venkov and Angelov, 2003; Michael, et al., 1999; Elassar and El-Khair, 2003; Ivanov, et al., 2007; Scott, et al., 1995) and for the preparation of a large number of heterocyclic compounds (Naringrekar, and Stella, 1990; Cindric, et al., 2004) they have a wide variety of applications in medicine, biochemistry, coordination chemistry and photonic technologies (Shi, 2005; El-hashim 2007; Fonseca, et al., 2005). Some  $\beta$ -enaminones are pharmacologically active and exhibit anticonvulsant activity (Cox, et al., 2002; Mulzac, et al., 1993; Edfiogho, et al., 2007; Ananthalakshmi, et al., 2006).

In recent years, environmentally benign synthetic methods have received considerable attention and some solvent-free protocols have been developed. Catalyzed synthesis of imines under solvent-free conditions using microwave irradiation has been reported (Kaupp, 2005).

The Schiff bases are of interest because they have long been known to show photochromism and thermochromism in the solid state. Photochromism is produced by an intermolecular proton transfer associated with a change in the  $\pi$ -electron configuration (Zhao, et al., 2001; Zgierski, and Grabowska, 2000; Hadjoudis, et al., 1987).

The intramolecular hydrogen bonds and the proton transfer equilibrium in Schiff bases determine their physical and biological properties. For this reason these phenomena have been studied by several groups using various methods (Dziembowska, 1998; Wozniak, et al., 1995; Inabe, et al., 1994; Fish, et al., 1995; Przybylski, et al., 2002). Transformations between the imine form and enamine form have been studied in several groups. (Cohen et al., 1964) studied the H-tautomerism of salicylaldehydes, while it was established by Ogawa et al., 1998.

## 2.5. Electronic Spectra

Direct evidence of orbital energy levels can be obtained from electronic spectra. The energy of the light observed as electrons are raised to higher levels is the difference in energy between the orbital energy levels. Much information about bonding and electronic structures in complexes has come from the study of electronic spectra (Greenwood and Earnshaw, 1997; Miessler, and Tarr, 1999).

The electronic spectra of the Schiff bases exhibit three main peaks: at about 270, 333 and 372 nm. The first and the second peaks are attributed to benzene  $\pi$ - $\pi^*$  and imino  $\pi$ - $\pi^*$  transitions, respectively. These bands were not significantly affected by chelation. The third band in the spectra of the ligand (372 nm) is assigned to  $n$ - $\pi^*$  transition. This band is shifted to a longer wavelength (28 nm) along with increasing in its intensity. This shift may be attributed to the donation of the lone pairs of the nitrogen atoms of the Schiff base to the metal ion ( $N \rightarrow M$ ).

Tanabe-Sugano diagrams are used in coordination chemistry to predict absorptions in the UV and visible electromagnetic spectrum of coordination compounds (Abd-Elzaher, 2001).

A Tanabe-Sugano diagram is a graph which plots the energy of different spectroscopic terms (on the y-axis) against the size of the ligand field (on the x-axis). The units used for each are the Racah Parameter B. This choice of unit means that the diagram takes account of electron-electron repulsion effects, which an Orgel diagram cannot. It is mainly used to predict the energy of any absorption bands that are predicted but not observed in the UV/visible spectra of transition metal complexes from the energies of those that can be seen, and can also be used to predict the size of the ligand field necessary to cause high-spin to low-spin transitions.

One of the characteristic features of many d-block metal complexes is their colour. The colours are due to absorption of light in the visible region of the spectrum. Studying the electronic spectra can provide details about the structure and bonding in complexes. Absorptions arise from transitions between electronic energy levels:

- Transitions between metal d-orbitals (d-d transitions)
- Transitions between metal and ligand orbitals that transfer charge from one to the other (the charge can go either way). Charge transfer bands give intense absorptions and d-d bands are much weaker. CT bands usually occur at higher energies than d-d transitions although in some spectra the d-d bands can still be masked by the CT bands.

MLCT = metal to ligand charge transfer

LMCT = ligand to metal charge transfer

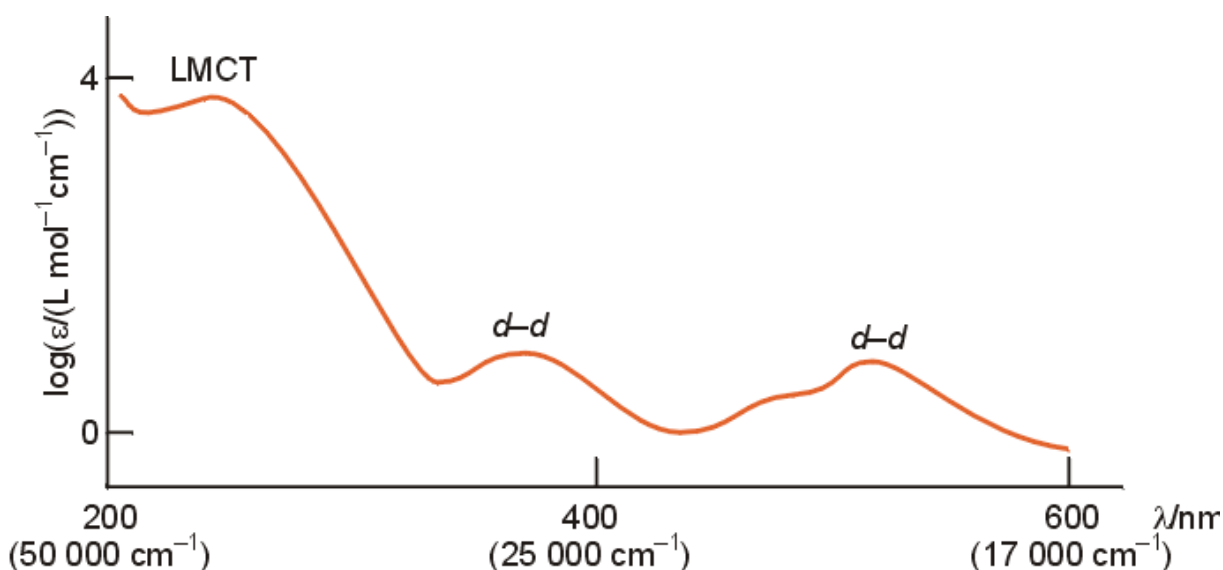
- Absorption bands in electronic spectra for d-block complexes are usually broad.
- Molecular rotations and vibrations occur much more slowly than the absorption of a photon of light.
- Thus an electronic spectrum will record a range of energies that will correspond to different vibrational and rotational states.

Complexes that possess a centre of symmetry can have that momentarily lost during molecular vibrations. The timescale of this is long enough to allow mixing of the orbitals and a transition to occur. In a molecule which is non-centrosymmetric in the first place, mixing will occur to a greater extent and a more intense transition will be observed. i.e. tetrahedral complexes are more intensely coloured than

octahedral complexes (<http://chemistry.hull.ac.uk/lectures/sja/06513%20SJA%20handout%20notes.pdf>).

### 2.5.1. Metal-metal bonds

Metal-metal bonds are seen in low oxidation state metals from the early part of the d-block. Such bonds can be within a discrete molecule/ cluster, or in solid state compounds. They are stabilised by  $\pi$ -donor ligands (e.g. halides and alkoxides). When there are no ligands bridging between the two metal centres the presence of a metal metal bond can easily be assigned. In the cases where there are bridging ligands measurement of bond lengths and magnetic properties can be used to identify metal-metal bonding (<http://chemistry.hull.ac.uk/lectures/sja/06513%20SJA%20handout%20notes.pdf>).



### 2.5.2. Electronic Spectra of Ligands and Complexes

The most significant difference in the electronic spectra of the ligand and its complex was the shift of ligand based absorptions to lower frequencies (longer wavelengths) and the appearing newer bands in the complex in longer wavelength region. In complex the longest wave length absorptions have small extinction coefficients and are assigned to metal-ligand charge transfer (MLCT) bands, higher energy absorptions immediately adjacent have higher extinction coefficients



and can be regarded as intra ligand (IL) transition bands (<http://chemistry.hull.ac.uk/lectures/sja/06513%20SJA%20handout5%20notes.pdf>).

### 2.5.3. Electronic Spectral Data and Magnetic Properties of Copper(II)

Because the  $d^9$  configuration can be thought of as an inversion of  $d^1$ , relatively simple spectra might be expected, and it is indeed true that the great majority of Cu (II) compounds are blue or green because of a single broad absorption band in the region  $11000\text{-}16000\text{ cm}^{-1}$ . However, as already noted, the  $d^9$  ion is characterized by large distortions from octahedral symmetry and the band is unsymmetrical, being the result of a number of transitions which are by no means easy to assign unambiguously. The free ion  $^2D$  ground term is expected to split in a crystal field in the same way as the  $^5D$  term of the  $d^4$  ion and a similar interpretation of the spectra is likewise expected. Unfortunately this is now more difficult because of the greater overlapping of bands which occurs in the case of Cu(II).

The T ground term of the tetrahedrally coordinated ion implies an orbital contribution to the magnetic moment, and therefore a value in excess of  $\mu_{\text{spin-only}}$  (1.73BM). but the E ground term of the octahedrally coordinated ion is also expected to yield a moment [ $\mu_e = \mu_{\text{spin-only}}^{(1-2\lambda/10Dq)}$ ] in excess of 1.73BM, because of "mixing" of the excited T term into the ground term, and the high value of  $\lambda$  ( $850\text{ cm}^{-1}$ ) makes the effect significant. In practice, moments of magnetically dilute compounds are in the range 1.9-2.2 BM, with compounds whose geometry approaches octahedral having moments at the lower end, and those with geometries approaching tetrahedral having moments at the higher end, but their measurements cannot be used diagnostically with safety unless supported by other evidence (Greenwood and Earnshaw, 1997).

The electronic spectrum of the Cu(II) complex exhibits an absorption band in the range 743 nm, attributed to  $^2E_g \rightarrow ^2T_{2g}$  transition suggesting a distorted octahedral geometry. The other bands in the range 590 and 497 nm can be assigned to the transitions:  $^2B_{1g} \rightarrow ^2B_{2g}$  and  $^2B_{1g} \rightarrow ^2E_g$  in order of increasing energy. But generally, such chelates exhibit a broad, structureless band with or without a shoulder

between 715–580 nm depending upon the strength of the field of the ligand (Sönmez, et al., 2003; Sönmez, and Şekerci, 2002).

The electronic spectra of the copper complexes exhibit bands in the region ca. 17,780–19,000  $\text{cm}^{-1}$  with a shoulder on the low energy side at 14,600–16,000  $\text{cm}^{-1}$ , and show that these complexes are distorted octahedral (Singh, et al., 2007; Raghu et al., 2002; Jubert, et al., 2002).

#### 2.5.4. Electronic Spectral Data and Magnetic Properties of High-Spin Octahedral and Tetrahedral Complexes of Cobalt(II)

Cobalt (II) is the only common  $d^7$  ion and because of its stereochemical diversity its spectra have been widely studied. In a cubic field, three spin-allowed transitions are anticipated because of the splitting of the free-ion, ground  $^4F$  term, and the accompanying  $^4P$  term. In the octahedral case the splitting is the same as for the octahedral  $d^2$  ion and the spectra can therefore be interpreted in a semi-quantitative manner using the same energy level diagram as was used for  $V^{3+}$ . In the present case the spectra usually consist of a band in the near infrared, which may be assigned as  $\nu_1 = ^4T_{2g}(F) \leftarrow ^4T_{1g}(F)$ , and another in the visible, often with a shoulder on the low energy side. Since the transition  $^4A_{2g}(F) \leftarrow ^5T_{1g}(F)$  is essentially a 2-electron transition from  $t_{2g}^5 e_g^2$  to  $t_{2g}^3 e_g^4$  it is expected to be weak, and the usual assignment is  $\nu_2$  (shoulder)  $= ^4A_{2g}(F) \leftarrow ^4T_{1g}(F)$   
 $\nu_3 = ^4T_{1g}(P) \leftarrow ^4T_{1g}(F)$ .

Indeed, some cases it is probable that  $\nu_2$  is not observed at all, but that the fine structure arises from term splitting due to spin-orbit coupling or to distortions from regular octahedral symmetry.

In tetrahedral fields the splitting of the free ion ground term is the reverse of that in octahedral fields so that, for  $d^7$  ions in tetrahedral fields  $^4A_{2g}(F)$  lies lowest but three spin allowed bands are still anticipated. In fact, the observed spectra usually consist of a broad, intense band in the visible region (responsible for the colour and often about 10 times as intense as in octahedral compounds) with a weaker

one in the infrared. The only satisfactory interpretation is to assign these, respectively, as,  $\nu_3 = {}^4T_1 (P) \leftarrow {}^4A_2(F)$  and  $\nu_2 = {}^4T_1 (F) \leftarrow {}^4A_2(F)$  in which case  $\nu_1 = {}^4T_2 (F) \leftarrow {}^4A_2(F)$  should be in the region  $3000-5000 \text{ cm}^{-1}$ .

Table 1 gives data for a number of octahedral and tetrahedral complexes, the values of  $10Dq$  and  $B$  having been derived by analysis of the spectra. It is clear from these data that the “anomalous” blue colour of octahedral  $\text{CoCl}_2$  arises because  $6\text{Cl}^-$  ions generate such a weak crystal field that the main band in its spectrum is at an unusually low energy, extending into the red region (hence giving a blue colour) rather than the green-blue region (which would give a red colour) more commonly observed for octahedral  $\text{Co(II)}$  compounds.

Magnetic properties provide a complementary means of distinguishing stereochemistry. The T ground term of the octahedral ion is expected to give rise to a temperature dependent orbital contribution to the magnetic moment whereas the A ground term of the tetrahedral ion is not. As a matter of fact, in a tetrahedral field the excited  ${}^4T_2(F)$  term is “mixed into” the ground  ${}^4A_2$  term because of spin-orbit coupling and tetrahedral complexes of  $\text{Co}^{II}$  are expected to have magnetic moments given by  $\mu_e = \mu_{\text{spin-only}}^{(1-\lambda/10Dq)}$ , where  $\lambda = -170 \text{ cm}^{-1}$  and  $\mu_{\text{spin-only}} = 3.87 \text{ BM}$ . Thus the magnetic moments of tetrahedral complexes lie in the range 4.4-4.8 BM, whereas those of octahedral complexes are around 4.8-5.2 BM at room temperature, falling off appreciably as the temperature is reduced (Greenwood and Earnshaw, 1997).

Table 1. Electronic Spectral data of Complexes of Cobalt(II)

octahedral					
complex	$\nu/\text{cm}^{-1}$	$\nu/\text{cm}^{-1}$ (weak)	$\nu/\text{cm}^{-1}$ 0(main)	$10Dq/\text{cm}^{-1}$	$B/\text{cm}^{-1}$
$[\text{Co}(\text{bipy})_3]^{2+}$	11300		22000	12670	791
$[\text{Co}(\text{NH}_3)_6]^{2+}$	9000		21100	10200	885
$[\text{Co}(\text{H}_2\text{O})_6]^{2+}$	8100	16000	19400	9200	825
$\text{CoCl}_2$	6600	13300	17250	6900	780
tetrahedral					
complex	$\nu/\text{cm}^{-1}$	$\nu/\text{cm}^{-1}$	$\nu/\text{cm}^{-1}$	$10Dq/\text{cm}^{-1}$	$B/\text{cm}^{-1}$
$[\text{Co}(\text{NCS})_4]^{2-}$		7780	16250	4550	691
$[\text{Co}(\text{N}_3)_3]^{2-}$		6750	14900	3920	658
$[\text{CoCl}_4]^{2-}$		5460	14700	3120	710
$[\text{CoI}_4]^{2-}$		4600	13250	2650	665

The solution spectra of cobalt(II) complexes exhibit absorption in the region ca. 8100–9,160( $\nu_1$ ), 12,500–15,700( $\nu_2$ ) and 18,600–20,500  $\text{cm}^{-1}$ ( $\nu_3$ ) respectively.

The spectra resemble to those of the complexes reported to be octahedral. The various bands can be assigned to:  $4T_{1g} \rightarrow 4T_{2g}(\text{F})$ ; ( $\nu_1$ ),  $4T_{1g} \rightarrow 4A_{2g}(\text{F})$ ; ( $\nu_2$ ),  $4T_{1g} \rightarrow 4T_{1g}(\text{P})$ ; ( $\nu_3$ ), respectively (Singh, et al., 2007; Raghu et al., 2002; Jubert, et al., 2002).

The electronic spectrum shows two bands at 760 and 523 nm attributed to  ${}^4T_{1g} \rightarrow {}^4A_{2g}$  ( $\nu_2$ ) and  ${}^4T_{1g}(\text{F}) \rightarrow {}^4T_{1g}(\text{P})$  ( $\nu_3$ ) transitions, respectively, in an octahedral geometry around the Co(II) ion. The bands observed at 261–357 nm and 445 nm are assigned to the  $\pi$ - $\pi^*$  transition of the azomethine group and charge-transfer bands (Sönmez, et al., 2003; Sönmez, and Şekerci, 2002).

### 2.5.5. Electronic Spectral Data and Magnetic Properties of Complexes of Nickel(II)

Nickel (II) is the only common  $d^8$  ion and its spectroscopic and magnetic properties have accordingly been extensively studied.

In a cubic field three spin-allowed transitions are expected because of the splitting of the free ion, ground  $^3F$  term and the presence of the  $^3P$  term. In an octahedral field the splitting is the same as for the octahedral  $d^3$  ion and the same energy level diagram can be used to interpret the spectra as was used for octahedral Cr(III). Spectra of octahedral Ni (II) usually do consist of three bands which are accordingly assigned as:

$$\nu_1 = {}^3T_{2g}(F) \leftarrow {}^3A_{2g}(F) = 10Dq; \quad \nu_2 = {}^3T_{1g}(F) \leftarrow {}^3A_{2g}(F); \quad \nu_3 = {}^3T_{1g}(P) \leftarrow {}^3A_{2g}(F)$$

with  $\nu_1$  giving the value of  $\Delta$ , or  $10Dq$ , directly. Quite often there is also evidence of weak spin-forbidden absorptions and, in  $[\text{Ni}(\text{H}_2\text{O})_6]^{2+}$  and  $[\text{Ni}(\text{dmsO})_6]^{2+}$ , for instance, the  $\nu_2$  absorption has a strong shoulder on it. This is ascribed to a transition to the spin singlet  $^1E_g$  which occurs when the  $^1E_g$  and  $^3T_{1g}(F)$  terms are in close proximity.

For  $d^8$  ions in tetrahedral fields the splitting of the free-ion ground term is the inverse of its splitting in an octahedral field, so that  $^3T_{1g}(F)$  lies lowest. In this case three relatively intense bands are to be expected, arising from the transitions:

$$\nu_1 = {}^3T_2(F) \leftarrow {}^3T_1(F); \quad \nu_2 = {}^3A_2(F) \leftarrow {}^3T_1(F); \quad \nu_3 = {}^3T_1(P) \leftarrow {}^3T_1(F)$$

Table 2 gives data for a number of octahedral and tetrahedral complexes.

Table 2. Electronic Spectral data of Complexes of Ni(II)

Octahedral				
complex	$\nu_1/\text{cm}^{-1}$	$\nu_2/\text{cm}^{-1}$	$\nu_3/\text{cm}^{-1}$	$10Dq/\text{cm}^{-1}$
$[\text{Ni}(\text{dmsO})_6]^{2+}$	7730	12970	24040	7730
$[\text{Ni}(\text{H}_2\text{O})_6]^{2+}$	8500	13800	25300	8500
$[\text{Ni}(\text{NH}_3)_6]^{2+}$	10750	17500	28200	10750
$[\text{Ni}(\text{en})_3]^{2+}$	11200	18350	29000	11200
$[\text{Ni}(\text{bipy})_3]^{2+}$	12650	19200		12650
tetrahedral				
complex	$\nu_1/\text{cm}^{-1}$	$\nu_2/\text{cm}^{-1}$	$\nu_3/\text{cm}^{-1}$	$10Dq/\text{cm}^{-1}$
$[\text{NiI}_4]^{2-}$		7040	14030	3820
$[\text{NiBr}_4]^{2-}$		7000	13230- 14140	3790
$[\text{NiCl}_4]^{2-}$		7549	14250- 15240	4090
$[\text{NiBr}_2(\text{OPPh}_3)_2]^{2-}$		7250	15580	3950

The T ground term of the tetrahedral ion is expected to lead to a temperature-dependent orbital contribution to the magnetic moment, whereas the A ground term of the octahedral ion is not, though “mixing” of the excited  ${}^3T_{2g}$  (F) term into the  ${}^3A_2$  (F) ground term is expected to raise its moment to:  $\mu_e = \mu_{\text{spin-only}}^{(1-\lambda/10Dq)}$  where  $\lambda = -315 \text{ cm}^{-1}$  and  $\mu_{\text{spin-only}} = 2.83 \text{ BM}$ . (This is the exact reverse of the situations found for  $\text{Co}^{\text{II}}$ . The upshot is that the magnetic moments of octahedral compounds are found to lie in the range 3.2-4.1 BM.

The electronic absorption data of the compounds, the bands in the 390–348 nm range are assigned to the  $n \rightarrow \pi^*$  transitions of the azomethine group. During the formation of the complexes, these bands are shifted to lower wavelength, suggesting that the nitrogen atom of the azomethine group is coordinated to the metal ion. The electronic spectrum of the  $\text{Cu}(\text{II})$  complex has bands in the 280–250 nm range and these bands may be due to the  $n \rightarrow \pi^*$  and  $\pi \rightarrow \pi^*$  transitions of the azomethine group.

Ni(II) complexes shows d-d transitions at 517 and 673 nm corresponding to  ${}^3A_{2g} \rightarrow {}^3T_{1g}(F)$  and  ${}^3A_{2g} \rightarrow {}^3T_{2g}(F)$ , respectively, which suggests mostly octahedral geometry (Sönmez, and Şekerci, 2002).

The solid reflectance spectra of the Ni(II) complex are consistent with the formation of an octahedral geometry with the appearance of three bands at:  $\nu_1$ : (5,860–11,070)  $\text{cm}^{-1}$ :  ${}^3A_{2g} \rightarrow {}^3T_{2g}$ ;  $\nu_2$ : (11,240–18,870)  $\text{cm}^{-1}$ :  ${}^3A_{2g} \rightarrow {}^3T_{1g}(F)$  and  $\nu_3$ : (21,830–27,470)  $\text{cm}^{-1}$ :  ${}^3A_{2g} \rightarrow {}^3T_{1g}(P)$ .

The solution spectra of Ni(II) complexes exhibit a well-discernable band with a shoulder on the low energy side. The other two bands generally observed in the region at ca. 16,570–17,240  $\text{cm}^{-1}$  ( $\nu_2$ ), and 26,860–28,000  $\text{cm}^{-1}$  ( $\nu_3$ ), are assigned to  ${}^3A_{2g} \rightarrow {}^3T_{1g}(F)$ , ( $\nu_2$ ), and  ${}^3A_{2g} \rightarrow {}^3T_{1g}(P)$  ( $\nu_3$ ), respectively (Singh, et al., 2007; Raghu et al., 2002; Jubert, et al., 2002).

## 2.6. Metal Complexes

A coordination compound or metal complex might be defined as a central atom or ion attached to a sheat of ions or molecules.

The chemistry of metals in solution is essentially the chemistry of their complexes. A metal ion in solution is coordinated to water molecules or to other ligands. The transition metal ions are fairly good Lewis acids, and their complexes are quite stable. The cations of the more electropositive metals such as the alkali metals and alkaline earth metals are weaker Lewis acids that form fewer and less stable complexes. Although they are hydrated in solution, the reaction with water is much weaker than in the case of transition metal ions.

Metal ions are almost never encountered without effective shielding from one another. In solution the shielding is provided by the solvent or some other ligand. In the solid state, cations are surrounded by anions.

In many cases the complexes found in well-ordered crystals do not persist in solution, because of solvent in competition with the ligands for metal coordination positions.

### **2.6.1. Metal Ion Control in Macrocyclic Synthesis**

One general synthetic route to macrocycles (L) has been through the application of metal template procedures; equimolar amounts of the organic precursors are reacted in the presence of a transition metal salt in alcoholic solution. Extension of the nature of the templating cation to include the alkaline earth metals and main group elements such as tin and lead was established in Belfast and in Sheffield. The compatibility between the radius of the templating cation and the 'hole' of the macrocycle contributes to the effectiveness of the synthetic pathway, and to the geometry of the product complex. If the cation radius is too large for the 'hole' then a [2+2] rather than a [1+1] condensation can occur. The nature of the donor atom is also important. If a strong interaction occurs between the metal and the donor atoms X then the terminal NH<sub>2</sub> and C=O groups of the probable intermediate can be brought into cis-alignment as required for ring closure to the [1+1] product. With weakly coordinating donors then the constraint leading to close proximity of the terminal units is raised and [2+2] product results (Fenton., 1986).

Mononuclear alkaline earth metal complexes of the [2+2] macrocycles provide interesting chemical features in their own right as well as serving, through the transmetallation reaction, as useful synthetic reagents (Fenton., 1986).

X-Ray crystallographic studies reveal that these complexes have 'sandwich' structures. Binuclear complexes of macrocyclic ligands have been the focus of much attention. They are of importance in several areas including the study of ferro— and anti-ferromagnetic exchange coupling, electron transfer properties, the binding and activation of small substrate molecules and as small molecule models for bimetallobiosite (Fenton, 1986).

Complexes of Schiff base ligands with structural similarities to phthalocyanines (N4-macrocycles) and other related compounds, are currently used as modifiers of the



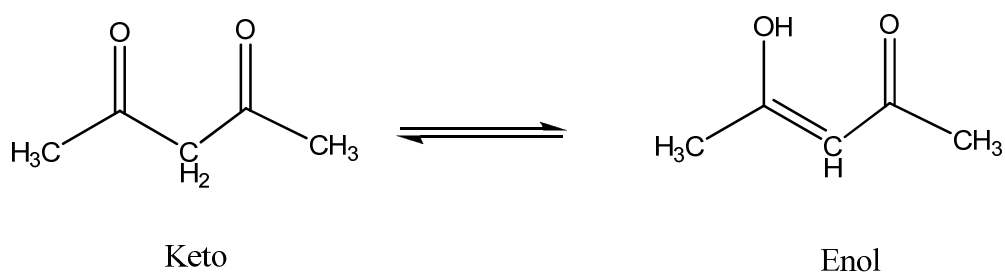
active surface of electrodes to improve their catalytic activity in the selective detection of organic pollutants and the entrainment of metals.

### 2.6.2. Analytical Applications

Equilibria involving complex formation are encountered frequently in analytical chemistry. Organic reagents that give insoluble complexes are used widely for separation, identification, and quantitative determination of metals. Metal complexes usually are insoluble, because the metal is incorporated into a large organic molecule and the resulting complex has no net charge. Some uncharged complexes are fairly volatile and can be sublimed; for example,  $\text{Fe}(\text{acetylacetonate})_3$  can be purified by sublimation at reduced pressure.

Because many uncharged complexes are insoluble in water but soluble in organic solvents, they also are used for separations based on solvent extraction procedures.

Acetylacetonone forms complexes used in solvent extraction procedures. Acetylacetonone exist in the keto and enol forms, which are in equilibrium:



Scheme 4. Keto-Enol Forms of Acetylacetonone

The enol form loses a proton and coordinates through both oxygen atoms to form a chelate ring. The term “chelate” (Grek “crab’s claw”) was first used by Morgan to describe the formation of similar complexes. The term metal chelate is now used to refer to the compounds formed as a result of chelation. Chelating ligands must have two or more points of attachment. Ammonia, with only one unshared pair of electrons, is a monodentate (one-toothed) ligand. Chelating ligands such as

acetylacetonate and ethylenediamine ( $\text{NH}_2\text{C}_2\text{H}_4\text{NH}_2$ ) are didentate (Douglas et al., 1993).

## 2.7. Characterization of Schiff Bases and Metal Complexes

IR study on metal complexes of ethylene diamine have been made by several groups of workers. Empirical assignment of  $\nu(\text{M-N})$  have been reported for  $[\text{M}(\text{en})_3]^{3+}$  ( $\text{M} = \text{Cr}^{3+}, \text{Co}^{3+}, \text{Zn}^{2+}, \text{Cd}^{2+}, \text{Fe}^{2+}, \text{Cu}^{2+}, \text{Pd}^{2+}, \text{Pt}^{2+}$ ). Bennett et al. found that, in a series of the  $\text{M}(\text{en})_3\text{SO}_4$  complexes, the  $\nu(\text{M-N})$  frequencies follow the order; (Nakamoto., 1997).

M =	Mn (II)	Fe (II)	Co(II)	Ni ( II)	Cu(II)	Zn(II)
$\nu$ ( $\text{cm}^{-1}$ )	391 <	397 <	402 <	410 <	485 >	405

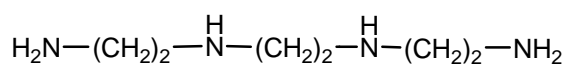
The MN stretching force constants of the hexamine complexes follows this order;

$\text{Pt (II)} \gg \text{Co (III)} > \text{Cr ( III )} > \text{Ni ( II)} \approx \text{Co(II)}$

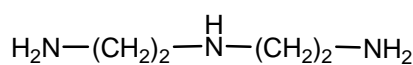
Lever and Mantovani assigned the MN stretching bands of  $\text{M}(\text{N-N})_2\text{X}_2$  [ $\text{M} = \text{Cu(II)}, \text{Co(II)}, \text{and Ni(II)}$ ;  $\text{N-N} = \text{en, dimethyl-en, etc.}$ ;  $\text{X} = \text{Cl, Br, etc.}$ ] type complexes by using the metal isotope technique. For this compounds, the CoN and NiN stretching bands have been assigned to  $400\text{-}230 \text{ cm}^{-1}$  and the CuN stretching vibrations have been located in the  $420\text{-}360 \text{ cm}^{-1}$  range (Nakamoto, 1997).

### 2.7.1. Complexes of Polyamines

Polyamines such as these shown below coordinate to a metal as tridentate or tetradentate ligands:

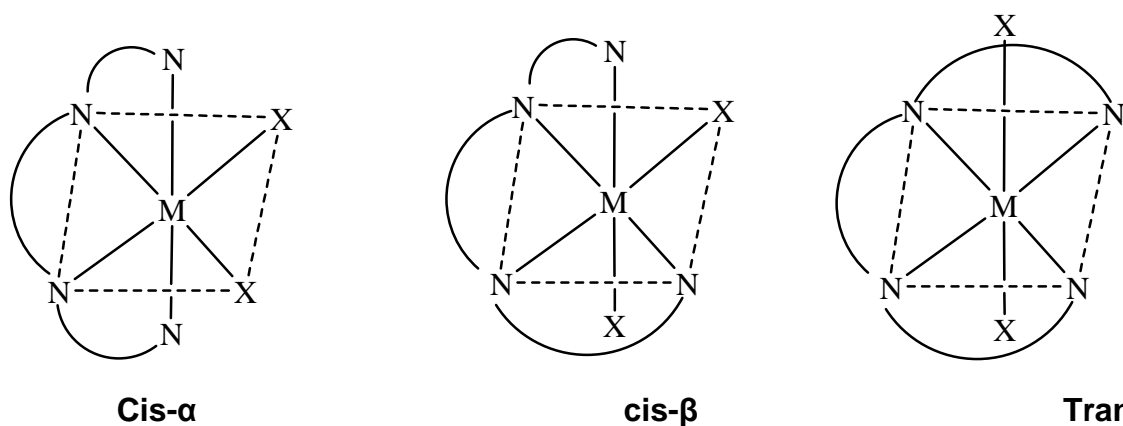


Tetradentate



Tridentate

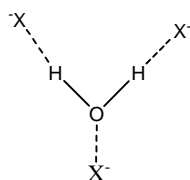
Buckingham and Jones measured the infrared spectra of  $[M(\text{trien})X_2]^+$ , where trien is triethylenetetramine, M is Co(II), Cr(II), or Rh(III), and X is a halogen or an acido anion. These compounds give three isomers,



which can be distinguished, for example, by the  $\text{CH}_2$  rocking vibrations in the 920-869  $\text{cm}^{-1}$  region. For  $[\text{Co}(\text{trien})\text{Cl}_2]\text{ClO}_4$ , cis- $\alpha$  isomer exhibits two strong bands at 905 and 871  $\text{cm}^{-1}$  and cis- $\beta$  isomer shows four bands at 918, 898, 868, and 862  $\text{cm}^{-1}$ , trans isomer gives only one band at 874  $\text{cm}^{-1}$  with a weak band at 912  $\text{cm}^{-1}$  (Nakamoto., 1997).

### 2.7.2. Lattice Water and Aqua Complexes

Water in inorganic salts may be classified as lattice or coordinated water. There is, however, no definitive borderline between the two. The former term denotes water molecules trapped in the crystalline lattice, either by weak hydrogen bonds to the anion or by weak ionic bonds to the metal, or by both:



Whereas the latter denotes water molecules bonded to the metal through partially covalent bonds. Although bond distances and angles obtained from X-ray and neutron-diffraction data provide direct information about the geometry of the water molecule in the crystal lattice, studies of vibrational spectra are also useful for this

purpose. It should be noted, however, that the spectra of water molecules are highly sensitive to their surrounding (Nakamoto, 1997).

In general lattice water absorbs at  $3550\text{-}3200\text{ cm}^{-1}$  (antisymmetric and symmetric OH stretchings) and at  $1630\text{-}1600\text{ cm}^{-1}$  (HOH bending). In the low-frequency region ( $600\text{-}200\text{ cm}^{-1}$ ) lattice water exhibits “librational modes” that are due to rotational oscillations of the water molecule, restricted by interactions with neighboring atoms. As are shown below, they are classified into three types depending upon the direction of the principal axis of rotation.

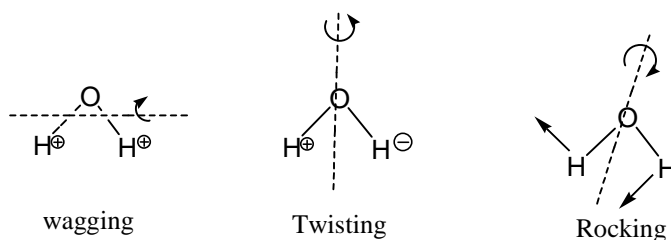


Figure 3. The three rotational modes of H<sub>2</sub>O in the solid state.

It should be noted, however, that these librational modes couple not only among themselves but also with internal modes of water (HOH bending) and other ions (SO<sub>4</sub><sup>2-</sup>, NO<sub>3</sub><sup>-</sup>, etc.) in the crystal (Woolins, 1994).

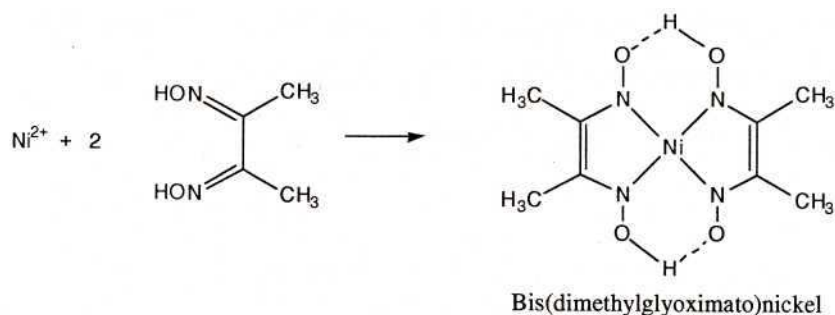
## 2.8. Stabilities of Coordination Compounds

The coordination process is an acid-base reaction. In general, an increase in basicity of the ligand and/or an increase in the acidity of the metal enhanced the stability of the complex formed. Ligands are Lewis bases (and usually Bronsted bases)- for example, NH<sub>2</sub>C<sub>2</sub>H<sub>4</sub>NH<sub>2</sub> (Douglas et al., 1993).

### 2.8.1. Effect of Metal Ion

Metal-chelate Schiff base complexes have played an important role in developing stereochemical models in main group and transition metal coordination chemistry, mainly due to their stability, ease of preparation, and structural variability.

Ni(II) will be precipitated quantitatively by the organic reagent dimethylglyoxime (Woolins, 1994).



Thermodynamic stabilities of the complexes formed by various metals follow some regular trends, such as those involving size and charge effects, factors that determine the Lewis acid strength of the metal ion.

Generally, the stabilities of complexes decrease with increasing atomic number for the electropositive metals—for example, group IIA or hard Lewis acids—and increase with increasing atomic number for the more noble metals (soft acids), following the general trend for the ionization energies. The ionic charge density ( $q/r$ ) is the determining factor for electropositive metal ions ( $d^0$ ); for example,  $\text{F}^-$  complexes of  $\text{Be}^{2+}$  are more stable than those of  $\text{Mg}^{2+}$ . Other factors must be considered for  $d^1$ - $d^9$  transition metal ions (Douglas 1993).

### 2.8.2. Classification of Metal Acceptor Properties

As previously mentioned, for the more electropositive metals (hard acids) the order of stability of the halide complexes is  $\text{F}^- > \text{Cl}^- > \text{Br}^- > \text{I}^-$ , but for highly polarizing (and also polarizable) soft acid metal ions such as  $\text{Hg}^{2+}$ , we see the reverse order. The most electropositive metals (hardest acids) show a great preference for forming complexes with hard ligands such as  $\text{F}^-$  or oxygen-containing ligands. As the electropositive character of the metals decreases (or the metal becomes softer), the complexes of N donors increase in stability with respect to those of O donors. Still more-electronegative (softer or more noble) metals form more stable complexes with soft donor atoms such as S relative to O, and P relative to N. The tendency to form stable olefin (alkene) complexes is greatest for the very soft noble metals (Douglas et al., 1993).

Table 3 shows metals classified according to their acceptor properties. The metals of class (a) are hard acids and show affinities for ligands that are roughly proportional to the basicities of the ligands toward the proton. The class (b) acceptors are soft acids, and they form stable olefin complexes. The border regions are not well-defined in all cases and, of course, the classification depends on the oxidation state of the metal ion. Copper (I) is a class (b) acceptor, but copper (II) is in the border region. Class (a) or hard acceptors form most stable complexes with hard ligand atoms in the second period (N, O or F), whereas soft class (b) acceptors form their most stable complexes with ligand atoms from the third or a later period (Douglas, 1993).

Table 3. Classification of metals according to acceptor properties

H																
Li	Be													B	C	
Na	Mg													Al	Si	
K	Ca	Sc	Ti	V	Cr	Mn	Fe	Co	Ni	Cu	Zn	Ga	Ge	As		
Rb	Sr	Y	Zr	Nb	Mo	Tc	Ru	Rh	Pd	Ag	Cd	In	Sn	Sb		
Cs	Ba	La <sup>b</sup>	Hf	Ta	W	Re	Os	Ir	Pt	Au	Hg	Tl	Pb	Bi	Po	
Fr	Ra	Ac <sup>c</sup>														

  Class (a)    
   Class (b)    
   Border region

<sup>a</sup>S. Ahlrand, J. Chatt, and N. R. Davies, *Q. Rev. Chem. Soc.* 1958, 12, 265.

<sup>b</sup>Lanthanides.

<sup>c</sup>Actinides.

### 2.8.3. Basicity and Structure of Ligand

Although class (a) metal atoms display a preference for different ligand atoms than do class (b) metals, with a given donor atom the stability constants generally increase as the basicity of the ligand increases. Thus the complexes of simple amines are generally more stable than those of  $\text{NH}_3$ , and the stability increases with the basicity of the amine. Generally the complexes of chelate ligands for example,  $\text{NH}_2\text{C}_2\text{H}_4\text{NH}_2$  are much more stable than those of monodentate ligands such as  $\text{NH}_3$ . This enhanced stability is referred to as the chelate effect.

Metal-chelate Schiff base complexes have played an important role in developing stereochemical models in main group and transition metal coordination chemistry, mainly due to their stability, ease of preparation, and structural variability (Douglas et al., 1993).

## 2.9. IR Spectroscopy

Primary(NH<sub>2</sub>) and secondary (NH) amines may be differentiated by using infrared spectra. Primary amines have two sharp N-H stretching bands near 3335 cm<sup>-1</sup>, a broad NH<sub>2</sub> scissoring band at 1615 cm<sup>-1</sup>, and NH<sub>2</sub> wagging and twisting bands in the 850-750 cm<sup>-1</sup> range. Secondary amines show only one N-H stretching band at 3335 cm<sup>-1</sup> and an N-H bending band at 1615 cm<sup>-1</sup>. The N-H wagging band for secondary amines appears at 715 cm<sup>-1</sup>. All aliphatic amines show C-N stretching bands at 1220-1020 cm<sup>-1</sup> (Khan, 1999; Stuart, 2004).

The effect of conjugation of C=C bond on C=N bond in diminishing the frequency of the later could be taken as very small in comparison with a similar decrease of 25-40 cm<sup>-1</sup> in the case of conjugation enones. (Sandhu, and Sain, 1987; Akitsu, and Einaga, 2006).

All IR spectra of the complexes of β-enaminones showed a common characteristic strong broad band in the region 3200–3600 cm<sup>-1</sup>, which confirmed the presence of water molecules coordinated to the metal ion. Furthermore, the strong bands assignable to stretching vibrations of the skeleton C=C and C=O groups, which are observed at 1556-1562 and 1598-1603 cm<sup>-1</sup> in the ligand, are all red-shifted to 1513 and 1565 cm<sup>-1</sup> in complex (Shi, et al., 2004; Greenhill, et al., 1991).

Metal complexes or chelates are largely covalent in nature and the spectra of such compounds are dominated by the contribution of the ligand and its coordination chemistry. The ligands may be small species, such as water or ammonium molecules, or large complex species, such as porphyrins. The infrared spectra of the Co(III), Cr(III) and Ni(II) hexamine complexes have been widely studied. and Figure 4 illustrates the infrared spectra of the Co(III), Cr(III) and Ni(II) hexamine complexes. The spectra indicate that the type of metal in the complex produces

important differences in the infrared bands of each complex. Significant differences in the wavenumber values of each complex are noted for the metal-NH<sub>3</sub> rocking (900-600 cm<sup>-1</sup>) and NH<sub>3</sub> bending (1400-1100 cm<sup>-1</sup>) bands. Bands due to N-H stretching and N-H bending are also observed in these spectra in the 3700-2500 and 1750-1500 cm<sup>-1</sup> regions, respectively (Stuart, 2004).

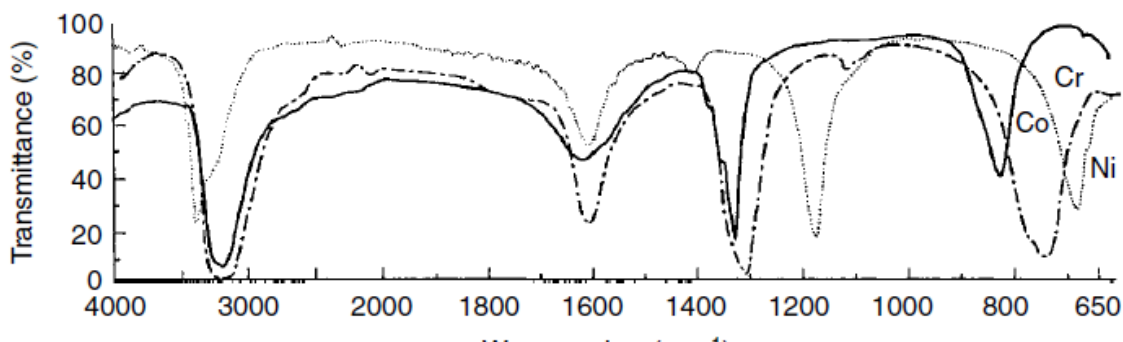
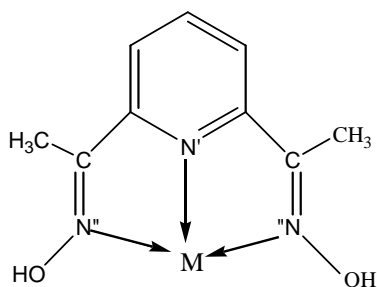


Figure 4. Infrared spectra of metal hexamine complexes (Nakamoto, 1997)

A useful band in the infrared spectra of carbonyl ligands in metal complexes is due to C-O stretching. The stretching wavenumber for a terminal carbonyl ligand in a complex correlated with the 'electron-richness' of the metal. The band position is determined by the bonding from the d orbitals of the metal into the  $\pi^*$  anti-bonding orbitals of the ligand. The bonding weakens the C-O bond and lowers the wavenumber value from its value in CO (Stuart, 2004).

The metal isotope technique has been used to assign the MN vibrations of metal complexes with many other ligands. For example Takemoto assigned the NiN', and NiN'' stretching vibrations of [Ni(DAPD)<sub>2</sub>]<sup>2-</sup> at 416-341 and 276 cm<sup>-1</sup>, respectively (Takemoto, 1973).



DAPD: 2,6-diacetylpyridine dioxime



In  $\text{Ni}(\text{DAPD})_2$ , where the Ni atoms is in the +IV state, the  $\text{NiN}''$ , and  $\text{NiN}'$  stretching bands are located at 509,8 - 472 and 394,8  $\text{cm}^{-1}$  respectively.

The Co-N stretching bands have been assigned to 400-230  $\text{cm}^{-1}$  and the Cu-N stretching vibrations have been located in the 420-360  $\text{cm}^{-1}$  range.

## 2.10. NMR Spectroscopy

NMR spectroscopy has been applied with limited success to the investigation of the structure of molecular complexes. The chemical shifts of the protons are generally shift to high fields in the complexes (Rao, and Ferraro, 1970; Nakamoto, 1997).

Sometimes the determination of chemical shifts may become difficult because the signals are too weak to be detected. The substance under examination may not be available in large amount or its solubility may be low or the inherent sensitivity of the NMR experiment for the nucleus in question may be low (Rao, and Ferraro, 1970; Nakamoto, 1997).

In the presence of a trace amount of water, exchange of hydrogens between amine molecules is extremely rapid. In aqueous solution, exchange is so rapid between ammonia and water molecules that separate O-H and N-H resonances are not obtained and only a single average proton resonance is obtained. Under these circumstances, ammonium ions, ammonia, and water exchange protons with one another sufficiently rapidly to give only a single line (Roberts 1959).

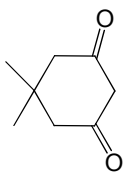
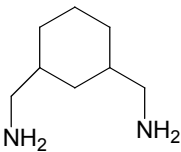
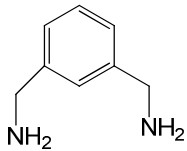
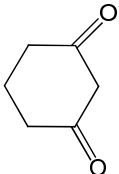
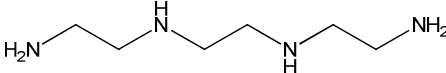
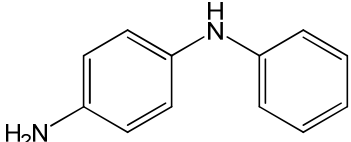
### 3 THE AIM OF THE WORK

The synthesis of some  $\beta$ -enaminones and their transition metal complexes was aimed in this study. Five new  $\beta$ -enaminones (**L1**, **L2**, **L3**, **L4**, **L5**) were synthesized by the reactions of 5,5-dimethyl-1,3-cyclohexanedione, 1,3-cyclohexanedione as diketones and *p*-amino diphenylamine, triethylenetetramine, 1,3-cyclohexane bis(methylamine) and *m*-xylylene daimine as diamines, respectively. The chemical structures of all  $\beta$ -enaminones were determined by analytical and spectral methods.

Of these  $\beta$ -enaminones **L1**, **L2**, **L3** were used as potential ligands for synthesizing their cobalt (II), copper (II), and nickel (II) complexes, whereas  $\beta$ -enaminones **L4**, **L5** were used for complexation with metal ions but no complex formation was observed. All the synthesized metal complexes were characterized by ICP-AES, magnetic susceptibility, DSC-TGA measurements, IR analyses and electronic spectral data.

Table 4 shows the structures of the ketone and amine employed in this study.

Table 4. Structures of the starting compounds

 5,5-Dimethyl-1,3-cyclohexanedione	 1,3-Cyclohexanebis(methylamine)	 <i>m</i> -xylylenediamine
 1,3-cyclohexanedione	 Triethylene tetramine	 <i>p</i> -Amino-diphenylamine

## 4. EXPERIMENTAL

### 4.1. General Procedures

All starting compounds and solvents for synthesis were purchased from Across, Aldrich, Sigma and E. Merck. Solvents and all reagents were technical grade and were purified and dried by distillation from appropriate desiccant when necessary. Concentration of solutions after reactions and extractions were achieved using a rotary evaporator at reduced pressure.

Analytical and preparative thin layer chromatography (TLC) was performed on silica gel HF-254 (Merck). Column chromatography was carried out by using 70-230 mesh silica gel (0.063-0.2 mm, Merck).

The structures of the compounds in this study were determined by the instruments mentioned below.

#### **Melting point:**

All melting points were measured in sealed tubes using an electrothermal digital melting point apparatus (Gallenkamp) and were uncorrected.

#### **Infrared Spectroscopy:**

The investigation of vibrational properties of the  $\beta$ -enaminones and the complexes were carried out on a Mattson 1000 Model FT-IR Spectrometer within the range of 4000 to 400  $\text{cm}^{-1}$ . The IR samples were prepared as KBr pellets.

#### **NMR**

$^1\text{H}$  NMR, COSY, APT spectra were recorded on a resolution fourier transform Bruker WH-400 NMR spectrometer with tetramethylsilane as an internal standard. Chemical shifts were reported in ppm relative to the solvent peak (DMSO-*d*6 at 2.5

and 3.3ppm for protons). Signals were designated as follows: s, singlet; d, doublet; t, triplet; q, quartet; m, multiplet.

### **Electronic Spectra**

The solid reflectance spectra were measured on a Shimadzu UV-3600 UV-VIS-NIR spectrophotometer.

### **Mass Spectra**

Mass spectra were recorded on a Micromass UK Platform II LC-MS spectrometer and AGILENT 1100 MSD LC-MS spectrometer.

### **Elemental analysis**

Elemental microanalyses of the separated solid chelates for C, H, N, were performed with a Elementar Analysensysteme GmbH varioMICRO CHNS analyser.

### **Magnetic Susceptibility**

Magnetic susceptibility measurements of the complexes in the solid state were determined at room temperature (20°C) with a MKI, MSBI/24093/6232 model (Sherwood Scientific Ltd., Cambridge, U.K.) magnetic susceptibility balance. It was calibrated with  $\text{HgCo(SCN)}_4$ . [mercury(II) tetrathiocyanatocobaltate(II)].

### **ICP Analysis**

Metal content of the complexes were measured on ICP-AES Varian model Liberty Series II analyser. The analyses were repeated twice to check the accuracy of the data.

## 4.2. Experiments

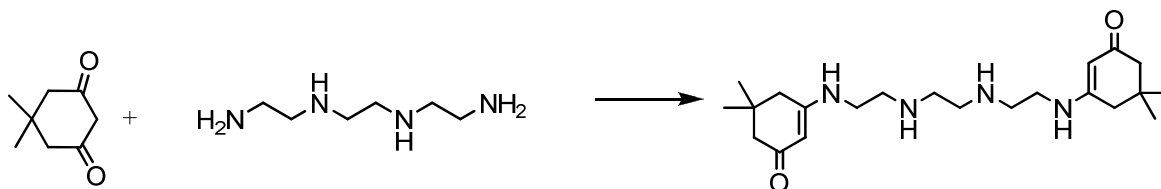
### 4.2.1 Synthesis of $\beta$ -enaminones

The  $\beta$ -enaminones were synthesized according to the below procedure:

The mixture of the ketone and the amine was refluxed in benzene using a Dean-Stark apparatus until all water was completely separated. The removal of water was very important because of the back hydrolysis of the imine. Benzene was evaporated and the precipitate was extracted with ethanol. The crude product was purified by silica gel column chromatography using a mixture of n-hexane/ethyl acetate mixture as eluent (Beckwith and Mayadunne, 2004).

All compounds, which were obtained using the above procedures, were separated and recrystallized twice from methanol or ethanol.

#### 4.2.1.1. Synthesis of 3,3'-(2,2'-(ethane-1,2-diylbis(azanediyl))bis(ethane-2,1-diyl))bis(azanediyl)bis(5,5-dimethylcyclohex-2-enone) (L1)



Scheme 5. Synthesis of 3,3'-(2,2'-(ethane-1,2-diylbis(azanediyl))bis(ethane-2,1-diyl))bis(azanediyl)bis(5,5-dimethylcyclohex-2-enone) (L1)

The mixture of the 5,5-dimethyl-1,3-cyclohexanedione (10 mmol) and the triethylenetetramine (5 mmol) were refluxed in benzene using a Dean-Stark apparatus until all water was completely separated. Benzene was evaporated and the precipitate was recrystallized from ethanol. Yield 75%; mp. 209-211 °C; IR ( $\text{cm}^{-1}$ ); 3324 and 3290  $\text{cm}^{-1}$  for N-H stretching of enamine and amine, 2880–3100 ( $\text{C-H}$  aliphatic), 1667 ( $\text{C=O}$  ketone), 1400-1550 ( $\text{C-H}$  aliphatic), 1143 ( $\text{C-N}$ ) (Figure 8).

<sup>1</sup>H-NMR (DMSO-d<sub>6</sub>) δ (ppm); 0.96 (s, 12H, CH<sub>3</sub>); 1.95 (s, 4H, CH<sub>2</sub>); 2.18 (s, 4H, CH<sub>2</sub>); 2.68 (m, 4H, CH<sub>2</sub>); 3.03 (m, 4H, CH<sub>2</sub>); 4.82 (s, 2H, vinylic CH); 6.86 (2H, enamine NH) (Figure 9).

**APT** (DMSO, 100MHz) δ (ppm): 28.45 (CH<sub>3</sub>), 32.68 (C(CH<sub>3</sub>)<sub>2</sub>), 42.77 (-HC=C(N)-CH<sub>2</sub>-C(CH<sub>3</sub>)<sub>2</sub>), 42.53 (C=C-NH-CH<sub>2</sub>-CH<sub>2</sub>-NH-), 47.32 (CH<sub>2</sub>-NH-CH<sub>2</sub>-CH<sub>2</sub>-NH-CH<sub>2</sub>), 52.29 (C=C-NH-CH<sub>2</sub>-CH<sub>2</sub>-NH) 50.75 (-C(=O)-CH<sub>2</sub>-C(CH<sub>3</sub>)<sub>2</sub>), 93.71 (vinylic CH), 163.41 (HC=C-NH-CH<sub>2</sub>), 194.33 (C=O, ketone) (Figure 10).

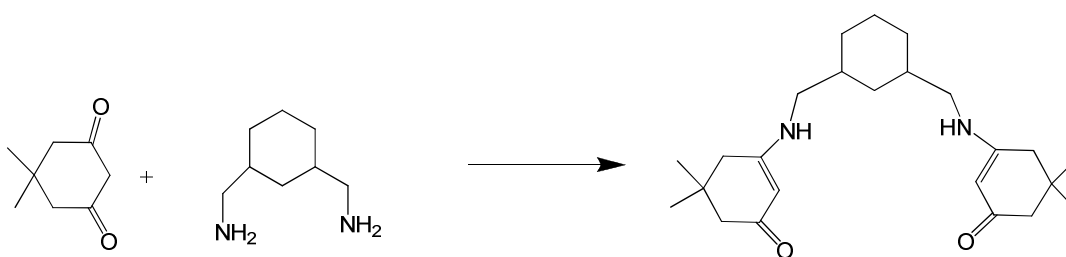
**UV**(nm): 219, 255, 287, 422 (Figure 11).

**LC-MS**: 394.3 [M+4H]<sup>+</sup>, 393.3 [M+3H]<sup>+</sup>, 392.3 [M+2H]<sup>+</sup>, 346.3 [M-44] (Figure 12).

Elemental Analysis (calculated): C, 67.66; H, 9.81; N, 14.35; O, 8.19

Elemental Analysis (measured): C, 67.85; H, 10.08; N, 13.94; O, 8.13

#### 4.2.1.2 Synthesis of 3,3'-(cyclohexane-1,3-diylbis(methylene))bis(azane diyl)bis(5,5dimethyl cyclohex-2-enone) (L2)



Scheme 6. Synthesis of 3,3'-(cyclohexane-1,3-diylbis(methylene))bis(azane diyl)bis(5,5dimethyl cyclohex-2-enone) (L2)

The mixture of the 5,5-dimethyl-1,3-cyclohexanedione (10mmol) and the 1,3-cyclohexanebis(methylamine) (5mmol) was refluxed in benzene using a Dean-Stark apparatus until all water was completely separated. Benzene was

evaporated and the precipitate was recrystallized from ethanol. Yield 94%; mp. 220-223°C; IR  $\nu(\text{cm}^{-1})$ ; 3263 (N-H enamin), 2880–3100 (C-H aliphatic), 1593 (C=O ketone), 1400-1500 (C-H aliphatic), 1149 (C-N) (Figure 14).

$^1\text{H-NMR}$  (DMSO- $d_6$ )  $\delta(\text{ppm})$ ; 0.96 (s, 6H,  $\text{CH}_3$ ); 1.21 (m, 2H,  $\text{CH}_2$ ); 1.38 (m, 4H,  $\text{CH}_2$ ); 1.55 (t, 2H,  $\text{CH}_2$ ); 1.72 (m, 2H, CH); 1.95 (s, 4H,  $\text{CH}_2$ ); 2.18 (s, 4H,  $\text{CH}_2$ ); 2.82 (d, 4H,  $\text{CH}_2$ ); 3.58 (b, 2H, NH); 4.8 (s, vinylic CH) (Figure 15).

APT (DMSO, 100MHz)  $\delta$  (ppm): 25.42 ( $\text{CH}_2$ ), 28.47 ( $\text{CH}_3$ ), 30.88 ( $\text{CH}_2$ ), 32.67 (C), 36.45 (CH), 42.54 (allylic  $\text{CH}_2$ ), 49.08 ( $\text{CH}_2$ ), 50.75 (N- $\text{CH}_2$ ), 93.66 (vinylic CH), 163.41 (vinylic C), 194.11 (C=O, ketone) (Figure 16).

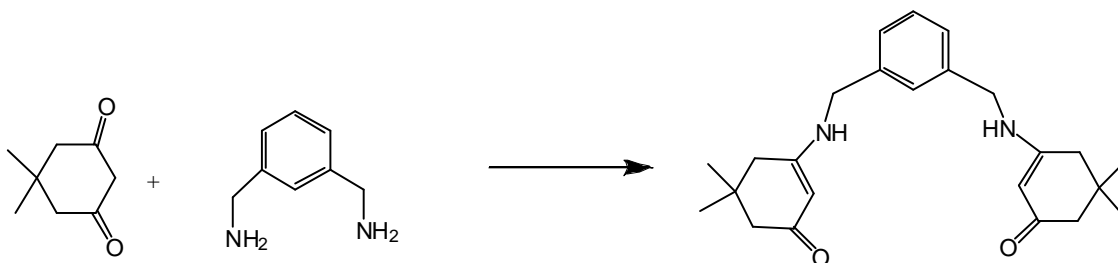
LC-MS: 387.3  $[\text{M}]^+$ , 265.2  $[\text{M}-\text{C}_8\text{H}_{11}\text{O}]$ , 140.13  $[\text{M}-\text{C}_{16}\text{H}_{22}\text{O}_2]$  (Figure 17).

UV (nm): 222, 260, 300, 423 (Figure 18).

Elemental Analysis (calculated): C, 74.57; H, 9.91; N, 7.25; O, 8.28

Elemental Analysis (measured): C, 74.22; H, 9.68; N, 7.18; O, 8.92

#### 4.2.1.3. Synthesis of 3,3'-(1,3-phenylenebis(methylene))bis(azanediy) bis(5,5-dimethyl cyclo hex-2-enone) (L3)



Scheme 7. Synthesis of 3,3'-(1,3-phenylenebis(methylene))bis(azanediy) bis(5,5-dimethyl cyclo hex-2-enone) (L3)

The mixture of the 5,5-dimethyl-1,3-cyclohexanedione (10 mmol) and the m-xylylenediamine (5 mmol) was refluxed in benzene using a Dean-Stark apparatus until all water was completely separated. Benzene was evaporated and the precipitate was recrystallized from ethanol. Yield 97%; mp. 230-231°C; IR  $\nu(\text{cm}^{-1})$ ; 3252 (N-H enamin), 2800–3050 (C-H aromatic and aliphatic), 1662 (C=O ketone), 1400-1550 (C-H aliphatic), 1141 (C-N) (Figure 20).

$^1\text{H-NMR}$  (DMSO- $d_6$ )  $\delta(\text{ppm})$ ; 0.97 (s,6H,  $\text{CH}_3$ ); 1.94 (s,4H,  $\text{CH}_2$ ); 2.25 (s,4H,  $\text{CH}_2$ ); 3.54 (b, 2H,NH); 4.21 (s,4H,  $\text{CH}_2$ ); 4.76 (s, vinylic CH); 7.18 (d, 1H, aromatic CH); 7.32 (t, 1H, aromatic CH); 7.54 (s, 1H, aromatic CH). (Figure 21).

APT (DMSO, 100MHz)  $\delta(\text{ppm})$ : 28.43 ( $\text{CH}_3$ ), 32.78 ( $\text{CH}_2$ ), 42.54 (allylic  $\text{CH}_2$ ), 46.01(C), 50.73 (N- $\text{CH}_2$ ), 94.68 (vinylic CH), 126.12 (aromatic CH), 128.67 (aromatic CH), 138.89 (aromatic C), 163.41 (vinylic C), 194.44 (C=O, ketone) (Figure 22).

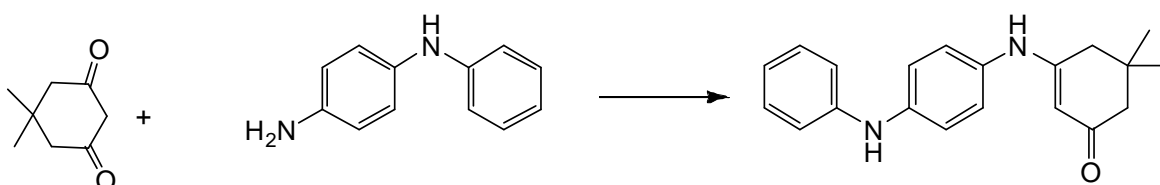
LC-MS: 381.2  $[\text{M}]^+$ , 258.1  $[\text{M}-\text{C}_8\text{H}_{11}\text{O}]$ , 140.13  $[\text{M}-\text{C}_{16}\text{H}_{20}\text{NO}]$  (Figure 23).

UV(nm): 219, 261, 312, 428 (Figure 24).

Elemental Analysis (calculated): C, 75.75; H, 8.48; N, 7.36; O, 8.41

Elemental Analysis (measured): C, 75.90; H, 8.32; N, 7.36; O, 8.42

#### 4.2.1.4. Synthesis of 5,5-dimethyl-3-(4-(phenylamino)phenylamino)cyclo hex-2-enone (L4)



Scheme 8. Synthesis of 5,5-dimethyl-3-(4-(phenylamino)phenylamino)cyclo hex-2-enone (L4)



The mixture of the 5,5-dimethyl-1,3-cyclohexanedione (10 mmol) and the p-amino-diphenylamine (10 mmol) was refluxed in benzene using a Dean-Stark apparatus until all water was completely separated. Benzene was evaporated and the precipitate was recrystallized from ethanol to give red-brown crystals. Yield 80%; mp. 210-212°C; IR  $\nu(\text{cm}^{-1})$ ; 3299 and 3222 (N-H enamin), 2800–3050 (C-H Aromatic and aliphatic), 1596 (C=O ketone) ,1450-1550 (C=C and C-H aliphatic), 1152 (C-N) (Figure 26).

$^1\text{H-NMR}$  (DMSO-*d*6)  $\delta$  (ppm); 1,03 ( s,6H, CH<sub>3</sub>); 2.08 ( s,2H, CH<sub>2</sub>); 2.22 ( s,2H, CH<sub>2</sub>); 5.20 ( s, vinylic CH); 7.06 (m, 5H, aromatic CH); 7.22 (m, 5H, aromatic CH) 8.23 (s, 1H,NH); and 8.62 (s, 1H,NH) (Figure 27).

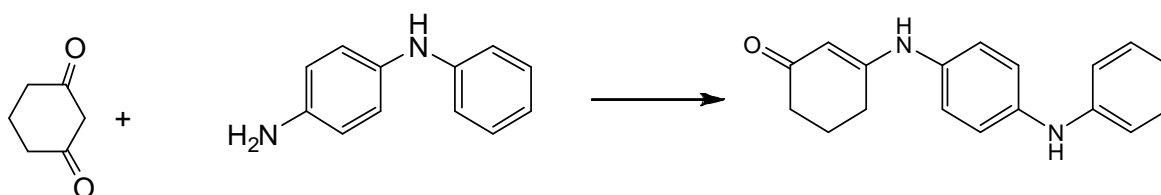
APT (DMSO, 100MHz)  $\delta$  (ppm) : 27.98 (CH<sub>3</sub>), 32.26 (CH<sub>2</sub>-C(CH<sub>3</sub>)<sub>2</sub>-CH<sub>2</sub>), 41.92 (CH<sub>2</sub>), 50.21(CH<sub>2</sub>), 95.70 (vinylic CH), 116.44-129.14 (aromatic CH), 130.80-143.42 (aromatic C), 161.04 (vinylic C), 194.76 (C=O, ketone) (Figure 28).

UV(nm): 267, 300, 396, 475 (Figure 29).

Elemental Analysis ( calculated): C, 78.40; H, 7.24; N, 9.14; O, 5.22

Elemental Analysis (measured) : C, 78.02; H, 7.17; N, 9.01; O, 5.80

#### 4.2.1.5 Synthesis of 3-(4-(phenylamino)phenylamino)cyclohex-2-enone (L5)



Scheme 9. Synthesis of 3-(4-(phenylamino)phenylamino)cyclohex-2-enone (L5)

The mixture of the 1,3-cyclohexanedione (10 mmol) and the p-amino-diphenylamine (10 mmol) was refluxed in benzene using a Dean-Stark apparatus until all water was completely separated. The removal of water was very important because of the back hydrolysis of the  $\beta$ -enaminone. Benzene was evaporated and the precipitate was recrystallized from ethanol to give dark green crystals. Yield 58%; mp. 207-208°C; IR  $\nu(\text{cm}^{-1})$ ; 3282 (N-H enamin), 3212 (N-H, amin), 2800–3050 (C-H Aromatic and aliphatic), 1598 (C=O ketone) ,1400-1550 (C-H aliphatic), 1144 (C-N) (Figure 31).

$^1\text{H-NMR}$  (DMSO- $d_6$ )  $\delta$  (ppm); 1.89 ( m,2H,  $\text{CH}_2\text{-CH}_2\text{-CH}_2$ ); 2.14 (t, 2H,NH-C- $\text{CH}_2\text{-CH}_2$ ); 2.46 ( t,2H, C(=O)- $\text{CH}_2\text{-CH}_2$ ); 5.15 (s,1H, vinylic CH); 6.83 (t, 1H, aromatic CH); 7.05 (m, 4H, aromatic CH); 7.22 (t, 2H, aromatic CH); 8.18 (s, 1H,NH);  $\delta$ 8.65 (s, 1H,NH); (Figure 32).

APT (DMSO, 100MHz)  $\delta$  (ppm): 22.10 ( $\text{CH}_2\text{-CH}_2\text{-CH}_2$ ), 28.88 (2H,NH-C- $\text{CH}_2\text{-CH}_2$ ), 36.92 (C(=O)- $\text{CH}_2\text{-CH}_2$ ), 97,55 (vinylic CH), between 116.96-129.64 (aromatic CH), 131.31 (aromatic C), 140.98 (aromatic C), 143.90 (aromatic C), 163.33 (vinylic C), 195.68 (C=O, ketone) (Figure 33).

UV(nm): 265, 293, 384, 471 (Figure 34).

Elemental Analysis (calculated): C, 77.67; H, 6.52; N, 10.06; O, 5.75

Elemental Analysis (measured): C, 77.38; H, 6.49; N, 9.94; O, 6.19

#### 4.2.2. Synthesis of Metal Complexes

Synthesis of complexes 1-18 was carried out in two different ways. The solvents were selected so that the ligand precursors and metal chlorides were fully dissolved but the complex precipitated out. All complexes were synthesized at room temperature. Finally, the powdered complexes were obtained with a yield of 30-50 %.

The metal complexes were synthesized according to the below procedures, either procedure 1 (complexes 1, 2, 3, 7, 8, 9, 13, 14, 15) or procedure 2 (complexes; 4, 5, 6, 10, 11, 12, 16, 17, 18) were used.

#### **4.2.2.1 Procedure 1 (in-situ method) :**

A mixture of the 5,5-dimethyl-1,3-cyclohexanedione (10 mmol) and the appropriate metal chloride ( $\text{CuCl}_2 \cdot 2\text{H}_2\text{O}$ ,  $\text{CoCl}_2 \cdot 6\text{H}_2\text{O}$  or  $\text{NiCl}_2 \cdot 6\text{H}_2\text{O}$ ) in ethanol was stirred about 15 min. This was followed by the addition of ethanolic solution of 10 mmol amine; the resultant mixture was stirred for about 2 h. A solid powder product formed, it was filtered, washed with ethanol and then with ether and dried in vacuum (Prasad et al., 2005).

The amines used in complexation study were; triethylenetetramine m-xylenylenediamine and 1,3-cyclohexanebis(methylamine).

#### **4.2.2.2 Procedure 2:**

Ethanolic solution of 10 mmol  $\beta$ -enaminone and 10 mmol appropriate metal chloride ( $\text{CuCl}_2 \cdot 2\text{H}_2\text{O}$ ,  $\text{CoCl}_2 \cdot 6\text{H}_2\text{O}$  or  $\text{NiCl}_2 \cdot 6\text{H}_2\text{O}$ ) was stirred about 2h. A solid powder product formed, it was filtered, washed with ethanol and then with ether and dried in vacuum (Namsan 2001).

Characterization of complexes were achieved by FT-IR, UV-VIS-NIR, magnetic susceptibility, DTA-TGA and ICP-AES analysis.

The colors, yields, magnetic moment, melting points and electronic spectra of the isolated solid ligands and the complexes were compiled in Table 5, 6 and 7.

The pictures of the ligands and complexes are given in Figures 5, 6 and 7.

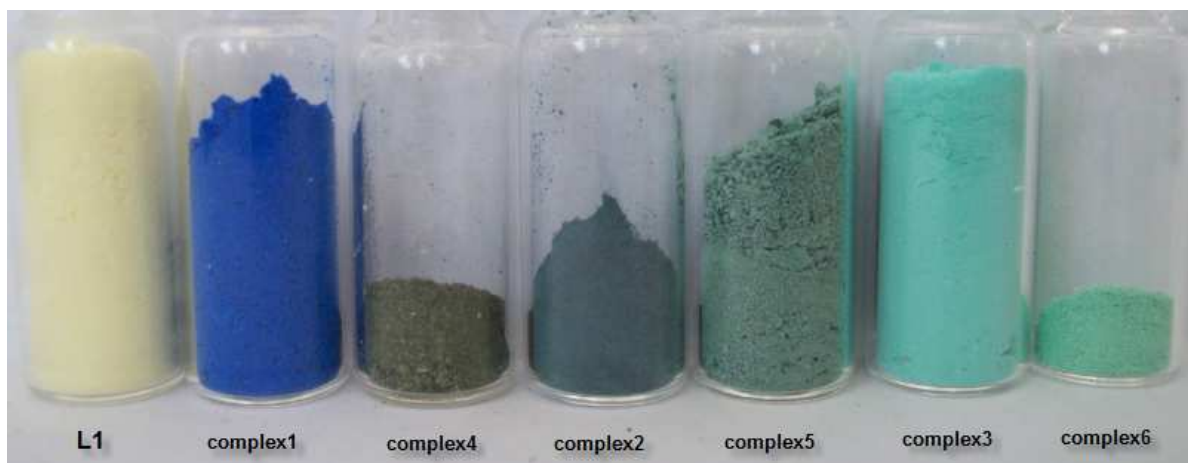


Figure 5. Colors of Ligand L1 and its complexes

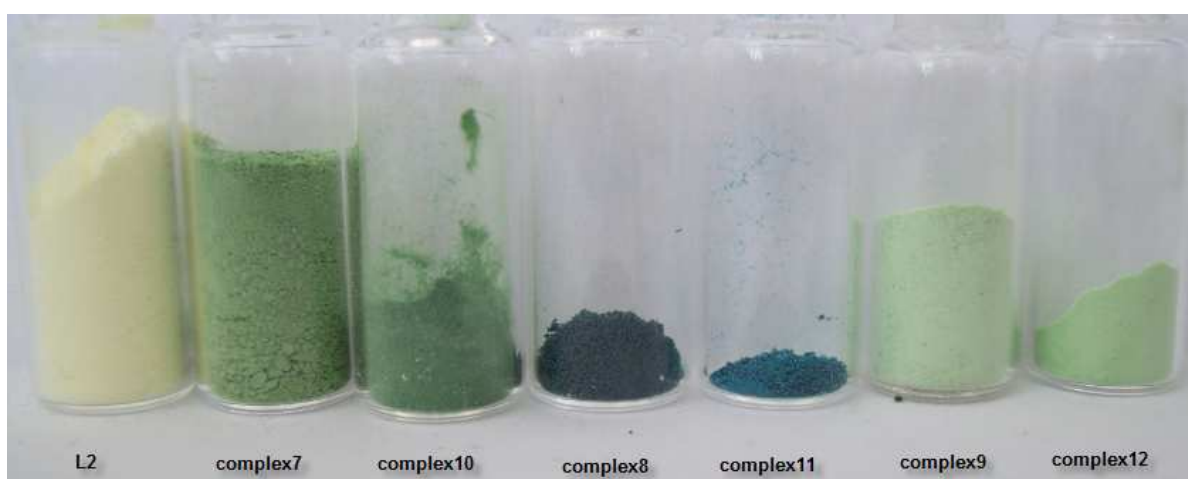


Figure 6. Colors of Ligand L2 and its complexes

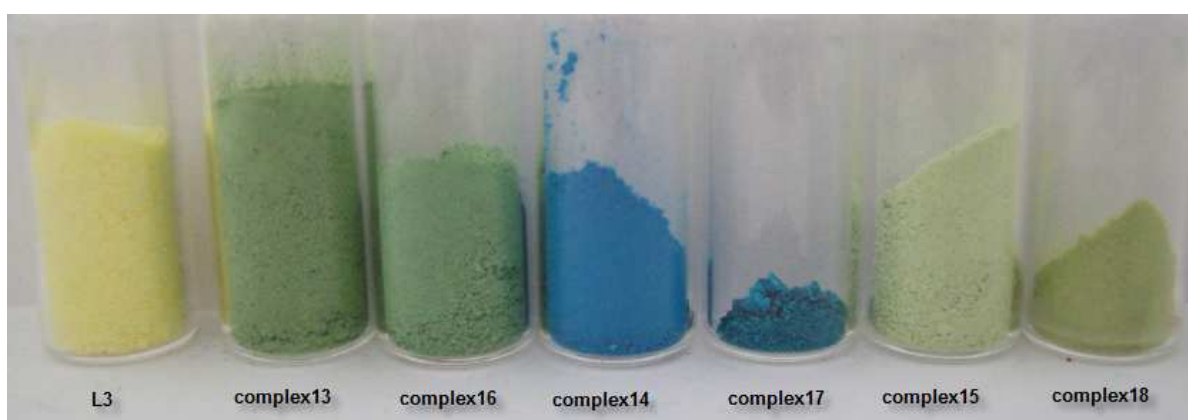


Figure 7. Colors of Ligand L3 and its complexes

Table 5. The experimental results of 3,3'-(2,2'-(ethane-1,2-diylbis (azanediyl))bis (ethane-2,1-diyl))bis(azanediyl)bis (5,5-dimethyl cyclohex-2-enone) (L1) and its metal complexes

Ligand and complexes	Complex No	Color	M.p. °C	Yield %	Magnetic moment B.M.	Electronic spectra		ICP Analysis	
						Intramolecular CT transitions of the ligand $\pi-\pi^*$ , $n-\pi^*$	d-d transitions	Percent of metal (%) measured	Percent of metal (%) calculated
L1;		Yellow	209-211	75	-	220-300b 420	-	-	-
L1-(Cu(Cl) <sub>2</sub> .2H <sub>2</sub> O) <sub>2</sub> (in-situ)	Complex 1	Dark blue	224-226	45	2.96	264 b	620 b	24.53	25.32
L1-(Co(Cl) <sub>2</sub> .6H <sub>2</sub> O) <sub>2</sub> (in-situ)	Complex 2	Gray	248	40	5.56	247b 450sh	610-720b	26.63	25.21
L1-(Ni(Cl) <sub>2</sub> .6H <sub>2</sub> O) <sub>2</sub> (in-situ)	Complex 3	Light blue	>>300	38	5.18	245 b, 295 sh, 400	645 b	24.06	22.71
L1-(Cu(Cl) <sub>2</sub> .2H <sub>2</sub> O) <sub>2</sub> (L1+metal salt)	Complex 4	Dark green	204-206	35	2.92	220-300b, 380sh	620b	25.05	25.95
L1-(Co(Cl) <sub>2</sub> .6H <sub>2</sub> O) <sub>2</sub> (L1+metal salt)	Complex 5	Green	223-226	31,5	5.67	255 b, 310sh	626 665 705	24.11	23.95
L1-(Ni(Cl) <sub>2</sub> .6H <sub>2</sub> O) <sub>2</sub> (L1+metal salt)	Complex 6	Light blue	>>300	35	5.86	240s, 300sh, 400	640 b	23.90	22.71

Table 6. The experimental results of 3,3'-(cyclohexane-1,3-diylbis (methylene))bis (azanediyl)bis(5,5dimethylcyclohex-2-enone) (L2) and its metal complexes

Ligand and complexes	Complex No	Color	M.p. °C	Yield %	Magnetic moment B.M.	Electronic spectra		ICP Analysis	
						Intramolecular CT transitions of the ligand $\pi-\pi^*$ , $n-\pi^*$	d-d transitions	Percent of metal (%) measured	Percent of metal (%) calculated
L2;	L2	Yellow	220-223	94	-	218, 262, 314, 425	-	-	-
L2-(Cu(Cl) <sub>2</sub> .2H <sub>2</sub> O) <sub>2</sub> (in-situ)	Complex 7	Green	172	54	2.72	270, 420	650-800	23.65	
L2-(Co(Cl) <sub>2</sub> .6H <sub>2</sub> O) <sub>2</sub> (in-situ)	Complex 8	Dark blue	>300	28	6.66	290, 360sh	485sh 630	26.99	23.04
L2-(Ni(Cl) <sub>2</sub> .6H <sub>2</sub> O) <sub>2</sub> (in-situ)	Complex 9	Light green	>300	35	6.70	290. 410	680	27.62	
L2-(Cu(Cl) <sub>2</sub> .2H <sub>2</sub> O) <sub>2</sub> (L2+metal salt)	Complex 10	DarkKhaki	>300	34	2.76	280b	770b	23.52	
L2-(Co(Cl) <sub>2</sub> .6H <sub>2</sub> O) <sub>2</sub> (L2+metal salt)	Complex 11	Dark blue	>300	68	7.84	230, 300	502 614b	28.65	23.04
L2-(Ni(Cl) <sub>2</sub> .6H <sub>2</sub> O) <sub>2</sub> (L2+metal salt)	Complex 12	Light green	>300	77	5.30	240,290, 400	680b	24.80	

Table 7. The experimental results of 3,3'-(1,3-phenylenebis(methylene))bis(azanediy) bis (5,5-dimethylcyclohex-2-enone) (L3) and its metal complexes

Ligand and complexes	Complex No	Color	M.p. °C	Yield %	Magnetic moment B.M.	Electronic spectra		ICP Analysis	
						Intramolecular CT transitions of the ligand $\pi-\pi^*$ , $n-\pi^*$	d-d transitions	Percent of metal (%) measured	Percent of metal (%) calculated
L3;	L3	Yellow	230-231	97	-	220, 259, 310, 425	-	-	-
L3-(Cu(Cl) <sub>2</sub> .2H <sub>2</sub> O) <sub>2</sub> (in-situ)	Complex 13	Green	152	53	2.72	270b	730b	20.10	23.31
L3-(Co(Cl) <sub>2</sub> .6H <sub>2</sub> O) <sub>2</sub> (in-situ)	Complex 14	darkcyan	272	31	7.35	270	580 630	24.59	-
L3-(Ni(Cl) <sub>2</sub> .6H <sub>2</sub> O) <sub>2</sub> (in-situ)	Complex 15	Light green	>300	64	5.87	230,295, 420	690	25.95	22.07
L3-(Cu(Cl) <sub>2</sub> .2H <sub>2</sub> O) <sub>2</sub> (L3+metal salt)	Complex 16	Green	156	15	2.66	270b	770b	20.03	23.31
L3-(Co(Cl) <sub>2</sub> .6H <sub>2</sub> O) <sub>2</sub> (L3+metal salt)	Complex 17	darkcyan	252	32	7.09	230, 300	585, 620, 660	24.08	22.07
L3-(Ni(Cl) <sub>2</sub> .6H <sub>2</sub> O) <sub>2</sub> (L3+metal salt)	Complex 18	Light green	>300	40	6.21	270, 415	690b	26.40	

Table 8. Characteristic IR bands of the Ligands and the Complexes (cm<sup>-1</sup>)

	Compound	$\nu(\text{H}_2\text{O})$	$\nu(\text{N-H})$	$\nu(\text{C-H})$	$\nu\text{C}=\text{O}$	$\nu(\text{H-O-H})$	$\nu(\text{C-H})$	$\nu(\text{C-N})$
	L1	-	3290	2951-2585	1667	-		1143
	L2	-	3290	2951-2585	1596	-		1143
	L3	-	3250	2945-2818	1662	-	1555-1450	1141
	L4		3299-3222	2959-2871	1596	-	1500-1550	1152
	L5		3280-3208	2945-2850	1597	-	1500-1550	1142
1	L1-(Cu(Cl) <sub>2</sub> .2H <sub>2</sub> O) <sub>2</sub> (in-situ)	3450	3225-3302	2950	1572	628	1454	1133
2	L1-(Co(Cl) <sub>2</sub> .6H <sub>2</sub> O) <sub>2</sub> (in-situ)	3412	3192-3115	2950	1580	666	1456	1146
3	L1-(Ni(Cl) <sub>2</sub> .6H <sub>2</sub> O) <sub>2</sub> (in-situ)	-	3291-3241	2934	1577	683	1454	1166
4	L1-(Cu(Cl) <sub>2</sub> .2H <sub>2</sub> O) <sub>2</sub>	3409	3254-3144	2946-2881	1585	607	1450-1470	1146
5	L1-(Co(Cl) <sub>2</sub> .6H <sub>2</sub> O) <sub>2</sub>	3500-3200	3200-3000	2960-2886	1588	609	1451-1480	1144
6	L1-(Ni(Cl) <sub>2</sub> .6H <sub>2</sub> O) <sub>2</sub>	3460	3320-3166	2974-2884	1589	607	1454-1478	1168
7	L2-Cu(Cl) <sub>2</sub> .2H <sub>2</sub> O (in-situ)	3445	3324-3137	2923	1577	588	1500-1454	1149
8	L2-Co(Cl) <sub>2</sub> .6H <sub>2</sub> O (in-situ)	3565	3384-3236	2917	1588	609	1495-	1149
9	L2-Ni(Cl) <sub>2</sub> .6H <sub>2</sub> O (in-situ)	-	3520-3200	2928-2857	1599	Covered with broad band	1508-1462	1146
10	L2-Cu(Cl) <sub>2</sub> .2H <sub>2</sub> O	3450	3351-	2917-2846	1637	599	1517-1456	1149
11	L2-Co(Cl) <sub>2</sub> .6H <sub>2</sub> O	3428	3247-3087	2923	1637	587	1456	1155
12	L2-Ni(Cl) <sub>2</sub> .6H <sub>2</sub> O	3439	3241-	2925-2857	1627	Covered with broad band	1503	1157
13	L3-Cu(Cl) <sub>2</sub> .2H <sub>2</sub> O (in-situ)	3428	3296-3225	2950	1585	581	1489	1152
14	L3-Co(Cl) <sub>2</sub> .6H <sub>2</sub> O (in-situ)	3549	3417-3285	2928	1591	596	1489	1155
15	L3-Ni(Cl) <sub>2</sub> .6H <sub>2</sub> O (in-situ)	3565	3318-3247	2945	1588	587	1490-1448	1133
16	L3-Cu(Cl) <sub>2</sub> .2H <sub>2</sub> O	3439	3340-3323	2928	1607	Covered with broad band	1459	1155
17	L3-Co(Cl) <sub>2</sub> .6H <sub>2</sub> O	3549	3395-3082	2906	1593	590	1481	1160
18	L3-Ni(Cl) <sub>2</sub> .6H <sub>2</sub> O	3587	3280	2840	1588	Covered with broad band	1511	1149



The  $\beta$ -enaminone ligands and its complexes were very stable at room temperature as solid. The ligand was soluble in common organic solvents, but its metal complexes were soluble only in DMSO except complexes 1, 2, 3, 4, 5, 6, 8, 11, 12, 17, 18. They were soluble also in water.

Table 9. Solubilities of all new compounds

		Water	Methanol	Ethanol	Ether	CH <sub>3</sub> CN	CHCl <sub>3</sub>	CCl <sub>4</sub>	DMSO	THF
	<b>L1</b>	IS	S	S	IS	IS	IS	IS	S	S
	<b>L2</b>	IS	S	S	IS	IS	IS	IS	S	S
	<b>L3</b>	IS	S	S	IS	IS	IS	IS	S	S
<b>1</b>	<b>L1-(Cu(Cl)<sub>2</sub>.2H<sub>2</sub>O)<sub>2</sub> (in-situ)</b>	S	$\delta$	IS	IS	IS	IS	IS	S	IS
<b>2</b>	<b>L1-(Co(Cl)<sub>2</sub>.6H<sub>2</sub>O)<sub>2</sub> (in-situ)</b>	S	$\delta$	IS	IS	IS	IS	IS	S	IS
<b>3</b>	<b>L1-(Ni(Cl)<sub>2</sub>.6H<sub>2</sub>O)<sub>2</sub> (in-situ)</b>	S	$\delta$	IS	IS	IS	IS	IS	S	IS
<b>4</b>	<b>L1-(Cu(Cl)<sub>2</sub>.2H<sub>2</sub>O)<sub>2</sub></b>	S	$\delta$	IS	IS	IS	IS	IS	S	IS
<b>5</b>	<b>L1-(Co(Cl)<sub>2</sub>.6H<sub>2</sub>O)<sub>2</sub></b>	S	$\delta$	IS	IS	IS	IS	IS	S	IS
<b>6</b>	<b>L1-(Ni(Cl)<sub>2</sub>.6H<sub>2</sub>O)<sub>2</sub></b>	S	$\delta$	IS	IS	IS	IS	IS	S	IS
<b>7</b>	<b>L2-Cu(Cl)<sub>2</sub>.2H<sub>2</sub>O (in-situ)</b>	IS	$\delta$	IS	IS	IS	IS	IS	S	IS
<b>8</b>	<b>L2-Co(Cl)<sub>2</sub>.6H<sub>2</sub>O (in-situ)</b>	S	$\delta$	IS	IS	IS	IS	IS	S	IS
<b>9</b>	<b>L2-Ni(Cl)<sub>2</sub>.6H<sub>2</sub>O (in-situ)</b>	IS	$\delta$	IS	IS	IS	IS	IS	S	IS
<b>10</b>	<b>L2-Cu(Cl)<sub>2</sub>.2H<sub>2</sub>O</b>	IS	$\delta$	IS	IS	IS	IS	IS	S	IS
<b>11</b>	<b>L2-Co(Cl)<sub>2</sub>.6H<sub>2</sub>O</b>	S	$\delta$	IS	IS	IS	IS	IS	S	IS
<b>12</b>	<b>L2-Ni(Cl)<sub>2</sub>.6H<sub>2</sub>O</b>	S	$\delta$	IS	IS	IS	IS	IS	S	IS
<b>13</b>	<b>L3-Cu(Cl)<sub>2</sub>.2H<sub>2</sub>O (in-situ)</b>	IS	$\delta$	IS	IS	IS	IS	IS	S	IS
<b>14</b>	<b>L3-Co(Cl)<sub>2</sub>.6H<sub>2</sub>O (in-situ)</b>	IS	$\delta$	IS	IS	IS	IS	IS	S	IS
<b>15</b>	<b>L3-Ni(Cl)<sub>2</sub>.6H<sub>2</sub>O (in-situ)</b>	IS	$\delta$	IS	IS	IS	IS	IS	S	IS
<b>16</b>	<b>L3-Cu(Cl)<sub>2</sub>.2H<sub>2</sub>O</b>	IS	$\delta$	IS	IS	IS	IS	IS	S	IS
<b>17</b>	<b>L3-Co(Cl)<sub>2</sub>.6H<sub>2</sub>O</b>	S	$\delta$	IS	IS	IS	IS	IS	S	IS
<b>18</b>	<b>L3-Ni(Cl)<sub>2</sub>.6H<sub>2</sub>O</b>	S	$\delta$	IS	IS	IS	IS	IS	S	IS

IS:insoluble; S: soluble;  $\delta$ : partially soluble

## 5. EXPERIMENTAL RESULTS AND DISCUSSION

### 5.1. Compound 3,3'-(2,2'-(ethane-1,2-diylbis(azanediy))bis(ethane-2,1-diyl))bis(azanediy))bis(5,5- dimethylcyclohex-2-enone) (L1)

Characterization of 3,3'-(2,2'-(ethane-1,2-diylbis(azanediy))bis(ethane-2,1-diyl))bis(azanediy))bis(5,5-dimethylcyclohex-2-enone) (L1) was achieved by elemental analysis, FT-IR, UV-VIS-NIR, LC-MS, <sup>1</sup>H-NMR, COSY and APT spectroscopies.

Schiff base L1 have three tautomers which were ketoimine, iminoenol and ketoamine ( $\beta$ -enaminone).

The IR spectrum of 3,3'-(2,2'-(ethane-1,2-diylbis(azanediy))bis(ethane-2,1-diyl))bis(azanediy))bis(5,5-dimethylcyclohex-2-enone) (L1) shows two bands at 3324 and 3290  $\text{cm}^{-1}$  for N-H stretching of enamine and amine, at 2880-3100  $\text{cm}^{-1}$  for aliphatic C-H stretching, at 1667  $\text{cm}^{-1}$  for C=O stretching of enaminone, 1400-1550 for  $\text{CH}_2$  bending and at 1143  $\text{cm}^{-1}$  for C-N bending of enamine (Figure 8).

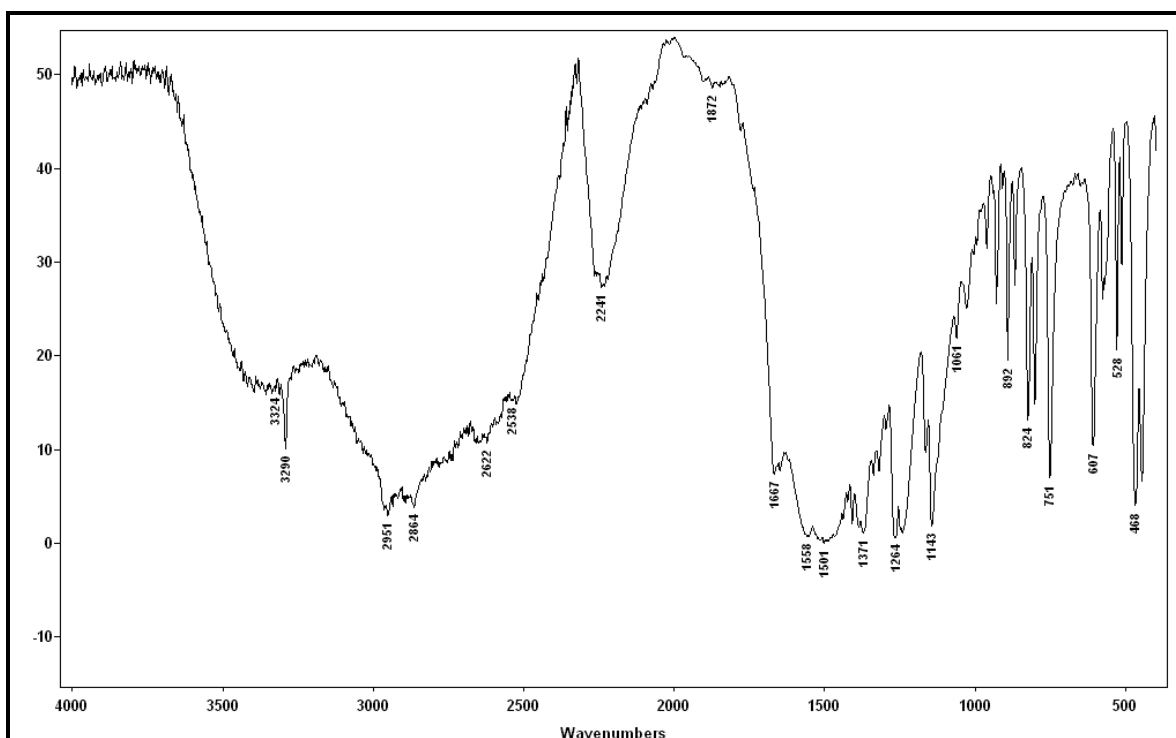


Figure 8. The IR spectrum of 3,3'-(2,2'-(ethane-1,2-diylbis(azanediy)) bis(ethane-2,1-diyl))bis(azanediy))bis(5,5-dimethylcyclohex-2-enone) (L1)

The  $^1\text{H-NMR}$  spectra of the  $\beta$ -enaminone was recorded in  $\text{DMSO-d}_6$ .  $\beta$ -enaminone (L1) showed four singlets at 0.96 ppm ( $\text{CH}_3$ ; 12H) **(1)**, 1.95 ppm ( $\text{CH}_2$ ; 4H) **(3)**, 2.18 ppm ( $\text{CH}_2$ , 4H) **(7)**, 2.68 (m, 4H,  $\text{CH}_2$ ) **(8)**, 3.03 (m, 4H,  $\text{CH}_2$ ) **(9)** and 4.82 ppm (vinylic  $\text{CH}$ ; 2H) **(5)** which corresponded to the cyclohexane group. A peak appears at 1.95 ppm was probably due to the methylene ( $-\text{C}(=\text{O})-\text{CH}_2-\text{C}(\text{CH}_3)_2$ ; 4H) protons. One further signal at 2.18 ppm, corresponded to methylene protons adjacent to the nitrogen atom at the  $\beta$ -position ( $-\text{HC}=\text{C}(\text{N})-\text{CH}_2-\text{C}(\text{CH}_3)_2$ ; 4H). The vinylic protons appeared at 4.82 ppm. Enamine NH protons appeared at 6.86 ppm. The single peak belonging to four protons, assigned with number 10, was not observed because its exact place was under DMSO peak. DMSO was the solvent which could dissolve the ligand. (Figure 9)

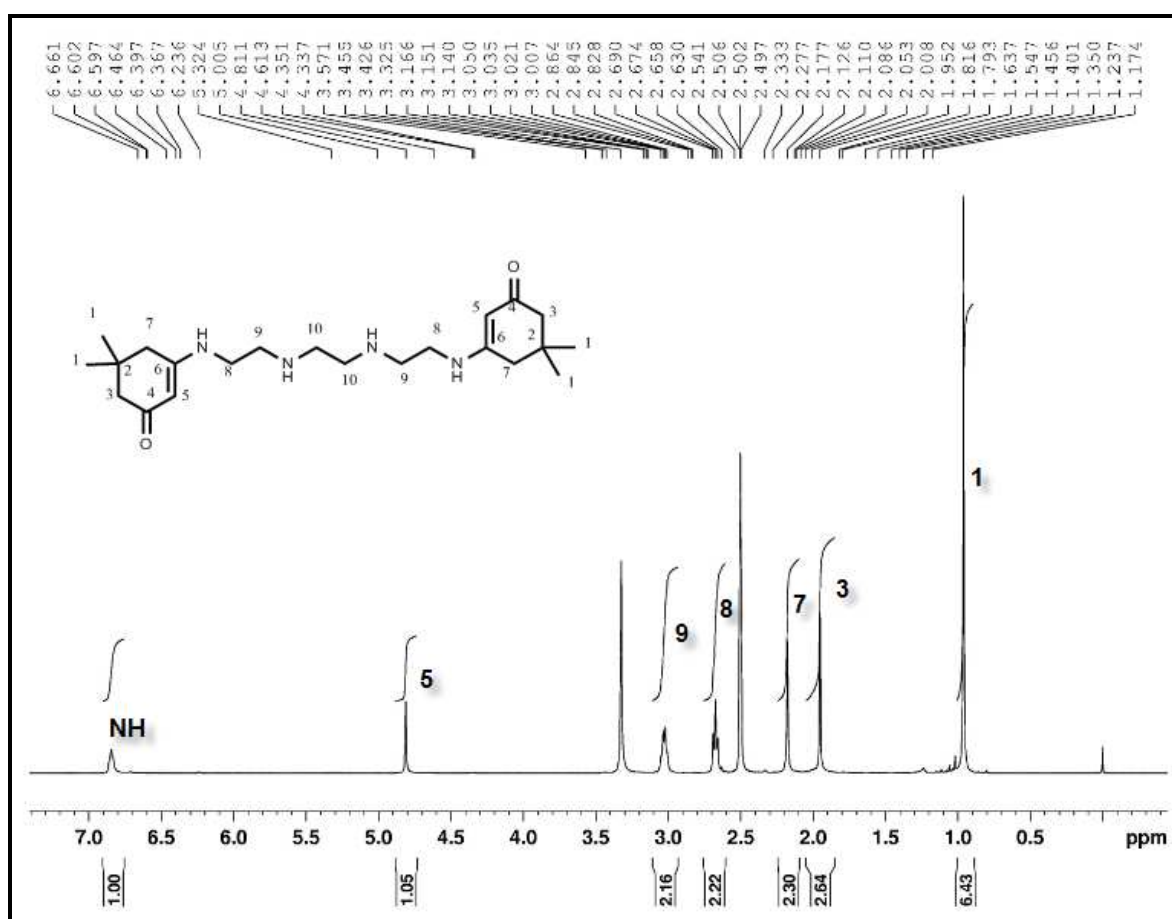


Figure 9. The  $^1\text{H-NMR}$  spectrum of 3,3'-(2,2'-(ethane-1,2-diylbis(azanediyl))bis(ethane-2,1-diyl))bis(azanediyl)bis(5,5-dimethylcyclohex-2-enone) (L1)

In the APT spectrum of compound L1 a signal at 28.45 ppm belonged to methyl carbons (**1**). The methylene carbons of cyclohexane ring appeared at 42.77 ppm (**7**), 47.32 ppm (**3**), and the methine carbon (**2**) appeared at 32.68 (C(CH<sub>3</sub>)<sub>2</sub>). The signals at 42.53, 50.75 and 52.29 ppm (**8**, **9**, **10**) belonged to the methylene carbons which were between two amine groups respectively. Vinylic methine carbon (**5**) showed a signal at 93.71 ppm. The signal at 194.33 ppm was due to ketone carbon (**4**) and the signal at 163.41 ppm belonged to enamine carbon (**6**) which was next to amine group (Figure 10).

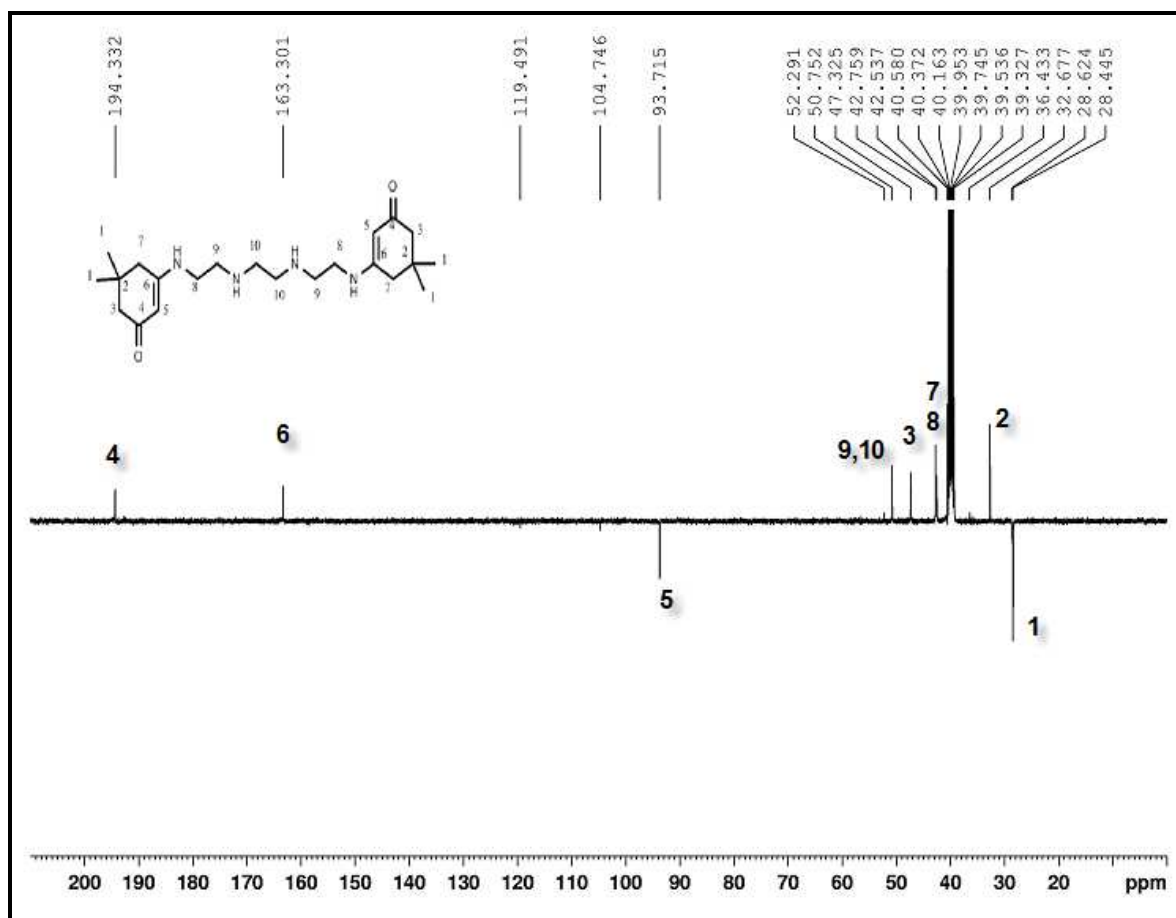


Figure 10. The APT spectrum 3,3'-(2,2'-(ethane-1,2-diylbis(azanediyl))bis(ethane-2,1-diyl))bis(azanediyl)bis(5,5-dimethylcyclohex-2-enone) (L1)

The UV spectrum of 3,3'-(2,2'-(ethane-1,2-diylbis(azanediyl))bis(ethane-2,1-diyl))bis(azanediyl)bis(5,5-dimethylcyclohex-2-enone) (L1) had four bands at 219 nm, 255 nm 287 nm ( $\pi$ - $\pi^*$ ) and 422 nm ( $n$ - $\pi^*$ ) (Figure 11).

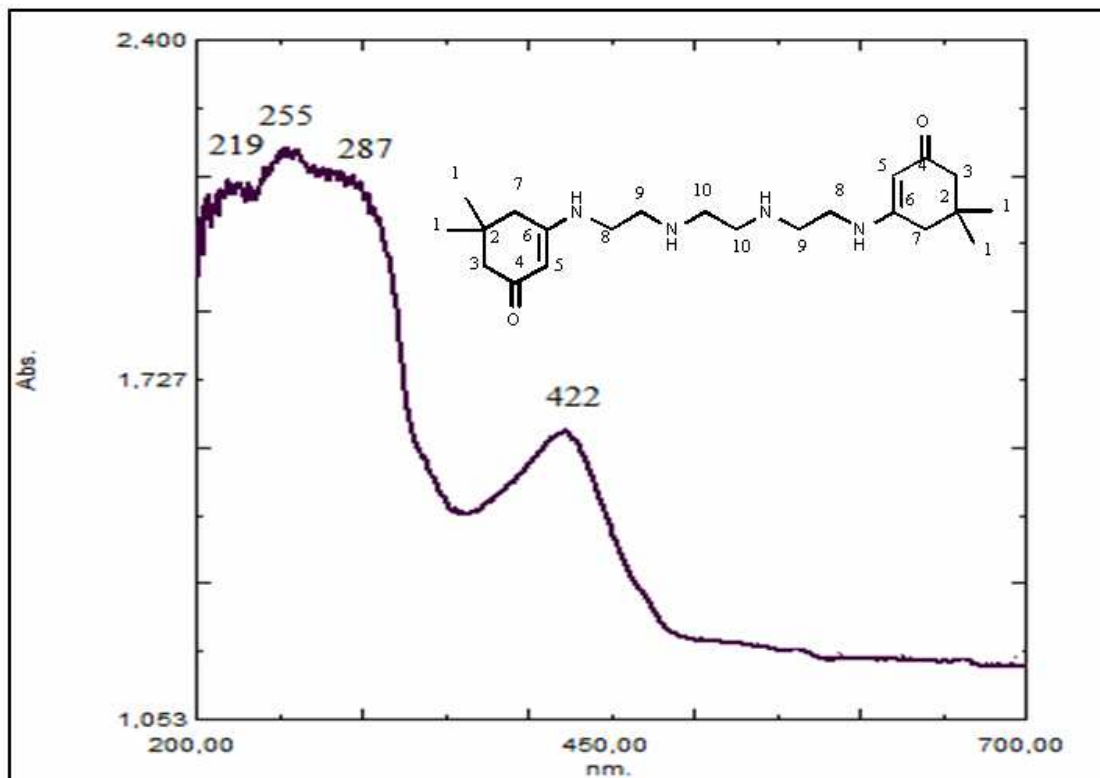


Figure 11. The UV spectrum of 3,3'-(2,2'-(ethane-1,2-diylbis(azanediyloxy))bis(ethane-2,1-diyl))bis(azanediyloxy)bis(5,5-dimethylcyclohex-2-enone) (L1)

The LC-MS spectrum of 3,3'-(2,2'-(ethane-1,2-diylbis(azanediyloxy))bis(ethane-2,1-diyl))bis(azanediyloxy)bis(5,5-dimethylcyclohex-2-enone) (L1) had three signals. The signals at 392.3, 393.3, and 394.3 belonged to molecular ion  $[M+2H]^+$ ,  $[M+3H]^+$  and  $[M+4H]^+$  respectively (Figure 12).

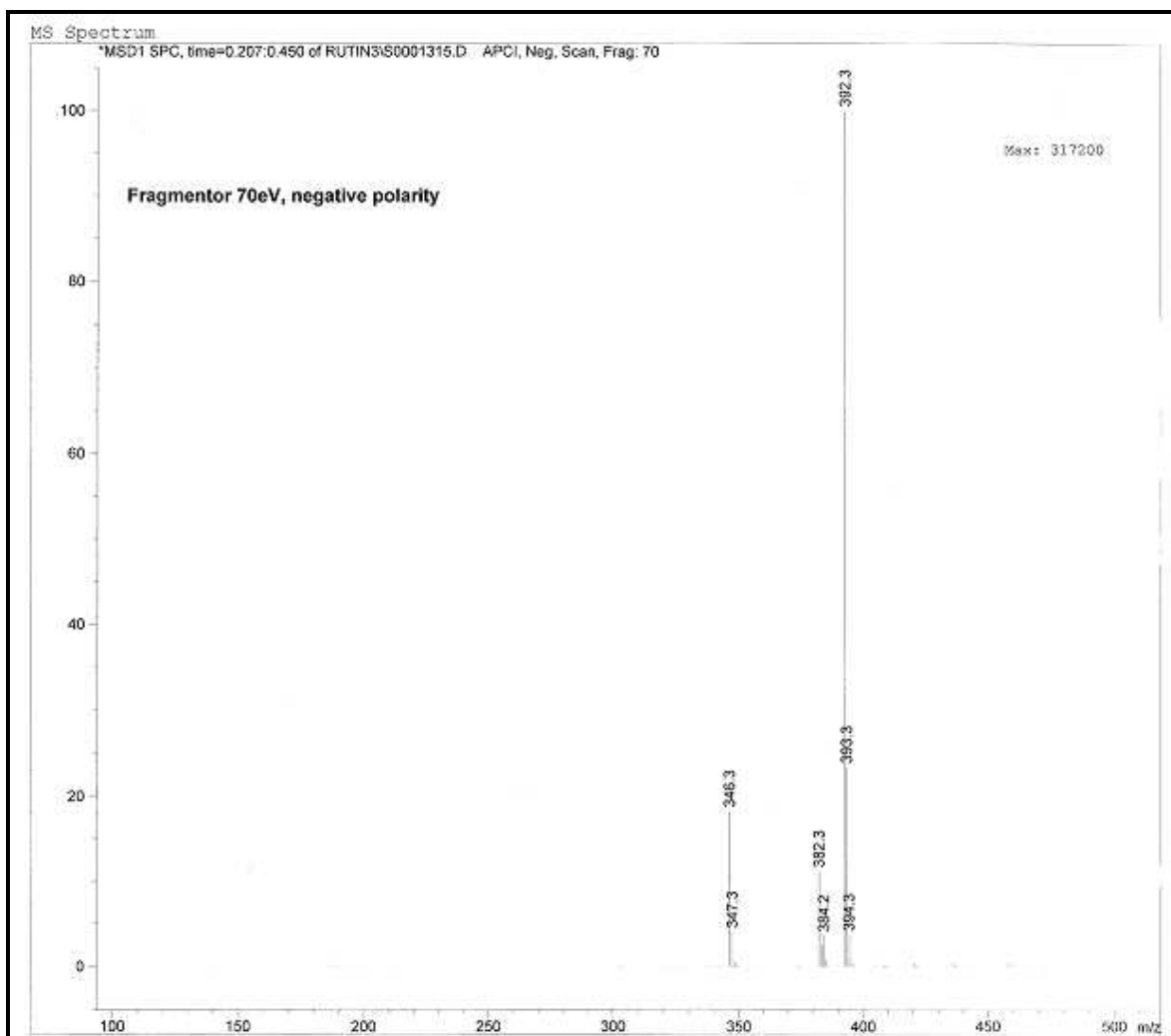


Figure 12. The LC-MS spectrum of 3,3'-(2,2'-(ethane-1,2-diylbis(azanediyl)) bis (ethane-2,1-diyl))bis(azanediyl)bis (5,5-dimethylcyclohex -2-enone) (L1)

Table 10. L1 COSY Hydrogen-interaction data

<sup>1</sup> H	δ ( ppm )	H-H COSY
1	0.96	-
3	1.96	7
7	2.18	3
8	2.68	9
9	3.04	8
5	4.82	-
NH	6.85	-

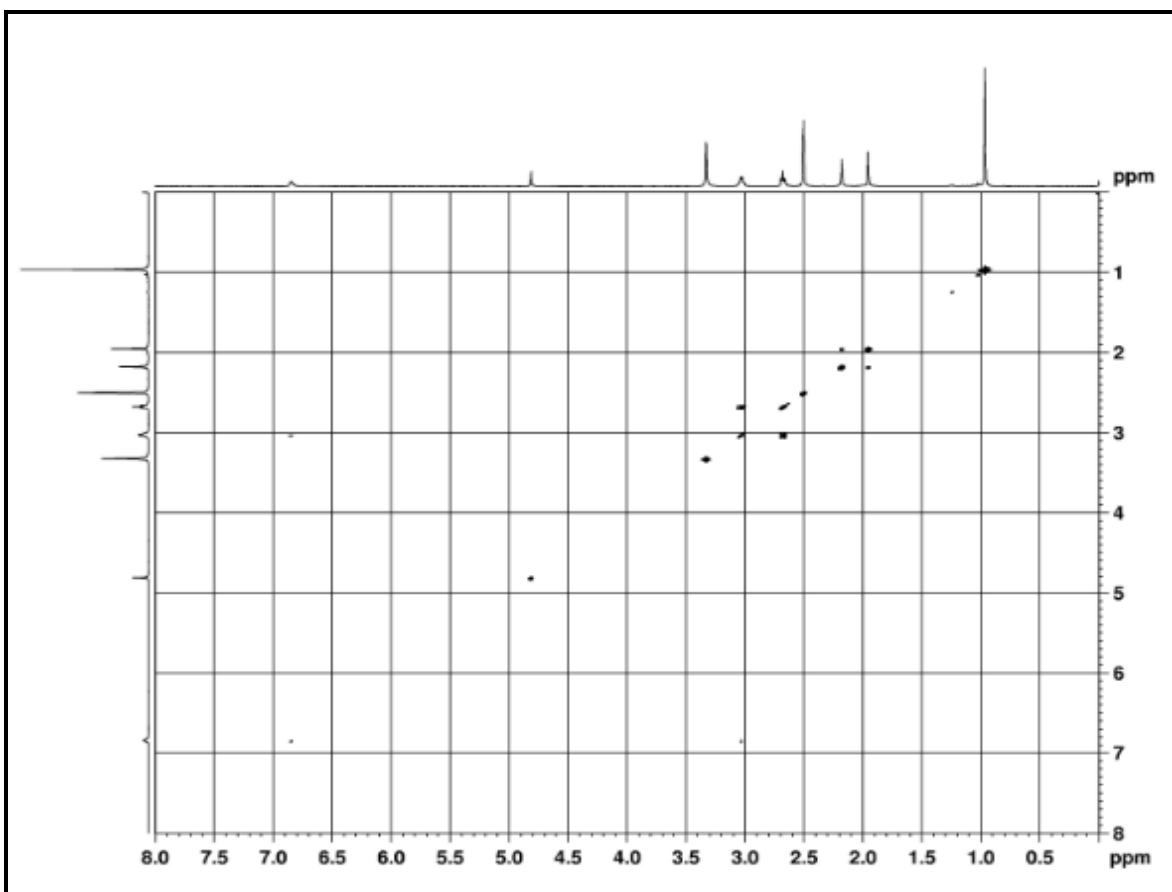
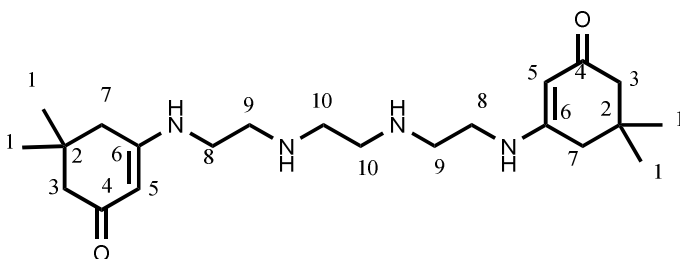


Figure 13. The COSY spectrum of 3,3'-(2,2'-(ethane-1,2-diylbis(azanediyl))bis(ethane-2,1-diyl))bis(azanediyl)bis(5,5-dimethylcyclohex-2-enone) (L1)



$^1\text{H}$  NMR spectra of  $\beta$ -enaminones show the signals of the vinyl protons between  $\delta=4.5\text{-}5.5$  ppm. The E-enaminone forms exhibited NH resonances in the range  $\delta=3.5\text{-}8.5$  ppm due to the strong intermolecular hydrogen bonding between the NH proton and the carbonyl oxygen. The  $^{13}\text{C}$  NMR spectra of these compounds reveal signals in the range  $\delta = 93\text{-}98$  ppm for vinyl carbon and  $\delta= 193\text{-}198$  ppm for carbonyl carbon. This proves that the carbonyl group is conjugated with the enamine group. In the IR spectra of the above compounds, the carbonyl band appears in the range of  $1620\text{-}1600\text{ cm}^{-1}$  and there is no band at  $1720\text{ cm}^{-1}$  which

indicates that the carbonyl bond is conjugated with the carbon-carbon double bond.

## 5.2 Compound 3,3'-(cyclohexane-1,3-diylbis(methylene))bis(azanediyl) bis(5,5dimethylcyclohex-2-enone) (L2)

Characterization of 3,3'-(cyclohexane-1,3-diylbis(methylene)) bis(azanediyl)bis(5,5dimethyl cyclohex-2-enone) (L2) was achieved by FT-IR, UV-VIS-NIR, LC-MS, <sup>1</sup>H-NMR and APT spectroscopy.

The IR spectrum of L2 showed bands at 3263 cm<sup>-1</sup> for N-H stretching of enamine, at 2880-3100 cm<sup>-1</sup> for aliphatic C-H stretching, at 1593 cm<sup>-1</sup> for C=O stretching of enamino, 1400-1500 for CH<sub>2</sub> bending and at 1149 cm<sup>-1</sup> for C-N bending of enamine (Figure 14).

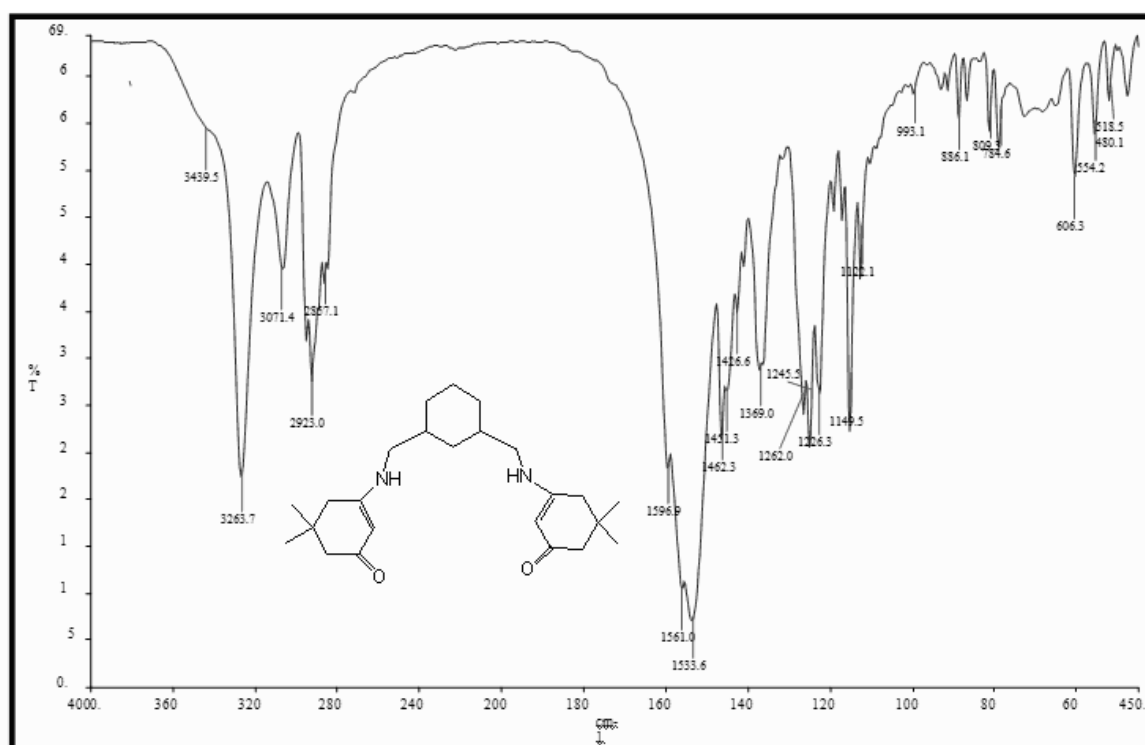


Figure 14. The IR spectrum of 3,3'-(cyclohexane-1,3-diylbis(methylene)) bis(azanediyl) bis(5,5dimethylcyclohex-2-enone) (L2)



The  $^1\text{H-NMR}$  spectrum of compound **L2** showed a singlet at 0.96 ppm for methyl protons (**1**) of dimedone. The multiplet at 1.21 ppm (**11**), 1.38 ppm (**10**) and a triplet at 1.55 ppm (**12**) were due to the methylene protons and a multiplet at 1.72 ppm was due to the methine proton (**9**) of cyclohexane ring. Methylene protons of dimedone (**2 and 6**) gave two singlets at 1.95 ppm and 2.18 ppm respectively. The doublet at 2.82 ppm belonged to the methylene protons (**8**) between cyclohexane ring and amine group. The broad band at 3.58 ppm belonged to NH protons of enamine group. Vinylic CH (**4**) gave a singlet at 4.80 ppm (Figure 15).

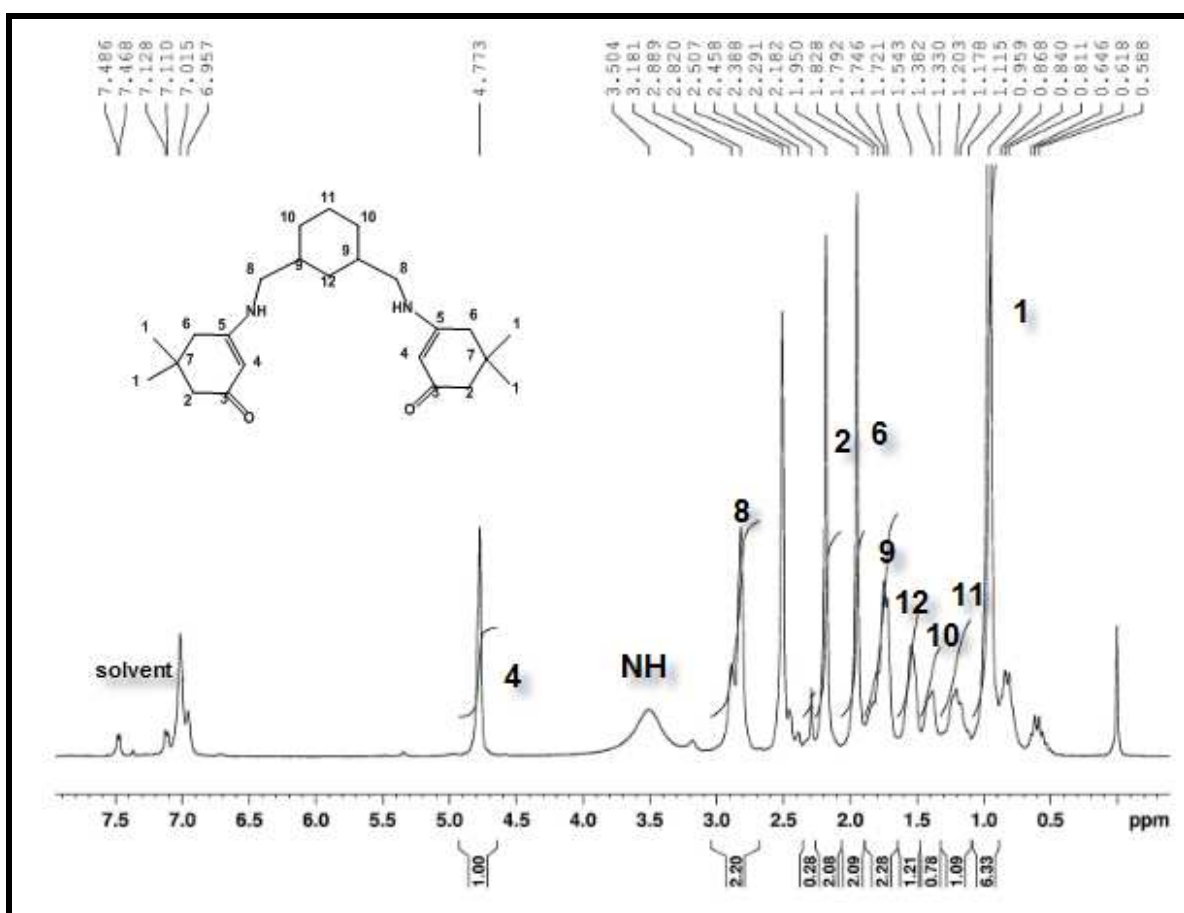


Figure 15. The  $^1\text{H-NMR}$  spectrum of 3,3'-(cyclohexane-1,3-diylbis(methylene)) bis(azanediyl) bis(5,5dimethylcyclohex-2-enone) **L2**

The APT spectrum of compound **L2** exhibited a signal at 28.47 ppm for the methyl carbon (**1**). The methylene carbon of cyclohexane ring appeared at

25.42 ppm (**11**), 30.88 ppm (**10**), and the methine carbon (**9**) appeared at 36.45 ppm. The signals at 49.078 ppm (**8**) belonged to the methylene carbon which was between cyclohexane ring and amine group. The methylene carbons of cyclohexanone showed signals at 42.54 ppm (allylic carbon) (**6**) and 50.75 ppm (**2**) and tertiary carbon at 32.67 ppm (**7**), respectively. Vinylic methine carbon (**4**) showed a signal at 93.66 ppm. The signal at 194.11 ppm was due to ketone carbon (**3**) and the signal at 163.41 ppm belonged to enamine carbon (**5**) which was next to amine group (Figure 16).

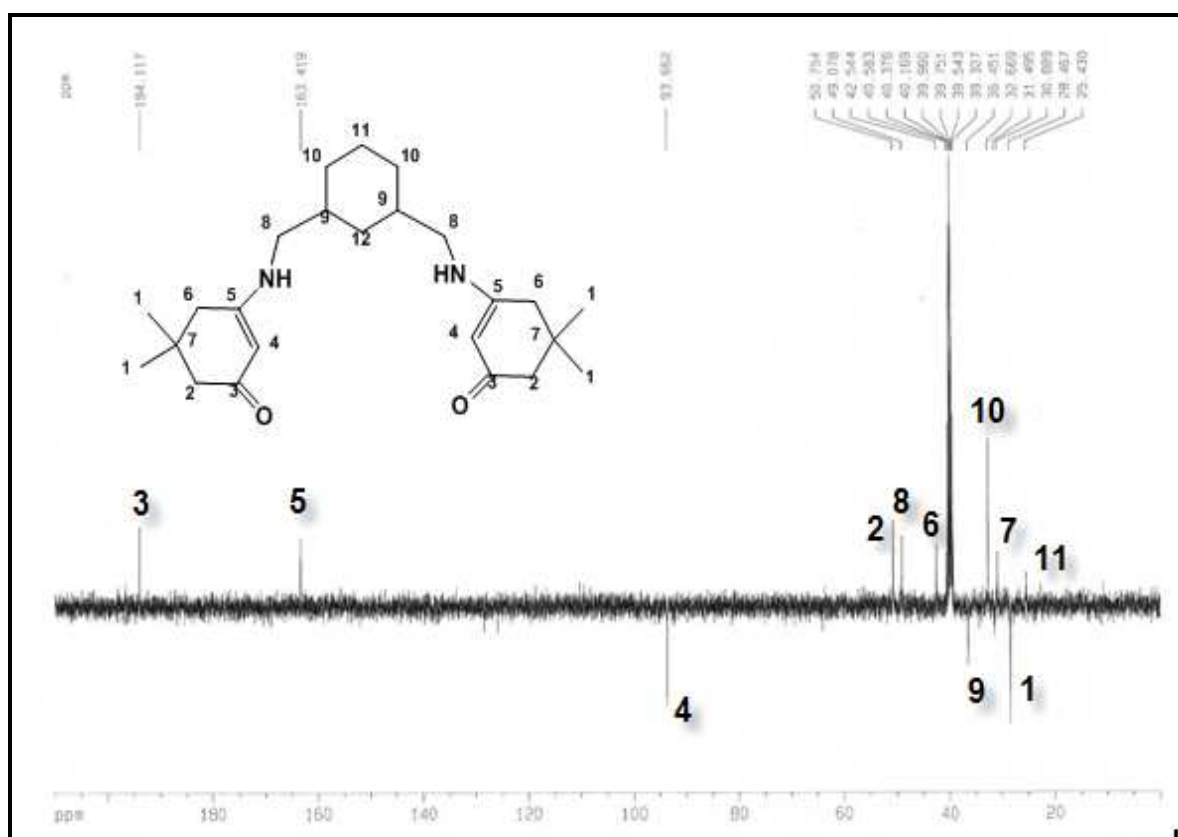


Figure 16. The APT spectrum of 3,3'-(cyclohexane-1,3-diylbis(methylene))bis(azanediy) bis(5,5dimethylcyclohex-2-enone) (**L2**)

The UV spectrum of 3,3'-(cyclohexane-1,3-diylbis(methylene))bis(azanediy)bis(5,5dimethyl cyclohex-2-enone) (**L2**) has four bands at 218 nm, 262 nm 314 nm ( $\pi$ - $\pi^*$ ) and 425 ( $n$ - $\pi^*$ ) nm (Figure 17).

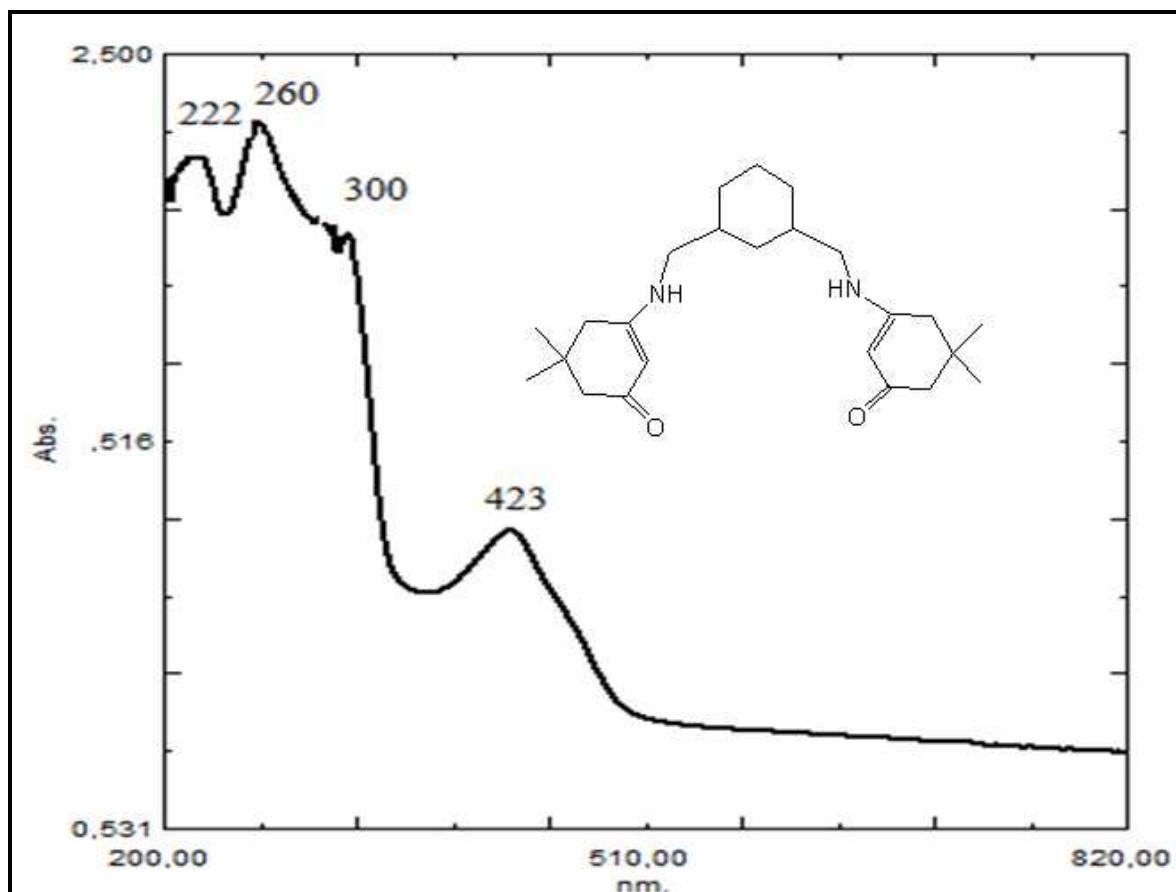


Figure 17. The UV spectrum of 3,3'-(cyclohexane-1,3-diylbis(methylene)) bis(azanediyl) bis(5,5dimethyl cyclohex-2-enone) (L2)

The LC-MS spectrum of 3,3'-(cyclohexane-1,3-diylbis(methylene))bis(azanediyl) bis (5,5dimethylcyclohex-2-enone) (**L2**) had three signals. The signal at 387.3 belonged to molecular ion  $[M+1H]^+$ . The loss of  $C_8H_{11}O$  group from  $[M]^+$  was proved by the  $m/z$ : 265.2  $[M - C_8H_{11}O]^+$ , the loss of  $C_{16}H_{22}O_2$  group from  $[M]^+$  was proved by the  $m/z$ : 140.1  $[M - C_{16}H_{22}O_2]^+$  (Figure 18).

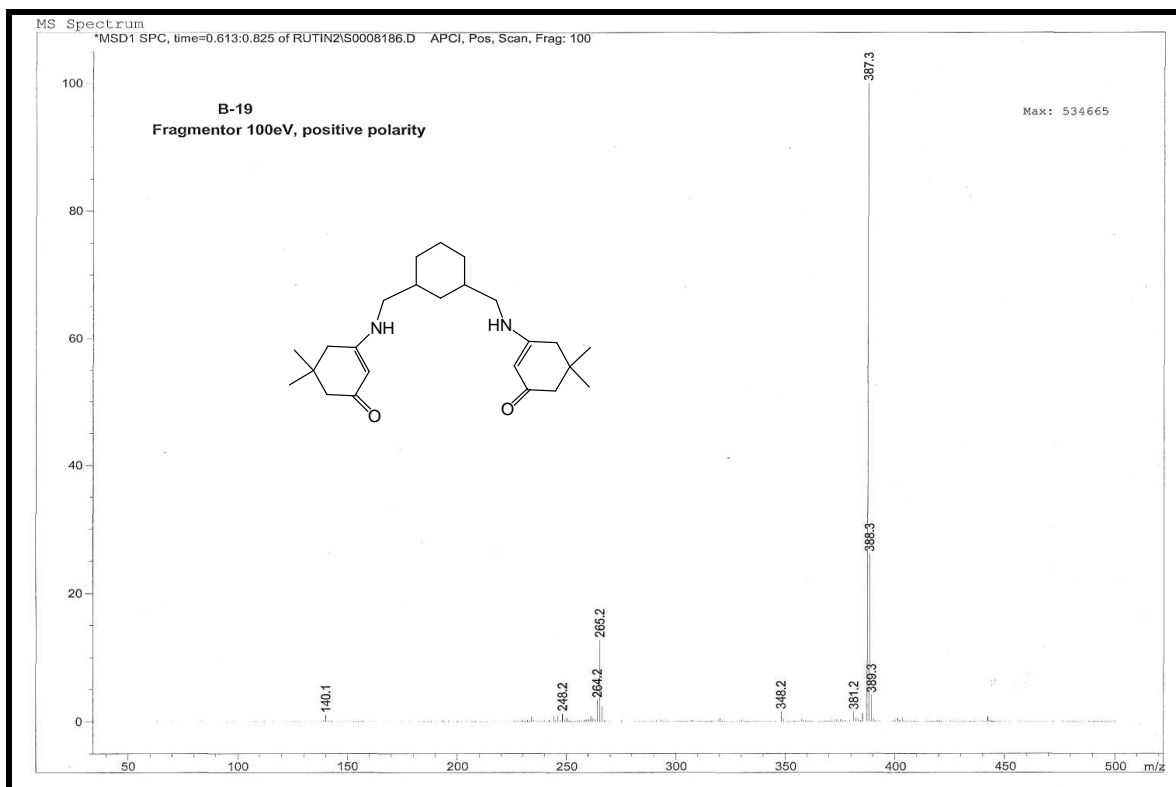


Figure 18. The LC-MS spectrum of 3,3'-(cyclohexane-1,3-diylbis(methylene)) bis(azanediy) bis(5,5dimethylcyclohex-2-enone) L2

Table 11. L3 COSY Hydrogen-interaction data

<sup>1</sup> H	δ ( ppm )	H-H COSY
1	0.96	-
11	1.21	10
10	1.38	11, 9
12	1.55	9
9	1.72	10, 12, 8
2	1.95	6
6	2.18	2
8	2.82	9
4	4.80	-
NH	3.58 Broad band	-

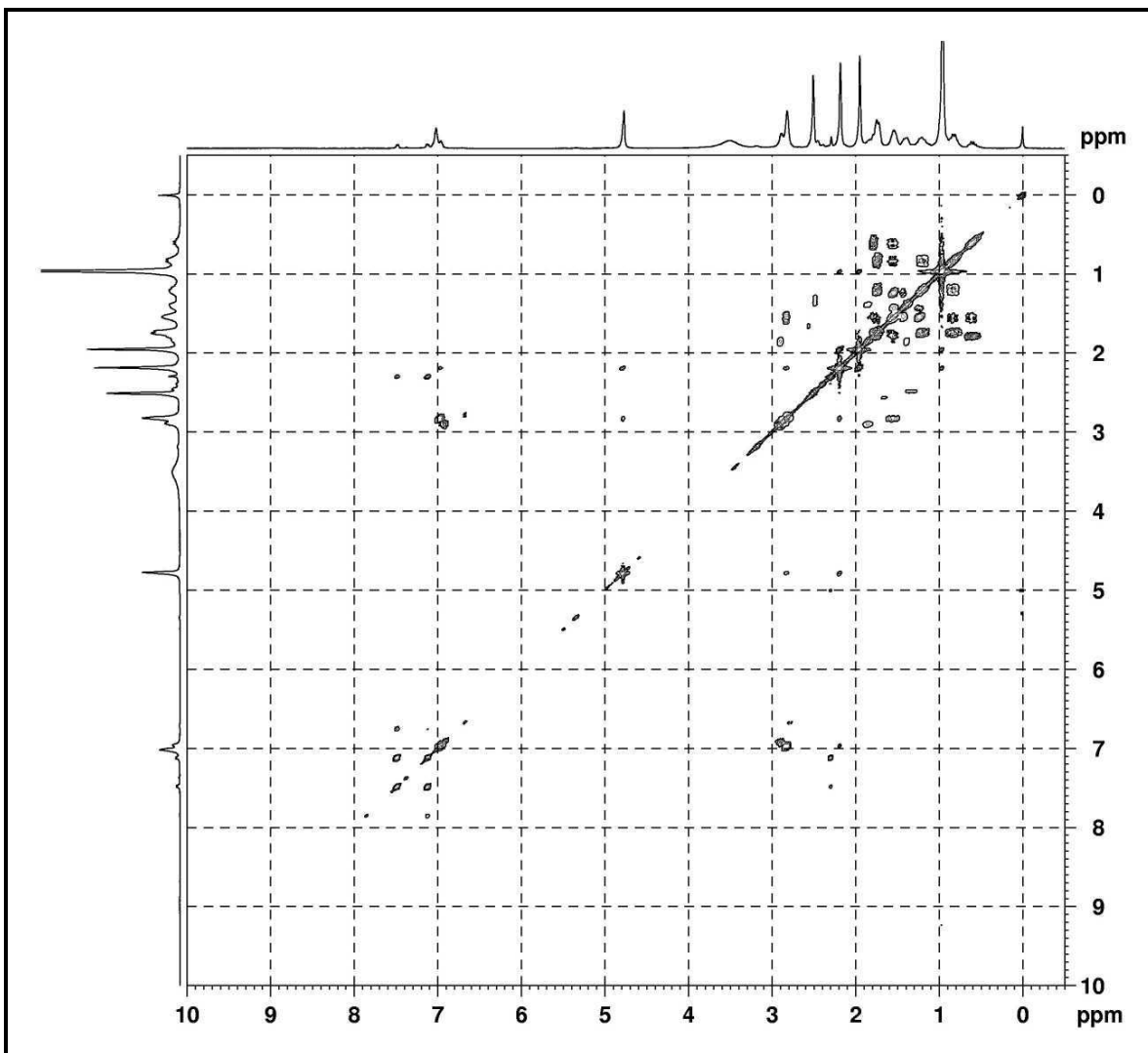
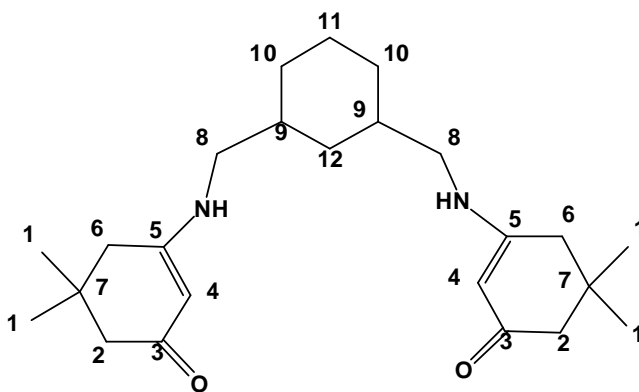


Figure 19. The COSY spectrum of 3,3'-(cyclohexane-1,3-diylbis(methylene)) bis (azanediy)bis(5,5dimethylcyclohex-2-enone) (L2)



### 5.3. Compound 3,3'-(1,3-phenylenebis(methylene))bis(azanediyl) bis(5,5-dimethyl cyclo hex-2-enone) (L3)

Characterization of 3,3'-(1,3-phenylenebis(methylene))bis(azanediyl) bis(5,5-dimethylcyclohex-2-enone) **L3** was achieved by FT-IR, UV-VIS-NIR, LC-MS, <sup>1</sup>H-NMR and APT spectroscopy.

The IR spectrum of **L3** showed bands at 3252 cm<sup>-1</sup> for N-H stretching of enamine, at 2880-3100 cm<sup>-1</sup> for aliphatic and aromatic C-H stretching, at 1662 cm<sup>-1</sup> for C=O stretching of enamionone, 1450-1550 for CH<sub>2</sub> bending and at 1141 cm<sup>-1</sup> for C-N bending of enamine (Figure 20).

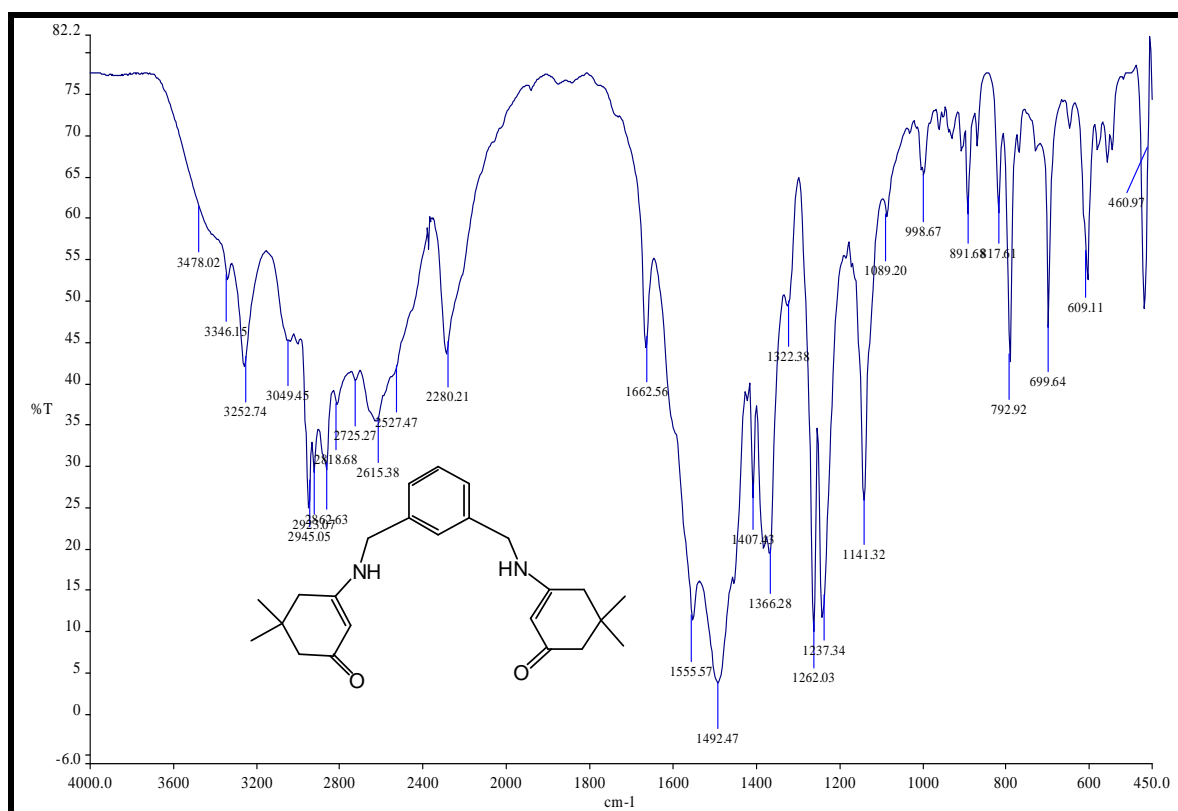


Figure 20. The IR spectrum of 3,3'-(1,3-phenylenebis(methylene))bis(azanediyl) bis(5,5-dimethylcyclohex-2-enone) (**L3**)

The <sup>1</sup>H-NMR spectrum of compound L3 showed a singlet at 0.97 ppm for methyl protons (**1**) of dimedone. The singlets at 1.94 ppm (**2**) and 2.24 (**6**) ppm is due to the methylene proton of dimedone group. The broad band at 3.54 ppm for

enamine protons of NH group. The singlet at 4.21 ppm belonged to the methylene proton (**8**) between benzene ring and amine group. Vinylic CH (**4**) gave a singlet at 4.76 and the benzene ring gave doublet at 7.18ppm, triplet at 7.32 ppm and singlet at 7.54 ppm, respectively (Figure 21).

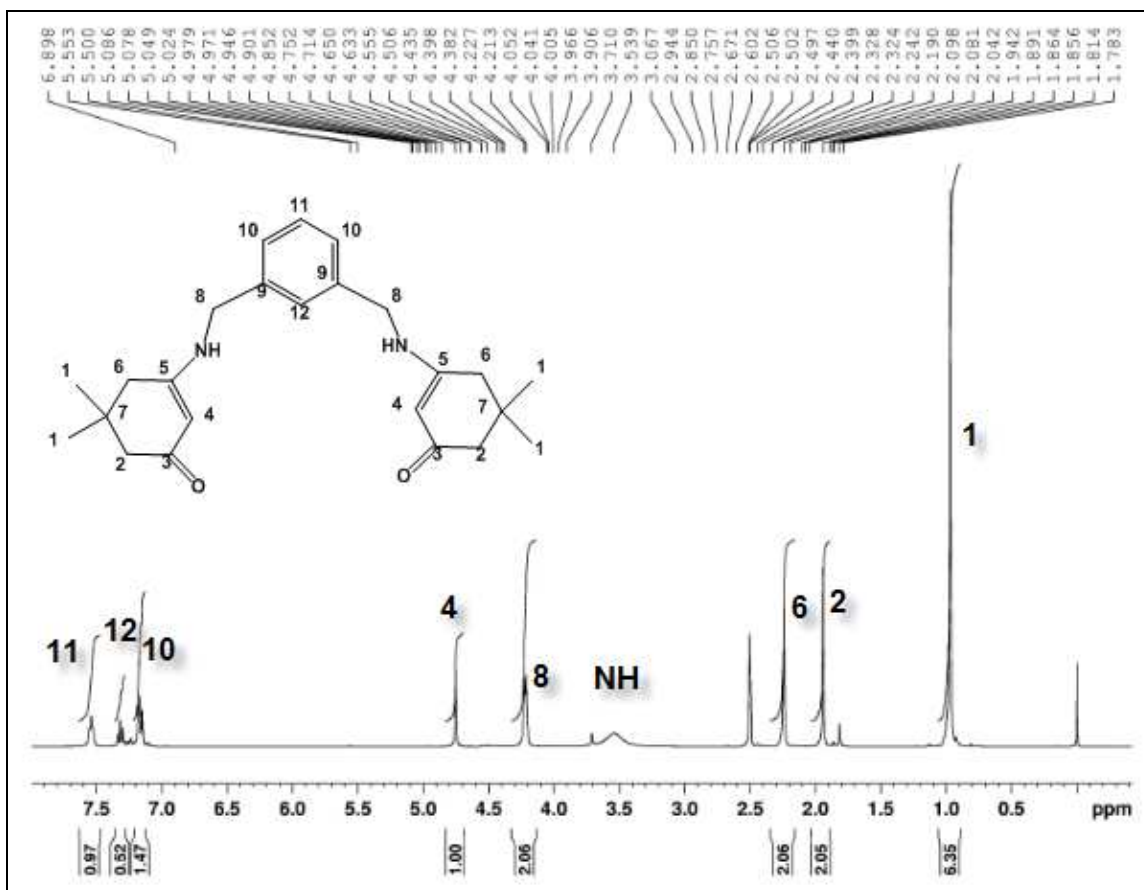


Figure 21: The <sup>1</sup>H-NMR spectrum of 3,3'-(1,3-phenylenebis (methylene)) bis(azanediyl) bis(5,5-dimethylcyclohex-2-enone) L3

The APT spectrum of compound L3 exhibited signal at 28.43 ppm for the methyl carbon (**1**). The methylene carbon (**7**) of cyclohexane ring appeared at 32.78 ppm and 42.45 ppm (**6**). The signals at 50.73 ppm belonged to the methylene carbon (**2**) which is between aromatic ring and amine group. The methine carbons (**8**) showed signal at 46.01 ppm. Vinylic methine carbon showed a signal at 94.68 ppm (**4**). The carbons of benzene ring exhibited signals at 126.12 ppm, 128.67 ppm, and 138.89 ppm. The signal at 194.44 ppm is due

to ketone carbon (**3**) and the signal at 163.41 ppm belonged to enamine carbon (**5**) which was next to amine group (Figure 22).

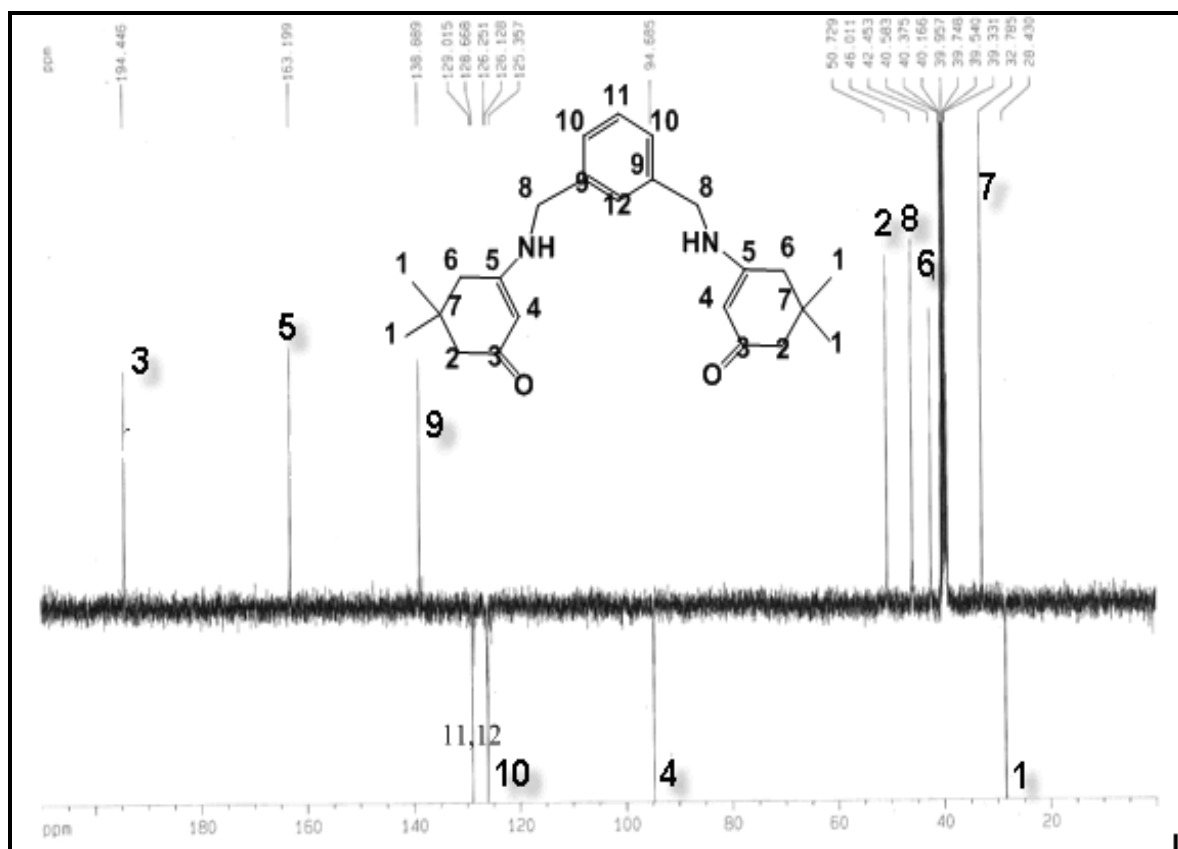


Figure 22. The APT spectrum of 3,3'-(1,3-phenylenebis(methylene))bis(azanediyl) bis(5,5-dimethylcyclohex-2-enone) (L3)

The UV spectrum of 3,3'-(1,3-phenylenebis(methylene))bis(azanediyl) bis(5,5-dimethylcyclohex-2-enone) **L3** had four bands at 219 nm, 261 nm, 312 nm ( $\pi$ - $\pi^*$ ) and 428 nm ( $n$ - $\pi^*$ ) (Figure 23).



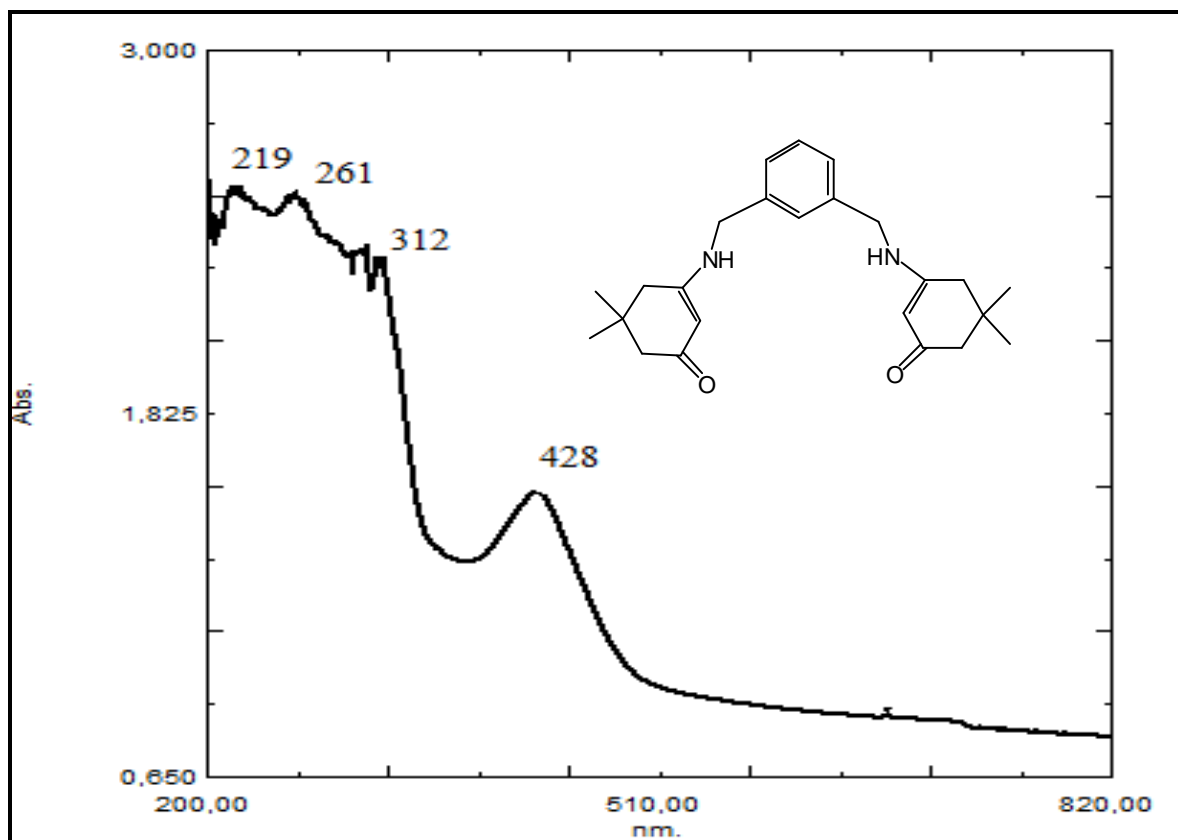


Figure 23. The UV spectrum of 3,3'-(1,3-phenylenebis(methylene))bis(azanediyl) bis(5,5-dimethylcyclohex-2-enone) (L3)

The LC-MS spectrum of 3,3'-(1,3-phenylenebis(methylene))bis(azanediyl) bis(5,5-dimethylcyclohex-2-enone) **L3** had three signals. The signal at 381.2 belonged to molecular ion  $[M+1H]^+$ . The loss of  $C_8H_{11}O$  group from  $[M]^+$  was proved by the  $m/z$ : 258.1  $[M- C_8H_{11}O]^+$ , the loss of  $C_{16}H_{20}NO$  group from  $[M]^+$  was proved by the  $m/z$ : 140.1  $[M- C_{16}H_{20}NO]^+$  (Figure 24).

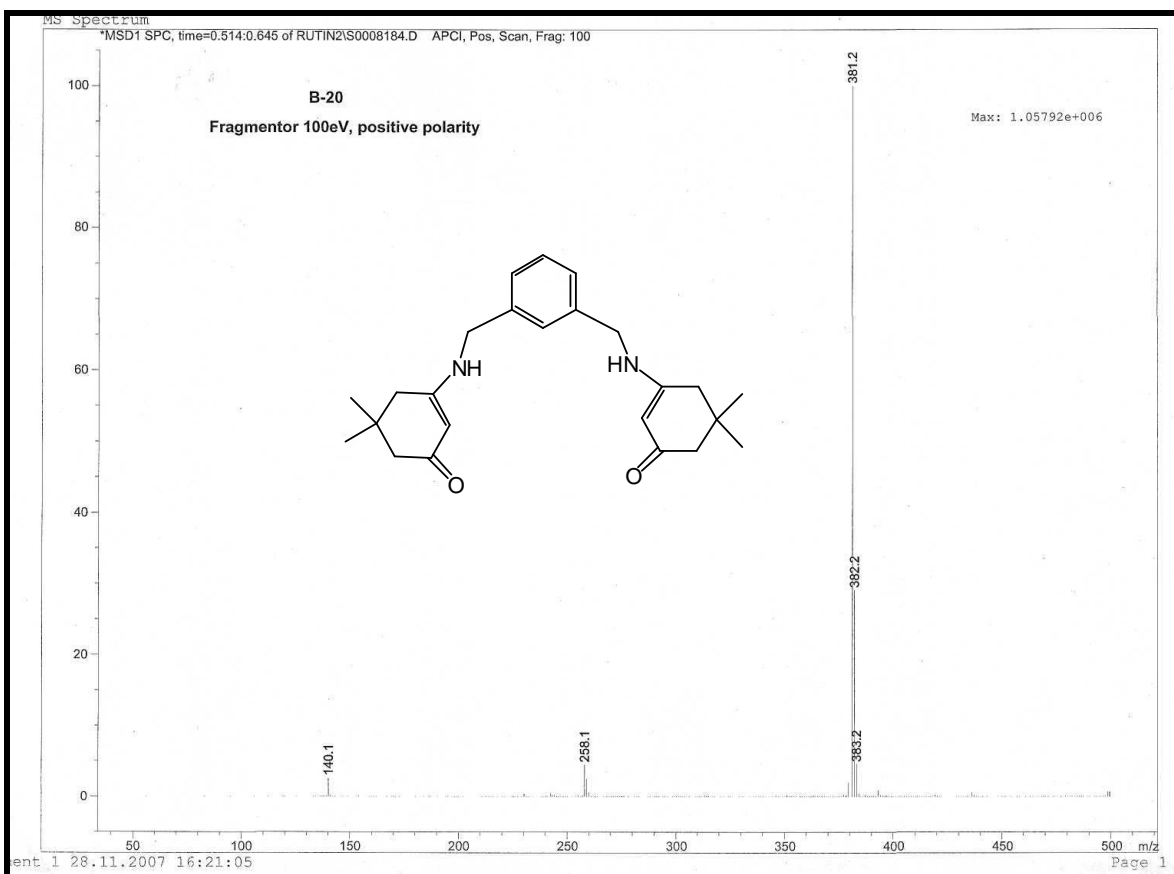


Figure 24. The LC-MS spectrum of 3,3'-(1,3-phenylenebis (methylene))bis (azanediy) bis(5,5-dimethylcyclohex-2-enone) (**L3**)

Table 12. L3 COSY Hydrogen-interaction data

<sup>1</sup> H	δ ( ppm )	H-H COSY
1	0.97	-
2	1.94	6
6	2.24	2
8	4.21	12
4	4.76	-
NH	3.54 Broad band	-
10	7.18	11
11	7.32	10
12	7.54	8

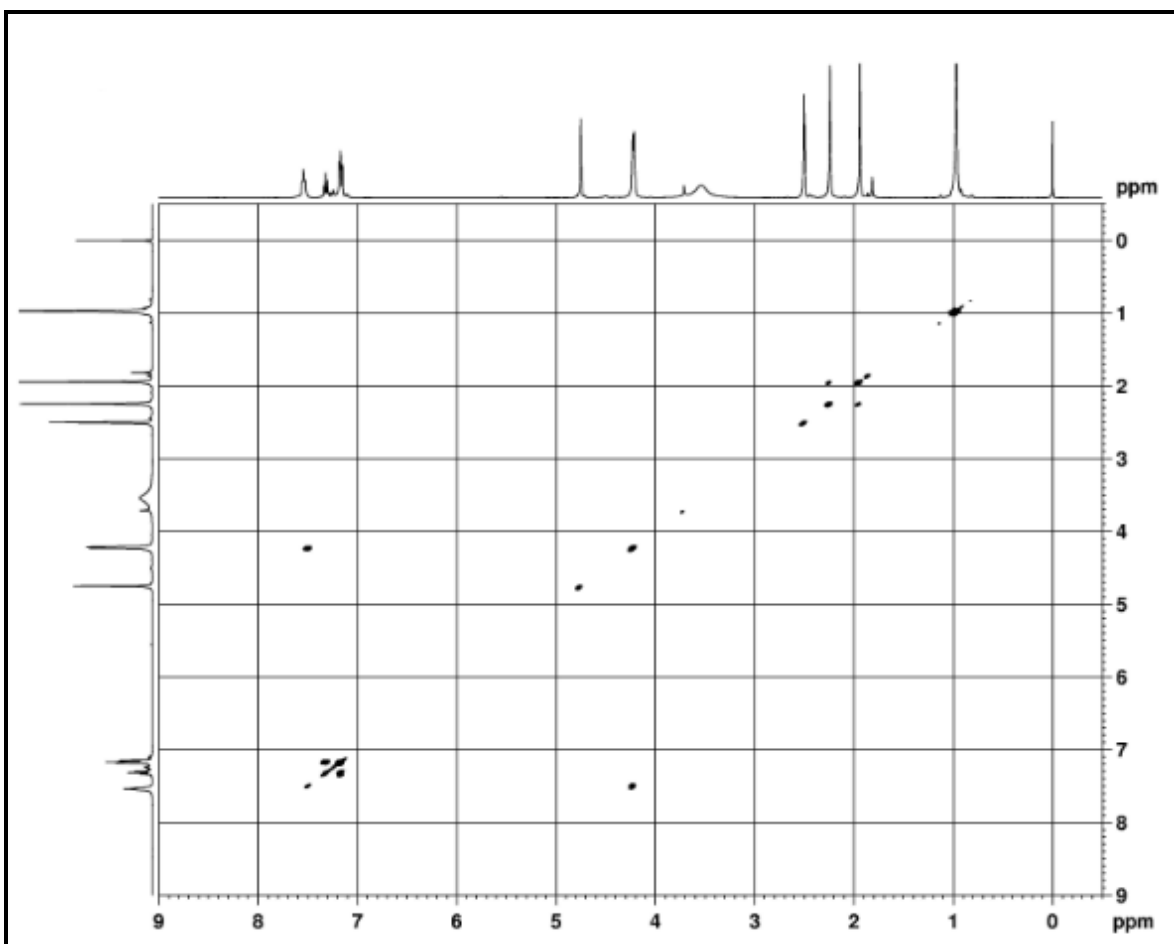
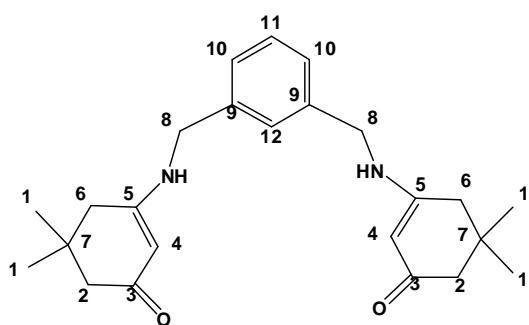


Figure 25. The COSY spectrum of 3,3'-(1,3-phenylenebis(methylene))bis (azanediy) bis(5,5-dimethylcyclohex-2-enone) (L3)



#### 5.4. Compound 5,5-dimethyl-3-(4-(phenylamino)phenylamino)cyclohex-2-enone (L4)

Characterization of 5,5-dimethyl-3-(4-(phenylamino)phenylamino)cyclohex-2-enone (L4) was achieved by FT-IR, UV-VIS-NIR,  $^1\text{H-NMR}$ , COSY and APT spectroscopy.

The IR spectrum of 5,5-dimethyl-3-(4-(phenylamino)phenylamino)cyclohex-2-enone (L4) showed bands at 3299 and 3222  $\text{cm}^{-1}$  for N-H stretching of enamine and amine, at 2880-3100  $\text{cm}^{-1}$  for aliphatic C-H stretching, at 1596  $\text{cm}^{-1}$  for C=O stretching of enaminone, 1400-1550 for  $\text{CH}_2$  bending and at 1152  $\text{cm}^{-1}$  for C-N bending of enamine (Figure 26).

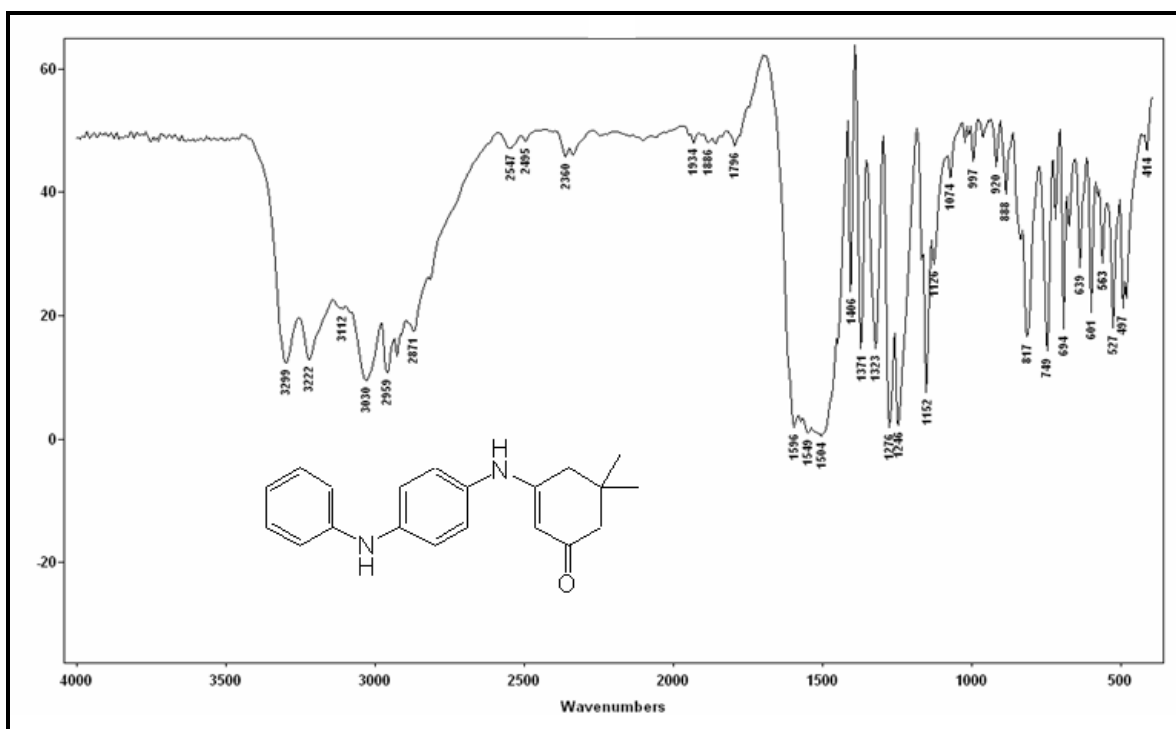


Figure 26. The IR spectrum of 5,5-dimethyl-3-(4-(phenylamino)phenylamino)cyclohex-2-enone (L4)

The  $^1\text{H-NMR}$  spectrum of compound **L4** showed a singlet at 1.04 ppm for methyl protons (**1**) of dimedone. The two singlets at 2.03 ppm (**7**), and 2.35ppm (**3**) were belonged to the methylene protons. Protons of aromatic benzene ring gave three multiple peak between 6.79 and 7.24 ppm (**9, 10, 11, 12, 13**). Vinylic CH (**5**) gave a singlet at 5.15 ppm. In the  $^1\text{H-NMR}$  spectrum of the compound, two small peak observed at 8.62 ppm (enamine **NH**) and 8.18 ppm (**NH** between two benzene) as a singlet were assigned to **NH** protons (Figure 27).

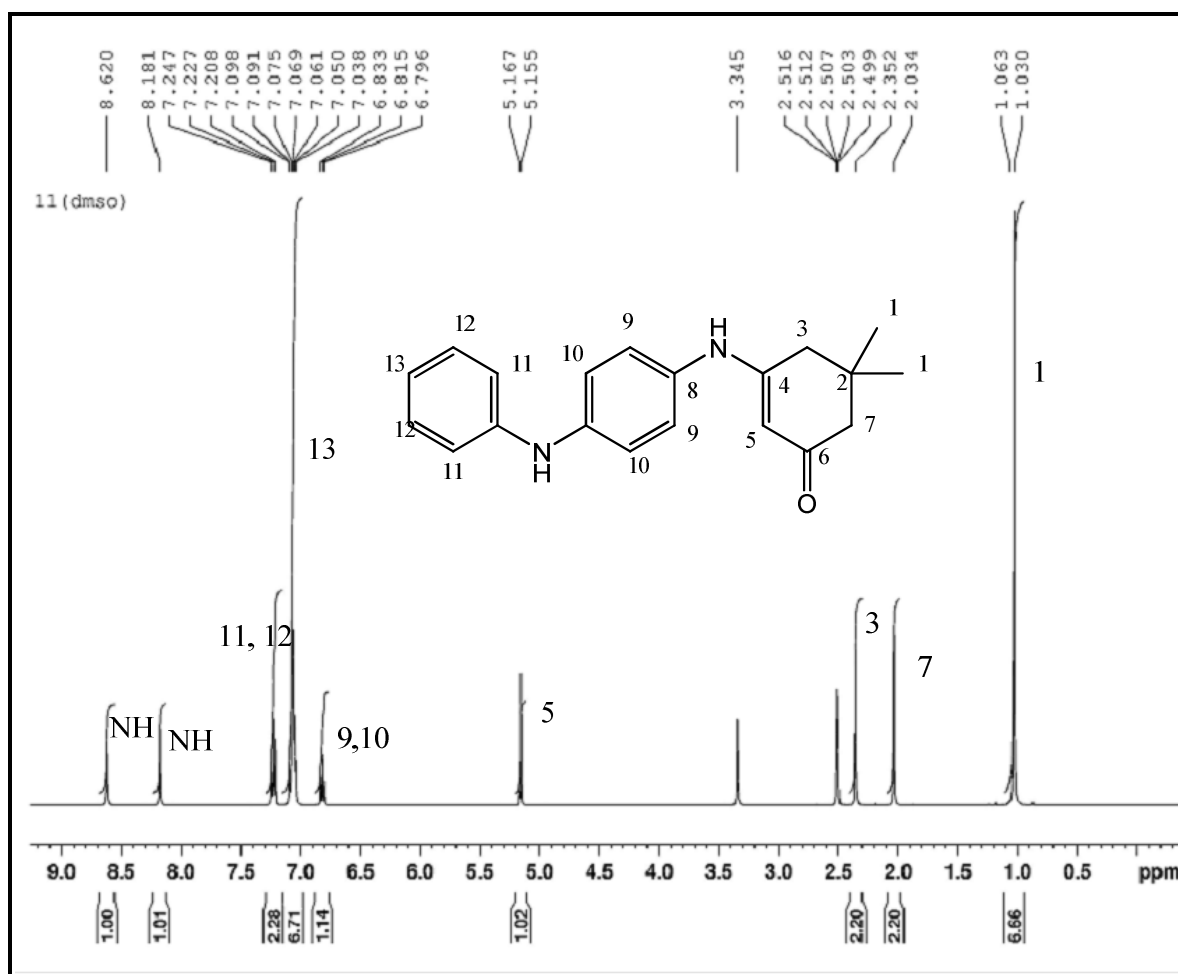


Figure 27. The  $^1\text{H-NMR}$  spectrum of 5,5-dimethyl-3-(4-(phenylamino)phenylamino)cyclohex-2-enone (**L4**)

The APT spectrum of compound L4 exhibited signal at 27.98 ppm for the methyl carbon (**C1**). The methylene carbons of cyclohexane ring appeared at 41.92 ppm (**C3**), 50.21 ppm (**C7**), and the carbon (**C2**) appeared at 32.26 ppm. Vinylic methine carbon (**C5**) showed a signal at 95.70 ppm. The signal at 194.76 ppm was due to ketone carbon (**C6**) and the signal at 161.04 ppm belonged to enamine carbon (**C4**), aromatic carbons appeared between 116.44 and 143.42 ppm (**C8-C13**) (Figure 28).

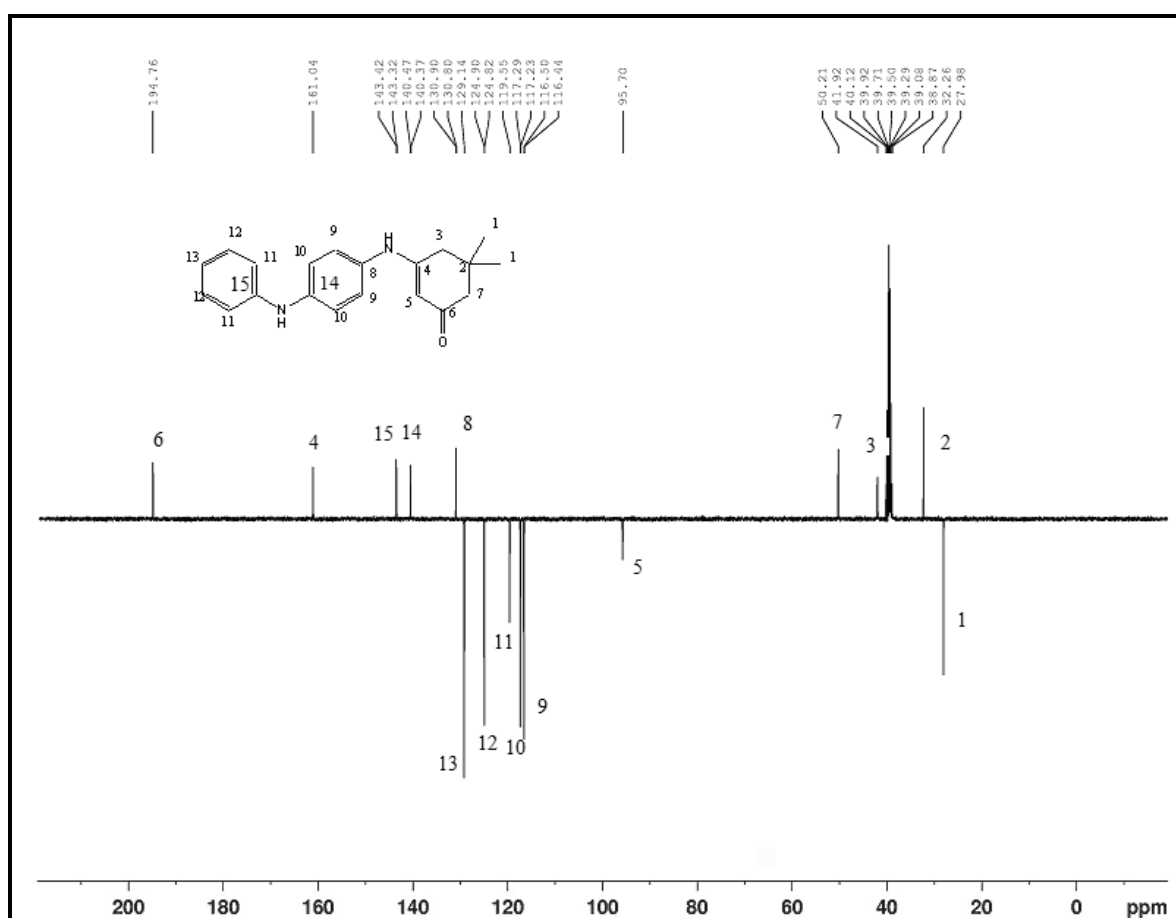


Figure 28. The APT spectrum of 5,5-dimethyl-3-(4-(phenylamino)phenylamino)cyclohex-2-enone (L4)

The UV spectrum of 5,5-dimethyl-3-(4-(phenylamino)phenylamino) cyclohex-2-enone (L4) had four bands at 267 nm, 300 nm, ( $\pi$ - $\pi^*$ ) 396 nm and 425 nm ( $n$ - $\pi^*$ ) (Figure 29).

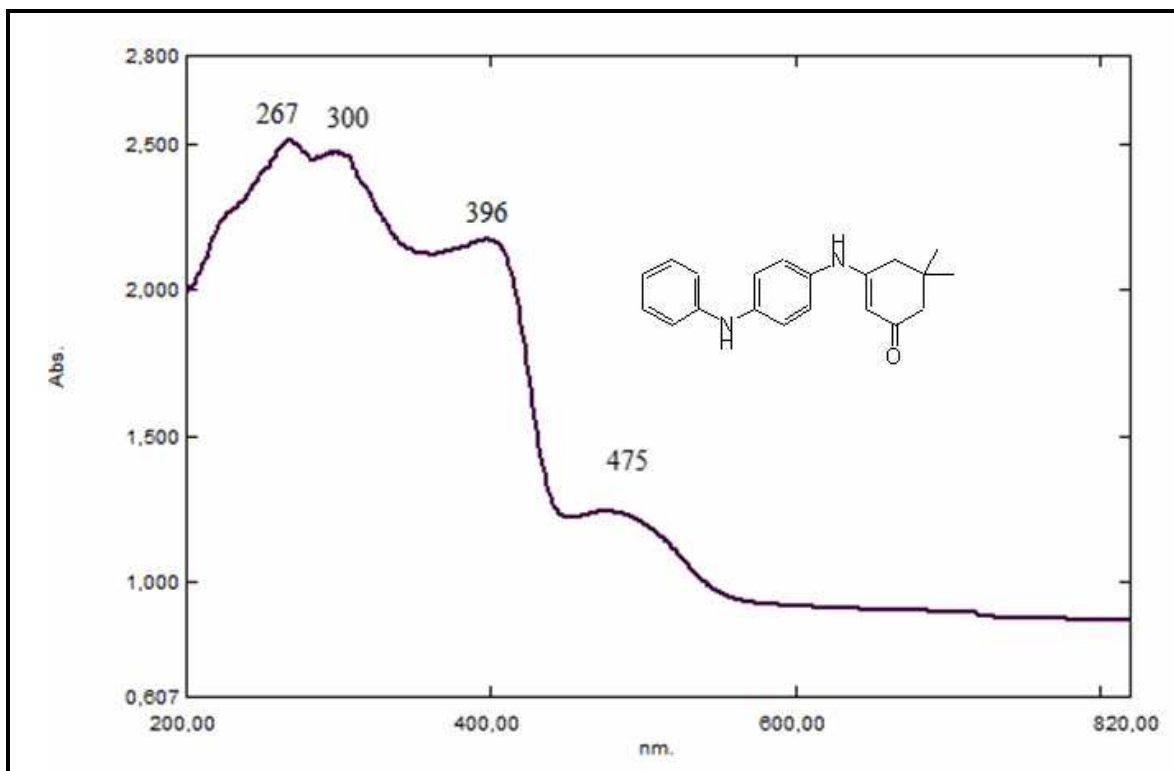


Figure 29. The UV spectrum of 5,5-dimethyl-3-(4-(phenylamino)phenylamino) cyclohex-2-enone (L4)

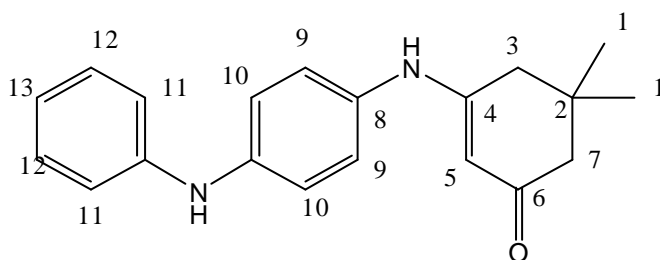


Table 13. L4 COSY Hydrogen-interaction.

<sup>1</sup> H	δ ( ppm )	H-H COSY
1	1.04	7
7	2.03	1,3
3	2.35	5,7
5	5.15	3
NH	8.18	-
NH	8.62	-

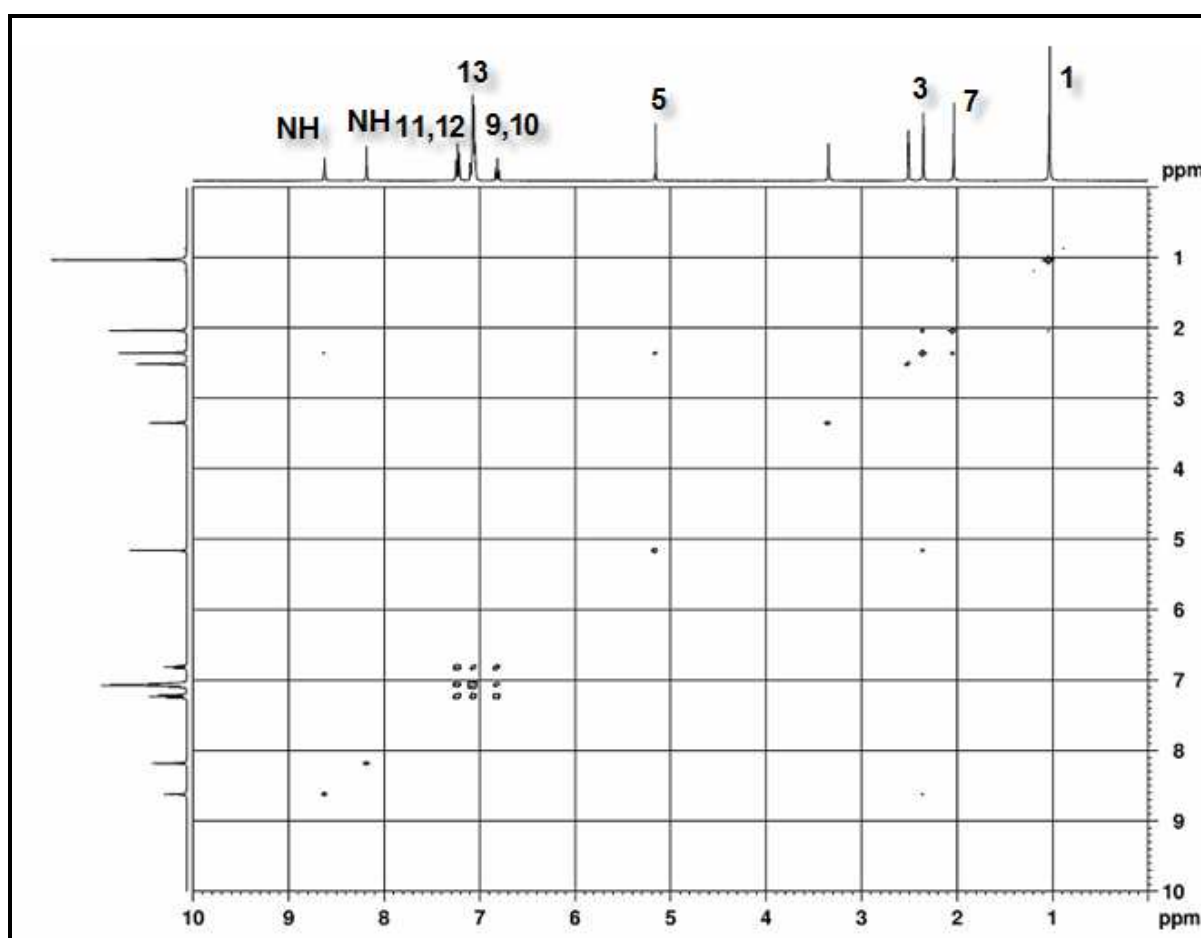


Figure 30. The COSY spectrum of 5,5-dimethyl-3-(4-(phenylamino)phenylamino)cyclohex-2-enone (L4)



## 5.5. Compound 3-(4-(phenylamino)phenylamino)cyclohex-2-enone (L5)

Characterization of 3-(4-(phenylamino)phenylamino)cyclohex-2-enone (L5) was achieved by FT-IR, UV-VIS-NIR,  $^1\text{H-NMR}$ , COSY and APT spectroscopy and X-Ray Crystallography.

The IR spectrum of 3-(4-(phenylamino)phenylamino)cyclohex-2-enone (L5) showed bands at 3289 and 3208  $\text{cm}^{-1}$  for N-H stretching of enamine and amine, at 2880-3100  $\text{cm}^{-1}$  for aliphatic C-H stretching, at 1597  $\text{cm}^{-1}$  for C=O stretching of enamione, 1400-1550 for  $\text{CH}_2$  bending and at 1142  $\text{cm}^{-1}$  for C-N bending of enamine (Figure 31).

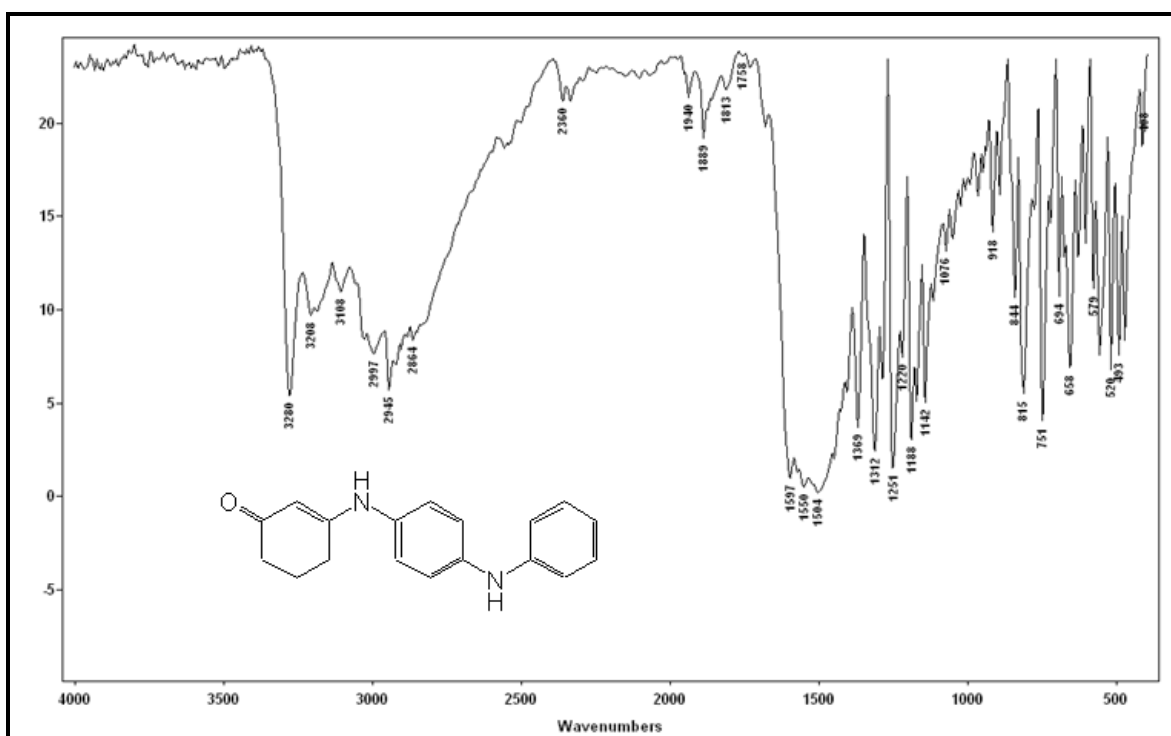


Figure 31. The IR spectrum of 3-(4-(phenylamino)phenylamino)cyclohex-2-enone (L5)

The  $^1\text{H-NMR}$  spectrum of compound L5 showed a multiplet at 1.89 ppm (**2**) and two triplets at 2.14 ppm (**3**), 2.49 ppm (**1**) for methylene protons of

cyclohexenone. Vinylic CH (**5**) gave a singlet at 5.15 ppm. Aromatic protons gave three multiple peak between 6,79 ppm and 7.24 ppm. In the  $^1\text{H-NMR}$  spectrum of the compound, two small peak observed at 8.18 (enamine **NH**) and 8.65 ppm (between two benzene) as a singlet was assigned to **NH** proton (Figure 32).

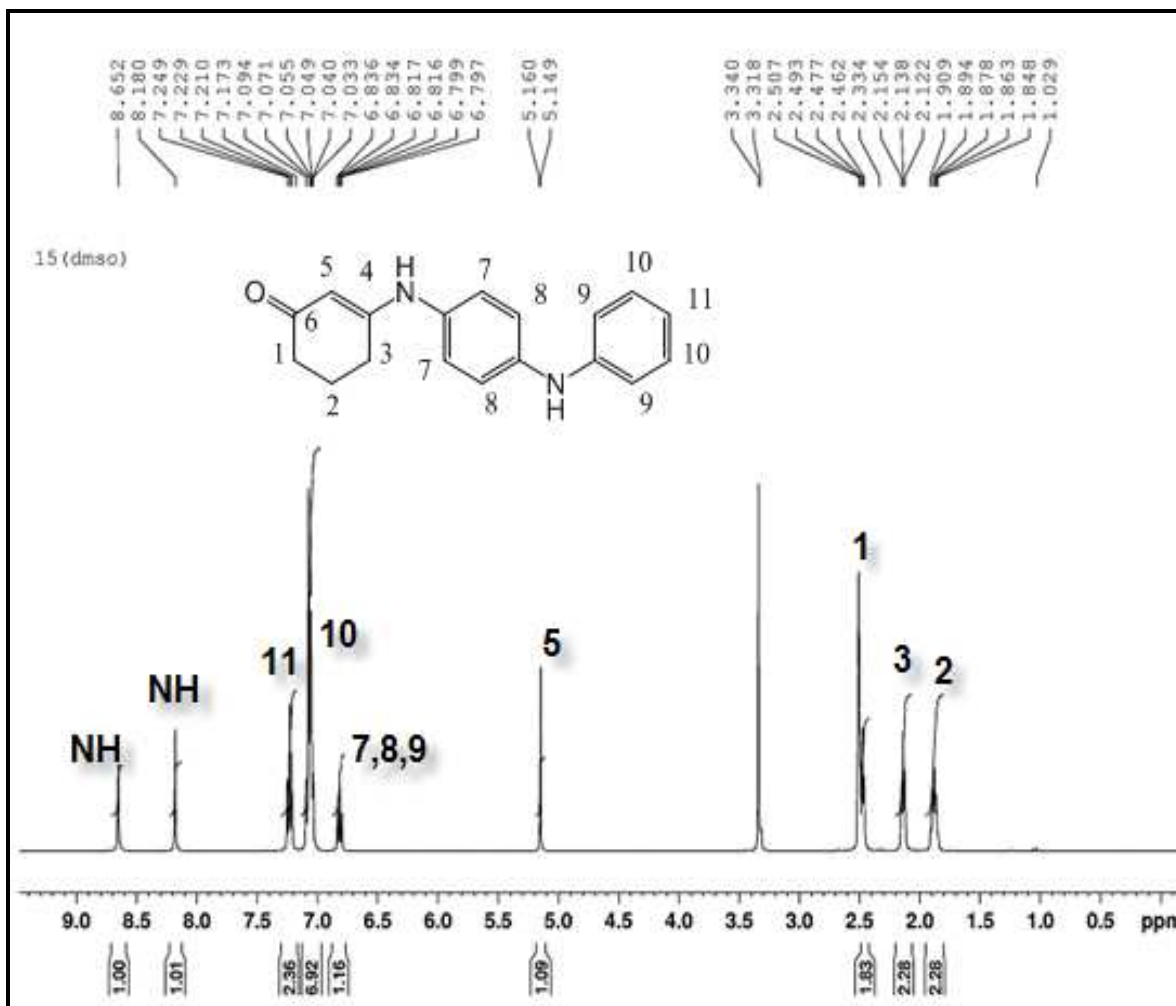


Figure 32. The  $^1\text{H-NMR}$  spectrum of 3-(4-(phenylamino)phenylamino)cyclohex-2-enone (L5)

The APT spectrum of compound L5 exhibited three signals at 22.10 ppm, 28.88 ppm, and 36.91 ppm for the methylene carbons (**2**, **3**, **1**) respectively. The signals between 116 ppm and 143 ppm belonged to the aromatic carbons (**7,14**). Vinylic methine carbon (**5**) showed a signal at 97.55 ppm. The signal at

195.67 ppm was due to ketone carbon (**6**) and the signal at 163.33 ppm belonged to enamine carbon (**4**) (Figure 33).

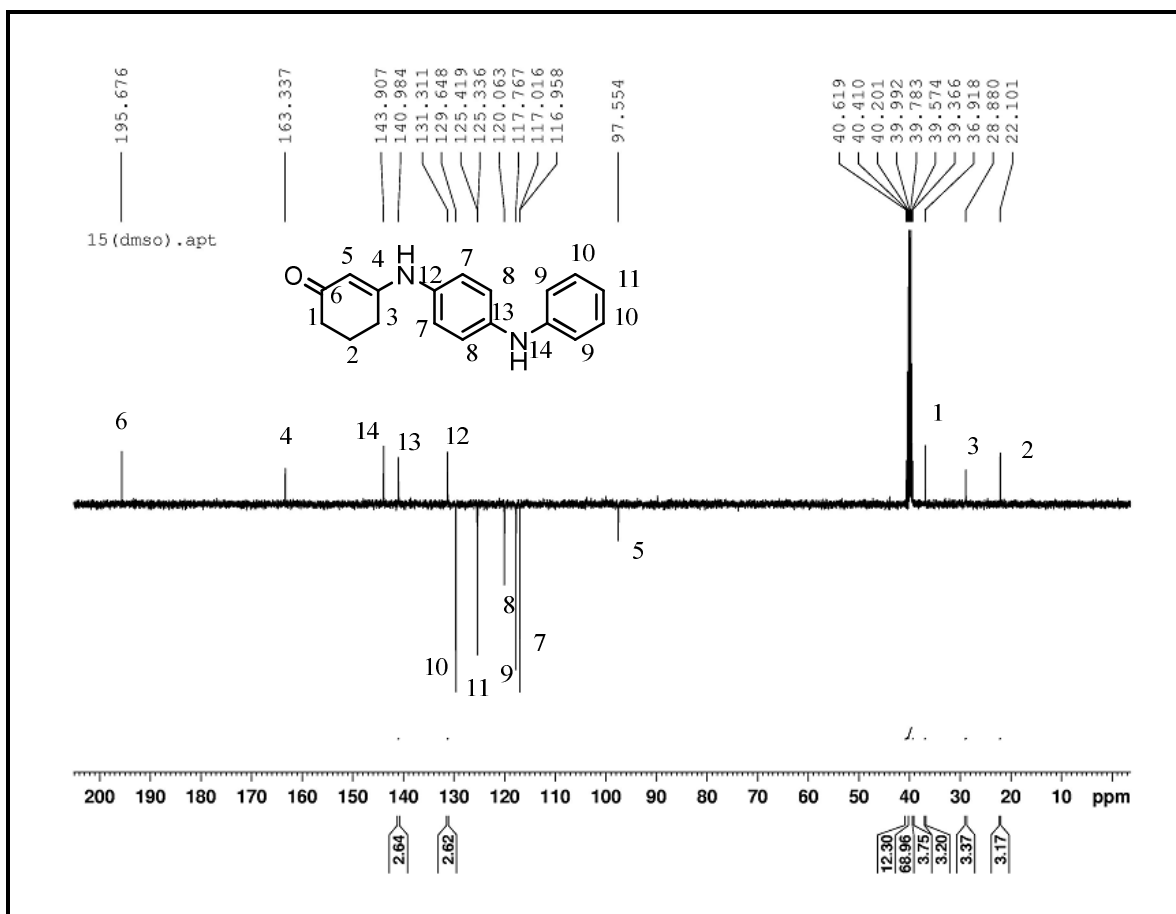


Figure 33. The APT spectrum of 3-(4-(phenylamino)phenylamino)cyclohex-2-enone (L5)

The UV spectrum of 3-(4-(phenylamino)phenylamino)cyclohex-2-enone (L5) had four bands at 265 nm, 293 nm ( $\pi$ - $\pi^*$ ) and 384 nm, 471 nm ( $n$ - $\pi^*$ ) (Figure 34).

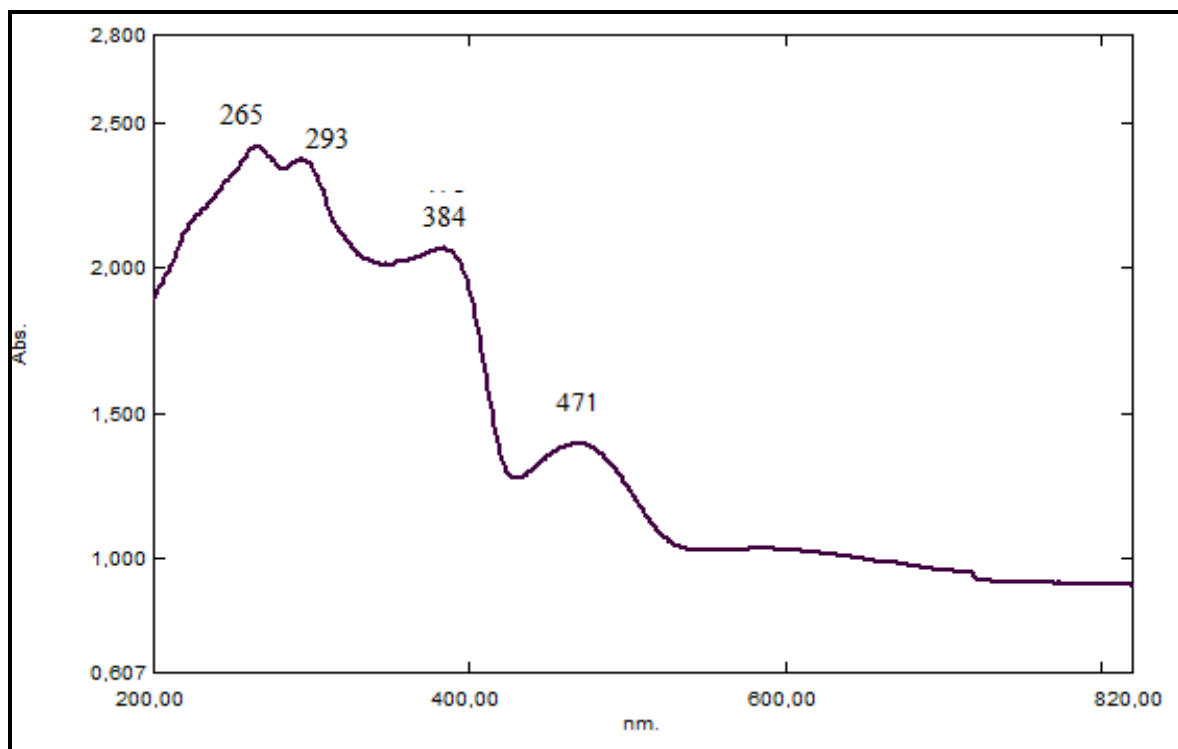


Figure 34. The UV spectrum of 3-(4-(phenylamino)phenylamino)cyclohex-2-enone (L5)

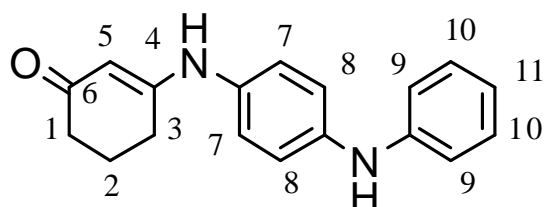


Table 14 . L5 COSY Hydrogen-interaction

$^1\text{H}$	$\delta$ ( ppm )	H-H COSY
2	1.89	3,1
3	2.14	2
1	2.49	2
5	5.15	-
7,8	6.81	7,8
10	7.05	9,11
11	7.22	10
NH	8.18	-
NH	8.65	-

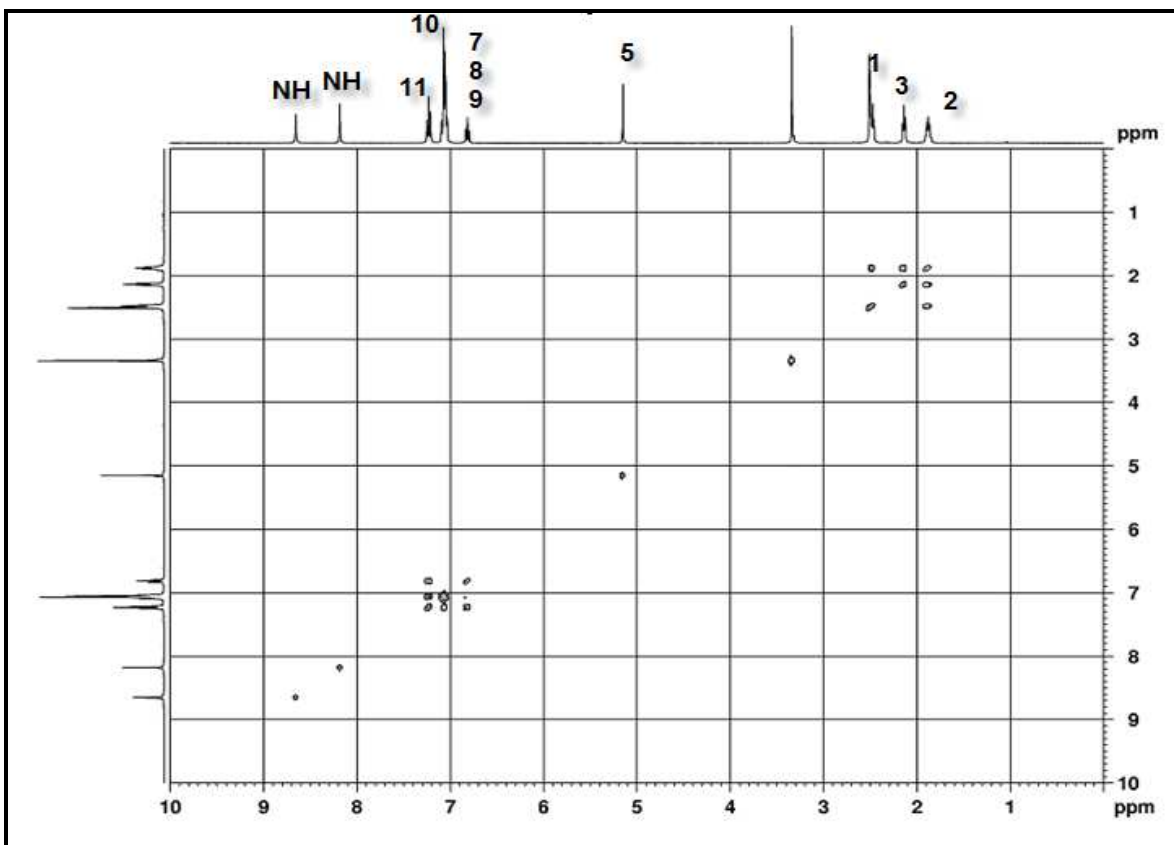


Figure 35. The COSY spectrum of 3-(4-(phenylamino)phenylamino)cyclohex-2-enone (L5)

The molecular structure and crystallographic numbering order of the atoms are shown in Fig36.

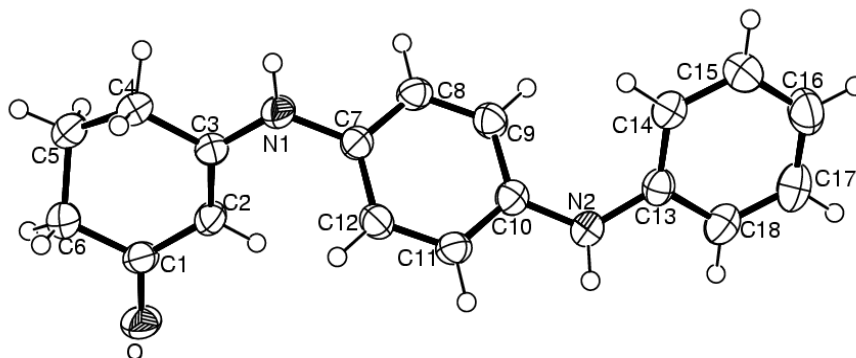


Figure 36. Molecular structure of 3-(4-(phenylamino)phenylamino)cyclohex-2-enone, showing 50% probability displacement ellipsoids

A summary of the key crystallographic information was given in Table 15. A suitable single-crystal was selected and mounted on an Enraf Nonius CAD-4 diffractometer. The structure was solved by direct methods with SHELXS-97 and refined by least squares on  $F_{\text{obs}}^2$  with SHELXL-97 (Sheldrick, 1997). All the hydrogen atoms were located from difference Fourier map and they were refined using riding model.

Table 15. Crystal data and details of the structure determination of 3-(4-(phenylamino) phenylamino)cyclohex-2-enone

$(\Delta\rho)_{\text{min}}, (\Delta\rho)_{\text{max}}$ ( $e \text{ \AA}^{-3}$ )	0.550,- 0.452
Crystal formula	$\text{C}_{18}\text{H}_{18}\text{N}_2\text{O}$
Formula weight	278.34
Crystal dimensions, [mm]	0.56x0.58x0.6
Temp, [K]	291(2)
Crystal system	Monoclinic
Space group	$P2_1/c$
a, [ $\text{\AA}$ ]	9.823(1)
b, [ $\text{\AA}$ ]	15.625(1)
c, [ $\text{\AA}$ ]	10.841(1)
$\beta$ , [ $^\circ$ ]	116.440(8)
Z; $D_{\text{calc}}$ , [ $\text{g cm}^{-3}$ ]	4; 1.24
Range of $\theta$ [ $^\circ$ ]	2.5 / 26.3
$\mu$ (MoK $\alpha$ ) [ $\text{mm}^{-1}$ ]	0.078
Reflections collected	3195
Reflections used in	3019
No. of refined	203
R / $R_w$ values	0.0590/ 0.1503
GOF	1.0880
Final shift	0.000

Some geometrical parameters (bond lengths, bond angles and torsion angles) can be seen in Table 16.

Table 16. Some geometrical parameters of 3-(4-(phenylamino)phenylamino)cyclohex-2-enone

<b>Bond lengths (Å)</b>	
O – C1	1.253(2)
N2 - C10	1.399(2)
N2 - C13	1.401(2)
N1 – C3	1.344(2)
N1 - C7	1.428(2)
C8 - C7	1.376(2)
C3- C2	1.369(2)
C3 – C4	1.502(2)
C10 - C11	1.392(3)
C10 - C9	1.394(2)
C13 - C14	1.388(3)
C13 - C18	1.392(2)
C1 - C2	1.414(3)
C7 - C12	1.391(2)
<b>Bond angles (°)</b>	
C10 - N2 - C13	127.02(16)
C3 - N1 - C7	126.40(15)
N1 – C3- C2	124.49(16)
C11 - C10 - C9	117.83(17)
C11 - C10 - N2	118.10(16)
C9 - C10 - N2	123.99(17)
C14 - C13 - C18	118.13(18)
C14 - C13 - N2	123.84(16)
C18 - C13 - N2	118.01(17)
C3 – C2 – C1	122.19(17)
C8 - C7 - C12	118.72(16)
C8 - C7 - N1	119.87(15)
C12 - C7 - N1	121.31(16)
O – C1 – C2	122.08(17)
<b>Torsion angles (°)</b>	
C7 - N1 – C3 – C2	-7.8(3)
C13 - N2 - C10 - C9	31.8(3)
C10 - N2 - C13 - C14	17.3(3)
C3 - N1 - C7 - C12	-48.6(3)
C3 – C2 – C1 - O	-
N2 - C13 - C14 - C15	178.34(18)

The discussion related with the crystallographic structure can be given by the following explanations.

The mean planes of the six-membered rings are twisted with respect to each other in order to minimize the steric hinderance (H2...H12 and H9...H14). Indeed, they make an angle of 48.80(6)° and 43.02(6) between the cyclohexanone ring and the phenyl rings and between the two phenyl rings, respectively. The conformation of the molecule can be also affected by the intermolecular hydrogen bonds in Fig 37. Geometrical details of these hydrogen bonds were given in Table 14. With the help of these donor-acceptor relationship, It can be said that, trans-keto form may be seen in the molecular conformation and this intermolecular tautomeric form may cause thermal and photochromic properties in the crystal structure such as molecular cis-keto form (Ogawa, et al., 2005). In the molecular structure, the C-O bond length is the most sensitive indicator of the type of tautomeric form. It is a single bond in the case of the enol-imino tautomers while it is shortened in the keto-amino tautomers. A distance of [1.253(2)Å] is observed for the C-O bond length of the title compound, which is slightly longer than the expected value of 1.222 Å for a double bond (Allen, et al., 1987) . According to the enol form and electron delocalizations some bond lengths can be deviated from the expected values (Allen, et al., 1987). In molecular structures of acyclic β-enaminones, conformational isomerism is usually expected, however, the title compound has a cyclic structure and shows only E isomer. Orientations related with two sides of the molecule can be given as follows with respect to cyclohexanone moiety. Cyclohexanone – disubstituted benzene [Z], cyclohexanone – phenyl [E].



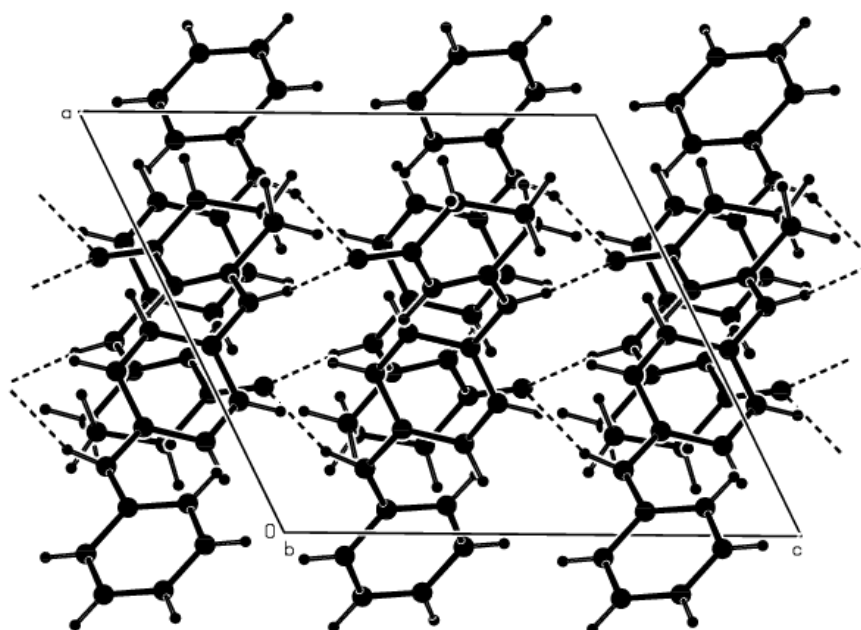


Figure 37. Packing diagram showing molecular orientation and hydrogen bonded chains

Table 17. Hydrogen bonding geometry ( $\text{\AA}$ ,  $^\circ$ ) for 3-(4-(phenylamino)phenylamino)cyclohex-2-enone

D-H...A	D-H	D...A	H...A	D-H...A
C11-H11...O <sup>(1)</sup>	0.93(2)	3.358(2)	2.655(1)	132.9( 1)
N2-H2N...O <sup>(1)</sup>	0.89(2)	2.942(3)	2.122(27)	151.7( 19)
N1-H1N...O <sup>(2)</sup>	0.91(2)	2.846(2)	1.954(22)	165.3( 2)

**Symmetry codes:** (1)  $-x+1, +y+1/2, -z+1/2+1$ ; (2)  $x, -y+1/2, +z-1/2$

## 5.6. $\beta$ -enaminone-Complexes

### 5.6.1. L1-Nickel Complexes

The electronic absorption studies of  $\beta$ -enaminone (L1) and its complexes were studied as solid. Electronic spectrum of ligand showed two characteristic absorption broad bands at 220-290 nm and 422 nm which might be assigned to the intra-ligand  $\pi$ - $\pi^*$  and  $n$ - $\pi^*$  transitions of the enaminone O=C-C=C-NH moiety. After complexation with nickel ion, the band at 422 nm shifted to 407 nm for complex 6, to 393 nm for complex 3 and a new broad band at 635 nm appeared suggesting that the nitrogen and oxygen atoms of the ligand were coordinated to the metal ion. This result might be due to the weakening of  $n$ - $\pi^*$  transitions of the ligand during complexation. In the literature, the band at  $15700\text{ cm}^{-1}$  (635 nm) was assigned to  ${}^3A_{2g}(F) \rightarrow {}^3T_{1g}(F)$  transition of nickel complexes in the octahedral geometry (Singh, et al., 2007; Raghu et al., 2002; Jubert, et al., 2002). For both of our Ni (II) complexes, complex 3 and 6 had their absorption bands at the same wavelength,  $15700\text{ cm}^{-1}$  (634 nm). These transitions were characteristic of octahedral geometry as in the literature. Measurements were recorded at room temperature and spectral data of the complexes were presented in Table 5.

Magnetic susceptibility data for complexes 3 and 6 were calculated at room temperature and the values lie at 5.18 B.M. for complex 3 and 5.86 B.M. for complex 6, which were somewhat larger than that expected for an ordinary paramagnetic Ni(II) compound (2.83 B.M.). This behavior probably indicated an intramolecular ferromagnetic coupling between the nickel ions. (Table 5)

When the IR spectra of L1 and the metal complexes 3 and 6 were compared, the most significant difference in the IR spectra of the ligand and complex were the shift of C=O stretching vibration to lower frequencies due to metal-ligand coordination. The ligand showed its carbonyl -C=O band at  $1667\text{ cm}^{-1}$ , and it was shifted to  $1591\text{ cm}^{-1}$  for complex 3 and to  $1588\text{ cm}^{-1}$  for complex 6. The bands at  $1111\text{ cm}^{-1}$  (for complex 3) and at  $1108\text{ cm}^{-1}$  (for complex 6) were assigned to the

$\nu(\text{C-N})$  vibration. The IR spectra information supported the suggestion of coordination of the nitrogen, and oxygen atom to the metal ion.

Further conclusive evidence of the coordination of this ligand with nickel ion was shown by the appearance of weak low frequency new bands for complex 3 at  $595\text{ cm}^{-1}$  and for complex 6 at  $589\text{ cm}^{-1}$ . These were assigned to the metal nitrogen (M-N) or metal-oxygen (M-O) vibrations.

The thermal behavior of complex 3 and 6 in  $\text{N}_2$  surroundings were studied by TG-DTA. The complex 3 and 6 were stable up to  $364^\circ\text{C}$  and  $360^\circ\text{C}$ , respectively, indicating the absence of lattice or coordinated water molecules and at these temperatures removal of the L1 molecules and finally transform to metaloxide with the total weight-losing rate 71.81% for complex 3 and 71.00 % for complex 6 were observed. The decomposition of the complexes above  $360^\circ\text{C}$ , indicated that the complexes are highly thermally stable.

Metal analysis of the complexes were measured on ICP-AES Varian model Liberty Series II analyser. The analyses were repeated twice to check the accuracy of the data. According to ICP analyses all ligands formed three-nuclear complexes with Ni(II), Cu(II) and Co(II) ions. This result may be because of large core of the ligands. The results are given in Table 5.

The reactions of Ni(II) chloride hexahydrate and L1 with two different methods afforded light blue complexes. The same colour and similar analysis results of the complexes might indicate that their structures are very similar to each other or they are the same complexes.

According to the amount of nickel atoms calculated from ICP analysis as three and calculated molecular weight as  $775\text{ g/mol}$  using TGA thermograms (29% weight loss corresponded to  $1.09\text{ g NiO}$  at  $650^\circ\text{C}$ ), the possible structure for the complex 3 and 6 are proposed as shown in Figure 38.

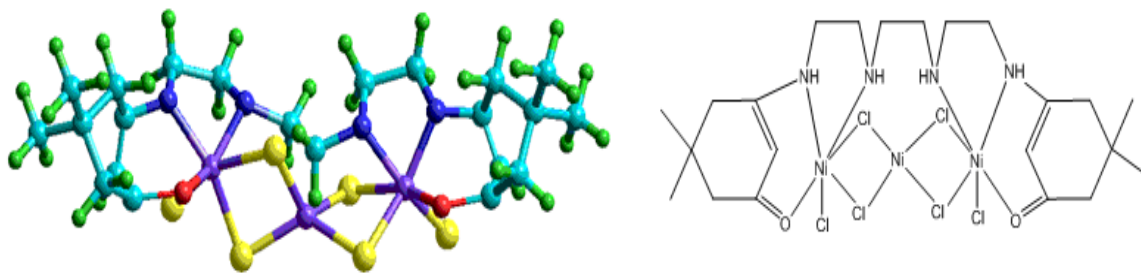


Figure 38: Possible structure of L1-Nickel complex

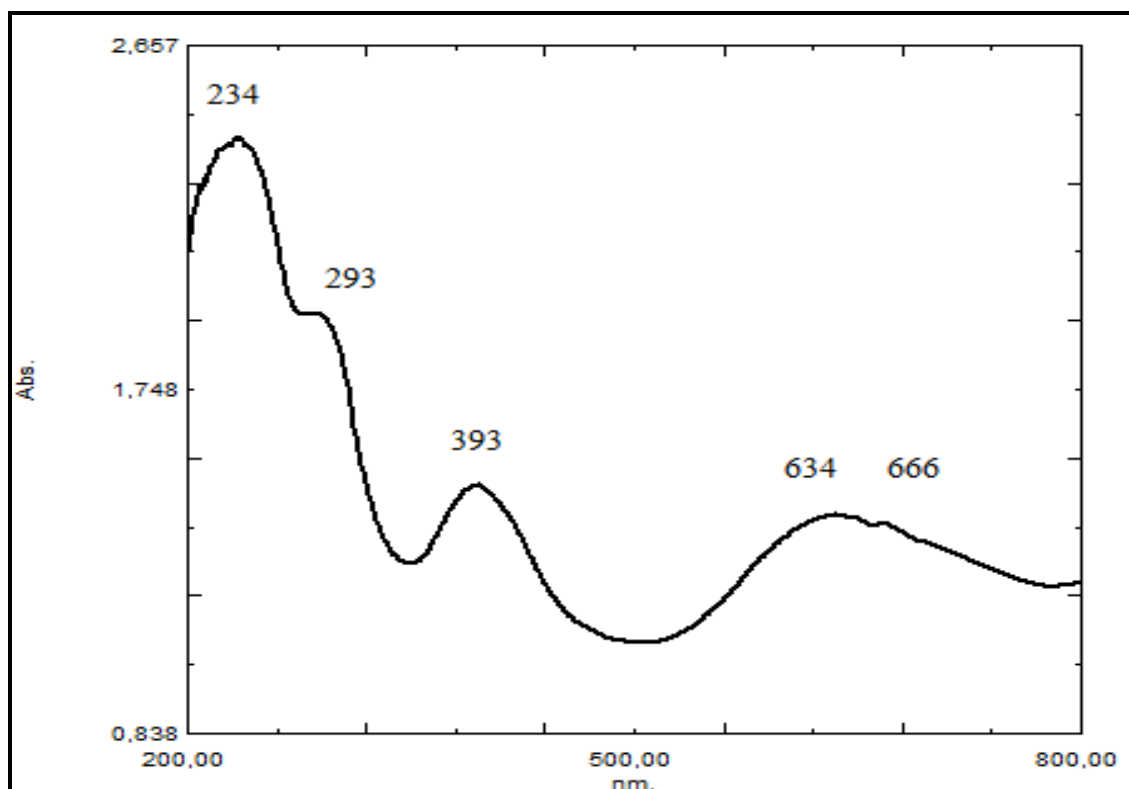


Figure 39: UV-VIS Spectrum of Complex 3

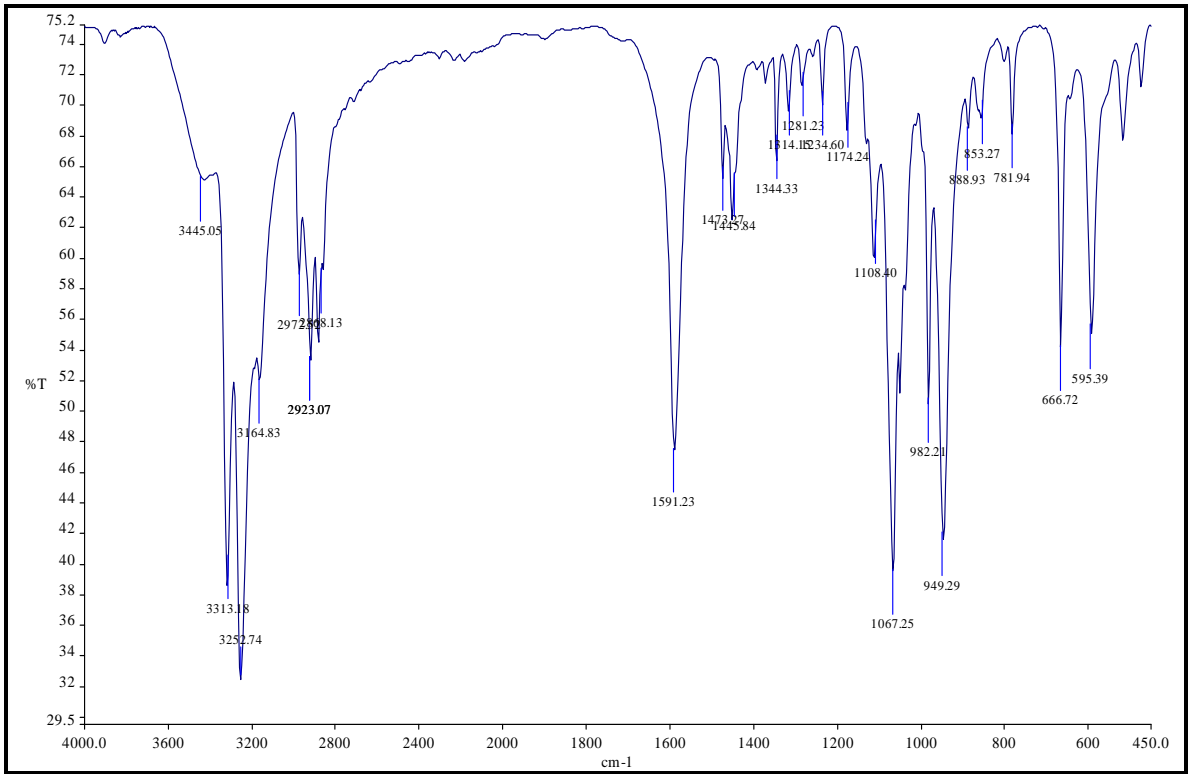


Figure 40: IR Spectrum of Complex 3

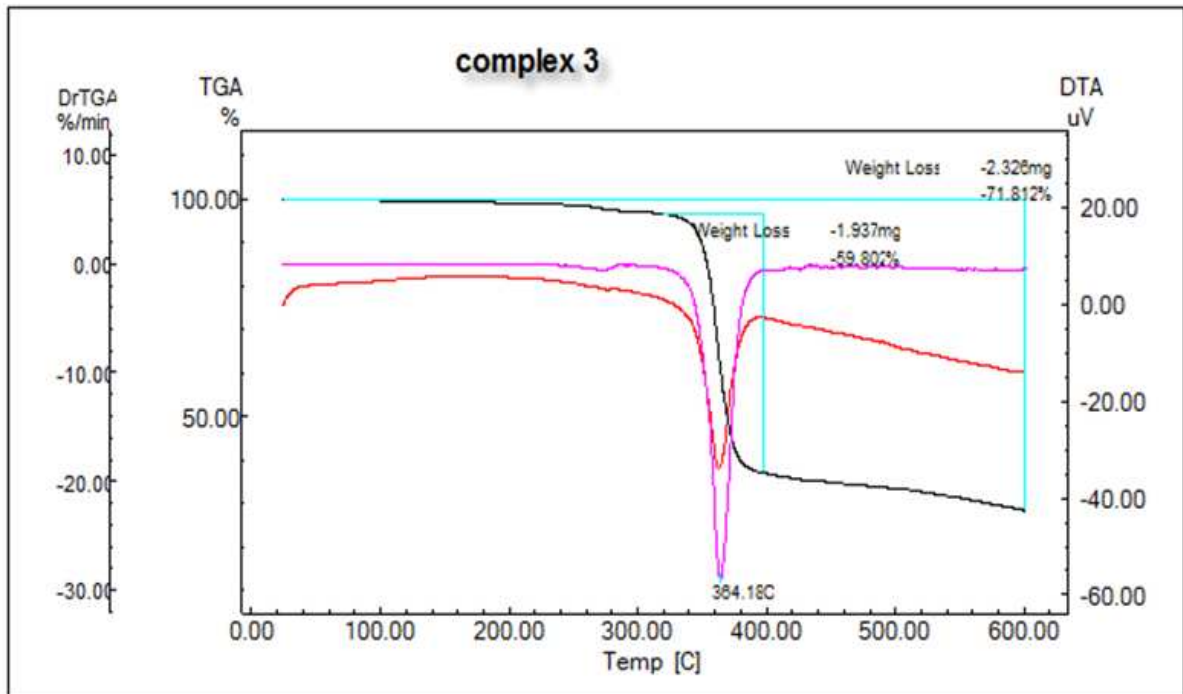


Figure 41 : DTA-TGA Thermogram of Complex 3

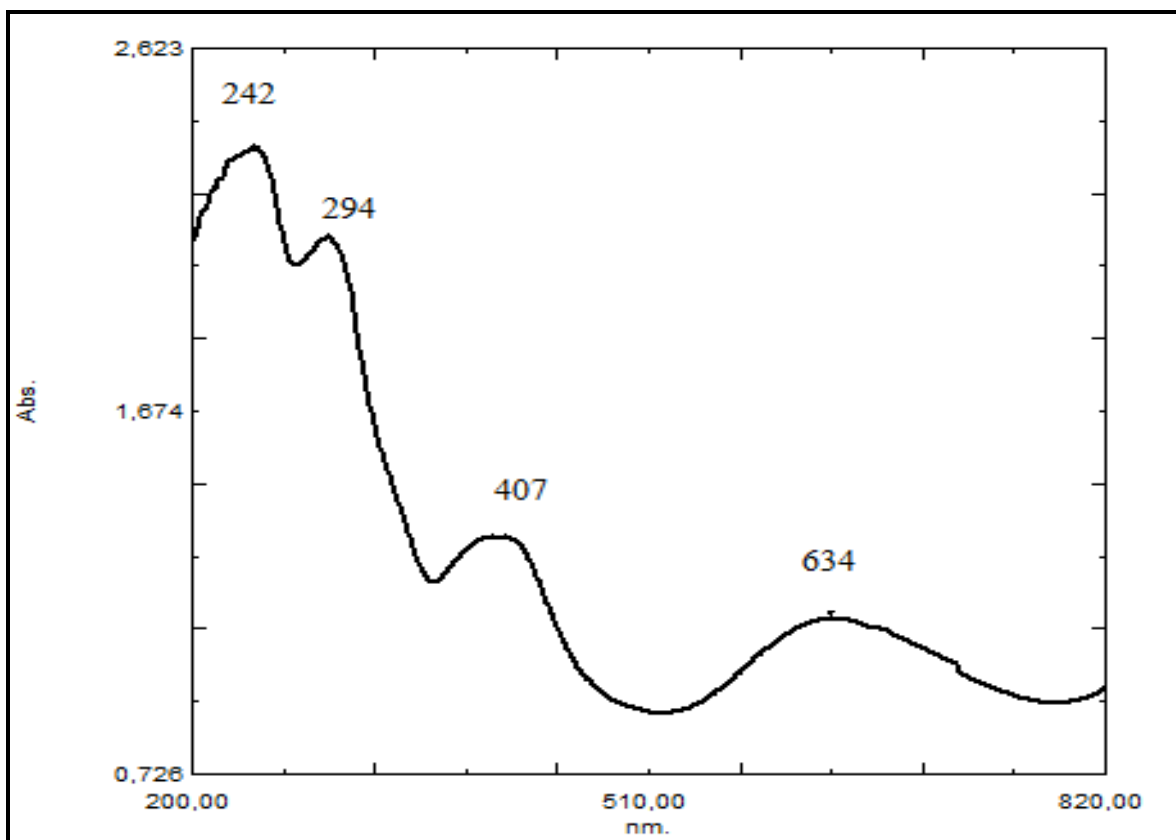


Figure 42: UV-VIS Spectrum of Complex 6

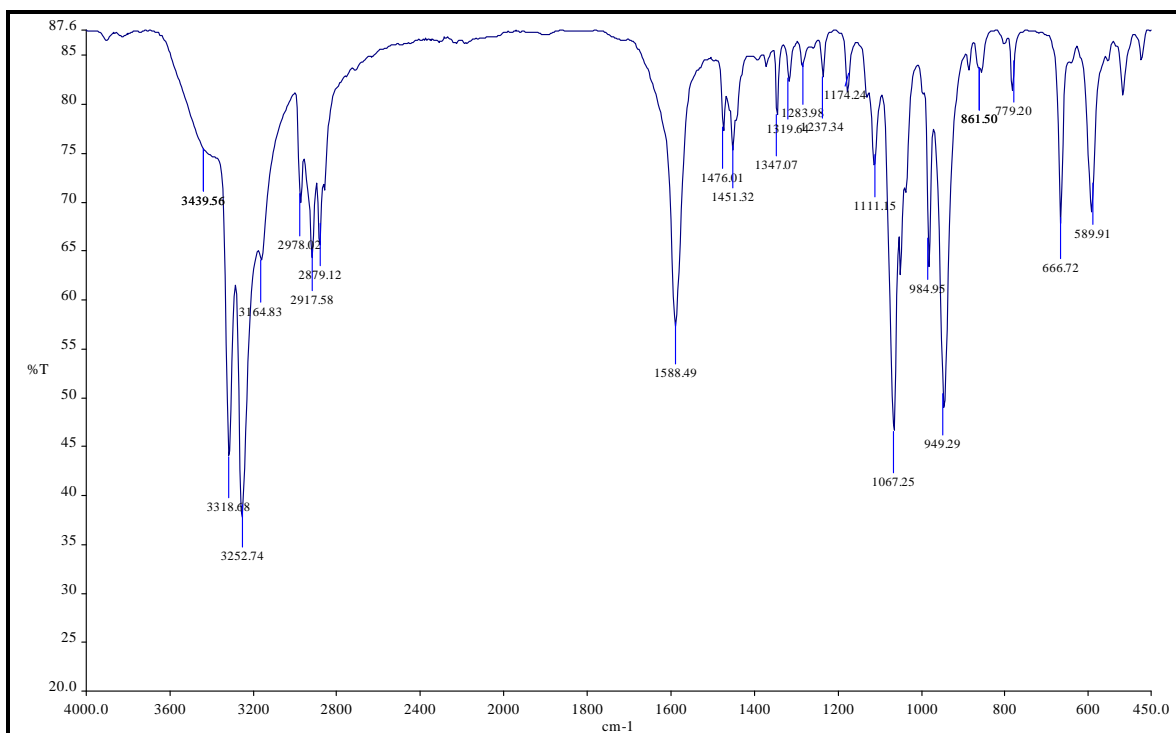


Figure 43: IR Spectrum of Complex 6

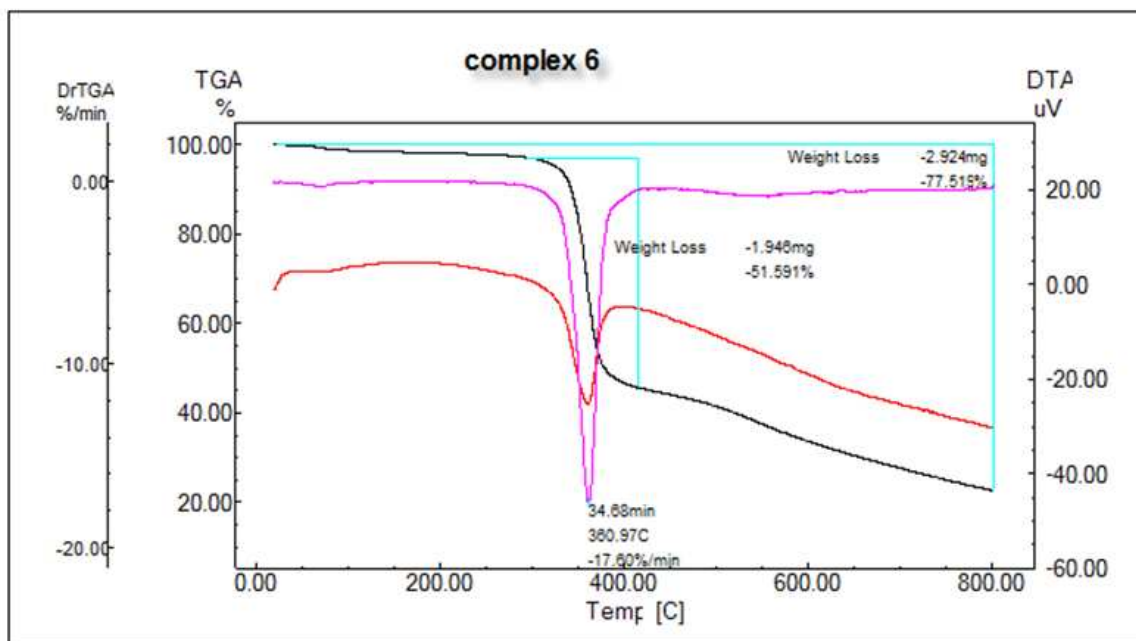


Figure 44 : DTA-TGA Thermogram of Complex 6

### 5.6.2. L2-Cobalt Complexes

In the electronic spectra, besides the shift of 423 nm band ( the intra-ligand  $n-\pi^*$  transition of the enaminone  $O=C-C=C-NH$  moiety) to 417 nm for complex 8 and to 408 nm for complex 11, a new broad band having three different maxima at 630, 668, and 689 nm for complex 8 and at 625, 664 and 688 nm for complex 11 appeared suggesting that the nitrogen and oxygen atoms of the ligand were coordinated to the metal ion. In the octahedral complexes of cobalt, the ground state term arising from this configuration was  $^4T_{1g}$  and there were three spin allowed transitions as  $^4T_{1g} \rightarrow ^4T_{2g}$ ,  $^4T_{1g} \rightarrow ^4A_{2g}$  and  $^4T_{1g}(F) \rightarrow ^4T_{1g}(P)$ . Bands at  $16666-14285\text{ cm}^{-1}$  (602-700 nm) and  $21275\text{ cm}^{-1}$  (470 nm) might be assigned to  $^4T_{1g} \rightarrow ^4A_{2g}$  and  $^4T_{1g}(F) \rightarrow ^4T_{1g}(P)$  transitions, respectively (Singh, et al., 2007; Raghu et al., 2002; Jubert, et al., 2002). For both of our Co (II) complexes, for complex 8 and 11, the absorption bands were observed at wavelenghts  $14530-16000\text{ cm}^{-1}$  (625-688 nm) and  $18450\text{ cm}^{-1}$  (542 nm) indicating octahedral geometry.

When the IR spectra of L2 and the metal complexes 8 and 11 were compared, the complexes showed a common characteristic strong broad band in the region

3100–3500  $\text{cm}^{-1}$  which confirmed the presence of water molecules coordinated to the metal ion. In addition, the presence of coordinating water molecules in all the complexes was indicated by two weak bands around 839 and 600  $\text{cm}^{-1}$ , which could be assigned to (OH) stretching, rocking and wagging vibrations, respectively.

According to TGA curves, decomposition of Co(II) complex started at a low temperature and completed at 600°C. The Co(II) complex decomposed and produced CoO as residue in the temperature ranges 25.0–250.0, 280.0–440.0 and 440.0–600.0 °C. In the decomposition process of the Co(II) complex, the mass losses corresponded to H<sub>2</sub>O leaving in the first stage of the decomposition. The first stage (25–250°C) with an experimental mass loss of 12.82 % (theoretical 13.59 %) for complex 8 and experimental mass loss of 12.05 % (theoretical 13.59 %) for complex 11, represent the loss of H<sub>2</sub>O. The second stage within the temperature range 280–440°C represents the loss of ligand.

The reactions of Co(II) chloride hexahydrate with L2 by two different methods afforded dark blue complexes. The possible structure for complexes is shown in Figure 45.

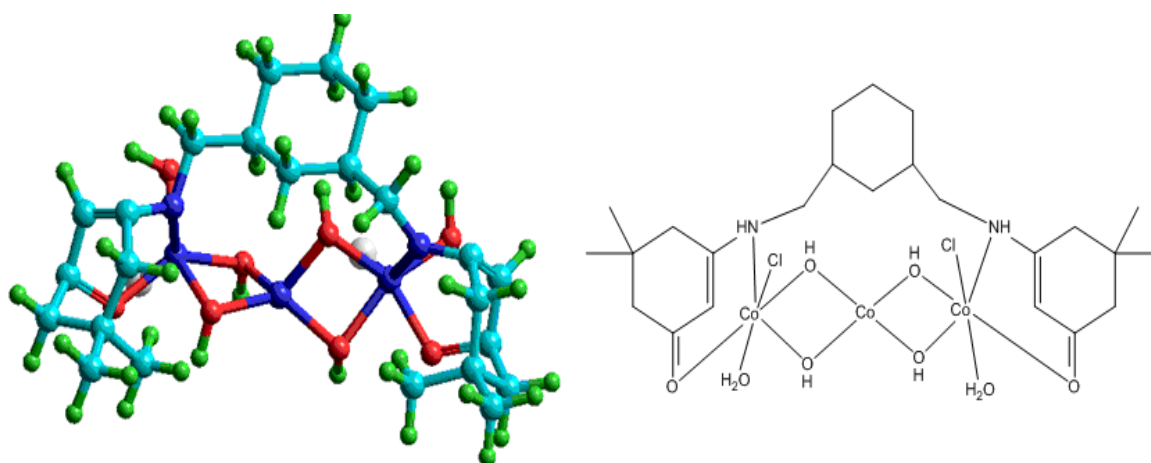


Figure 45: Possible structure of L2-Cobalt complex



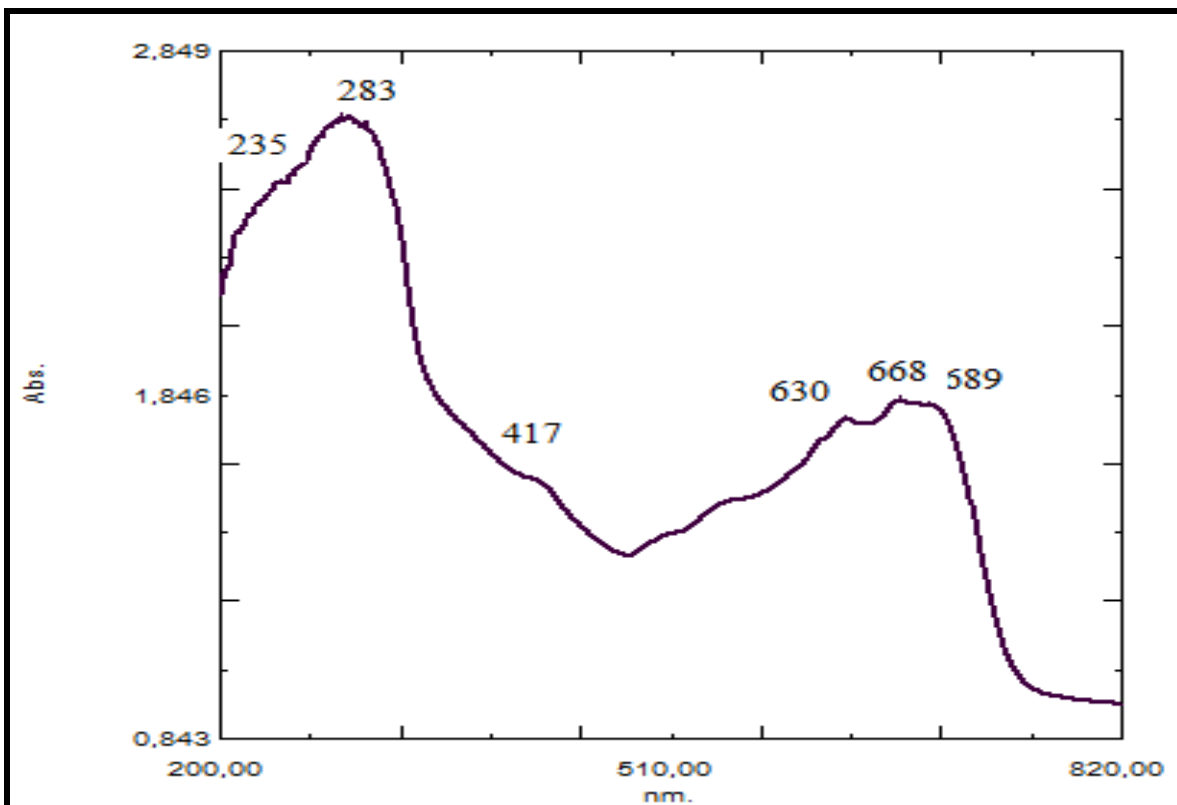


Figure 46: UV-VIS Spectrum of Complex 8

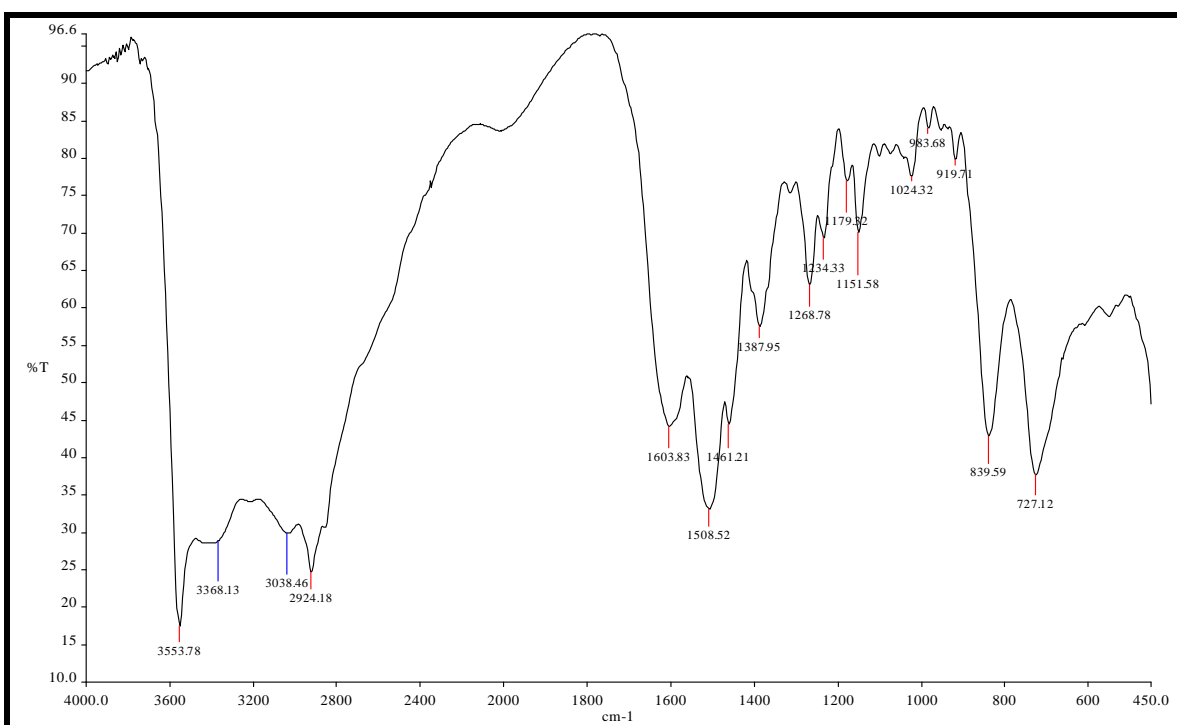


Figure 47: IR Spectrum of Complex 8

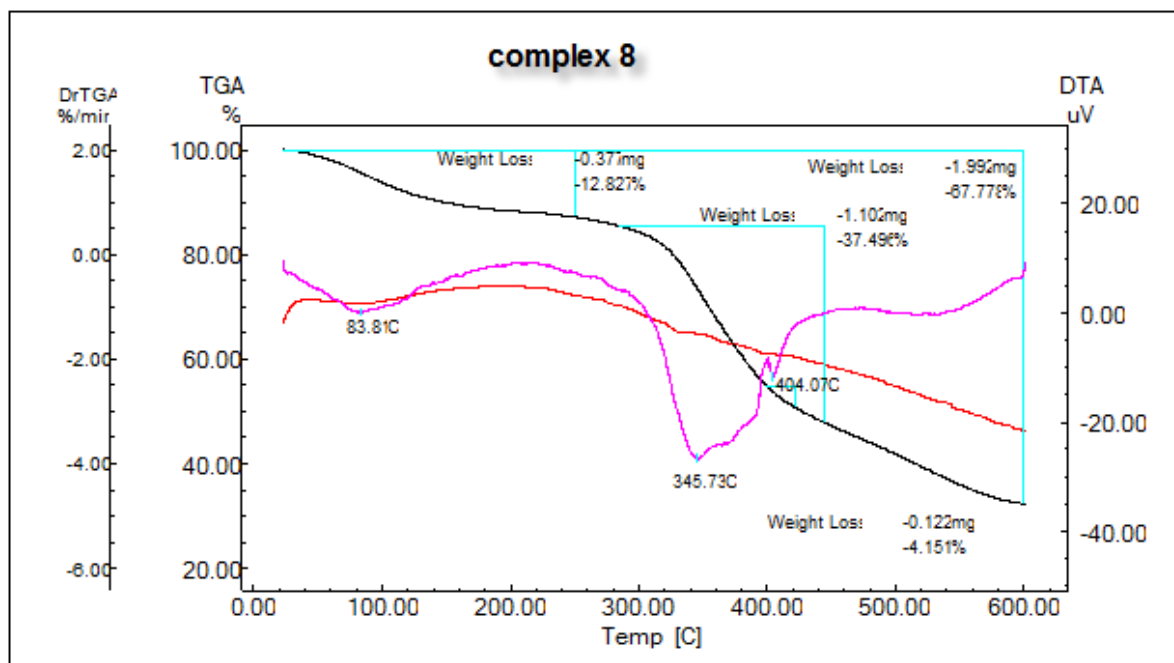


Figure 48: DTA-TGA Thermogram of Complex 8

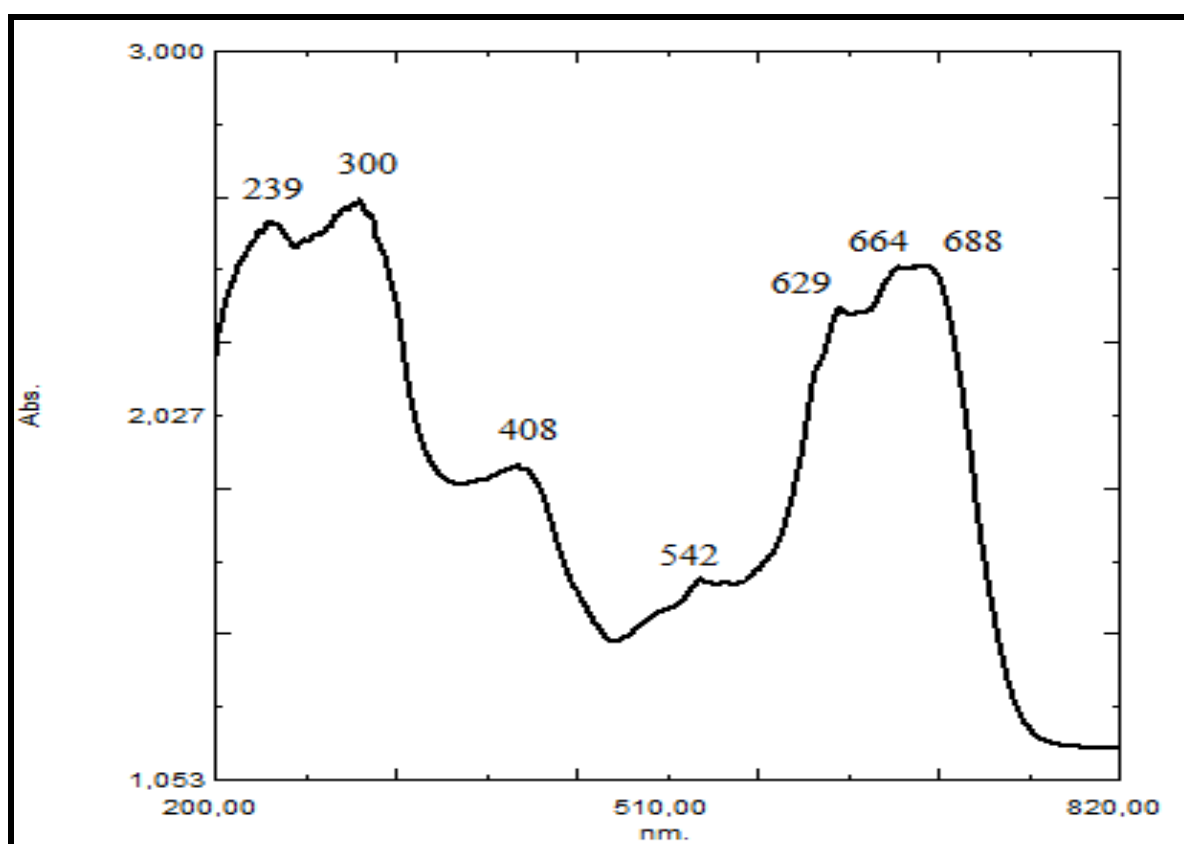


Figure 49: UV-VIS Spectrum of Complex 11

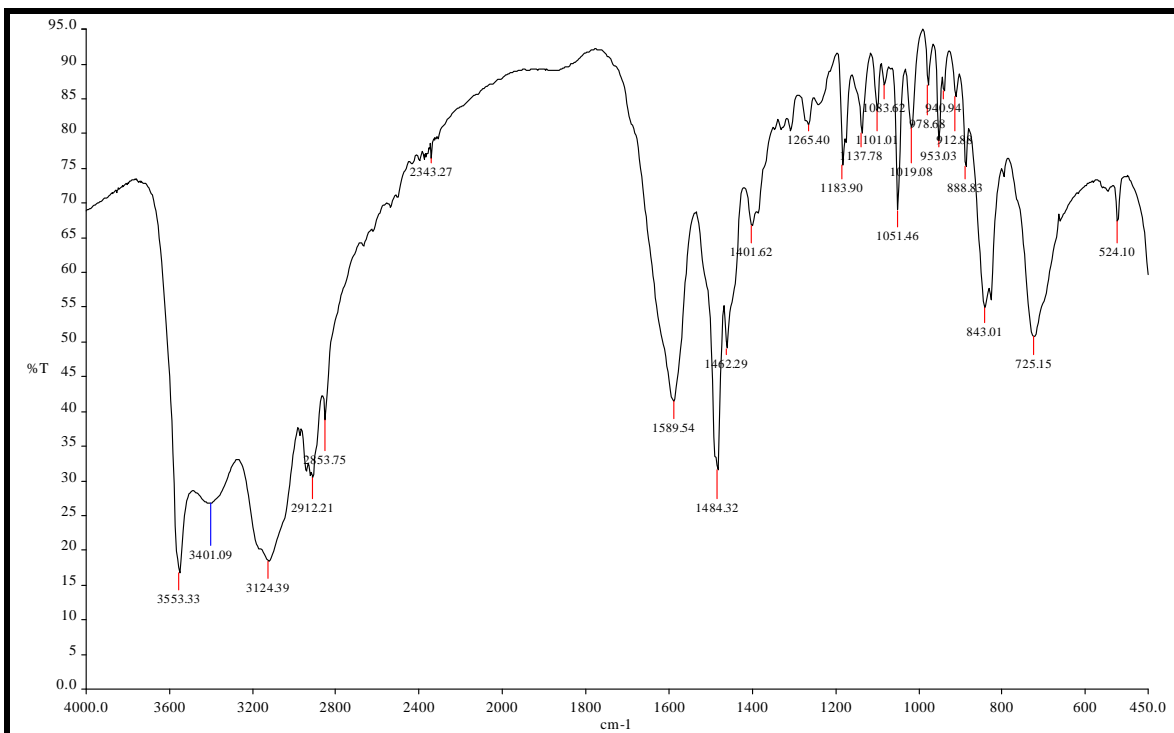


Figure 50: IR Spectrum of Complex 11

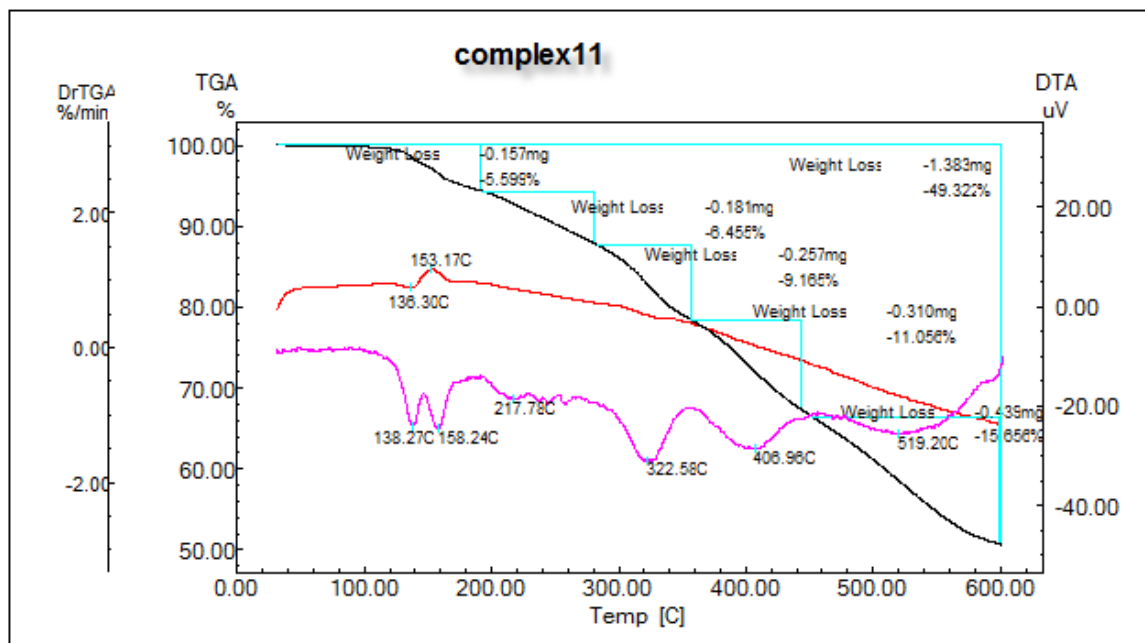


Figure 51: DTA-TGA Thermogram of Complex 11

### 5.6.3. L3-Copper Complexes

The electronic absorption studies of copper complex (L3) showed a broad band at 428 nm ( $n-\pi^*$ ), after complexation the band disappeared and a new very broad band at 740-760 nm appeared. The absorption band in the 600–800 nm range was assigned to the d–d transitions of the Cu (II) ion suggesting that six-coordinated complex was obtained which indicated octahedral geometry for the Cu (II) complex (Singh, et al., 2007; Raghu et al., 2002; Jubert, et al., 2002).

IR spectra of the complexes 13 and 16 showed broad bands in the region 3100-3500  $\text{cm}^{-1}$  which confirmed the presence of water molecules coordinated to the metal ion.

In the decomposition process of the Cu(II) complex, the first mass losses corresponded to  $\text{H}_2\text{O}$  leaving. The first stage (30–164°C) with an experimental mass loss of 3.96 % (theoretical 3.92 %) represents the loss of two  $\text{H}_2\text{O}$  molecules. The metal analysis results are given in Table 7.

The possible structure for the complexes 13 and 16 is proposed as shown in Figure. 52

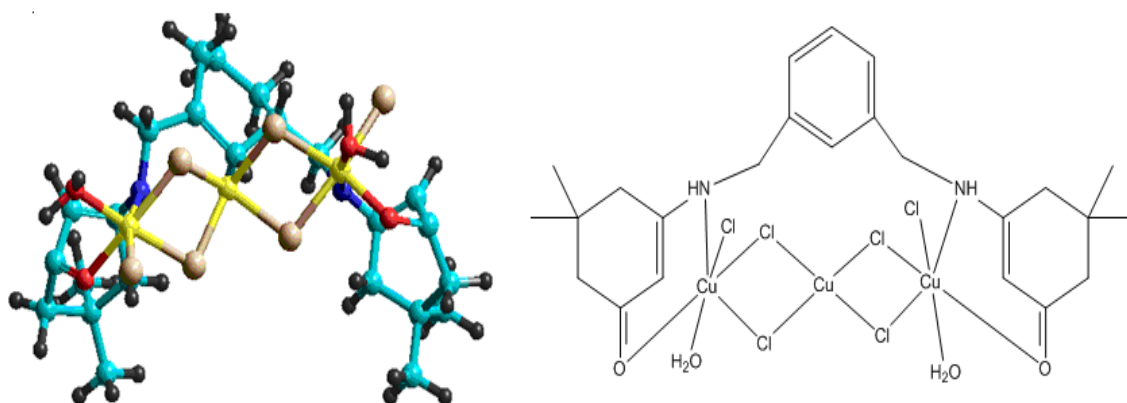


Figure 52: Possible structure of L3-Copper complex

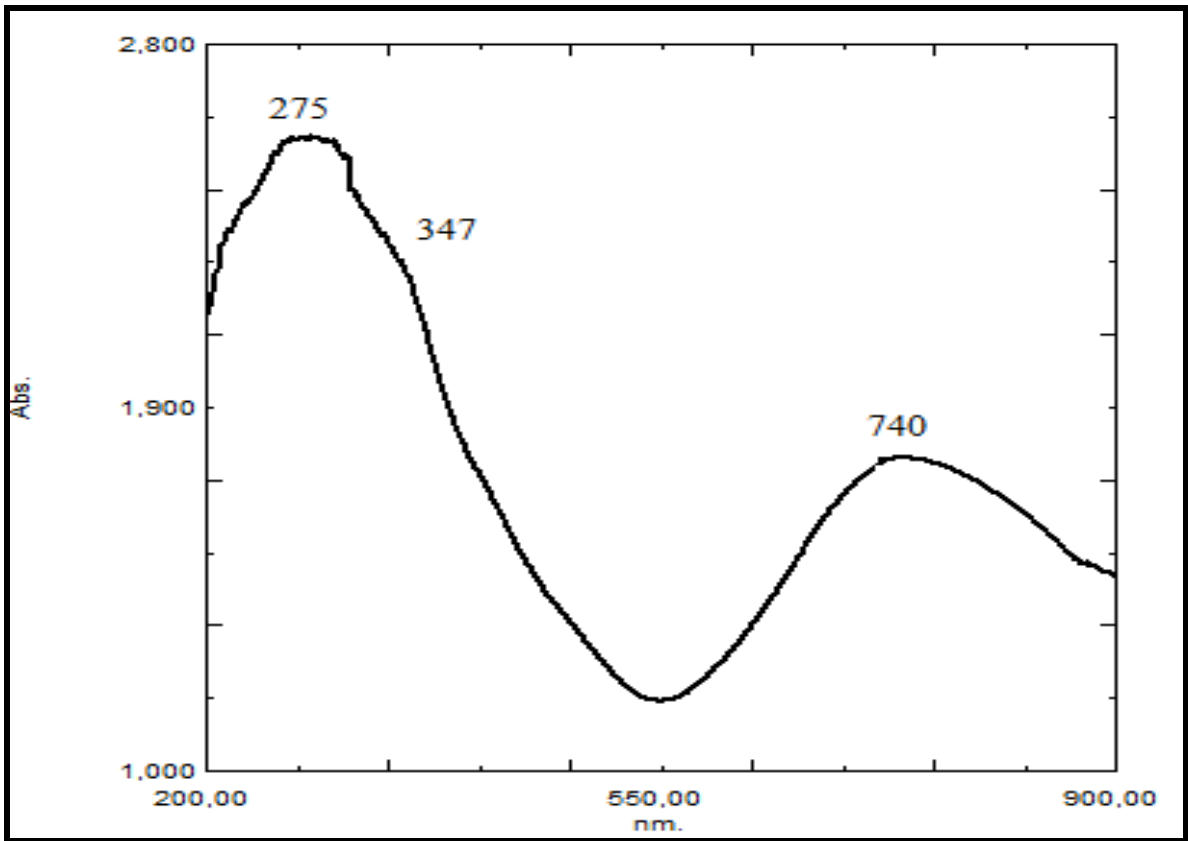


Figure 53: UV-VIS Spectrum of Complex 13

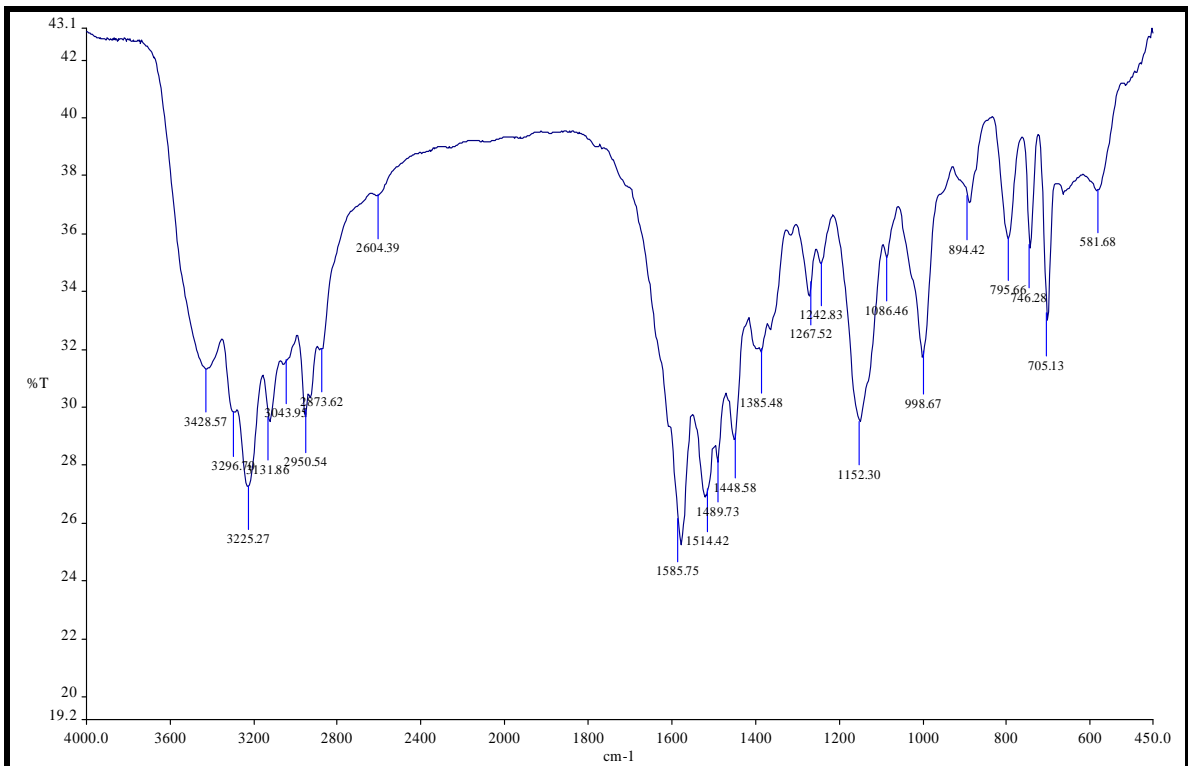


Figure 54: IR Spectrum of Complex 13

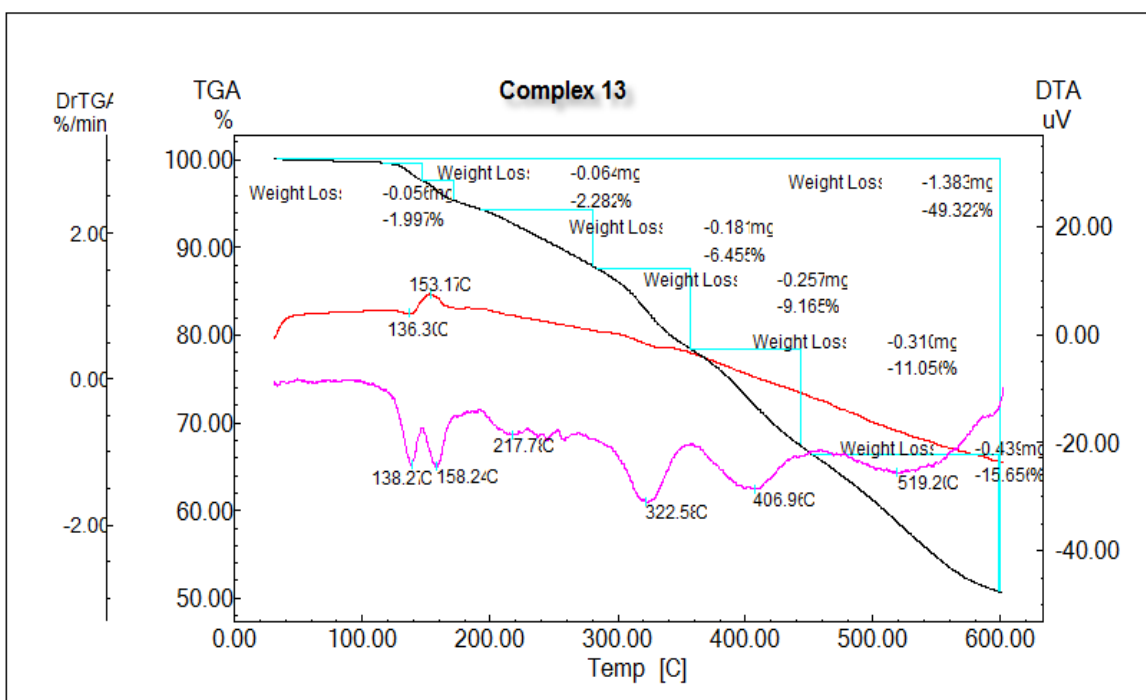


Figure 55: DTA-TGA Thermogram of Complex 13

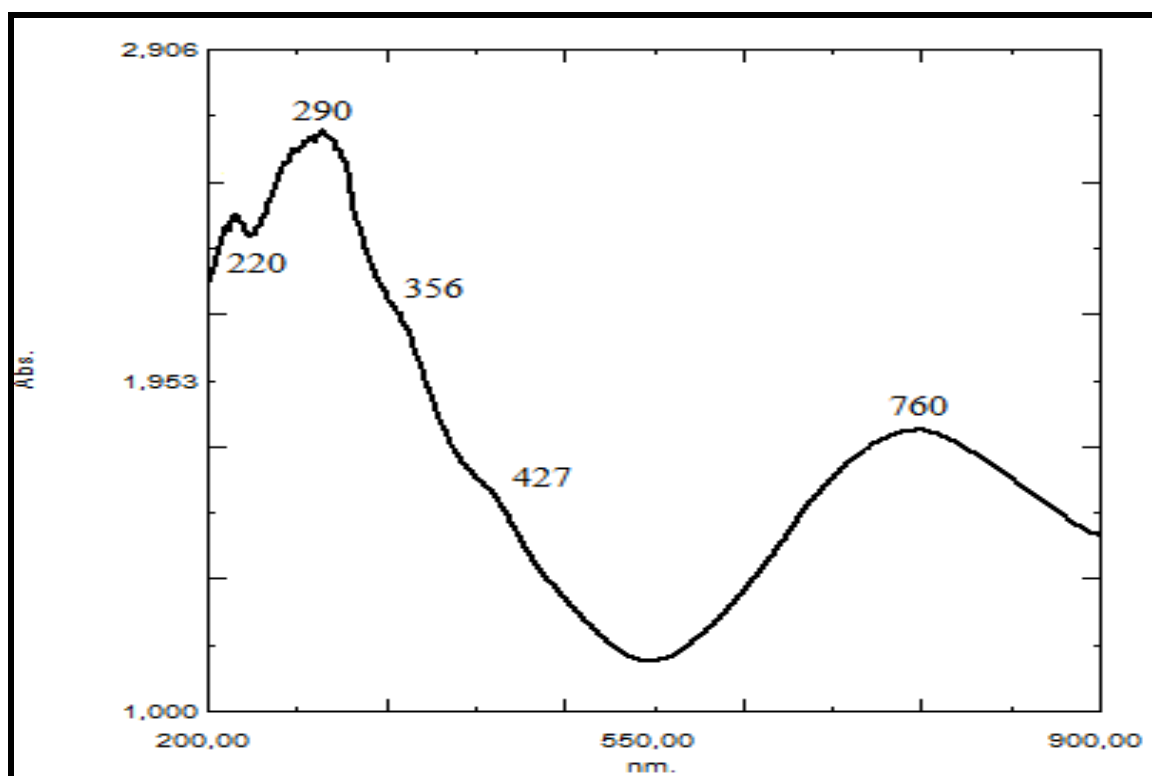


Figure 56: UV-VIS Spectrum of Complex 16

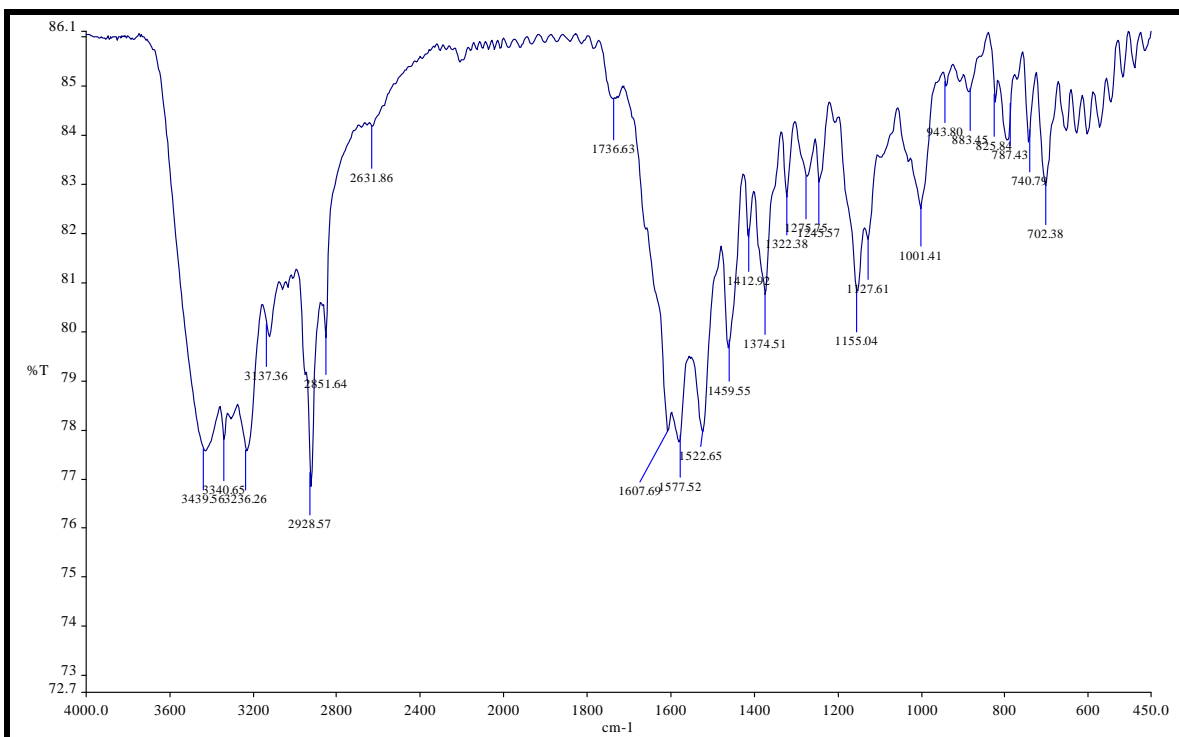


Figure 57: IR Spectrum of Complex 16

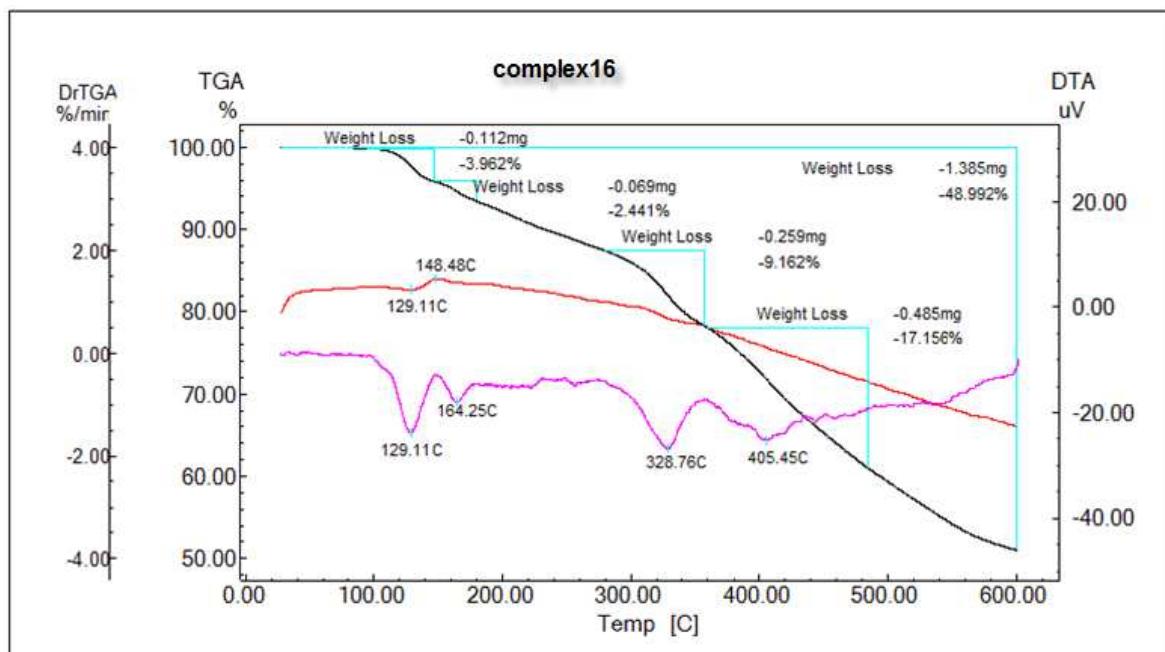


Figure 58: DTA-TGA Thermogram of Complex 16

#### 5.6.4. L1-Copper Complexes

The IR spectra of L1- complexes of nickel (3 and 6) and copper (1 and 4) were different from each other. In the IR spectra of Cu-L1 complexes, the bands in the 3100-3500  $\text{cm}^{-1}$  region appeared because of coordination to water.

Thermo-gravimetric measurements of the samples 1 and 4 were performed. In the complex 1 mass loss of 5.02 % was observed (theoretical mass loss for water molecules is 4.54 %) in two steps within the temperature range 25-220  $^{\circ}\text{C}$ . In the complex 4 a gradual mass loss of 6.04 % was observed (theoretical mass loss for water molecules is 6.74 %) in one step within the temperature range 25-220  $^{\circ}\text{C}$ . At the temperature of 360  $^{\circ}\text{C}$  the compounds start to decompose.

The reactions of Cu(II) chloride dihydrate and  $\beta$ -enaminone L1 afforded blue and dark green complexes according to two different complexation methods. The blue complex (complex 1) contain two water molecules and dark green complex (complex 4) contain three water molecules. The third water molecule is bonded to the central copper ion in complex 4.

The possible structures for the complexes 1 and 4 are proposed as shown in Figure 59 and 60.

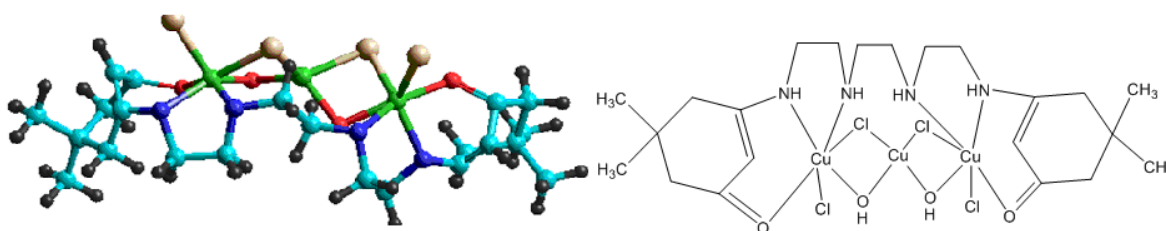


Figure 59. Possible structure of L1-Copper complex 1

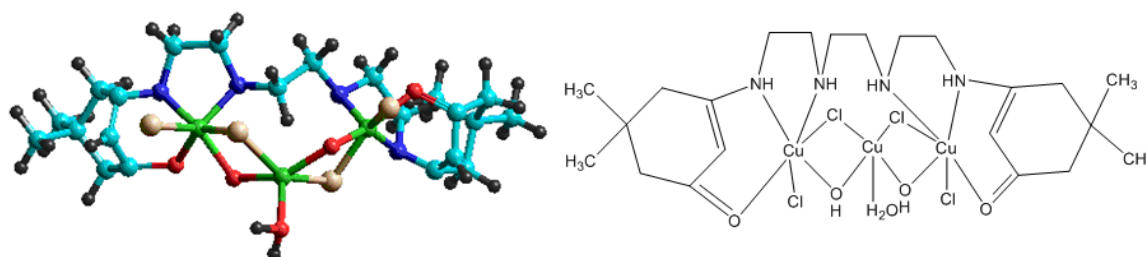


Figure 60. Possible structure of L1-Copper complex 4



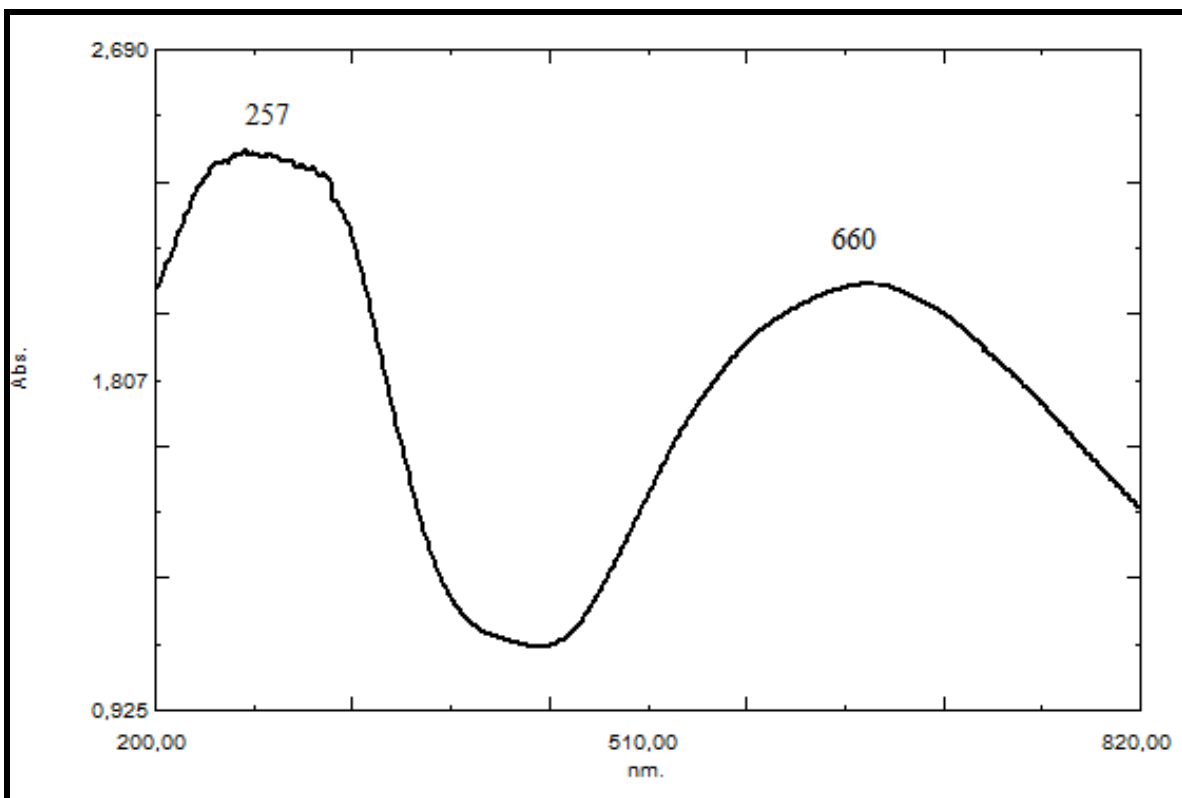


Figure 61: UV-VIS Spectrum of Complex 1

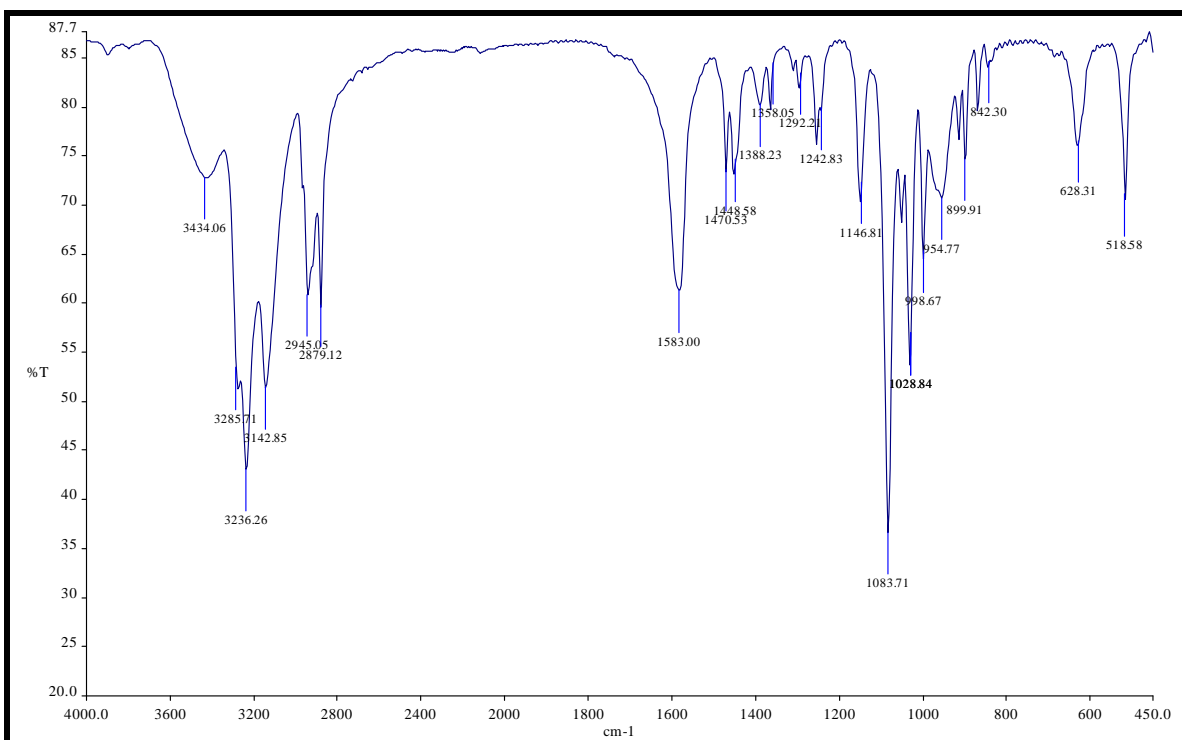


Figure 62: IR Spectrum of Complex 1

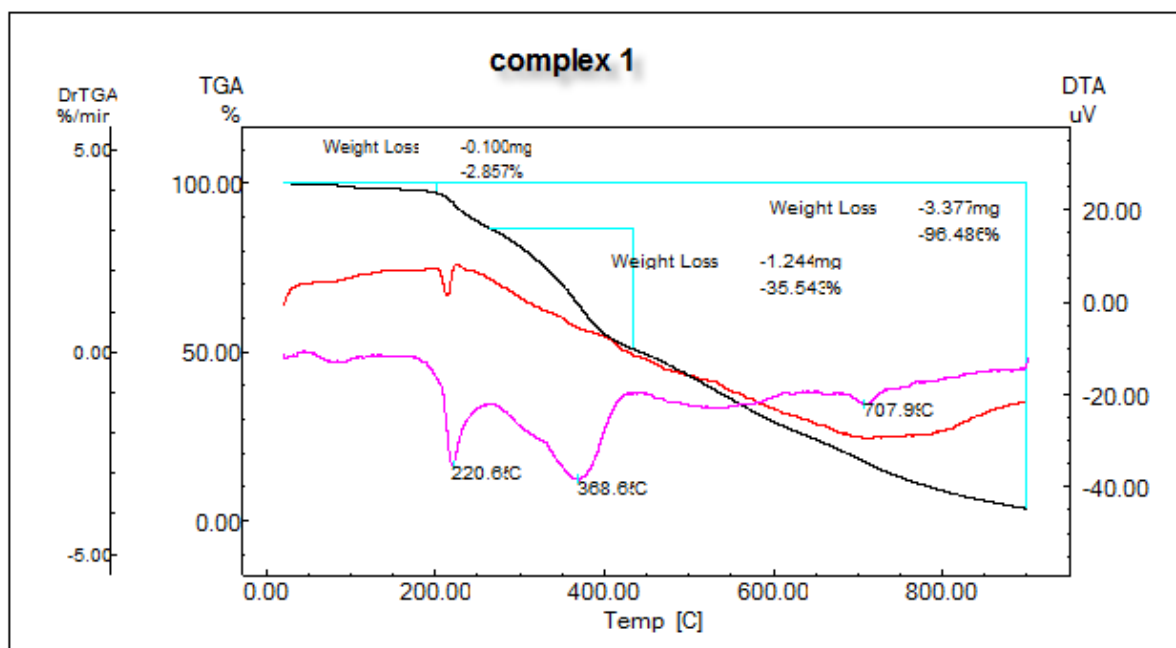


Figure 63: DTA-TGA Thermogram of Complex 1

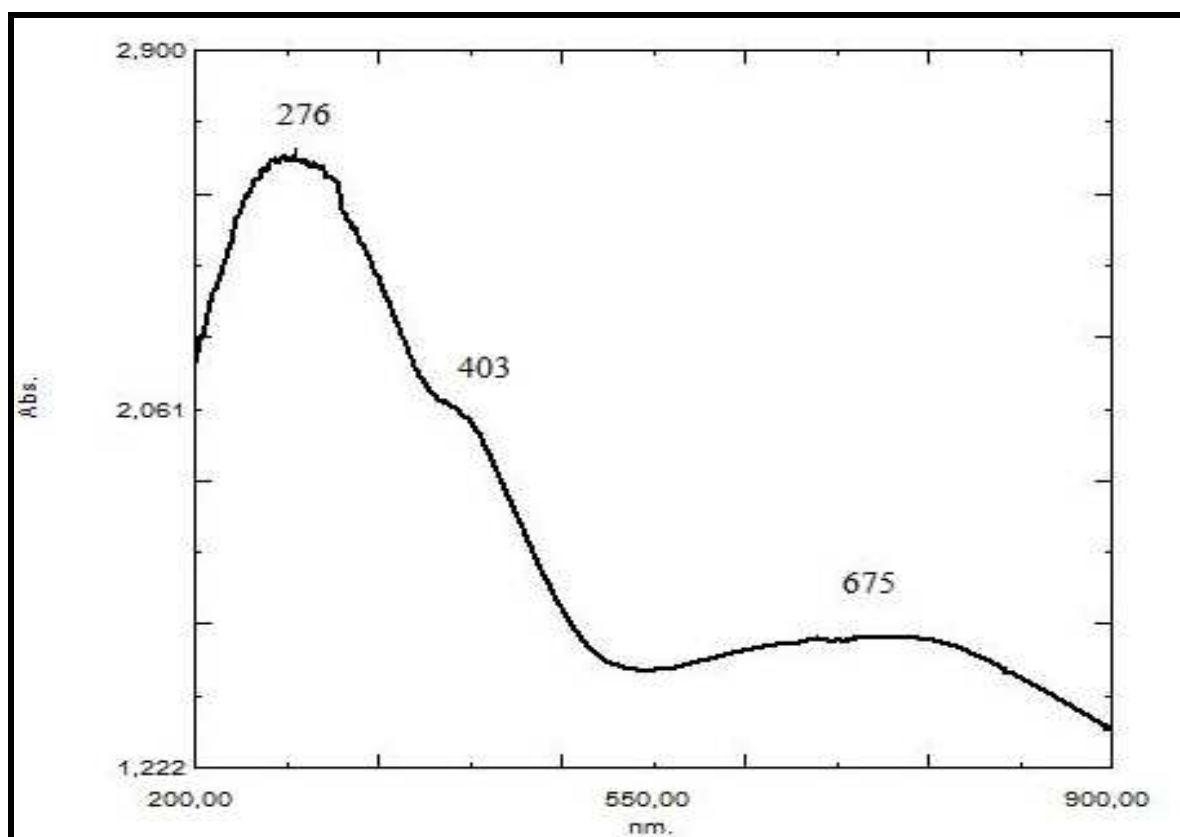


Figure 64: UV-VIS Spectrum of Complex 4

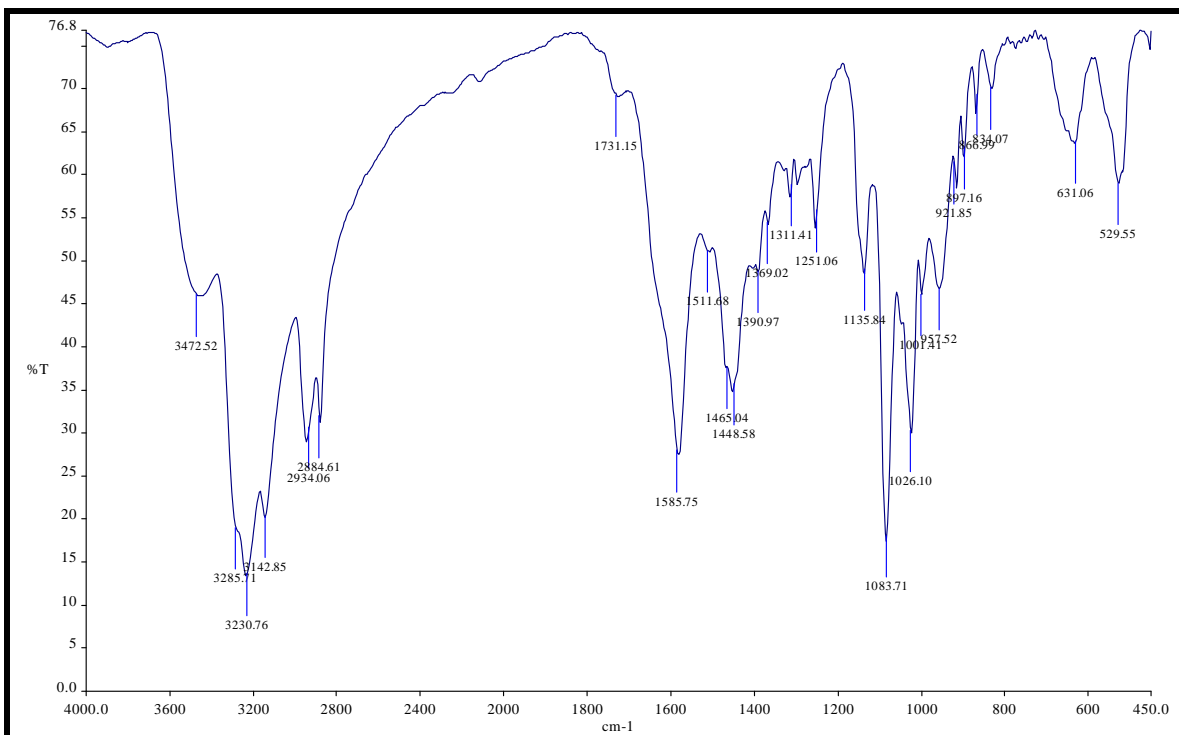


Figure 65: IR Spectrum of Complex 4

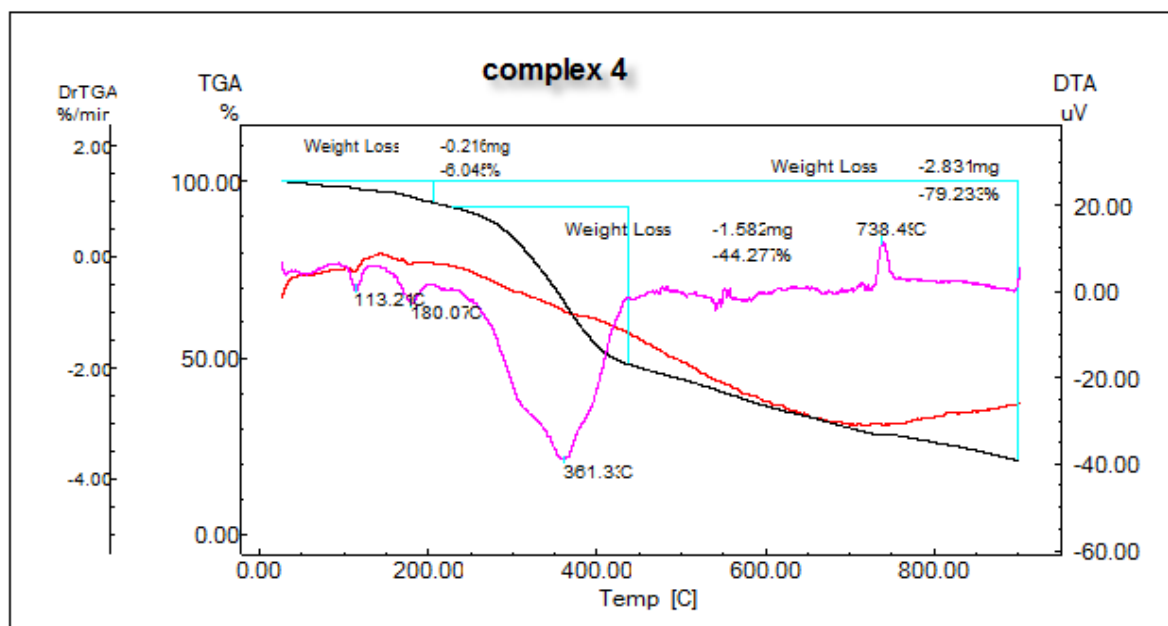


Figure 66: DTA-TGA Thermogram of Complex 4

### 5.6.5. L1 Cobalt Complexes

TGA thermograms showed decomposition temperature ranges 25-170 and 380-400 °C for complex 2 and 25-192 and 340-400 °C for complex 5. In the decomposition process of the Co (II) complexes, the mass losses corresponded to H<sub>2</sub>O leaving. For complex 2 at the first stage (25–170°C) with an experimental mass loss of 11.64 % (theoretical 9.71%) and for complex 5 experimental mass loss of 5.00% (theoretical 4.62%) represents the loss of H<sub>2</sub>O. The second stage within the temperature range 340–400°C represents the loss of ligand. The in-situ obtained complex (complex 2) contain four water molecules and all three cobalt atoms are bridged by  $\mu$ -OH groups. The two chlorides are bonded to two terminal cobalt atoms. The other cobalt complex (complex 5) contain only two water molecules so the cobalt atoms are attached to each other both by  $\mu$ -OH and chloride bridges.

The possible structure for the complexes 2 and 5 is proposed as shown in Figure 67 and 68.

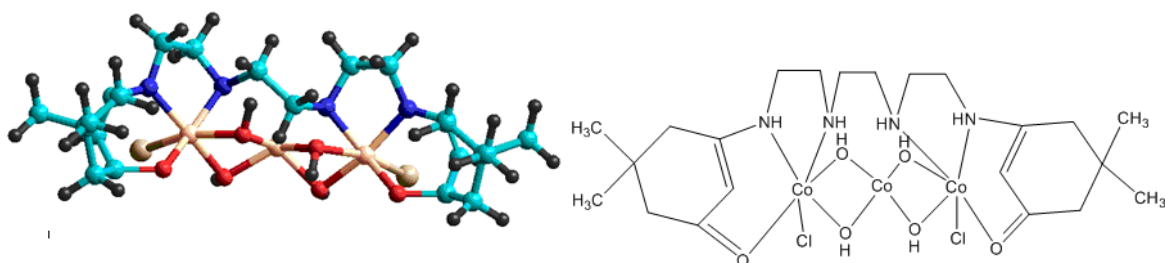


Figure 67. Possible structure of L1-Cobalt complex 2

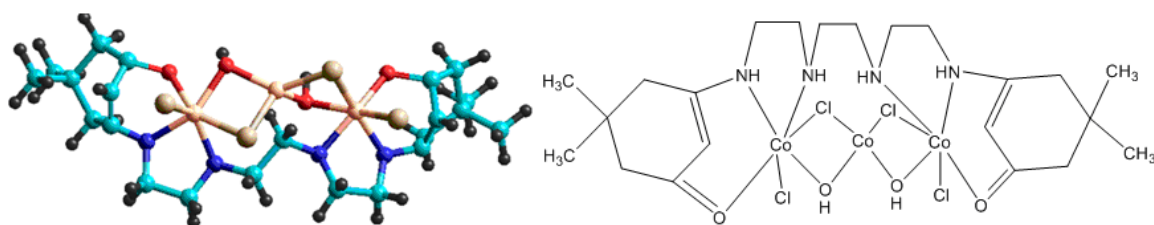


Figure 68. Possible structure of L1-Cobalt complex 5

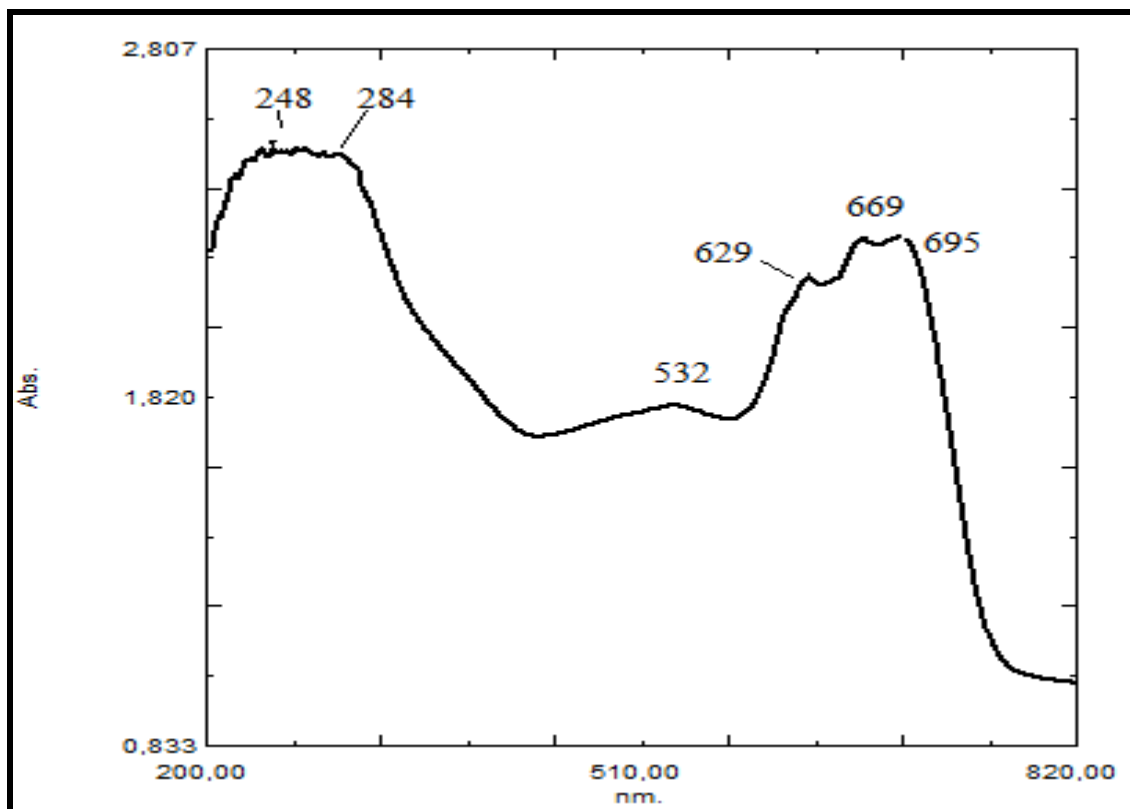


Figure 69: UV-VIS Spectrum of Complex 2

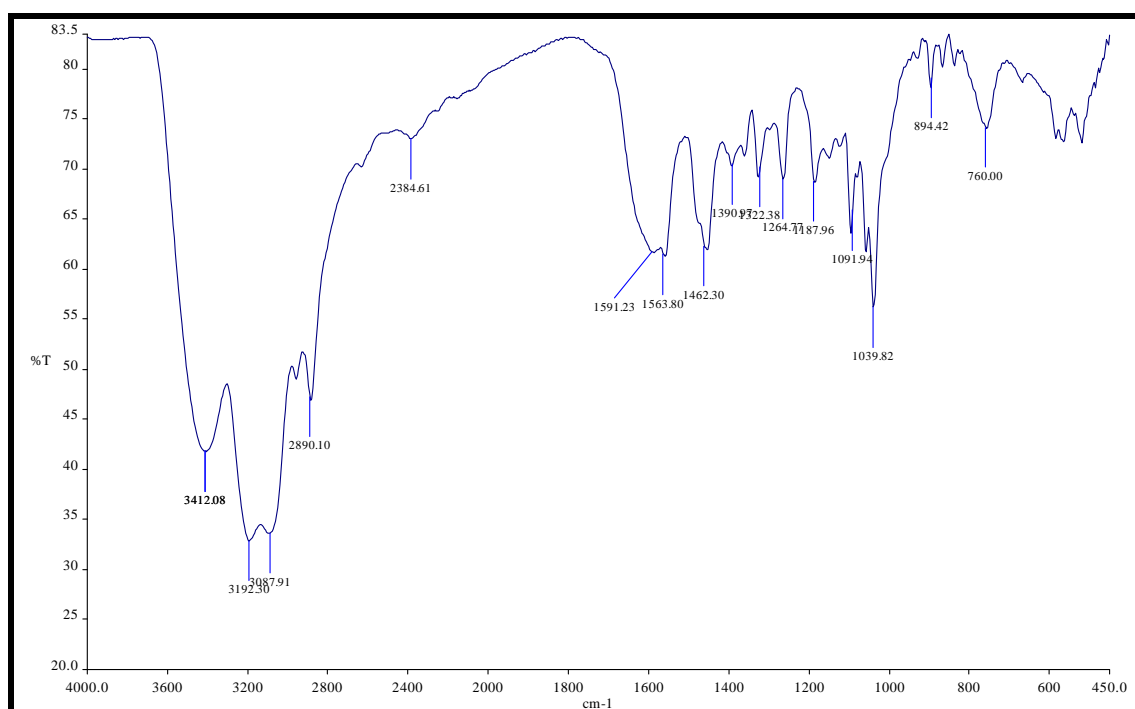


Figure 70: IR Spectrum of Complex 2

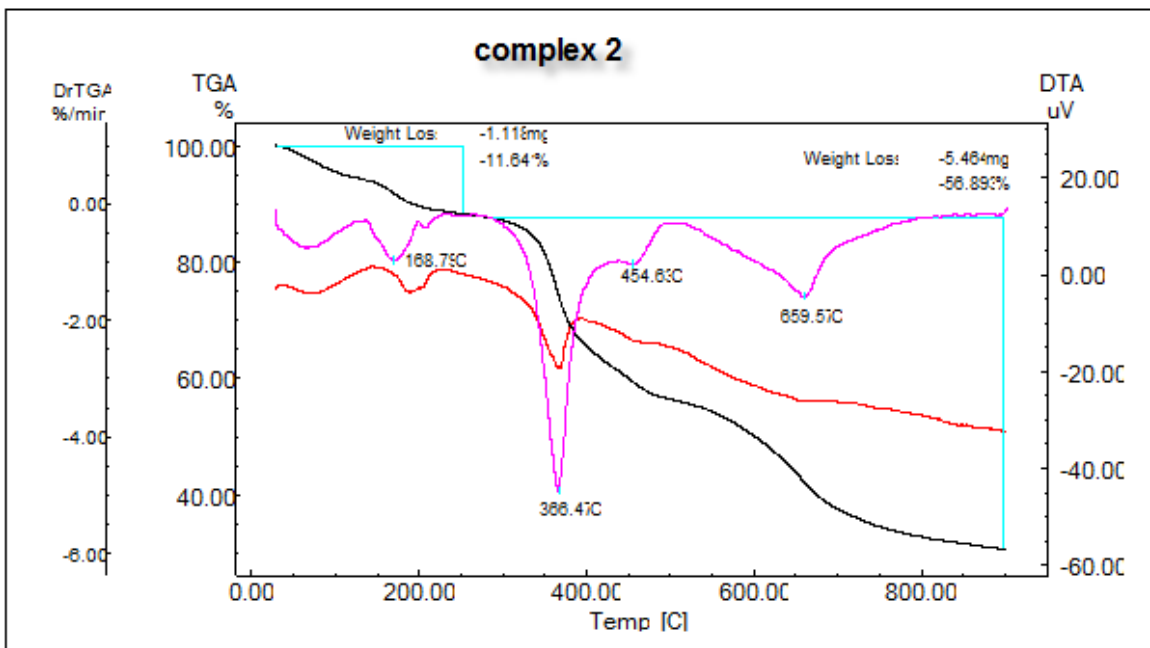


Figure 71: DTA-TGA Thermogram of Complex 2

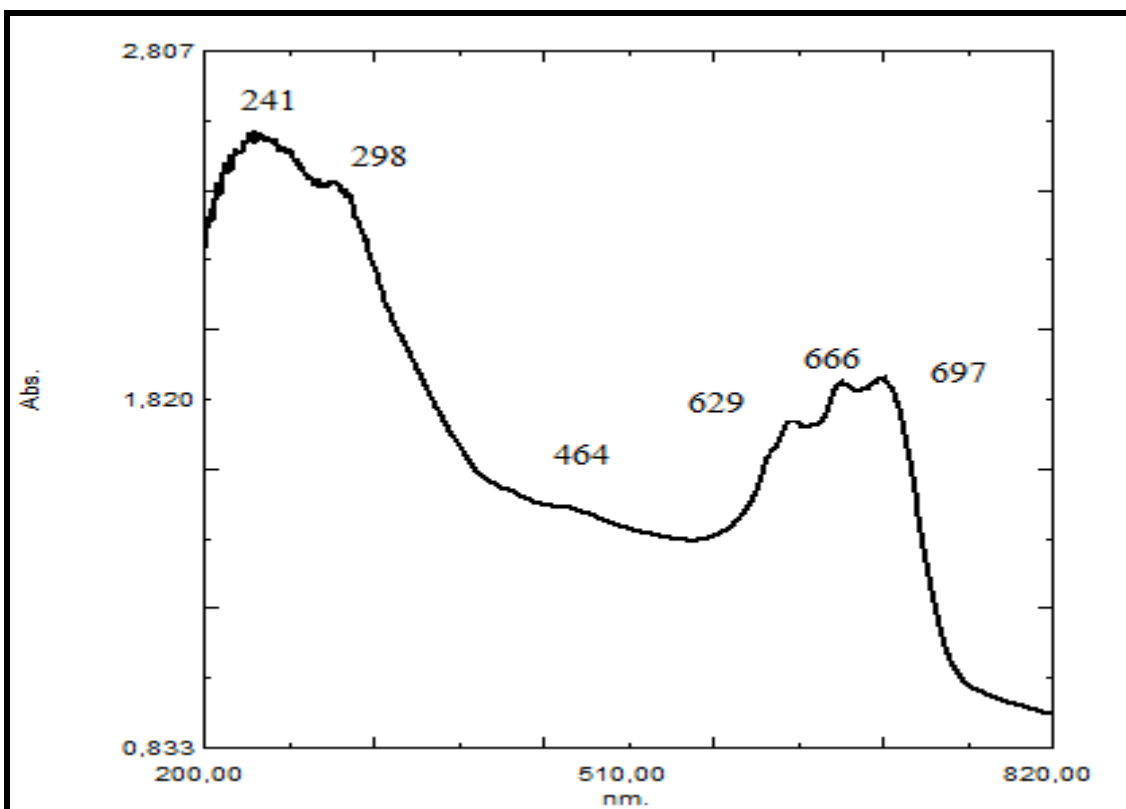


Figure 72: UV-VIS Spectrum of Complex 5

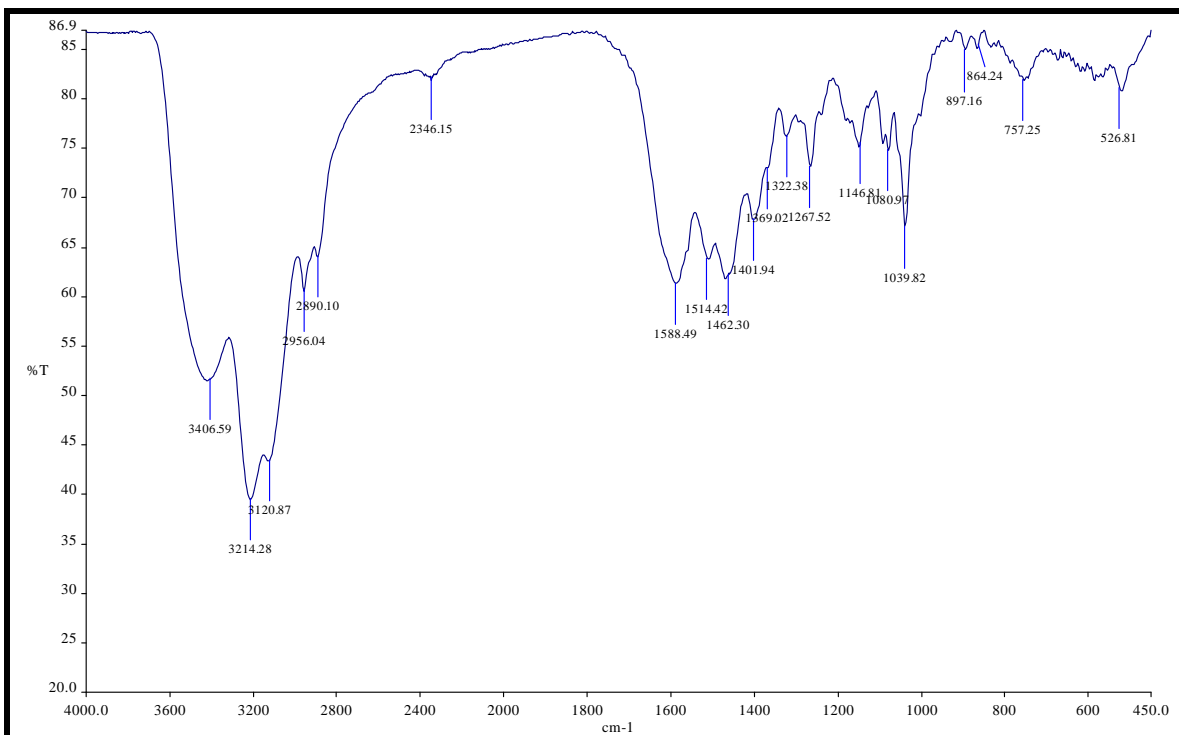


Figure 73: IR Spectrum of Complex 5

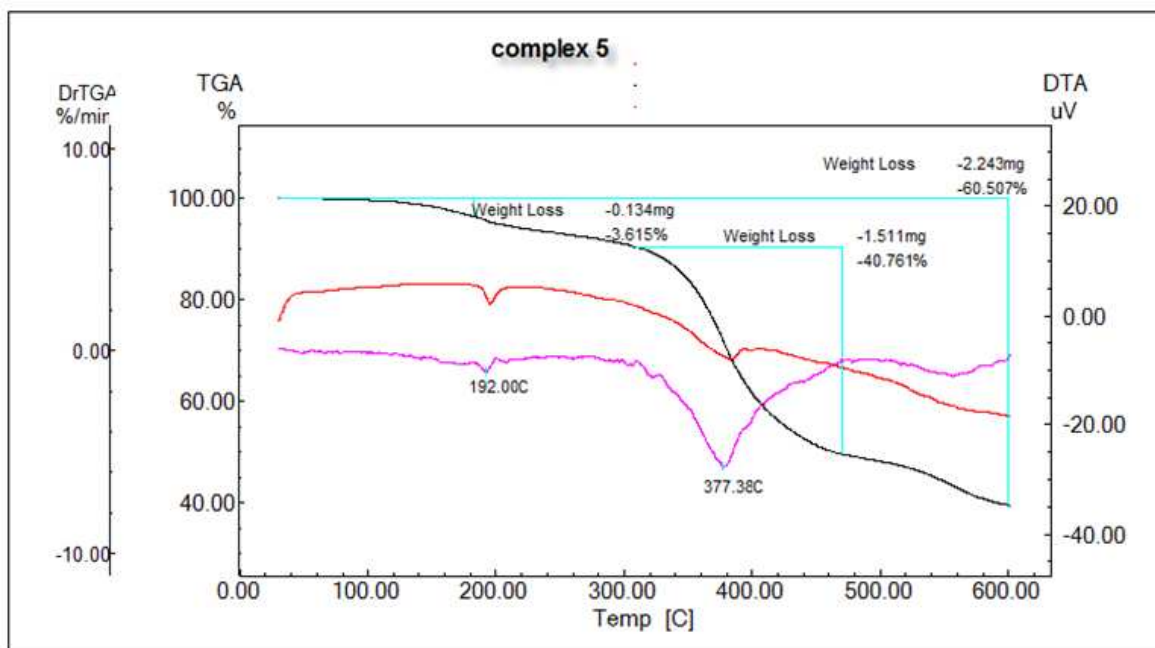


Figure 74 : DTA-TGA Thermogram of Complex 5

### 5.6.6. L3- Cobalt Complexes

Darkcyan coloured complexes of cobalt with L3 have similar properties and they contain two moles of water in their structures.

The possible structure for the L3 cobalt complex is proposed as shown in Figure 75.

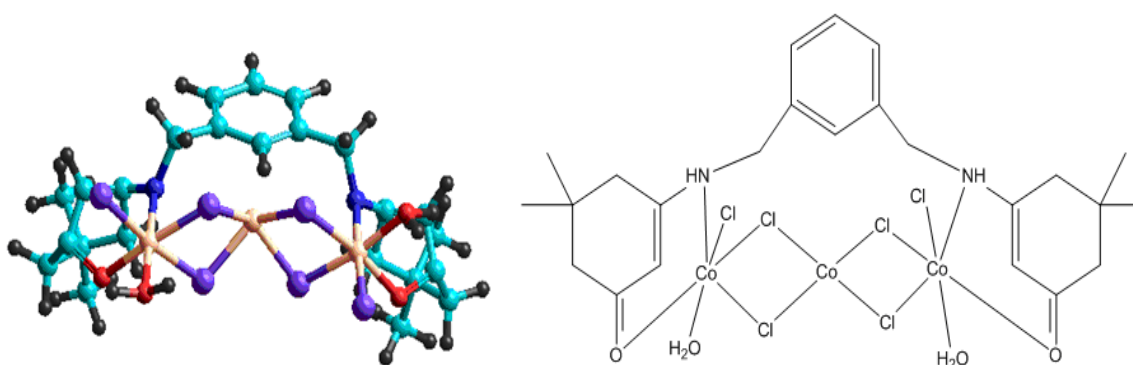


Figure 75. Possible structure of L3-Cobalt complex

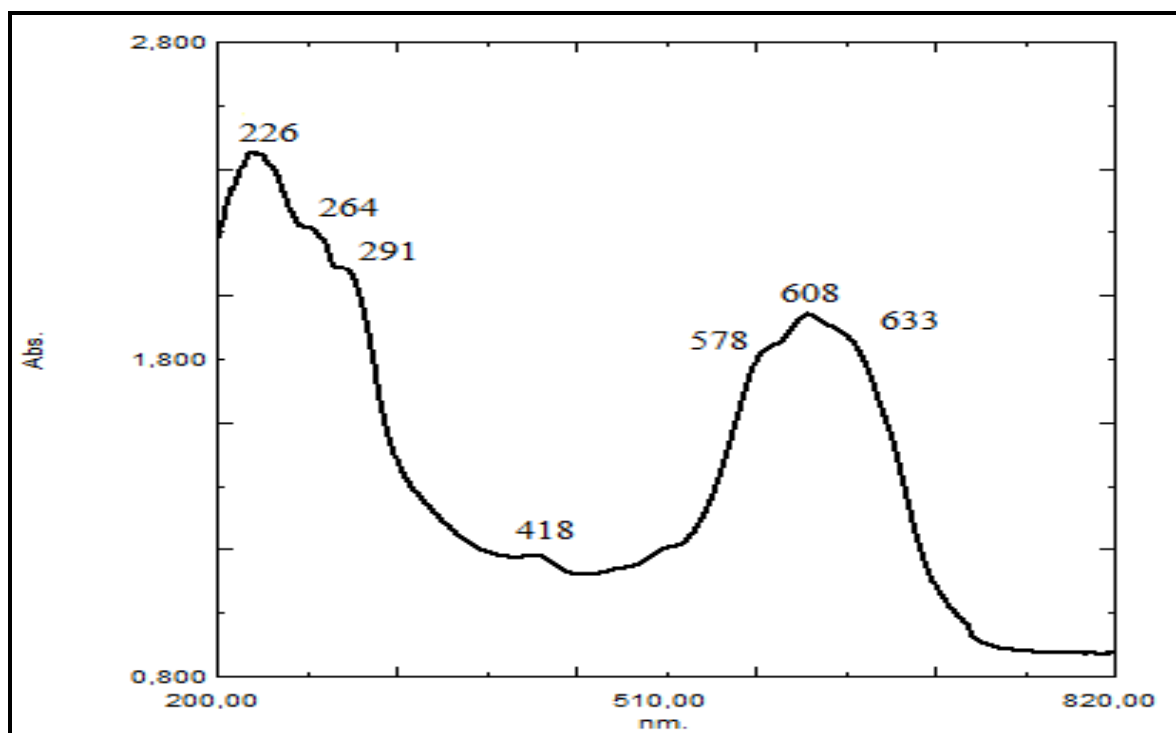


Figure 76: UV-VIS Spectrum of Complex 14



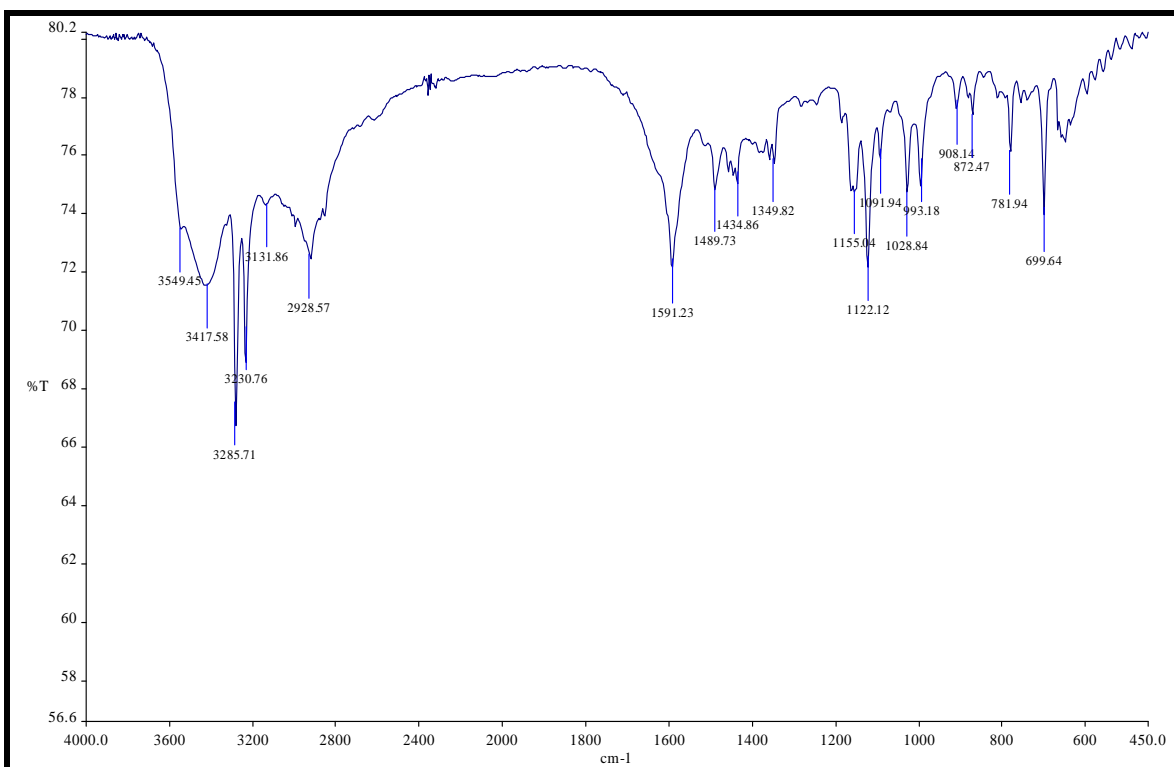


Figure 77: IR Spectrum of Complex 14

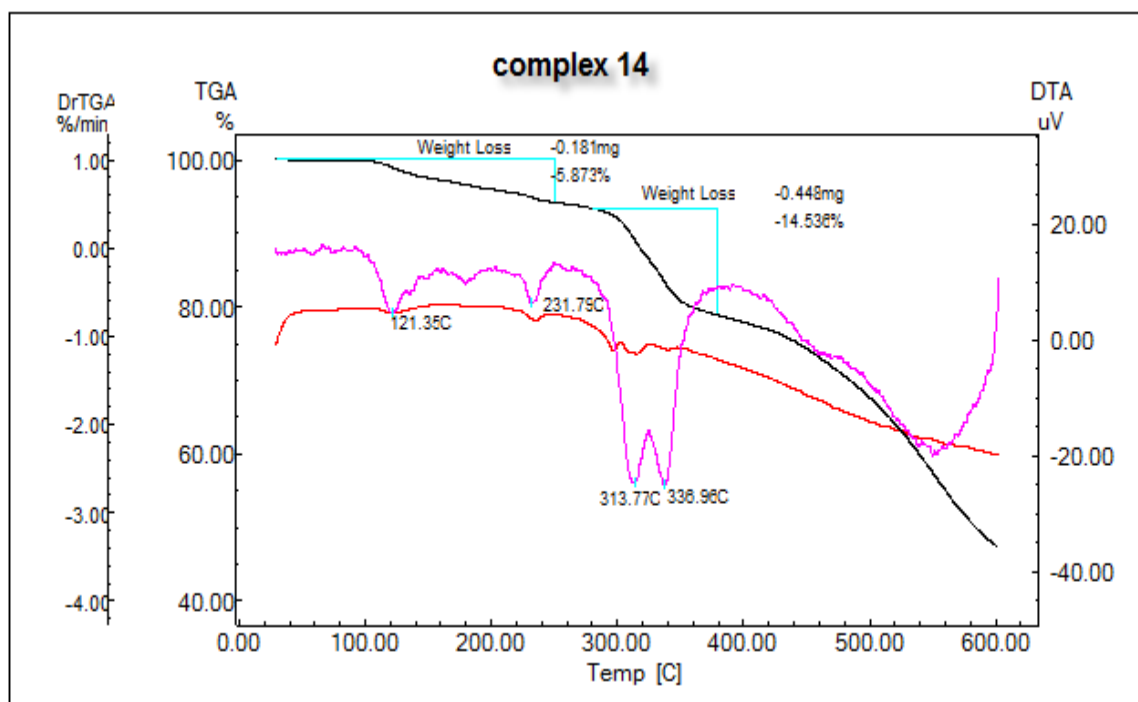


Figure 78: DTA-TGA Thermogram of Complex 14

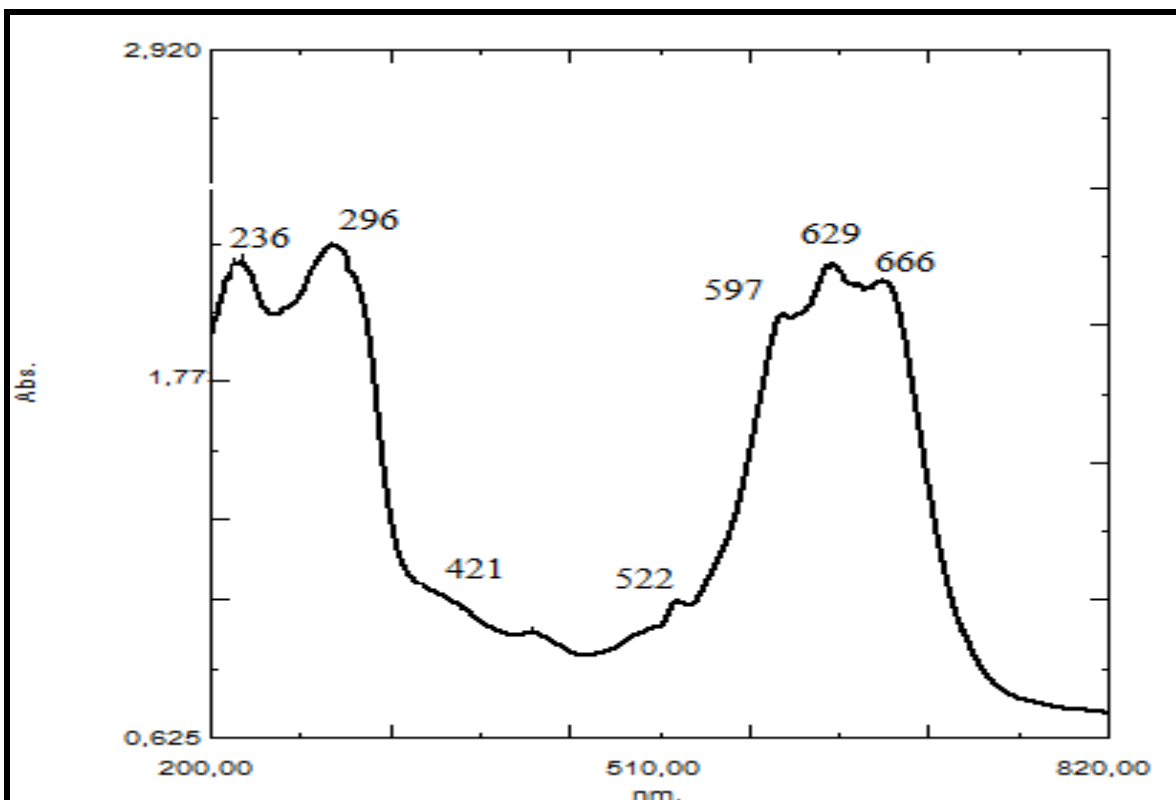


Figure 79: UV-VIS Spectrum of Complex 17

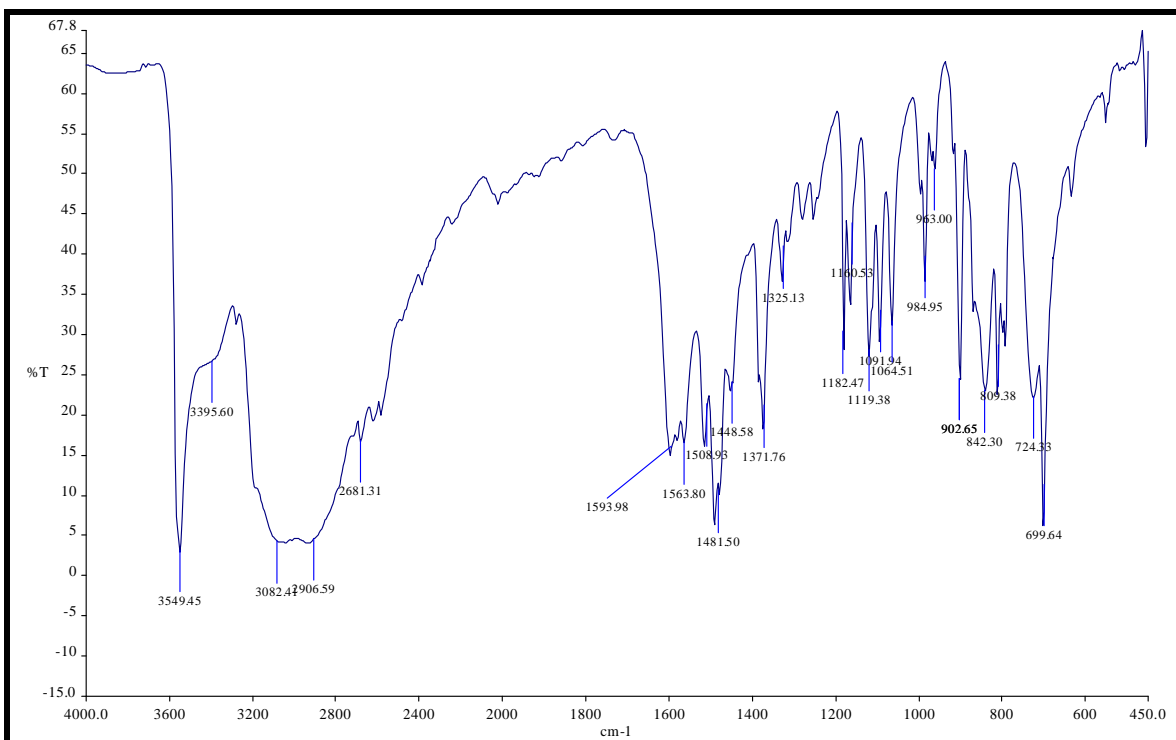


Figure 80: IR Spectrum of Complex 17

### 5.6.7. L3 Nickel Complexes

Ni-complexes of ligand L3 contain two water molecules different from L1 complexes of the same metal. Complex 15 and 18 which were obtained by two different methods from the same ligand L3 and the same metal nickel have similar properties. The proposed structure is shown in Figure 81.

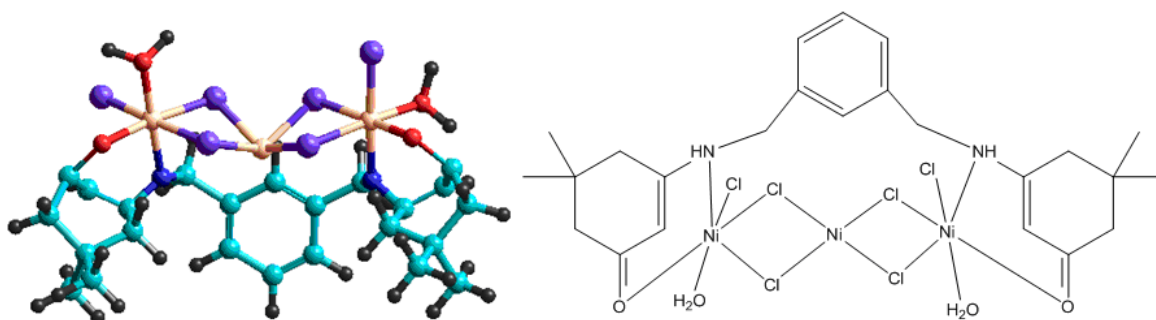


Figure 81. Possible structure of L3-Nickel complex

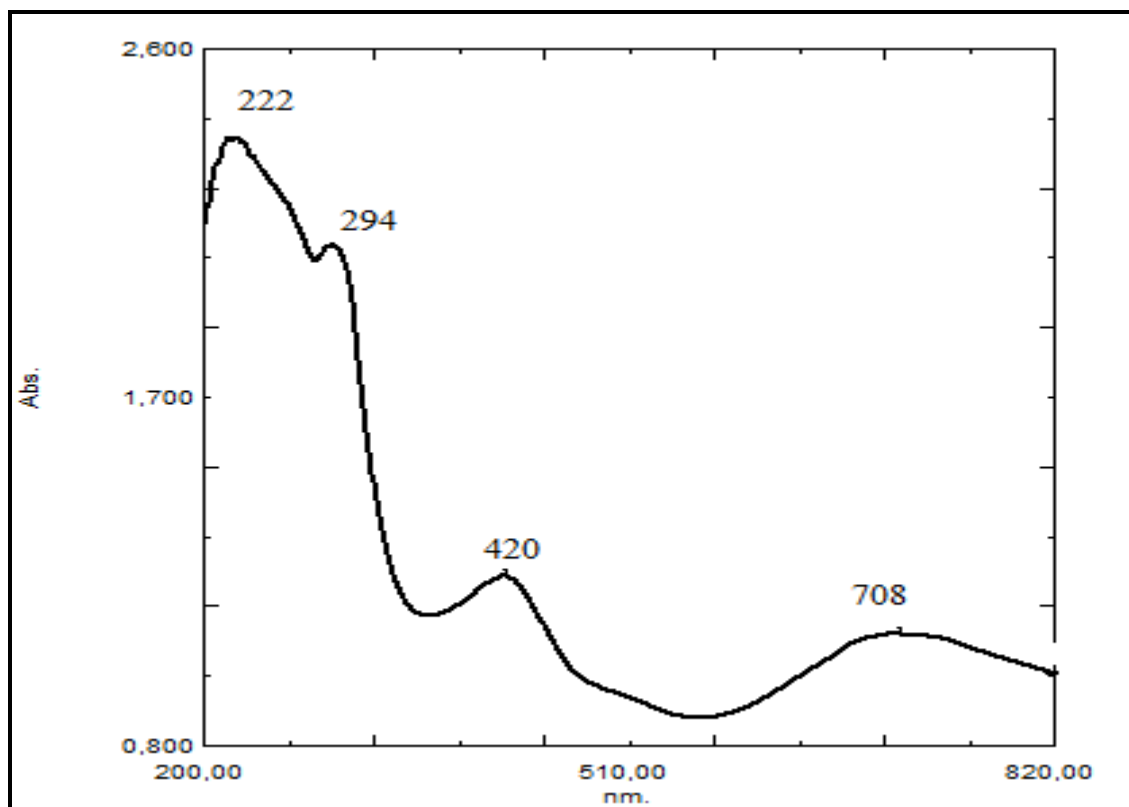


Figure 82: UV-VIS Spectrum of Complex 15

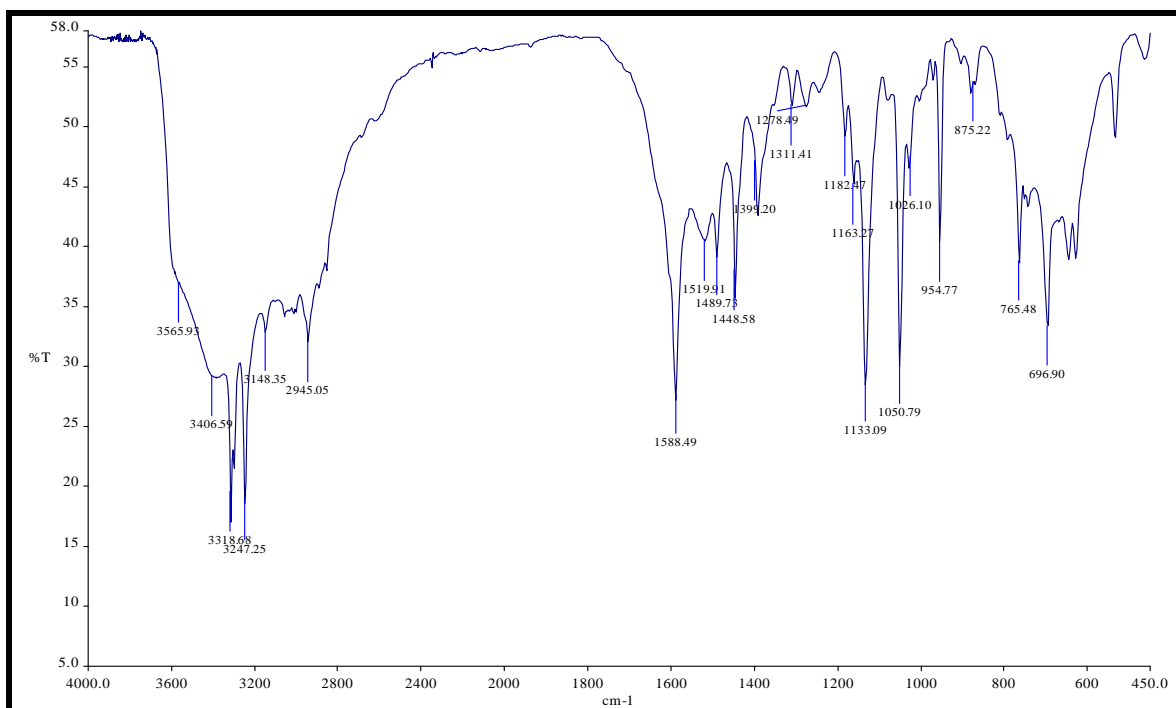


Figure 83: IR Spectrum of Complex 15

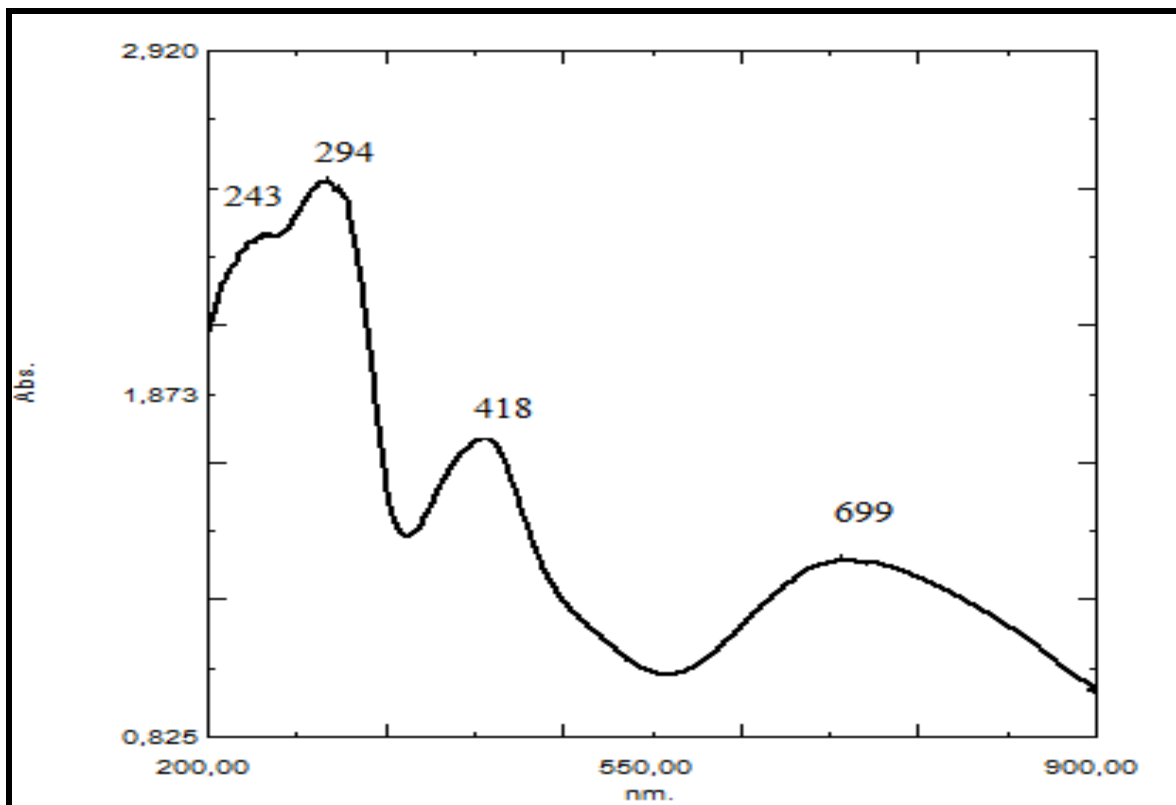


Figure 84: UV-VIS Spectrum of Complex 18

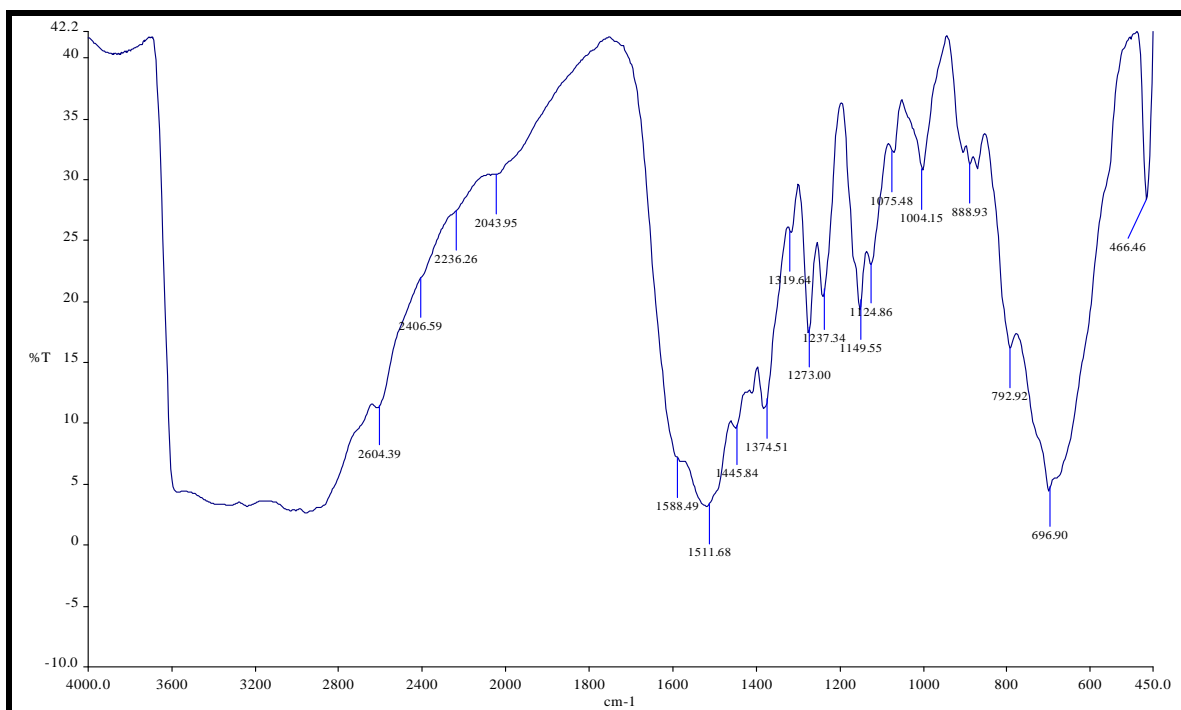


Figure 85: IR Spectrum of Complex 18

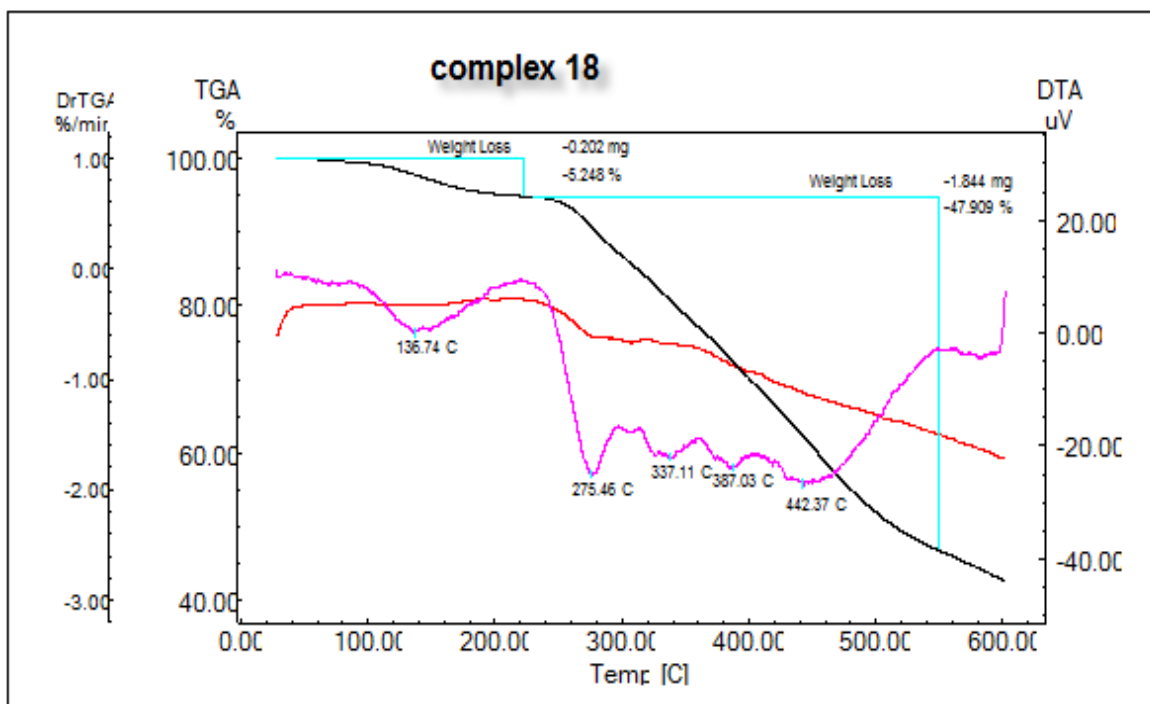


Figure 86: DTA-TGA Thermogram of Complex 18

### 5.6.8. L2-Copper Complexes

Copper complexes of ligand L2 ( complexes 7 and 10) have different colours according to the water contents their possible structures will be given after further analysis.

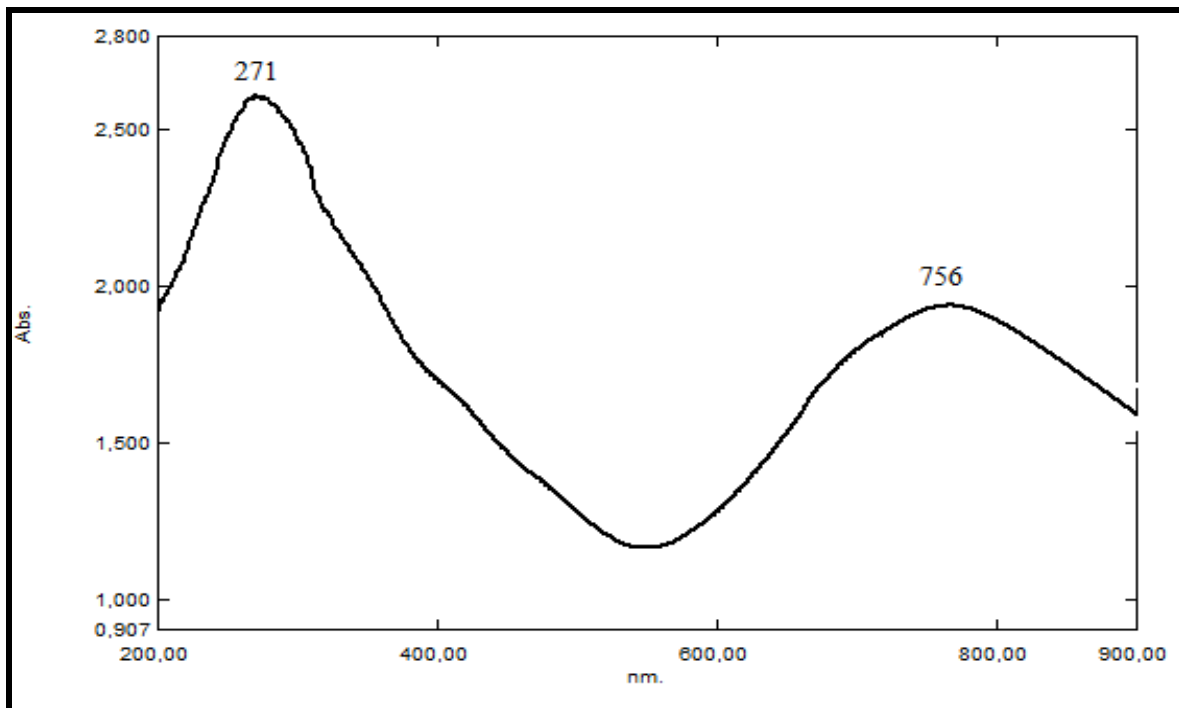


Figure 87: UV-VIS Spectrum of Complex 7

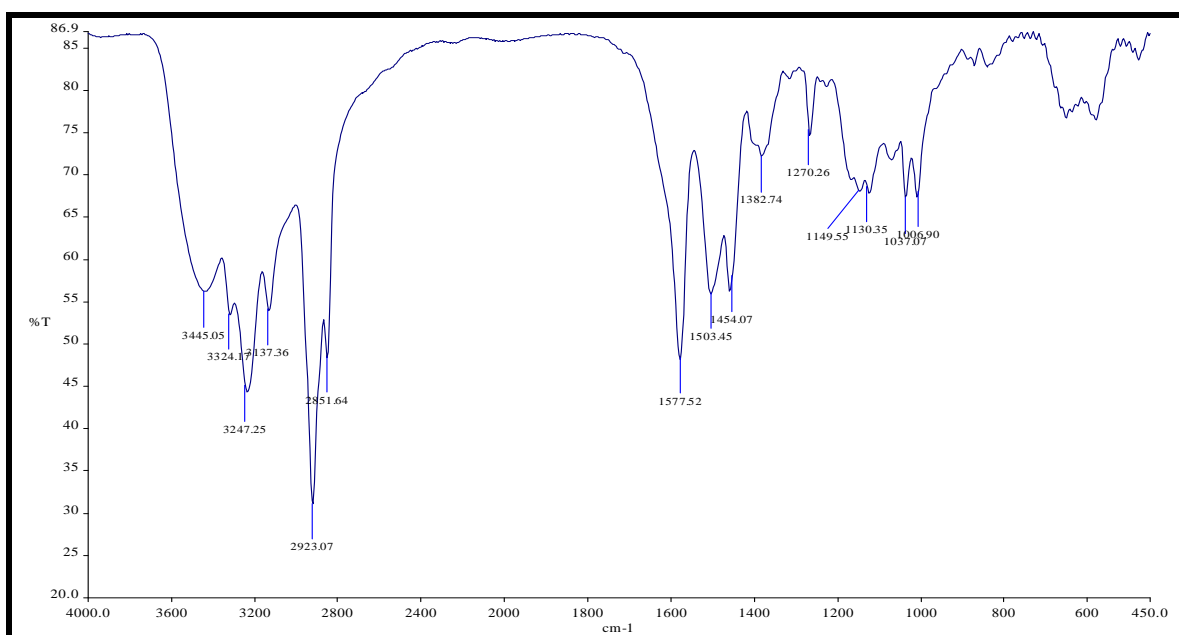


Figure 88: IR Spectrum of Complex 7

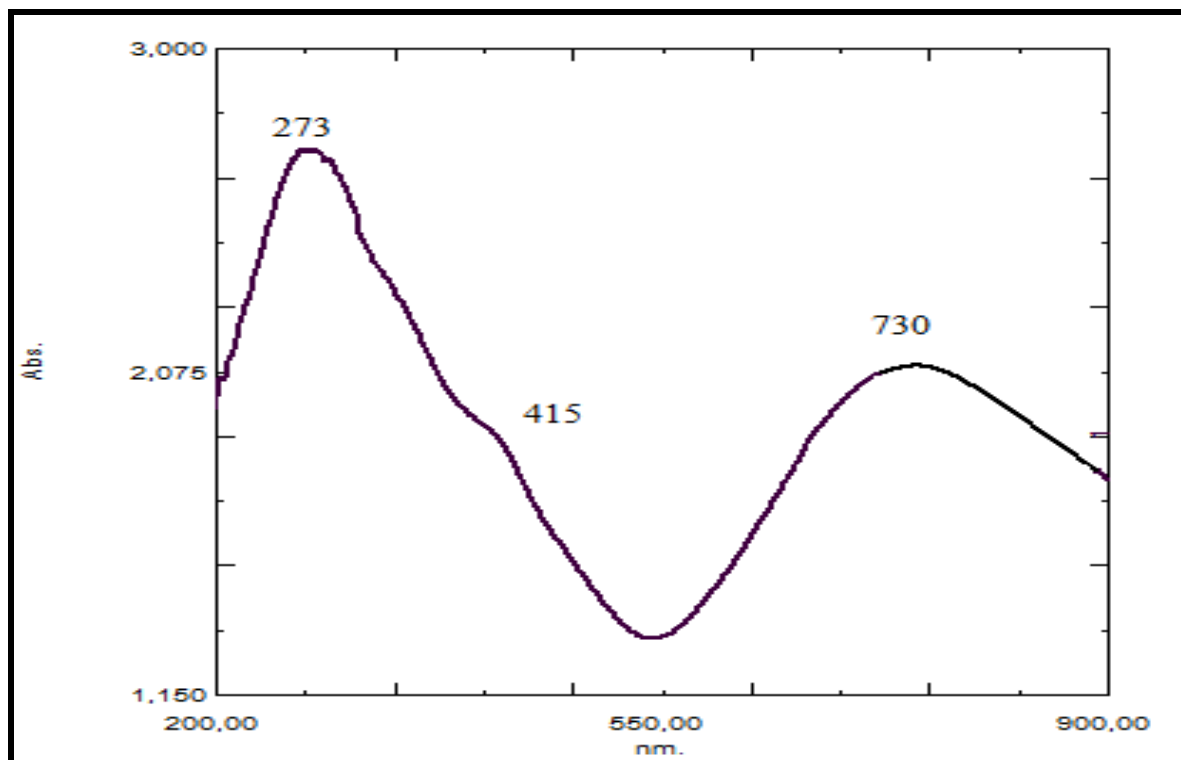


Figure 89: UV-VIS Spectrum of Complex 10

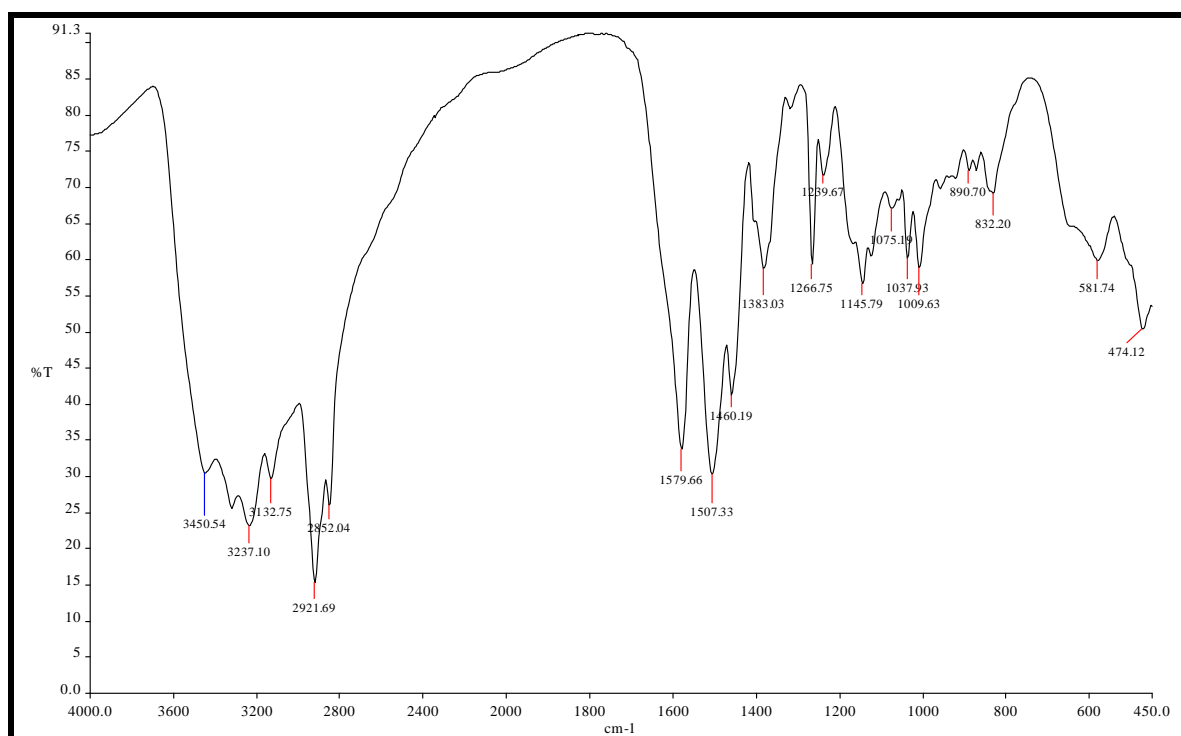


Figure 90: IR Spectrum of Complex 10

### 5.6.9. L2-Nickel Complexes

These nickel complexes (complexes 9 and 12) were light green and contained water molecules in their structures but the amount of water was not calculated. The possible structure of the complexes will be investigated after TGA analysis.

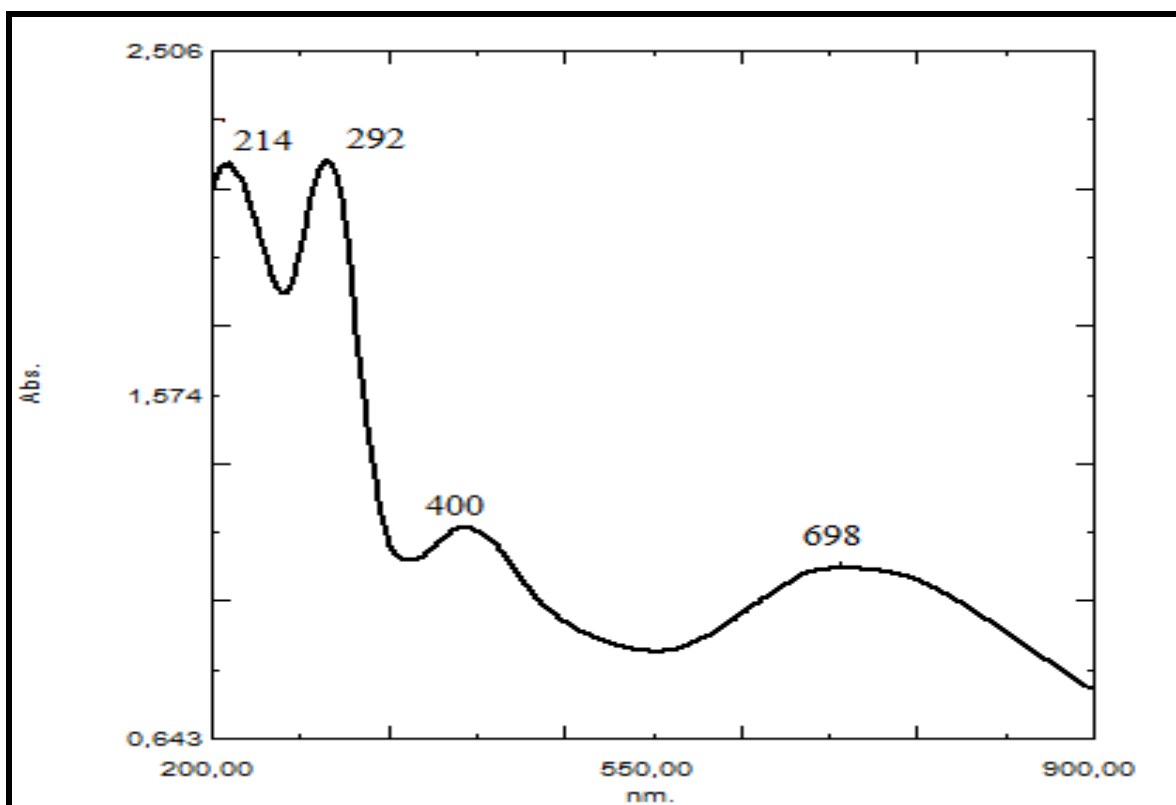


Figure 91: UV-VIS Spectrum of complex 9



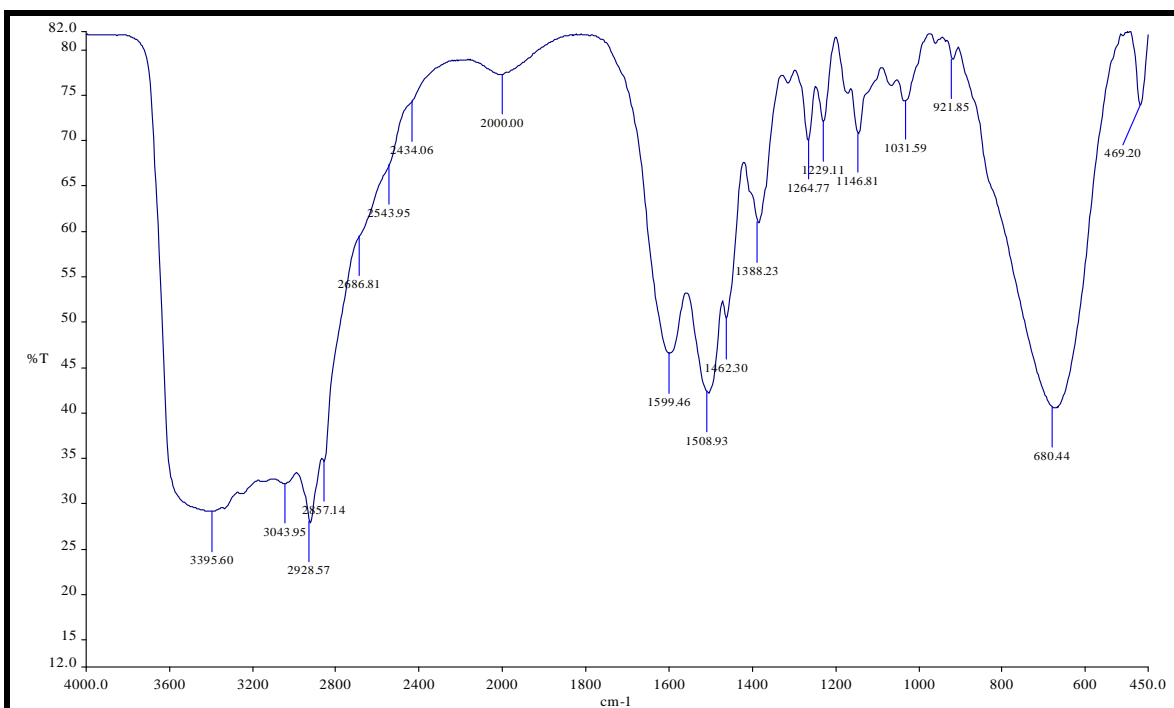


Figure 92: IR Spectrum of Complex 9

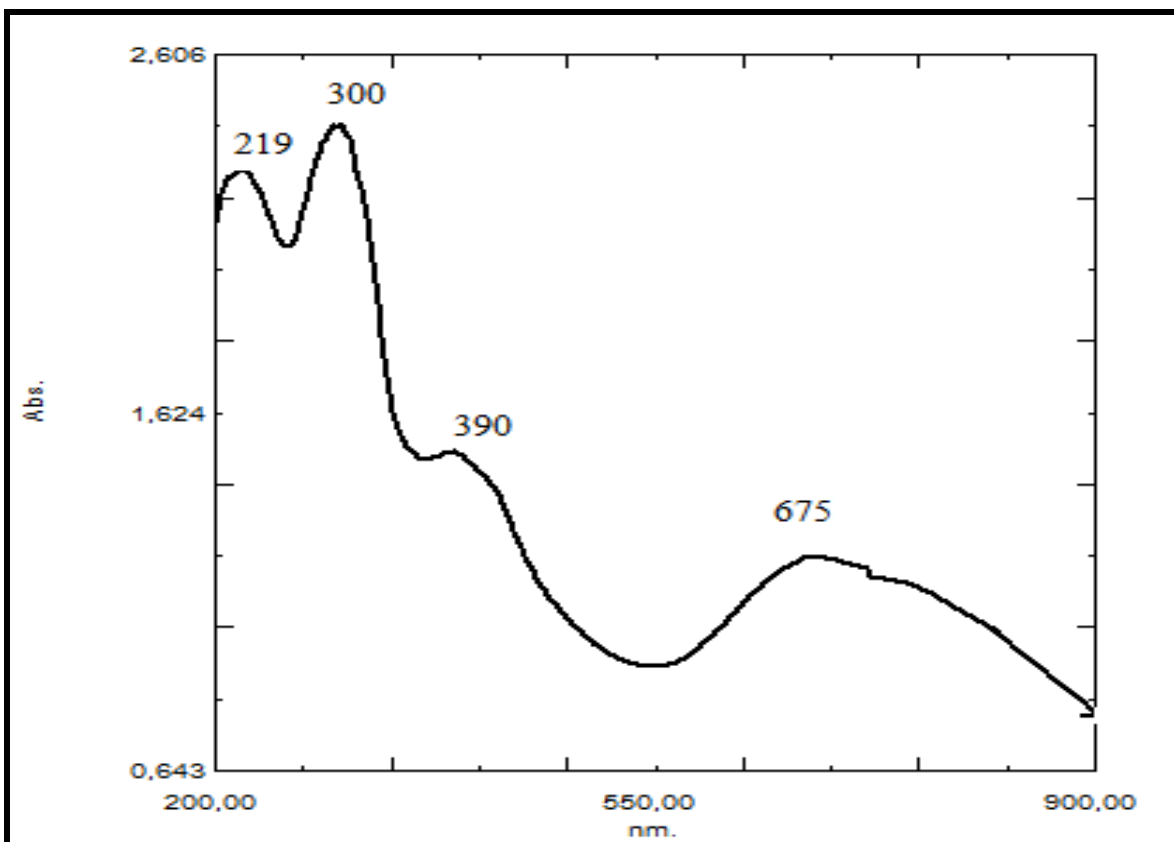


Figure 93: UV-VIS Spectrum of Complex 12

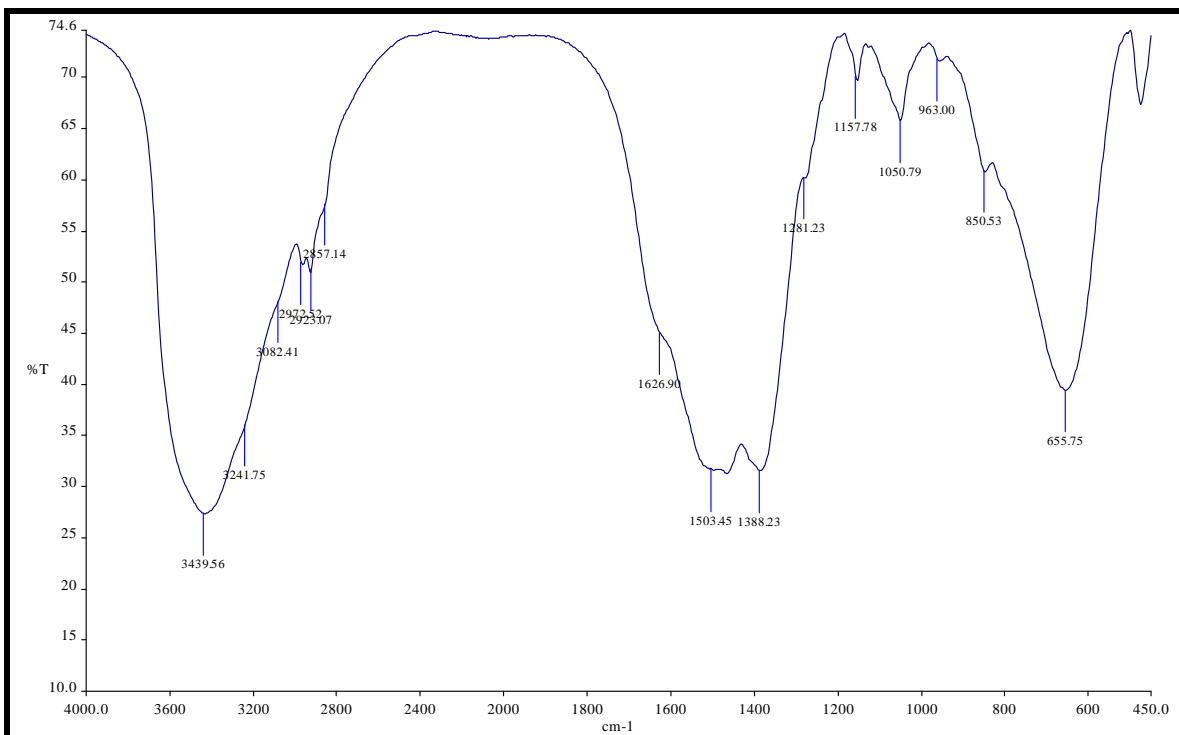


Figure 94: IR Spectrum of Complex 12

## 6. CONCLUSIONS

In an attempt to prepare five  $\beta$ -enaminone by the reaction of triethylenetetramine, 1,3-cyclohexanebis(methylamine), m-xylenediamine p-aminodiphenylamine, 1,3-cyclohexanedione and 5,5-dimethyl-1,3-cyclohexanediamine we have obtained some isomeric enaminones instead of imine-enols and keto-imines. The five enaminones were characterized by UV-VIS-NIR,  $^1\text{H-NMR}$ ,  $^{13}\text{CNMR}$ , FTIR and LC-MS spectra as well as elemental analysis.

According to the spectroscopic analyses, ketone amine ratio was 2:1 for L1,L2, L3 and 1:1 for L4, L5. Addition products were obtained in the Schiff base formation reactions as enaminone tautomers.

The first  $\beta$ -enaminone (**L1**), was obtained by condensation of the ketone, 5,5-dimethyl-1,3-cyclohexanedione, and triethylenetetramine in 75% yield.

The second product was, 3,3'-(cyclohexane-1,3-diylbis(methylene)) bis(azanediy) bis(5,5-dimethyl cyclohex-2-enone) (**L2**) and it was obtained by reacting, 5,5-dimethyl-1,3-cyclohexanedione with 1,3-cyclohexanebis(methylamine) in a quite high yield (94% ).

The third synthesis was realised according to procedure by using m-xylylendiamine and 5,5-dimethyl-1,3-cyclohexanedione to afford 3,3'-(1,3-phenylenebis(methylene))bis(azanediy) bis(5,5-dimethylcyclohex-2-enone) **L3** in 97% yield.

The fourth synthesis was realised according to procedure by using p-amino-diphenylamine and 5,5-dimethyl-1,3-Cyclohexanedione to afford 5,5-dimethyl-3-(4-(phenylamino)phenylamino)cyclohex-2-enone (L4) in 80% yield.

The last synthesis was realised by using 1,3-cyclohexanedione and p-amino-diphenylamine to afford 3-(4-(phenylamino)phenylamino)cyclohex-2-enone (L5) in 58% yield.

The  $\beta$ -enaminone L5 was analysed by single crystal X-ray diffraction. The enaminone molecule correspond to the *E* configuration of the double bond. The NMR shifts of the carbon and hydrogen atoms of the common segment of the five enaminones are alike. These two analyses allowed us to conclude that the common segments have similar electronic structure and that the double bond was in the *E* configuration in all five enaminones. The double bond is stabilized in the *E* configuration due to the internal hydrogen bond, N-H---O=C, either in the solid state or in a non polar solvent such as chloroform.

After the synthesis of the  $\beta$ -enaminones, the complexation studies have been realized. The complexes of the  $\beta$ -enaminones with three different metal cations Cu(II), Co(II) and Ni(II) were synthesized successfully by using two different methods.

The structures of  $\beta$ -enaminone metal complexes with Co(II), Ni(II), Cu(II), ions were confirmed by IR, and UV-VIS, magnetic susceptibility ICP-AES and TGA-DTA.

The yields of the complexes were in the range of 30-50%. Further stirring and heating did not increase the yield of the complexes. The low yields might be due to the steric hindrance around the coordination centre.

Eventhough many attempts for the preparation of metal complexes of  $\beta$ -enaminones (L4, L5) have been tried black coloured powders were obtained. Everytime when Cu(II), Co(II) and Ni(II) were used for complexation exact IR and NMR spectra could not be obtained for these compounds.

In the LC-Mass spectra of the  $\beta$ -enaminones the molecular ion peaks are in good agreement with their empirical formula as indicated from elemental analyses. The other peaks represent fragments of the molecular ion. The IR spectra show that L1 behaves as a neutral hexadentate ligand, coordinated to the metal ions via amine N and carbonyl O. L2 and L3 behaves as tetradentate ligand, coordinated to the

metal ions via amine N and carbonyl O. No molecular ion peak was observed for the metal complex of L1.

All complexes were obtained as coloured powder solids. They are antiferromagnetic as evidenced by magnetic susceptibility measurements.

$^{13}\text{C}$  NMR and  $^1\text{H}$  NMR spectrum could not be obtained clearly. The failure of taking NMR spectra of the complexes can be due to the paramagnetic properties of the complexes.

## REFERENCES

- Abd-Elzaher, M. M., 2001, Spectroscopic Characterization of Some Tetradentate Schiff Bases and Their Complexes with Nickel, Copper and Zinc, *J. Chin. Chem. Soc.*, 48, 153-158.
- Akitsu, T., Einaga, Y., 2006, Synthesis and crystal structures of the flexible Schiff base complex bis(N-1,2-diphenylethyl-salicydenaminato- $\kappa^2$ N,O)copper(II) (methanol): A rare case of solvent-induced distortion, *Polyhedron*, 25, 1089-1095.
- Alcantar, C.G., Yatsimirsky, A.K., Lehn, J.M., 2005, Structure-stability correlations for imine formation in aqueous solution *J. Phys. Org. Chem.* 18, 979-985.
- Allen, F. H., Kennard, O. Watson, D. Brammer, G. L., Orpen, A. G. Taylor, R., 1987, *J. Chem. Soc. Perkin Trans II.* 1-12.
- Ananthalakshmi, K.V.V., Edafiogho, I.O., Kombian, S.B. 2006, Concentration-dependent effects of anticonvulsant enaminone methyl 4-(4'-bromophenyl) aminocyclohex-3-en-6-methyl-2-oxo-1-oate on neuronal excitability in vitro, *Neuroscience.* 141, 345-356.
- Angyal, S. J., 1954, The Sommelet Reaction. *Org. React.*, 8, 197-206.
- Beckwith, A. L. J., Mayadunne, R. T. A., 2004, Diastereoselective radical cyclization reactions; the synthesis of O-methylcorytenchirine, *Arkivoc*, 80-93.
- Belmar, j., Pérez, F. R., Alderete, J., Zuniga, C., 2005, Synthesis and Tautomeric Studies of Enamines from 1-(n-Hexyl)-3-methyl-2-pyrazolin-5-one, *J. Braz. Chem. Soc.*, Vol., 16, No. 2, 179-189.
- Blaha K., Cervinka, O., 1966, Cyclic enamines and imines, *Advan. Hetrocycl. Chem.*, 6, 147-227.
- Bukhari, I. F., 2002, Preparation, Characterization and Biological Evaluation of Schiff-Base Metal Complexes of Some Drug Substances, PHD thesis Pakistan.
- Calligaris, M., Nardin G., Randaccio, L., 1972, *Coord. Chem. Rev.*, 7, 385-403.
- Casellato U., and Vigato, P. A., Fenton, D. E., Vidali, M., 1979, Compartmental ligands: routes to homo- and hetero-dinuclear complexes, *Chem. Soc. Rev.*, 8, 199.
- Chaaban, I., Greenhill, J. V. and Akhtar, P., 1979, Enaminones in the mannich reaction. Part 2. Further investigations of internal mannich reactions, *J. Chem. Soc., Perkin Trans.*, 1, 1593 – 1596.

- Cindric, M., Vrdoljak, V., Strukan, N., Brbot –Saranovic, A., Novak, P., Kamenar, B., 2004, The new molybdenum(V) complexes with differently N-substituted  $\beta'$ -hydroxy- $\beta$ -enaminones, *Inorg. Chim. Acta*, 357, 931–938.
- Cockenll, A. F., Harrison, R.G., 1977, *The Chemistry of Double Bonded Functional Groups*, ed. S. Patai, Interscience, New York, Suppl., A, part 1, p. 288.
- Cohen, M.D., Schmidt, G.M.J. and Flavian, S., 1964, *Topochemistry. VI. Experiments on photochromy and thermochromy of crystalline anils of salicylaldehydes*, *J. Chem. Soc.*, 2041.
- Cox, D.S., Scott, K.R., Gao, H., Eddington, N.D., 2002, Effect of P-Glycoprotein on the Pharmacokinetics and Tissue Distribution of Enaminone Anticonvulsants: Analysis by Population and Physiological Approaches, *J. Pharmacol Exp. Ther.*, 302, 3, 1096-1102.
- Dorris, M., 1999, *Reversing the Effects of Formalin Fixation “PhD Thesis”*, UK.
- Douglas B., Mcdaniel D., Alexander J., 1993, *Concept and Models of Inorganic Chemistry*, third ed., John Wiley & Sons, Inc. New York.
- Dziembowska, T., 1998, Resonance assisted intramolecular hydrogen bond in Schiff bases, *Pol. J. Chem.*, 72 193-209.
- Eberlin, M. N., Takahata, Y., Kascheres, C., 1990, The use of AM1 in structural analyses of primary and secondary enaminones, *J. Mol. Struct. (Theochem)*, 207, 143-156.
- Elmalı, A., Kabak, M., Kavlakoglu, Elerman, E. Y., Durlu, T. N., 1999, Tautomeric properties, conformations and structure of N-(2-hydroxy-5-chlorophenyl) salicylaldimine, *J. Mol. Struct.*, 510, 207-214.
- Elassar, A.-Z. A., El-Khair, A. A., 2003, Recent Developments in the Chemistry of Enaminones, *Tetrahedron*, 59, 8463.
- El-hashim, A. Z., Edafiogho, I. O., Kombian, S.B., Yousif, M.H., 2007, Anti-tussive and bronchodilator actions of enaminone, E121 U.S patent, Pub. No.: US 2007/0167518 A1.
- Fenton, D.E., 1986, Tetraimine Schiff base macrocycles derived from heterocyclic dicarbonyls, *Pure & Appl. Chem.*, Vol.58, No.11, 1437-1444.
- Fish, R.G., Groundwater, P.W., Morgan, J.J.G., 1995, The photo-epimerisation of gossypol Schiff's bases, *Tetrahedron: Asymmetry*, 6, 873-876.
- Fonseca, T.L.; De Oliveira H.C.B.; Amaral, O.A.V.; Castro, M.A. MP2 static first hyperpolarizability of azo-enaminone isomers *Chem. Phys. Lett.* 2005, 413, 356–361.

- Gallardo, C., Trujillo, A., Fuentealba, M., Vega, A., Carrillo, D., Manzur, Carolina., 2007, Organometallic 1,5-Benzodiazepine And 1,5-Benzodiaze Pinium Compounds: Synthesis, Characterization, X-Ray Diffraction Structures And Theoretical Investigation, J. Chil. Chem. Soc, 52, No 3, 1266-1270.
- Gilli, P., Bertolasi, V., Ferretti, V., Gilli, G., 2000, Evidence for Intramolecular N-H--O Resonance-Assisted Hydrogen Bonding in  $\alpha$ -Enaminones and Related Heterodienes. A Combined Crystal-Structural, IR and NMR Spectroscopic, and Quantum-Mechanical Investigation, J. Am. Chem.Soc. 122, 10405–10417.
- Golcu, A., Tumer, M., Demirelli, H., Wheatley, R.,A., 2005, Cd(II) and Cu(II) complexes of polydentate Schiff base ligands: synthesis, characterization, properties and biological activity, Inorg. Chim. Acta, 358, 1785-1797.
- Greenwood, N.N. and Earnshaw, A., 1997, Chemistry of the elements, second edition elsevier, U.K, 1131-1200.
- Hadjoudis, M., Vitterakis, I., Moustakali, and Mavridis, I., 1987, Photochromism and thermochromism of schiff bases in the solid state and in rigid glasses, Tetrahedron, 43, 1345-1360.
- Harada, K., 1970, The Chemistry of the Carbon-Nitrogen Double Bond, ed. S. Patai, Interscience, New York, p. 255.
- Hatfield, W. E., Inman, G. W., 1969, Spin-spin coupling in magnetically condensed complexes. IX. Exchange coupling constants for tetranuclear Schiff's base complexes of copper(II), J. Inorg Chem., 8, 1376-1378.
- Holm, R. H., Everett G. W., Chakravarty, A. A., 1966, Metal Complexes of Schiff. Bases and  $\beta$ -Ketoamines, Prog. Inorg. Chem., 7, 83.
- <http://chemistry.hull.ac.uk/lectures/sja/06513%20SJA%20handout5%20notes.pdf>
- Iqbal, M. S., Khurshid S. J., Iqbal, M. Z., 1993, Preparation, characterization, and biologic evaluation of copper(II) - Schiff base complexes derived from anthranilic acid and aldoses, Can. J. Chem., 71, 629.
- Inabe, T., Luneau, I., Mitani, T., Maruyama, Y., Takeda, S., 1994, Proton Transfer in N-(2-Hydroxy-1-naphthylmethylene)-1-pyrenamine and N,N'-Bis(2-hydroxy-1-naphthylmethylene)-p-phenylenediamine, Crystals Bull. Chem. Soc. Jpn., 67, 612-621.
- Ivanov, I.; Nikolova, S.; Angelov, P.; Kochovska,E., 2007, Regioselective acylation of  $\beta$ -enaminones of homoveratrylamine, Arkivoc, 11-17.
- Jarrahpour, A.A., Khalili, D., 2006, Synthesis of Some New bis-Schiff Bases of Isatin and 5-Fluoroisatin in a Water Suspension Medium, Molecules, 11, 59-63.



- Jubert, C., Mohamadou, A., Gerard, C., Brandes, S., Tabard, A., Barbier, J-P., 2002, Equilibrium and structural studies of complexes with a hexadentate ligand containing amide, amine and pyridyl nitrogen donors. Crystal structures of copper(II), nickel(II) and cobalt(III) complexes, *J. Chem. Soc., Dalton Trans.*, 2660–2669.
- Junior V. L., Constantino M.G., Da Silva G.V.J., Neto A.C., Tormena C. F., 2007, NMR and Theoretical Investigation of the Keto–Enol Tautomerism in Cyclohexane-1,3-diones, *J. Mol. Struct.*, 828, 54–58.
- Kalinowski, H.-O., Berger, S., Braun, S., 1984, *<sup>13</sup>C NMR Spektroskopie*, Georg Thieme Verlag: Stuttgart, New York, pp. 174-176
- Katritzky, A.R., Ghiviriga, I., Oniciu, D.C., More O'Ferrall, R.A., Walsh, S. M., 1997, Study of the Enol–enaminone Tautomerism of  $\alpha$ -Heterocyclic Ketones by Deuterium Effects on <sup>13</sup>C Chemical Shifts, *J. Chem. Soc. Perkin Trans.*, 2, 2605-2608.
- Kaupp, G., 2005, Organic Solid-State Reactions with 100% Yield, *Top. Curr. Chem.*, 254, 95-183.
- Kaye, P. T., Nyokong, T., Watkins G. M., Wellington, K.W., 2002, *Arkivoc*, Vol.9, 9-18
- Kayser R. H., Pollack, R. M., 1977, Intramolecular general base catalysis of Schiff base hydrolysis by carboxylate ions, *J. Am. Chem. Soc.*, 99, 3379-3386.
- Khan, T. A., Shagufta, M., 1999, Transition metal ion directed bimetallic macrocyclic complexes, *Trans. Met. Chem.*, 24: 669-671.
- Kubickia, M., Bassyounib, H.A.R., Coddington, P.W., 2000, Hydrogen bonding in three anticonvulsant enaminones, *J. Mol. Struct.*, 525, 141–152
- Layer, R. W., 1963, The Chemistry of Imines, *Chem. Rev.*, 63, 489-510.
- Ligtenbarg, A.G.J., Hage, R., Meetsma, A., Feringa, B.I., 1999, Hydrogen bonding properties and intermediate structure of N-(2-carboxyphenyl) salicylideneimine, *J. Chem., Soc., Perkin Trans.*, 2, 807-812
- Macho, V., Kralik, M., Hudec, J., Cingelova, J., 2004, One stage preparation of Schiff's bases from nitroarenes, aldehydes and carbon monoxide at presence of water, *J.Mol. Catal. A: Chem.*, 209, 69-73.
- McClure. M.R., Holcombe, J., 2004, Synthesis and Nmr Characterization of Cobalt(III) Complexes with Triethylenetetramine, 2,2-Bipyridine and 1,10-Phenanthroline *J. Coord. Chem.*, Vol. 57, No. 11, 907–915.
- Michael, J. P., de Koning, C. B., Gravestock, D., Hosken, G. D., Howard, A. S., Jungmann, C. M., Krause, R. W. M., Parsons, A. S., Pelly, S. C., Stanbury,

- T. V., 1999, Enaminones: Versatile Intermediates for Natural Product Synthesis, *Pure Appl. Chem.*, 71, 979.
- Miessler, G.L., Tarr, D.A., 1999, *Inorganic chemistry*, second ed., Wiley, USA.
- Mohamed, G.G., El-Gamel, N.E.A., El-Dien, F.A.N., 2001, *Synth. React. Inorg. Met.-Org. Chem.*, 31(2), 347–358.
- Mulzac, D.; Scott, K. R., 1993, Profile of Anticonvulsant Activity and Minimal Toxicity of Methyl 4- [ (p-Chlorophenyl)amino]-6-Methyl-2-Oxo- Cyclohex-3-En- 1-Oate and Some Prototype Antiepileptic Drugs in Mice and Rats, *Epilepsia*, 34(6),1141-1146.
- Nakamoto, K., 1968, *Infrared and Raman Spectra of Inorganic and Coordination Compounds*, Wiley-Interscience, New York.
- Nakamoto. K., 1997, *Infrared and Raman Spectra of Inorganic and Coordination Compounds*, Part B, 5th ed., John Wiley and Sons, Inc., Canada.
- Namsan, O. S.M., 2001, *Synth. React., Inorg.Met.Org.Chem.*,31(8), 1433-1442.
- Naringrekar, V. H.; Stella,V. J., 1990, Mechanism of Hydrolysis and Structure Stability Relationship of Enaminones as Potential Prodrugs of Model Primary Amines, *J. Pharm. Sci.*, 79, 138-146.
- Nazır, H., Yıldız, M., Yılmaz, H., Tahir, M. N., Ülkü, D., 2000, Intramolecular hydrogen bonding and tautomerism in Schiff bases. Structure of N-(2-pyridil)-2-oxo-1-naphthylidenemethylamine, *J. Mol. Struct.* 524, 241.
- Niederhoffer, E. C., Timmons, J. H., Martell, A. E., 1984. Thermodynamics of Oxygen Binding in Natural and Synthetic Dioxygen Complexes, *Chem. Rev.* 84:137-203.
- Ogawa, K., Kasahara, Y., Ohtani, Y., Harada, J., 1998, Crystal Structure Change for the Thermochromy of N-Salicylideneanilines. The First Observation by X-ray Diffraction, *J. Am. Chem.Soc.*, 120, 7107-7108.
- Ogawa, K., Fujiwara, T., Harada, J., 2005, *Acta Cryst.*, A61, 330-331.
- Olah G. A., Kuhn, S. J., 1964, *Friedel Crafts and Related Reactions*, ed. G. A. Olah, Interscience, New York, vol. III, part II, 1191.
- Perrin, D. D., 1967, *Organic Analytical Reagents*, MirPubl., Moscow.
- Prasad, R., Malamathur,N., 2002, Synthesis and characterization of Cr(III), Fe(III), Co(II), Ni(II), Cu(II) and Zn(II) complexes of 2,12-dimethyl-3-13-di-n-propyl-1,4,11,14-tetraazacycloeicosa- 1,3,11,13-tetraene, *J.Serb.Chem.Soc.* 67 (12) 825–832.

- Prasad, N., Agrawal, M., Sharma, S., 2005, Cobalt(II) complexes of tetraazamacrocycles derived from  $\beta$ -diketones and diaminoalkanes, *J. Serb. Chem. Soc.* 70 (4) 635–641.
- Przybylski, P., Jasiński, K., Brzezinski, B., Bartl, F., 2002, Spectroscopic studies and PM5 semiempirical calculations of new Schiff bases of gossypol with amino derivatives of crown ethers, *J. Mol. Struct.*, 611, 193-201.
- Raman, N., Muthuraj, V., Ravichandran, S., Kulandaisamy, A., 2003, Synthesis, characterisation and electrochemical behaviour of Cu(II), Co(II), Ni(II) and Zn(II) complexes derived from acetylacetone and *p*-anisidine and their antimicrobial activity, *Proc. Indian Acad. Sci. (Chem. Sci.)*, Vol. 115, No. 3, 161–167.
- Rao, C.N.R., Ferraro, J.R., 1970, Spectroscopy In Inorganic Chemistry, Vol.1, Academic press, New York.
- Roberts, J. D., 1959, Nuclear Magnetic Resonance Applications to Organic Chemistry, McGraw-Hill Book Company, Inc. New York Toronto London, 63-83.
- Rodriguez, J.M., Hamilton, A.D., 2006, Intramolecular Hydrogen Bonding Allows Simple Enaminones to Structurally Mimic the *i*, *i* + 4, and *i* + 7 Residues of an  $\alpha$ -Helix, *Tetrahedron Lett.*, 47,7443-7446.
- Sandhu, J.S., Sain, B., 1987, Some Recent Advances In The Chemistry Of Imines, In Particular Cycloaddition Reactions, *Heterocycles*, 26, (3), 777-818.
- Schiøtt B., Iversen B. B., Madsen G.K. H., Larsen in Enzymatic Reactions, *Proc. Natl. Acad. Sci. USA*, 95, 12799–12802.
- Schilf, W., Kamiński, B., Kolodziej, B., Grech, E., 2004, The NMR study of hydrogen formation in some tris((-salicylidene)amino)ethylamine derivatives in solution and in the solid state, *J. of Mol. Struc.*, 708, (2004), 33-38.
- Scott, K.R., Nicholson, J.M., Edafiogho, I.O., 1995, Enaminone Esters, U.S patent, patent No:5468775).
- Sheldrick, G. M., 1997, SHELXS-97 and SHELXL-97. Programs for Crystal Structure Analysis (Release 97-2). University of Göttingen, Germany.
- Shi, Y.C., Yang, H.M. Shen, W.B. Yan, C.G. Hu, X.Y., 2004, Syntheses and crystal structures of ferrocene-containing enaminones and their copper complexes, *Polyhedron*, 23, 15-21.
- Shi, Y.C., Yang, H.M., Song, H.B., Liu, Y.H., 2004, Syntheses and crystal structures of a ferrocene-containing enaminone and its copper complex, *Polyhedron*, 23, 1541-1546.

- Shi, Y.C., Yang, H.M., Song, H.B., Yan, C.G., Hu, X.Y., 2004, Syntheses and crystal structures of the potential tridentate ligand formed from condensation of ferrocenoylacetone and S-benzylthiocarbamate and its bivalent metal complexes, *Polyhedron* 23, 567-573.
- Shi, Y.C., 2005, 3-[(2-Hydroxyphenyl)amino]-1-phenylbut-3-en-1-one ethanol solvate, *Acta Crystallogr. Sect. E: Struct. Rep. Online*. E61, 1130–1132.
- Shi, Y.C., Sui, C-X., Song, H-B., Jian, P-M., 2005, Syntheses and crystal structures of a tridentate enaminone and its copper complex, *J. Coord. Chem.*, Vol. 58, No. 4, 363–371.
- Shikama, K., 1998, The Molecular Mechanism of Autoxidation for Myoglobin and Hemoglobin: a Venerable Puzzle, *Chem. Rev.*, 1357–1373.
- Simunek, P., Bertolasi, V., Peskova, M., Machacek, V., Lycka, A., 2005, Solution and solid state structure and tautomerism of azo coupled enaminone derivatives of benzoylacetone, *Org. Biomol.chem.*, 3, 1217-1226.
- Singh, D. P., Kumar, R., Malik, V., 2007, Synthesis and characterization of complexes of Co(II), Ni(II), Cu(II), Zn(II), and Cd(II) with macrocycle 3,4,11,12-tetraoxo-1,2,5,6,9,10,13,14-octaazacyclohexadeca- 6,8,14, 16-tetraene and their biological screening, *Trans. Met. Chem.*, 32:1051–1055.
- Sinha, S.C., Das, S., Li, L.S., Lerner, R.A., Barbas, C.F., 2007, Preparation of integrin  $\alpha(v)\beta(3)$ -targeting Ab 38C2 Constructs, *Nature Protocols.*, 2, 2, 449-456.
- Sönmez, M., Şekerci, M., 2002, Synthesis and Characterization of Cu(II), Co(II), Ni(II) and Zn(II) Schiff Base Complexes from 1-Amino-5-benzoyl-4-phenyl-1H-pyrimidine-2-one with Salicylaldehyde, *Polish J. Chem.*, 76, 907–914.
- Sönmez, M., Levent, A., Şekerci, M., 2003, Synthesis And Characterization Of Cu(II), Co(II), Ni(II) And Zn(II) Complexes Of Schiff Base Derived From 1-Amino-5- Benzoyl-4-Phenyl-1H-Pyrimidine-2-One And 3-Hydroxy salicylaldehyde, *Synth. React. Inorg. Met. –Org. Chem.*, Vol. 33, No. 10, 1747–1761.
- Stuart, B., 2004, *infrared spectroscopy:Fundamentals and applications* John Wiley & Sons, Ltd). New york.
- Takemoto, j., 1973, *Inorg.chem.*, 12, 949.
- Turner, M. Koksal, H. Serin S. Digrak, M., 1999, *Trans. Met. Chem.*, 24, 13.
- Ünver, H., 2001, Synthesis And Spectroscopic Studies In Some New Schiff Bases, *Spectrosc. Lett.*, 34, 783-791.
- Van Der Poel, H., Van Koten, G., Vrieze, K., 1980, *Org.chem.*, 19,1145.

- Vazzana, I., Terranova, E., Mattioli, F., Sparatore, F., 2004, *Arkivoc*, 364-374.
- Venkov, A. P., Angelov, P. A., 2003, Synthesis of Unsymmetrical  $\beta$ -Enamino Ketones, *Synthesis*, 14, 2221-2225.
- Vishnu, J. R., 1980, *Arch. Pharm. (Weinheim)*, 313, 471-476.
- Wagger, J., Bevk, D., Meden, A., Svete J., Stanovnik B., 2006, Enaminone-Based Synthesis of Dipodazine Derivatives, *Helv. Chim. Acta*, Vol. 89.
- Wennerbeck, I., 1973, Polarized ethylenes. V. Ultraviolet spectra, experimental results, and PPP [Pariser-Parr-Pople] calculations, *Acta Chem. Scand.* 27, 258-270.
- Woolins, J.D., 1994, *Inorganic Experiments*, VCH Verlagsgesellschaft Weinheim, Germany, 10-11.
- Wozniak, K., He, H., Klinowski, J., Jones, W., Dziembowska, T., Grech, E., 1995, Intramolecular hydrogen bonding in N-salicylideneanilines. X-ray diffraction and solid-state NMR studies, *J. Chem. Soc. Faraday Trans.*, 91 77-85.
- Yıldız, M., 2004, Synthesis and Spectroscopic Studies of Some New Polyether Ligands of the Schiff Base Type, *Spectrosc. Lett.*, 37, 367-381.
- Yıldız, M., Kılıç, Z., Hökelek, T., 1998, Intramolecular hydrogen bonding and tautomerism in Schiff bases. Part I. Structure of 1,8-di[N-2-oxophenyl-salicylidene]-3,6-dioxaoctane, *J. Mol. Struct.*, 441, 1-10.
- Zhao, J., Zhao, B., Liu, J., Xu, W., Wang, Z., 2001, Spectroscopy study on the photochromism of Schiff Bases N,N'-bis(salicylidene)-1,2-diaminoethane and N,N'-bis(salicylidene)-1,6-hexanediamine, *Spectrochim. Acta*, 57A, 149-154.
- Zgierski, M.Z., Grabowska, A., 2000, Theoretical approach to photochromism of aromatic Schiff bases: A minimal chromophore salicylidene methylamine, *J. Chem. Phys.*, 113, 7845.
- Zhuo, J. C., 1997, NMR of Enaminones Part 3- $^1\text{H}$ ,  $^{13}\text{C}$  and  $^{17}\text{O}$  NMR Spectroscopic Studies of Acyclic and Cyclic N-Aryl Enaminones: Substituent Effects and Intramolecular Hydrogen Bonding, *Magn. Reson. Chem.*, 35, 21-29.
- Zhuo, J. C., 1997, NMR of Enaminones Part 2- $^{17}\text{O}$  NMR Spectra of Primary and Secondary Enaminones: Evaluation of Substituent Increments and Intramolecular Hydrogen Bonding, *Magn. Reson. Chem.*, 35, 311-312.
- Zhuo, J. C., 1998, Part 8- $^1\text{H}$ ,  $^{13}\text{C}$  and  $^{17}\text{O}$  NMR spectra of primary and secondary 1,2-disubstituted enaminones: configuration, conformation and intramolecular hydrogen bonding, *Magn. Reson. Chem.*, 36, 565-572.

## **CURRICULUM VITAE**

**Name & Surname** : Mahir TİMUR

**Place of Birth** : Antakya

**Date of Birth** : 06.12.1972

**Marial Status** : married

### **Education and**

#### **Academic Life** **High School**

: 1986-1989 Antakya Merkez Lisesi

#### **B.Sc.**

: 1994-1998 Hatay Mustafa Kemal University  
Department of Chemistry

: 1998-2001 Hatay Mustafa Kemal University

#### **M.Sc.**

Department of Chemistry Organic Chemistry Section

**Foreign Language** : English

### **Work Experience**

1998-2001 : Research Assistance,  
Hatay Mustafa Kemal University ,  
Chemistry Department

2001- Research Assistance,  
Hacettepe University,